Analytical approaches to the study of hyaluronan and hyaluronidases:

Development and application of hyphenated chromatographic and electrophoretic methods

Dissertation

zur Erlangung des Doktorgrades der Naturwissenschaften (Dr. rer. nat.)

der Fakultät für Chemie und Pharmazie

der Universität Regensburg

vorgelegt von

Martin Rothenhöfer

aus Coburg

2013

Die vorliegende Arbeit entstand in der Zeit von Januar 2010 bis Januar 2013 unter der Leitung von Prof. Dr. Armin Buschauer und Prof. Dr. Günther Bernhardt am Institut für Pharmazie der Fakultät für Chemie und Pharmazie der Universität Regensburg.

Das Promotionsgesuch wurde eingereicht am 12. Februar 2013.

Tag der mündlichen Prüfung: 08. März 2013

Prüfungsausschuss:

Vorsitzender:	Prof. Dr. Jörg Heilmann
Erstgutachter:	Prof. Dr. Armin Buschauer
Zweitgutachter:	Prof. Dr. Günther Bernhardt
Prüfer:	Prof. Dr. Frank-Michael Matysik

„Beim Erforschen und Versuchen

hört man auch die Frömmsten fluchen.“

Prof. Dr. Hans-Jürgen Quadbeck-Seeger (*1939), German chemist

Contents

Curriculum vitae

Personal information

Name:	Martin Rothenhöfer
Date of birth:	October 12, 1984
Place of birth:	Coburg, Germany
Marital status:	Single
Nationality:	German

Education

01/2010 – today	Doctoral candidate University of Regensburg Department of Pharmaceutical and Medicinal Chemistry II
01/2010	Licensure as a pharmacist (*Approbation als Apotheker*)
11/2009	Part three of the pharmaceutical exam (*3. Abschnitt der Pharmazeutischen Prüfung*)
05/2009 – 10/2009	Practical training Bayer HealtCare AG, Wuppertal Cardiology Research (Vascular Diseases)
11/2008 – 04/2009	Practical training Sonnen-Apotheke (community pharmacy), Neustadt bei Coburg
10/2008	Part two of the pharmaceutical exam (*2. Abschnitt der Pharmazeutischen Prüfung*)
08/2006	Part one of the pharmaceutical exam (*1. Abschnitt der Pharmazeutischen Prüfung*)
10/2004 – 09/2008	Studies of pharmacy University of Regensburg
06/2004	General qualification for university entrance (*Allgemeine Hochschulreife*)
09/1995 – 06/2004	Arnold-Gymnasium (secondary school), Neustadt bei Coburg

Funding

02/2010 – 01/2013	PhD fellowship, German National Academic Foundation (*Studienstiftung des deutschen Volkes*)
10/2004 – 10/2008	Bavarian governmental scholarship (*Stipendium nach dem Bayerischen Begabtenförderungsgesetz*)

Publications, oral presentations, and posters

Peer-reviewed journal articles (published results prior to the submission of this thesis)

Rothenhöfer, M.; Scherübl, R.; Bernhardt, G.; Heilmann, J.; Buschauer, A. Qualitative and quantitative analysis of hyaluronan oligosaccharides with high performance thin layer chromatography using reagent-free derivatization on amino-modified silica and electrospray ionization-quadrupole time-of-flight mass spectrometry coupling on normal phase. *J. Chromatogr. A* **2012,** 1248, 169-177.

Grundmann, M.; Rothenhöfer, M.; Bernhardt, G.; Buschauer, A.; Matysik, F. M. Fast counter-electroosmotic capillary electrophoresis–time-of-flight mass spectrometry of hyaluronan oligosaccharides. *Anal. Bioanal. Chem.* **2012,** 402, 2617-2623.

Oral presentations

Rothenhöfer, M.; Grundmann, M.; Scherübl, R.; Hamberger, J.; Bernhardt, G.; Heilmann, J.; Matysik, F. M.; Buschauer, A. Analytical approaches to the study of hyaluronan and hyaluronidases. *Graduate student meeting of the German Pharmaceutical Society (DPhG Doktorandentagung)* **2012**, Nov. 14 – Nov. 17, Weimar.

Rothenhöfer M. Analytik von Hyaluronsäure-Oligosacchariden mittels CE–MS-Kopplung und Ionenchromatographie: Vorstellung des Projekts (German). *Meeting of PhD students of the German National Academic Foundation (Forum Natur, Studienstiftung des deutschen Volkes)* **2011**, June 2 – June 5, Berlin.

Poster presentations

Rothenhöfer, M.; Scherübl, R.; Bernhardt, G.; Heilmann, J.; Buschauer, A. HPTLC of purified hyaluronan oligosaccharides: reagent-free derivatization and densitometric quantification on amino-modified silica, TLC–ESI–Q-TOF-MS coupling on normal phase. *Annual meeting of the German Pharmaceutical Society (DPhG Jahrestagung)* **2012**, Oct. 11 – Oct. 13, Greifswald.

Rothenhöfer, M.; Grundmann, M.; Bernhardt, G.; Matysik, F. M.; Buschauer, A. At-line CE–ESI-TOF-MS analysis of hyaluronan oligosaccharide degradation by hyaluronidases. *6th Summer School Medicinal Chemistry* **2012**, Sept. 26 – Sept. 28, Regensburg.

Co-authored poster

Grundmann, M.; Rothenhöfer, M.; Bernhardt, G.; Buschauer, A.; Matysik, F. M. Coupling capillary electrophoresis to time-of-flight mass spectrometry – achieving fast separations in capillaries. Presented by M. Grundmann, *Wissenschaftsforum Chemie* **2011**, Sept. 4 – Sept. 7, Bremen.

Acknowledgements and declaration of collaborations

First, I want to thank my supervisor Prof. Dr. Armin Buschauer for giving me the opportunity to work on my scientific project in his research group and for useful discussions on this thesis.

I also express gratitude to my second supervisor Prof. Dr. Günther Bernhardt for scientific advice and for hints to improve the style of this thesis. Furthermore, I thank Prof. Bernhardt for taking the nice photographs depicted in Chapter 10 to illustrate the CAM assay.

My most sincere thanks are due to all persons and institutions who contributed to this work by collaboration, excellent cooperation, and technical assistance. The nature of these collaborations and the contributions of the respective partners and colleagues are stated below.

I am indebted to Prof. Dr. Frank-Michael Matysik (Institute of Analytical Chemistry, Chemo- and Biosensors, University of Regensburg) and his group for collaboration concerning CZE–ESI-TOF-MS coupling. Development and characterization of the method (Chapter 3) were carried out together with Dr. Marco Grundmann, contributing equally to conceptual design, realization, and interpretation of the respective experiments.

HPTLC and TLC–MS method development (Chapter 5) was concerted work (with equal contributions) with Rosmarie Scherübl from the group of Prof. Dr. Jörg Heilmann (Department of Pharmaceutical Biology, University of Regensburg). I wish to express my warmest thanks for this successful collaboration. I am also deeply grateful to Prof. Heilmann for offering us cooperation with regard to these HPTLC and TLC–MS experiments as well as for numerous fruitful discussions and mentoring. I thank Josef Kiermaier from the Center of Chemical Analysis (University of Regensburg) for performing the TLC–MS coupling experiments.

The kind gift of recombinant human hyaluronidases for *in vitro* characterization (Chapter 7) by Gregory I. Frost, PhD (Halozyme Therapeutics, San Diego, CA, USA) is gratefully acknowledged.

Samples of synovial fluid (Chapter 8) were kindly provided by the Department of Orthopedics (University of Regensburg/Asklepios Klinikum, Bad Abbach).

I wish to thank Prof. Dr. Achim Göpferich (Department of Pharmaceutical Technology, University of Regensburg) for the possibility to perform rheological studies (Chapter 8) in his

lab. Special thanks go to his coworker Dr. Ferdinand Brandl for instructions concerning the rheometer.

I owe sincere gratitude to Prof. Dr. Joachim Wegener (Institute of Analytical Chemistry, Chemo- and Biosensors, University of Regensburg) for cooperation concerning electric cell–substrate impedance sensing (ECIS) as well as for providing endothelial cells for crystal violet assay and flow cytometry (Chapter 9). Special thanks are addressed to his coworkers Barbara Goricnik and Nadja Hinterreiter for performing the ECIS measurements.

Maria Beer-Krön from our group is gratefully acknowledged for outstanding technical assistance with regard to cell culture and performing crystal violet cell proliferation assays (Chapter 9).

Furthermore, I show appreciation to Prof. Dr. Sigrid Karrer (Department of Dermatology, University of Regensburg) for providing samples collected from wounds (Chapter 9).

I am deeply indebted to PD Dr. Dietrich Paper for instructions and help concerning the CAM assay as well as for contribution of expert knowledge with regard to evaluation and interpretation of the results (Chapter 10).

I thank Dr. Jörg Teßmar (Department of Pharmaceutical Technology, University of Regensburg) for providing bFGF (Chapter 10). Technical assistance of Petra Pistor concerning the preparation of histological samples from chorioallantoic membranes is acknowledged (Chapter 10).

For technical assistance I also wish to thank my student apprentice Verena Lehner.

I also show appreciation to all former and present members of the Department of Pharmaceutical and Medicinal Chemistry II. Especially the colleagues from the hyaluronidase and hyaluronidase inhibitor field are acknowledged for collaboration and fruitful discussions.

Many thanks are due to the German National Academic Foundation (Studienstiftung des deutschen Volkes) for a PhD fellowship.

I want to extend special thanks to all friends, especially Amelie Kaufner, Benjamin Kaufner, Rosmarie Scherübl, Kira Bürger, and Julia Maier-Bort, for personal support.

Furthermore, I owe sincere gratitude to my parents for their support and for believing in me.

Finally, I thank Caroline for her love and for always being at my side.

Abbreviations

2D	Two-dimensional
δ	Phase angle
λ	Wavelength
A	Peak area
A_λ	Absorbance at wavelength λ (λ given in nm)
APS	Ammonium peroxodisulfate
AU	Arbitrary unit(s)
bFGF	Basic fibroblast growth factor
BSA	Bovine serum albumin
BTH	Bovine testicular hyaluronidase
CAM	Chorioallantoic membrane
CD	Cluster of differentiation
CPD	Citrate-phosphate-dextrose
CTAB	Cetyltrimethylammonium bromide
C(Z)E	Capillary (zone) electrophoresis
DMSO	Dimethyl sulfoxide
E	Electrode potential
E_λ	Extinction at wavelength λ (λ given in nm)
EC	Enzyme Commission (number)
ECIS	Electric cell–substrate impedance sensing
EDTA	Ethylenediamin tetraacetate
ELISA	Enzyme-linked immunosorbent assay
EOF	Electroosmotic flow
ERK	Extracellular signal-regulated kinase
ESI	Electrospray ionization
f	Female
FACE	Fluorophore-assisted carbohydrate electrophoresis
FCS	Fetal calf serum
FSC	Forward scatter
g	Gravitational acceleration, 9.81 m/s²
G*	Complex shear rigidity modulus
|G*|	Absolute value of the complex shear rigidity modulus
G’	Storage modulus
G’’	Loss modulus

GA	D-Glucuronic acid
GPI	Glycosylphosphatidylinositol
HA	Hyaluronan, hyaluronic acid
HAS	Hyaluronan synthase
HEPES	4-(2-hydroxyethyl)piperazine-1-ethanesulfonic acid
HMW	High molecular weight
HPAEC	High performance anion exchange chromatography
HPLC	High performance liquid chromatography
HPTLC	High performance thin layer chromatography
Hsp72	Heat shock protein 72
Hyal	Hyaluronidase
IC_{50}	Concentration of an inhibitor required to give 50% inhibition of enzyme activity
IgG	Immunoglobulin G
IU	International unit(s)
K_m	Michaelis constant
LED	Light-emitting diode
LMW	Low molecular weight
LOD	Limit of detection
LOQ	Limit of quantification
m	Male
MALDI	Matrix assisted laser desorption ionization
mRNA	Messenger ribonucleic acid
MS	Mass spectrometry
MW	Molecular weight
m/z	Mass-to-charge (ratio)
N	Number of replicates
n_x (*x* = 1, 2, 3, …)	Saturated hyaluronan oligosaccharide comprising *x* disaccharide moieties, “even-numbered”
n_x (*x* = 1.5, 2.5, 3.5, …)	Hyaluronan oligosaccharide with an incomplete disaccharide moiety (only D-glucuronic acid, no *N*-acetyl-D-glucosamine) at the reducing end, “odd-numbered”
n_x* (*x* = 1, 2, 3, …)	Unsaturated hyaluronan oligosaccharide comprising *x* disaccharide moieties
NAG	*N*-Acetyl-D-glucosamine
NaOAc	Sodium acetate
NF-κB	Nuclear factor kappa B
NMR	Nuclear magnetic resonance
PAD	Pulsed amperometric detection

PAGE	Polyacrylamide gel electrophoresis
PBS	Phosphate-buffered saline
PEG	Poly(ethylene glycol)
PH-20	Testicular hyaluronidase (sperm adhesion molecule 1, SPAM1)
Q-TOF-MS	Quadrupole time-of-flight mass spectrometry
R^2	Coefficient of determination
R_f	Retardation factor (in thin layer chromatography)
rh	Recombinant human
RHAMM	Receptor for hyaluronan-mediated motility
RSD	Relative standard deviation
SD	Standard deviation
SDS	Sodium dodecyl sulfate
SEM	Standard error of the mean
S/N	Signal-to-noise ratio
SSC	Side scatter
TBE	Tris/borate/EDTA (buffer)
TEMED	*N*,*N*,*N'*,*N'*-tetramethylethylenediamine
TLC	Thin layer chromatography
TOF-MS	Time-of-flight mass spectrometry
Tris	Tris(hydroxymethyl)aminomethane
UV	Ultra violet
v_{max}	Maximum velocity
v/v	Volume per volume
w/v	Weight per volume

1 General introduction

1.1 Hyaluronan

1.1.1 Structure and properties: a chemical point of view

The polysaccharide hyaluronan (hyaluronic acid, HA) was isolated from bovine vitreous humor by Meyer and Palmer in 1934.[1] Having identified uronic acid and hexosamine as constituents of this substance, they suggested the name "hyaluronic acid", a combination of "hyaloid" (vitreous) and "uronic acid".[1] At physiological pH, the carboxylic groups of the acidic polysaccharide (pK_a = 3–4) are predominantly deprotonated.[2] Hence, the term "hyaluronan" is preferably used today.

In 1954, the exact chemical structure of hyaluronan was elucidated (Figure 1.1).[3] Hyalobiurionic acid, the repeating unit of the polymer, consists of D-glucuronic acid and *N*-acetyl-D-glucosamine, linked by a β-1,3 glycosidic bond.[3] Depending on the origin, hyaluronan is polydisperse with each molecule of the unbranched polymer comprising about 2000–25000 disaccharide moieties,[4] connected by β-1,4 glycosidic bonds.[2-5] As each disaccharide unit has a molecular mass of approximately 400 Da and an average length of ca. 1 nm,[2] these degrees of polymerization correspond to molecular masses of 0.8–10 MDa and extended lengths of 2–25 µm.

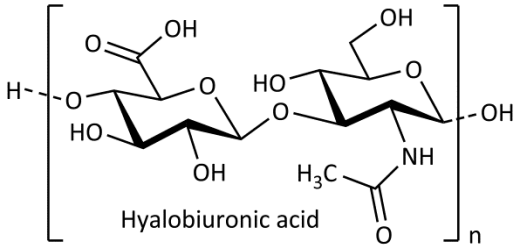

Hyaluronic acid (hyaluronan): n = 2000–25000

Figure 1.1: General structure of hyaluronan. The biopolymer consists of β1→4-linked hyalobiuronic acid* (D-glucuronic acid β1→3-linked with *N*-acetyl-D-glucosamine). Depending on the source, the native polysaccharide usually comprises n = 2000–25000 disaccharide moieties.[4]

Within the family of glycosaminoglycans, hyaluronan differs from chondroitin sulfate, dermatan sulfate, keratan sulfate, heparin, and heparan sulfate by being the only non-sulfated exception. Moreover, hyaluronan is the only glycosaminoglycan, which is not

* In literature, the term "hyalobiuronic acid" is inconsistently used for both the repeating disaccharide unit (as depicted in Figure 1.1) and its deacetylated derivative.

covalently linked to a protein core, forming a proteoglycan, but is secreted directly into the extracellular space during synthesis.[6]

In a way, the common depiction (also used in this work) of hyaluronan as a sequence of disaccharide units, drawn in the same orientation, is misleading. Although hyaluronan molecules are simple linear polysaccharide chains, the secondary and tertiary structures of this biomolecule are more complex.

Hyaluronan in solution has been assumed to form a tape-like, two-fold helix with each disaccharide rotated by 180° compared to its neighboring repeating units.[7] The existence of hydrophobic patches within the molecule was suggested, allowing for self-aggregation as well as for formation of reversible tertiary structures, correlated to the biological properties.[7-9] Recently, this theory was rejected by Almond et al. due to the observation that the proposed two-fold helices occurred only transiently in very restricted regions of the polysaccharide chains.[10, 11] Instead, a dynamic local conformation was determined, which (in average) could approximately be described as a contracted four-fold helix.[10] With regard to the high concentrations of hyaluronan in the extracellular matrix and the high degrees of polymerization, the reported NMR methods were not ideal to prove or exclude the formation of structures of higher order under physiological conditions. Hence, Raman spectrometry and Raman optical activity (ROA) were applied to this problem, providing further evidence against the existence of tertiary structures of hyaluronan.[12]

Moreover, the theory of stable networks was often referred to the rheological properties of hyaluronan in aqueous solution.[9] By contrast, in a review of analytical studies, Cowman and Matsuoka drew the conclusion that the behavior of hyaluronan was quite typical for a linear semi-flexible polymer of the respective chain length.[13] Due to its flexibility, its viscoelastic properties, and the space-filling structure, hyaluronan provides perfect conditions for tissue remodeling and can serve as a kind of track for migrating cells.[11]

1.1.2 Occurrence and physiological relevance: a biological point of view

Physiologically, different amounts of hyaluronan can be found in tissues from all vertebrates as well as in the capsules of some strains of *Streptococci*.[2] It is an important constituent of embryonic and regenerating tissues, where it provides hydrated pericellular zones (facilitating cell rounding during mitosis) and pathways for cell migration.[2, 4] Among mature tissues, an extraordinarily high concentration of hyaluronan (7.5 mg/mL) can be found in rooster comb, whereas umbilical cord probably has the highest hyaluronan content (4 mg/mL) of all mammalian tissues.[2]

However, half of the 7–8 g of hyaluronan in the body of an average adult human is located in the different layers of the skin.[2] Considering the wet tissue mass, the hyaluronan content of

the dermis (ca. 0.5 mg/g) is higher than that of the epidermis (ca. 0.1 mg/g).[2] Nevertheless, the different contents of cells result in opposed conditions with regard to the concentration in the extracellular matrix of dermis (ca. 0.5 mg/mL) and epidermis (2–4 mg/mL).[2] Considering the high content and the observed turnover time of less than one day within the epidermal matrix, hyaluronan seems to be important for migration and shape changes of keratinocytes during differentiation.[14]

In hyaline cartilage, hyaluronan forms aggregates of several hundred million Dalton with chondroitin sulfate proteoglycans (aggrecans).[15] Thereby, hyaluronan serves as backbone and retains high concentrations of aggrecan molecules in the matrix, which are essential for the biomechanical properties of the cartilage tissue.[2, 15]

As hyaluronan was first isolated from bovine vitreous humor,[1] it is not surprising that the human vitreous body also contains relatively high amounts (0.1 mg/g wet weight) of hyaluronan.[2] The isolation of hyaluronan from synovial fluid was also described, when research on this substance was still in the fledgling stages in 1939.[16] With a hyaluronan content of 3–4 mg/mL, synovial fluid has one of the highest concentrations in the human body.[2] Later, hyaluronan was proven to be responsible for the viscosity of synovial fluid.[17] Ogston and Stanier suggested a mainly lubricant function of hyaluronan, considering the viscoelastic properties less relevant under physiological conditions.[18] With regard to the pathology of osteoarthritis and rheumatoid arthritis, the role of hyaluronan is discussed controversially.[19-23] Nevertheless, hyaluronan is not only physiologically present in the eye and joints. Ophthalmology (e. g. cataract surgery) and orthopedics (treatment of osteoarthritis) are also typical examples for the use of this biopolymer as medical device, mainly owing to its viscoelasticity and its high capacity to bind water.[24]

The matrix produced by the cumulus cells around the oocyte also contains significant amounts of hyaluronan (ca. 0.5 mg/mL).[2] Probably the hyaluronan-rich matrix facilitates ovulation and transport of the oocyte.[25] During fertilization, the matrix of the expanded cumulus cell–oocyte complex probably forms a barrier, which can only be overcome by fully functional sperm.[25] The sperm hyaluronidase and its role during fertilization will be discussed in Section 1.2.2.

Apart from the mentioned examples of physiological functions, directly related to the physicochemical properties of the polymer, hyaluronan can also cause biological effects via interaction with hyaluronan binding proteins (hyaladherins), especially with cell surface hyaluronan receptors (*cf*. Section 1.2.3). Moreover, hyaluronan and hyaluronan-derived oligosaccharides are proposed to influence many different physiological and patho-physiological processes in a size-dependent manner (*cf*. Section 1.2.5).

1.2 Hyaluronidases and hyaluronan metabolism

1.2.1 Occurrence and classification of hyaluronidases

Hyaluronan degrading enzymes have been identified in bacteria (bacteriophage-associated as well as bacterial enzymes), some species of fungi, nematodes, leeches, crustaceans, venoms from arthropods (insects, scorpions, spiders) and vertebrates (stonefish, snakes, lizards, mammals), and other vertebrate sources (tissues, body fluids).[26-29] According to the conventional classification by Meyer, hyaluronidases are usually sorted into three main families with regard to their catalytic mechanism (Figure 1.2).[30]

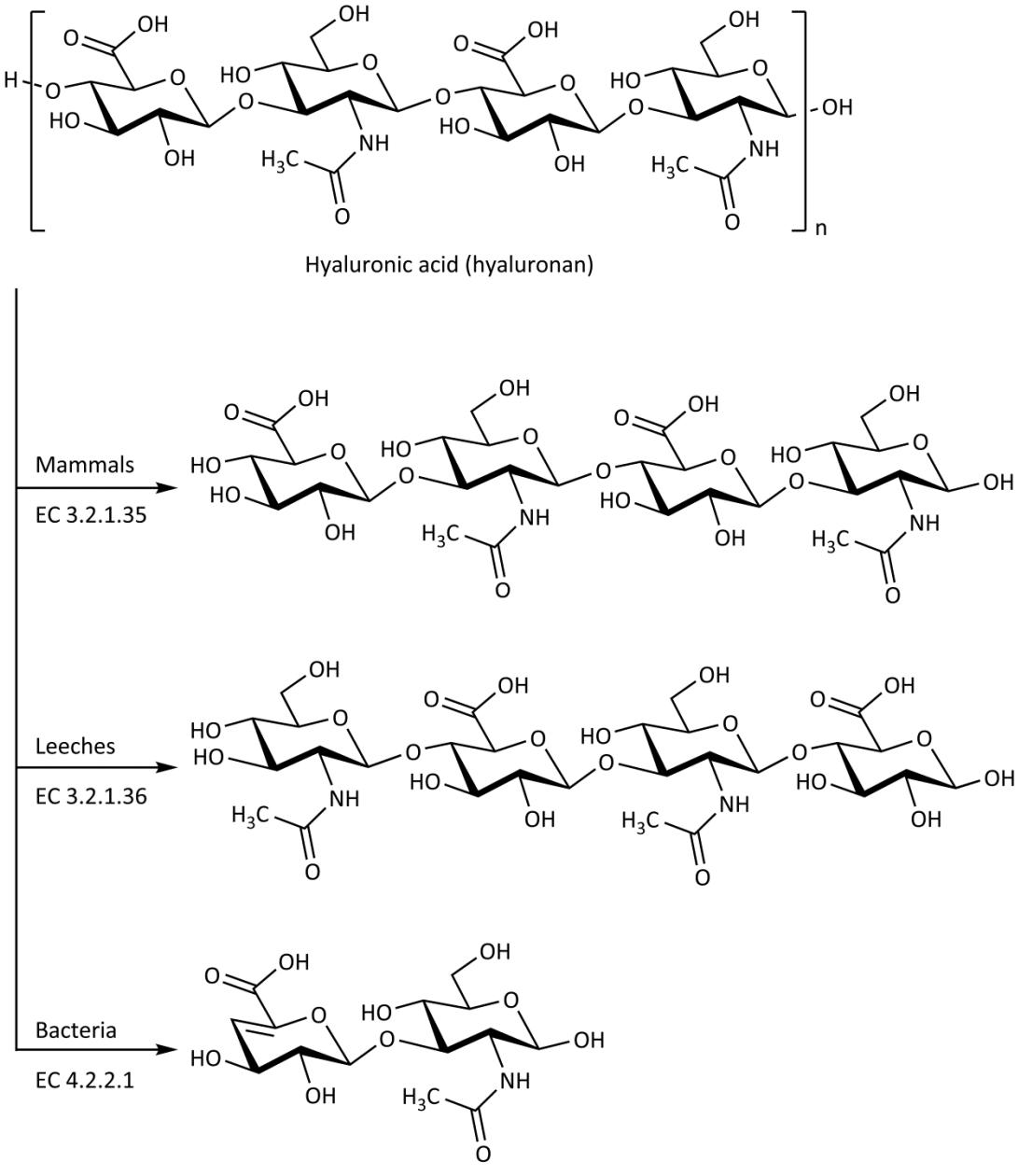

Figure 1.2: Classification of hyaluronidases according to Meyer.[30]

The hyaluronidases from mammals and other vertebrates as well as the bee venom hyaluronidase are typical examples of the first group (EC 3.2.1.35).[28, 30-32] The mechanism of these endo-β-*N*-acetyl-D-hexosaminidases is characterized by the hydrolysis of the β-1,4 glycosidic bonds of hyaluronan. Tetra- and hexasaccharides accumulate as end products.[31] Some hyaluronidases from this family were proven to accept chondroitin sulfates and dermatan sulfates as alternative substrates.[31, 33] By contrast, stonefish hyaluronidase was reported to be unique within this group with regard to its substrate specificity for hyaluronan.[34] Moreover, mammalian isoenzymes exhibit differences concerning pH profile, minimal substrates, and product spectra.[32, 35] From many studies, mainly using bovine testicular hyaluronidase (BTH), it is known that both hydrolysis and transglycosylation reactions occur with these enzymes.[32, 35-42]

The second group (EC 3.2.1.36) includes hyaluronidases from crustaceans, nematodes, and the salivary glands of leeches.[28, 30, 31] These enzymes are endo-β-D-glucuronidases and hydrolyze the β-1,3 glycosidic bonds of hyaluronan. Hence, the products of the reaction have a D-glucuronic acid moiety at the reducing end. Similar to the first group, the main products are tetra- and hexasaccharides.[31] The leech enzyme, purified and characterized by Yuki and Fishman, was specific for hyaluronan.[43] Most probably, this hyaluronidase serves as spreading factor increasing the permeability of the skin of the host.[28] By analogy, the hyaluronidases (showing activity also against chondroitin sulfate A) from nematodes, excreted by the parasites during intestinal invasion, were reported to contribute to pathological enteritis.[44] Hence, these enzymes might be potential drug targets for the therapy of nematode infections.

The same is the case for hyaluronidases from microbial pathogens. In contrast to both other types of hyaluronidases, the bacterial enzymes (EC 4.2.2.1, formerly EC 4.2.99.1) catalyze a β-elimination reaction.[28, 30, 31, 45] Except for *Streptomyces hyalurolyticus* hyaluronidase, which degrades hyaluronan to mixtures of unsaturated tetra- and hexasaccharides, the main product of microbial hyaluronan lyases is the unsaturated disaccharide 3-(4-deoxy-β-D-gluc-4-enuronosyl)-*N*-acetyl-D-glucosamine.[45] Moreover, the hyaluronidases from *Streptococci*, *Staphylococci, Clostridia*, *Streptomyces*, and other microorganisms exhibit different substrate specificities, with *Streptomyces hyalurolyticus* hyaluronidase being highly specific for hyaluronan.[45] Probably, the best characterized bacterial hyaluronidases are those of the group B *Streptococci*, namely *Streptococcus agalactiae* and *Streptococcus pneumonia*e. These enzymes are supposed to exhibit a catalytic mechanism comprising an initial random cleavage step and further processive exolytic degradation of the residual polysaccharide chain.[46-51] Apart from the function of hyaluronidases as spreading factor, the produced disaccharides are discussed to serve as nutrients for the bacteria.[52] Recently, the use of host hyaluronan as carbon source by *Mycobacterium tuberculosis* was reported, although no hyaluronidase had previously been identified in the genome of this human pathogen.[53] The

authors also described successful inhibition of hyaluronan-dependent growth of *Mycobacteria* by L-ascorbic acid-6-*O*-hexadecanoate,[53] a potent hyaluronidase inhibitor found in our group.[54]

1.2.2 Human hyaluronidases

Hyaluronidases from venoms and human pathogens are potential drug targets. The same holds for human hyaluronidases, which are still far from being understood with regard to their physiological and pathophysiological role. Six hyaluronidase-like sequences have been identified in the human genome: *HYAL1*, *HYAL2*, and *HYAL3* clustered on chromosome 3p21.3; *HYAL4*, *PH-20*, and *HYALP1* on chromosome 7q31.3.[55] The human paralogs exhibit a sequence identity of about 40%, whereas a much higher degree of homology was observed for orthologous human and murine genes.[31, 55]

HYAL1 is expressed in many tissues. Highest levels of mRNA were detected in liver, heart, spleen, kidney, and bone marrow.[56] The gene was proven to encode the soluble acid-active hyaluronidase found in human plasma.[57] Although differing in molecular mass and some other characteristics, similar hyaluronidases were isolated from human liver,[58] serum,[59] and urine.[60] As acid-active hyaluronidase is assumed to be a lysosomal enzyme, its presence in plasma as well as its pH optimum clearly below the lysosomal pH of 4.5 seem mysterious.[61] *HYAL1* was described as a candidate tumor suppressor gene, also known as *LUCA-1* due to its observed deletion in lung cancer.[62, 63] By contrast, overexpression of Hyal-1 was reported to promote growth and aggressiveness of malignant tumors of breast,[64, 65] bladder,[66] and prostate.[67] This controversial role is further supported by recent studies, in which blocked as well as high expression of Hyal-1 inhibited proliferation of prostate cancer cells.[68] In addition to this ambiguous involvement in cancer, inactivating mutations of the *HYAL1* gene were observed in the lysosomal storage disorder mucopolysaccharidosis IX.[69, 70]

Recently, a putative second type of mucopolysaccharidosis IX was proposed from a study with mice lacking Hyal-2, the protein encoded by *HYAL2*.[71] In human tissues, the *HYAL2* gene (also known as *LUCA-2*) is widely expressed, except in brain, with highest mRNA levels found in spleen.[56, 72] Hyal-2 was reported to be either a lysosomal protein or membrane-bound via a glycosylphosphatidylinositol (GPI) anchor.[72, 73] Recently, Hyal-2 was proven to be the only hyaluronidase present in platelets.[74, 75] The enzyme is commonly believed to cleave hyaluronan incompletely, yielding fragments down to 20 kDa.[72, 73] Thus, Hyal-1 and Hyal-2, the major hyaluronidases in human somatic tissues, are hypothesized to contribute to the degradation of hyaluronan in a concerted and successive manner (*cf*. Section 1.2.3).[55, 61] By contrast, Hamberger proved the presence of smaller fragments (10–15 kDa) after incubation of hyaluronan with Hyal-2.[75] The products of Hyal-2 are supposed to induce the production of proinflammatory cytokines and to play an important role in wound healing (*cf*. Section

1.2.5).[74] Overexpression of Hyal-2 in murine astrocytoma cells promoted the formation of highly vascularized and invasive tumors in brain, whereas subcutaneous tumorigenicity of these glioma cells was not increased, indicating an interaction with the extracellular matrix of the brain.[76] By contrast, murine fibroblasts were reported to become more sensitive to tumor necrosis factor alpha (TNF-α) by Hyal-2 overexpression, resulting in increased apoptosis.[77]

Although *HYAL3* is widely expressed in humans, no activity of the Hyal-3 protein was proven up to now.[61] Hence, its physiological relevance remains an enigma. Particularly high expression can be found in bone marrow and testis.[56] Human and murine Hyal-3 share about 80% of their amino acid sequence, which is a much higher sequence identity than that of the respective Hyal-1 enzymes (73%).[55] As Hyal-3 was reported to contribute to the hyaluronidase activity in murine sperm and to be expressed also in human sperm, the enzyme was proposed to play a role in fertilization in both species.[78] Considering the stem cell-like state of both bone marrow and testis, it was hypothesized that Hyal-3 might be relevant for stem cell regulation and fetal development.[31, 55]

HYAL4 gene expression was determined on the mRNA level in skeletal muscle and placenta.[56] Recently, human Hyal-4 was proven to be an endo-β-*N*-acetylgalactosaminidase with specificity for chondroitin sulfate, thus being the first chondroitin sulfate hydrolase identified in a higher organism.[79]

In 1993, the GPI-anchored human sperm head protein PH-20 (also termed sperm adhesion molecule 1, SPAM1), encoded by *PH-20*, was proven to exhibit hyaluronidase activity.[80] Expression of the *PH-20* gene is relatively specific for testis, although it was also proven in placenta, fetal tissue, some other tissues, and a few malignant tumors.[56, 61] However, the major physiological function of PH-20 is probably its role during fertilization, which is described in detail in a recent review article by Martin-DeLeon.[81] Two different forms of the enzyme were identified.[82] One variant, bound to the plasma membrane via the GPI anchor, has a molecular mass of 64 kDa and exhibits hyaluronidase activity at both neutral and acidic pH.[80, 82] A second form with a molecular mass of 53 kDa and activity only at acidic pH, is released during the acrosome reaction.[82] Hyaluronidase activity of PH-20 bound to the plasma membrane of the sperm enables degradation and penetration of the hyaluronan-rich cumulus extracellular matrix around the oocyte, whereas hyaluronidase released from the acrosome is responsible for hydrolysis of hyaluronan in the zona pellucida matrix.[25, 83] However, GPI-anchored hyaluronidase seems to fulfill a second function as a membrane receptor for hyaluronan, inducing sperm signaling.[83] PH-20 bound to the inner acrosome membrane may also be involved in second or tertiary binding of the sperm to the zona pellucida or its penetration.[83, 84] It should be noted that the well-known enzyme isolated

from bovine testis (BTH)[85] was proven to be nothing else than a soluble fragment of membrane-bound bovine PH-20 enzyme.[86]

Due to two deletions causing premature termination of transcription, *HYALP1* is a pseudogene in humans but the corresponding ortholog may encode an active protein in other species.[56]

1.2.3 Hyaluronan metabolism

Hyaluronan levels in the human body are regulated by a dynamic interplay of anabolic and catabolic processes. Approximately one third of the 15 g of hyaluronan present in the body of a 70 kg adult human is replaced every day.[61] However, the turnover rate strongly depends on the tissue. Whereas hyaluronan of the epidermis is reported to be replaced within 1–2 days[61] or even less than one day,[14] this process takes about 1–3 weeks in cartilage tissue.[61] By contrast, intravenously injected hyaluronan has a half-life of only 2.5–4.5 min, determined in rabbit.[87]

Three highly conserved isoforms of hyaluronan synthases (HAS1, HAS2, and HAS3), the enzymes of hyaluronan anabolism, have been identified in mammals up to now.[88-90] In contrast to other macromolecules, hyaluronan is not synthesized intracellularly, but extruded to the extracellular space by the transmembrane hyaluronan synthases, thus allowing for the extraordinarily high degree of polymerization.[89] HAS1 exhibits the lowest, HAS3 the highest activity of the three isoenzymes.[90] However, the different hyaluronan synthases differ not only in the rate of hyaluronan formation. Whereas recombinant murine HAS1 and HAS2 were reported to synthesize hyaluronan molecules of 0.2–2 MDa, the products of HAS3 reached molecular masses of only 0.1–1 MDa.[91] Extremely large hyaluronan of more than 2 MDa was observed in cell culture medium of stable transfectants, expressing the HAS2 protein.[91] Moreover, HAS2 is probably the major source of hyaluronan during embryogenesis, and knock-out mice showed early lethality owing to severe cardiac and vascular abnormalities.[92] Whereas HAS2 therefore seems to be important for the production of large amounts of high molecular weight hyaluronan during developmental processes and tissue growth, HAS1 might be responsible for maintenance of the required minimal level of hyaluronan.[90] Finally, the smaller products of HAS3 might fulfill distinct functions within the extracellular matrix or induce cellular effects via hyaluronan receptors and the corresponding signaling cascades.[90]

Human hyaluronidases, the catabolic enzymes of hyaluronan metabolism, were already discussed in Section 1.2.2. The detailed mechanisms of hyaluronan catabolism are still unknown. One hypothesis proposes a concerted, but successive action of the two major somatic hyaluronidases, Hyal-1 and Hyal-2.[55, 61] According to this model, hyaluronan might

be fixed by hyaluronan receptors (*cf*. Section 1.2.4) at the cell membrane (putatively CD44), degraded by membrane-bound Hyal-2 to fragments of about 20 kDa, subsequently internalized by endocytosis, delivered to endosomes, and finally completely degraded in lysosomes by the action of Hyal-1, β-glucuronidase, and β-*N*-acetylglucosaminidase.[55, 61] Thereby, enrichment of the initial hyaluronan–CD44–Hyal-2 complex in microdomains (caveolae), where degradation of hyaluronan by Hyal-2 might take place, is conceivable.[93] However, this hypothetical model remains unproven and other aspects, like the contribution of free radicals to the cleavage of hyaluronan into smaller fragments, also have to be considered under pathological conditions.[61, 93]

1.2.4 Hyaluronan receptors

Recognition of hyaluronan by cellular receptors is a prerequisite for the regulation of both, the proposed mechanism of hyaluronan metabolism and the putative size-dependent effects on cellular function. The best characterized examples of hyaluronan receptors are the lymphocyte homing receptor CD44[94, 95] and RHAMM, the receptor for hyaluronan-mediated motility.[96] The CD44 epitope is present on the membrane surface of most vertebrate cells, but is shared by a group of proteins of 80–200 kDa.[97] The enormous heterogeneity of these proteins, encoded by a highly conserved gene, is caused by alternative splicing as well as post-translational modifications.[97, 98] These modifications, which differ between cell types and cell states, influence hyaluronan binding and receptor function.[99] Apart from its role in internalization and degradation of hyaluronan (*cf*. Section 1.2.3), CD44 probably mediates cell–matrix communication by interaction with the cytoskeleton via the ERM protein family (ezrin, radixin, moesin, and merlin) or the ankyrin.[94, 100] Moreover, CD44 was reported to interact with tyrosin kinases and specific GTPases.[100]

Both hyaluronan receptors, CD44 and RHAMM/CD168, were reported to form complexes with ERK1,2 in invasive breast cancer cells.[101] Like CD44, RHAMM exists in different variants as a result of alternative splicing.[96, 102] Moreover, RHAMM is not only localized at the cell membrane, but can also be found intracellularly.[96] Intracellular RHAMM may be involved in processes of cytoskeleton assembly.[100] Moreover, the fast dynamic appearance of RHAMM at the cell membrane under certain conditions seems to require some kind of intracellular storage of the protein.[96] By contrast, the protein is permanently present on the surface of malignant cells, where it seems to be involved in invasion and metastasis.[96, 100, 103] Hall et al. suggested that binding of hyaluronan to RHAMM promotes cell locomotion by protein tyrosin kinase mediated signaling via rapid phosphorylation and dephosphorylation of focal adhesion kinase (FAK).[104] In parallel with this transient phosphorylation, assembly and disassembly of focal adhesions were detected, pivotal processes for cell locomotion.[104] Hence, it is not surprising that RHAMM is also proposed to be involved in endothelial cell migration, angiogenesis, and wound healing.[105]

Less intensively studied hyaluronan receptors are the lymph vessel endothelial hyaluronan receptor (LYVE-1),[106] the toll-like receptor 4 (TLR4),[107, 108] the hyaluronan receptor for endocytosis (HARE),[109] and layilin.[110, 111]

1.2.5 Effects of hyaluronan and its oligosaccharide fragments: a matter of size?

As discussed above (*cf*. Section 1.2.2 and Section 1.2.3), both hyaluronidases and hyaluronan synthases produce oligosaccharides and polysaccharides of different chain lengths. However, the biological effects of hyaluronan and hyaluronan oligosaccharides are believed to be strongly size-dependent.[112] In this work, hyaluronan oligosaccharides are designated according to the number of disaccharide moieties (n = *x*) as n_x (Figure 1.3).

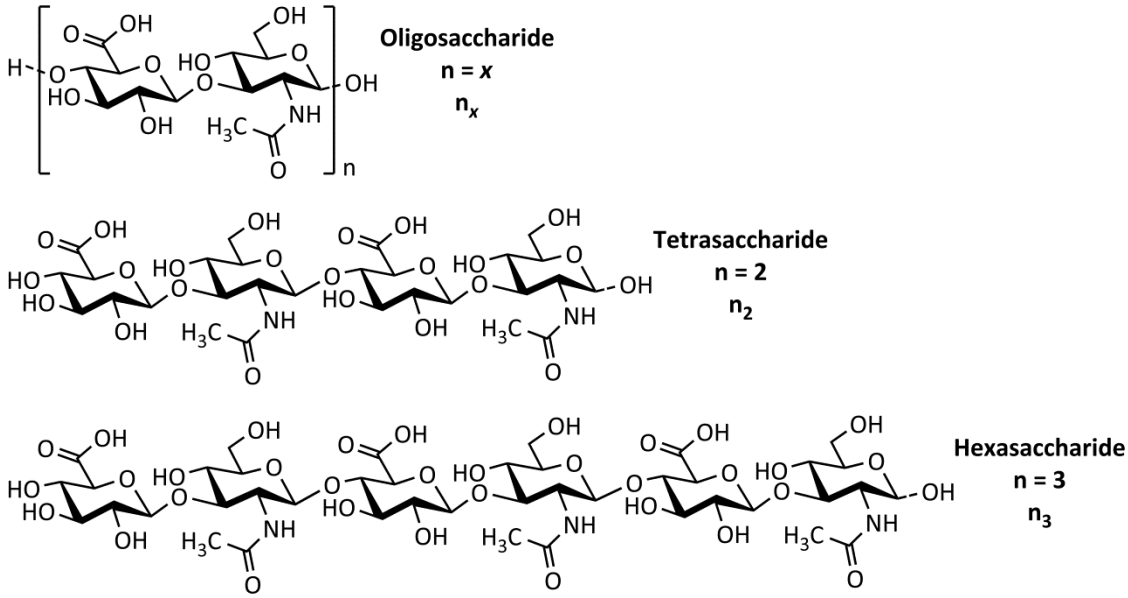

Figure 1.3: Oligosaccharides are designated as multiples of hyalobiuronic acid (disaccharide) as n_x (n = *x*), e. g. the tetrasaccharide (n = 2) as n_2 and the hexasaccharide (n = 3) as n_3.

Hyaluronan of an average molecular weight below approximately 500 kDa is often referred to as low molecular weight (LMW) hyaluronan.[112] This term is additionally used for poly-disperse mixtures containing a broad series of hyaluronan oligosaccharides with an average molecular weight of less than 10 kDa.

The proposed size-dependent physiological and pathophysiological functions are manifold. Hence, only examples can be discussed here. For a more detailed summary on this topic, see the review article by Asari.[112]

The role of hyaluronan and hyaluronan oligosaccharides in angiogenesis has been a matter of discussion since the 1980s. High molecular weight hyaluronan was described to be antiangiogenic,[113] whereas oligosaccharides were reported to induce angiogenesis.[114]

Differential effects on the proliferation of endothelial cells and the stability of cell layers were discussed.[115] Based on these results, hyaluronan and hyaluronan oligosaccharides are believed to modulate vascularization and wound healing, probably via the hyaluronan receptors CD44 and RHAMM.[102, 105, 116-120] Thereby, the involvement of size-dependent pro- and anti-inflammatory effects is also conceivable. High molecular weight hyaluronan was reported to inhibit the activation of NF-κB and the production of pro-inflammatory cytokines.[121, 122] By contrast, smaller fragments seem to act as pro-inflammatory stimuli via NF-κB activation and formation of cytokines, chemokines, and nitric oxide.[123-125] Toll-like receptor 4 (TLR4), identified as hyaluronan receptor, may also be involved in inflammatory processes.[107]

Moreover, the smallest oligosaccharides (n_2–n_9) might have unique effects, different from both low molecular weight as well as high molecular weight hyaluronan. The tetrasaccharide (n_2) was shown to induce heat shock protein 72 (Hsp72) and to suppress apoptosis under stress conditions.[126] By contrast, oligosaccharides of 3–9 disaccharide units (n_3–n_9) were reported to trigger apoptosis in cancer cells.[127] Thereby, these small oligosaccharides are thought to inhibit kinase activity, resulting from polyvalent binding of larger oligosaccharides and high molecular weight hyaluronan to cellular receptors, by competitive monovalent binding.[127, 128]

In view of these putative size-dependent effects, the importance of analytical methods for the determination of hyaluronan, hyaluronan oligosaccharides, and the enzymological particularities of the enzymes of hyaluronan metabolism (especially hyaluronidases) becomes obvious.

1.3 Analytical approaches to the study of hyaluronan, hyaluronan oligosaccharides, and hyaluronidases

1.3.1 Conventional methods

Meyer reviewed the hyaluronidase activity assays of his time and sorted them into biological, physicochemical, and chemical methods.[129] This classification was adopted for the conventional assays described below. Some of them, especially the biological assays, appear rather exotic and old-fashioned nowadays.

One typical biological assay, determines the spreading effect of hyaluronidase on co-administered dyes due to increased permeability of animal skin.[130] The method is based on the observation that extracts from mammalian testes contain a “spreading factor”,[131] which was made long before this “spreading factor” was identified as hyaluronidase.[132, 133]

Interestingly, comparable results were obtained from the spreading assay developed by Jaques in 1952[134] and physicochemical *in vitro* assays.[135] A second biological assay, measuring the degradation of the capsules of *Streptococci*,[136, 137] may also be considered obsolete.

The mucin clot prevention tests is an example of a physicochemical method.[129] In acidic solutions, hyaluronan and protein form fibrous clots, whereas flocculent or no precipitate is obtained after incubation with hyaluronidase, depending on the degree of digestion.[138-140] The spinnability method determines the destruction of the spinnability of dialyzed bovine synovial fluid by hyaluronidase, requiring a special apparatus for measurement of the length of the fiber which can be produced under defined conditions.[141] Both methods are unfavorable with regard to convenient and quantitative determination of hyaluronidase activity. Thus, they are no longer used today.

A conventional physicochemical method, which is still common for the measurement of hyaluronidase activity and for the estimation of the average molecular weight of hyaluronan, is viscosimetry. In 1940, Madinaveitia and Quibell published a method measuring the reduction of viscosity of extracts from vitreous humor by testicular extracts using an Ostwald viscosimeter.[142] Meyer describes this method as very accurate.[129] However, values for hyaluronidase activity determined by viscosimetry depend on the initial viscosity of the substrate solution, which is influenced by the average molecular weight of hyaluronan.[143] Nevertheless, due to the fast initial reduction of viscosity by mammalian hyaluronidases, the determination of hyaluronidase activity using an Ubbelohde viscosimeter was found to outperform the sensitivity of turbidimetry and colorimetry by a factor of 10.[33] For this reason, viscosimetry was recently used to determine the low activity of Hyal-2 in human platelets.[75] However, to obtain solutions with sufficient viscosity, hyaluronan must be present at relatively high concentrations. Moreover, viscosimetry is only applicable to high molecular weight hyaluronan of approximately 1500 disaccharide units and above. Determination of low molecular weight hyaluronan or hyaluronan oligosaccharides is not possible. Finally, the sensitivity of viscosimetry strongly depends on the type of hyaluronidase, as the decrease in viscosity per cleavage step is much more pronounced with the random mode of action observed for mammalian enzymes than for processive exolytic degradation by the bacterial hyaluronidases.[144]

The turbidimetric assay can be considered as a standard physicochemical assay for the determination of hyaluronidase activity and enzyme inhibition. This relatively old approach was first described by Kass and Seastone in 1944, who observed precipitation of high molecular mass hyaluronan (but not enzymatically digested material) after addition of acidified horse serum.[145] Subsequently, different modifications, using serum of other sources or purified protein fractions, were reported.[129, 146-150] With regard to the assay described by

Meyer,[129] saccharides of more than 6–8 kDa were reported to cause precipitation.[151] Today, quaternary ammonium salts with long lipophilic chains are preferably used instead of serum or serum proteins. Typical reagents are cetyltrimethylammonium bromide[152] or cetylpyridinium chloride.[153] In this work, a miniaturized version of the turbidimetric assay by Di Ferrante[152] is used.

The reducing ends resulting from the cleavage of the carbohydrate polymer by hyaluronidase activity were often determined using conventional chemical assays for reducing sugars.[129, 151] However, a more specific approach is the determination of the *N*-acetyl-D-glucosamine moiety at the reducing end. In 1933, Elson and Morgan described the colorimetric determination of glucosamine and chondrosamine (galactosamine) using an acidic solution of *p*-dimethylaminobenzaldehyde (Ehrlich's reagent).[154] One year later, the authors reported on a modification of this assay with regard to the corresponding *N*-acetylated hexosamines.[155] With regard to this article, the method is commonly referred to as "Morgan-Elson reaction" or "Morgan-Elson assay". Reissig et al., further optimized the assay.[156] This modified version, basically, is the one which is still frequently used today. Additional alterations of the protocol were described later, especially aiming at determination of hyaluronidase activity in serum or plasma.[157, 158] More recent modifications additionally considered the turbidity component of the extinction caused by protein in the samples[159] or used sensitive fluorescence measurement alternatively.[160]

For quantification of hyaluronan and hyaluronan oligosaccharides with regard to the uronic acid content, the carbazole assay can be used.[161, 162] If the respective amount of reducing *N*-acetyl-D-glucosamine ends is known (e. g. from Morgan-Elson reaction), the average chain length can also be calculated by combination of data from both assays. However, no information on size distribution is obtained by all chemical assays.

1.3.2 Chromatographic methods

Chromatographic techniques were already used in the very early days of hyaluronan research. In their first report on the chemical structure of hyaluronan, Weissmann et al. described paper chromatography and ion exchange chromatography of hyaluronan oligosaccharides for both preparative and analytical purposes.[3]

Although still used, planar chromatography is less popular with regard to the analysis of hyaluronan oligosaccharides today. Only a few articles describe thin layer chromatography (TLC) on silica plates with post-chromatographic derivatization[163-166] or, more recently, coupling to time-of-flight mass spectrometry (TOF-MS) using matrix assisted laser desorption ionization (MALDI).[164]

Liquid chromatography of hyaluronan oligosaccharides is mainly based on ion exchange, using silica-based (in part polymer-coated) amine columns[34, 42, 144, 167, 168] or different polymer-based anion exchange resins as stationary phases.[168-171] Detection of the analytes can be achieved by far-UV absorbance[34, 42, 144, 167, 168, 172] or pulsed amperometric detection (PAD).[169-171] Gel permeation chromatography (size exclusion chromatography) is often used for preparation of purified hyaluronan oligosaccharides.[35, 42, 114, 168, 170-172] Nevertheless, gel permeation chromatography was also applied to kinetic studies on hyaluronan degradation by hyaluronidase.[173] A different approach, using reversed-phase ion pair HPLC, was chosen by Cramer and Bailey for studies on BTH and its products.[36, 174]

1.3.3 Electrophoretic methods

Electrophoretic methods for the analysis of hyaluronan can be grouped into gel electrophoretic and capillary electrophoretic methods.

The degradation of hyaluronan by Hyal-2, resulting in products of a molecular weight of approximately 20 kDa, was often studied by agarose gel electrophoresis.[72, 175, 176] Oligosaccharides were thereby visualized with Stains-All, giving diffuse bands due to the polydispersity of analytes.[72, 175, 176] A higher resolution can be obtained by polyacrylamide gel electrophoresis (PAGE).[75, 114, 177, 178] West et al. used radioactive oligosaccharides.[114] The more recent protocols applied a combined alcian blue/silver staining.[75, 177, 178] Depending on the gel size and the exact protocol, oligosaccharides of 8–100 (n_8–n_{100})[177] or 5–50 (n_5–n_{50})[178] disaccharide units, respectively, gave distinct bands. Hence, gel electrophoresis is extremely valuable for medium-sized oligosaccharides of more than approximately 25 disaccharide moieties, as almost every other method is insufficient with regard to this size range. A variant of gel electrophoresis of hyaluronan oligosaccharides is fluorophore-assisted carbohydrate electrophoresis, showing excellent sensitivity but requiring fluorescent-labeled analytes.[179-181]

Gels can also be used to fill capillaries for capillary gel electrophoresis. This method is rarely applied to hyaluronan analysis.[182, 183] In most cases, capillary zone electrophoresis (CZE) with UV detection is used. Some of the first applications of CZE to the analysis of hyaluronan were reported by Grimshaw et al., who analyzed the hyaluronan content of vitreous humor[184] and synovial fluid.[185] They also used CZE for the determination of oligosaccharides derived from various glycosaminoglycans.[186] Pattanaargson et al. applied CZE to the measurement of hyaluronidase activity in animal venoms.[187] Subsequently, many authors described CZE for analysis of hyaluronan samples or the characterization of hyaluronidases.[32, 35, 188-190] However, UV detection is not ideal for hyaluronan oligosaccharides. Hence, MS is an interesting alternative, which was already applied successfully.[191]

1.3.4 Other methods

As described above, mass spectrometry is very frequently used after preparative purification or analytical separation of oligosaccharides (off-line or on-line).[40, 42, 164, 167, 168, 170-172, 191] Apart from analysis of the steric structure of hyaluronan (*cf*. Section 1.1.1),[9, 10] nuclear magnetic resonance (NMR) spectroscopy was also reported in the context of oligosaccharides from enzymatic[34, 144, 192] or (preparative) chemical[192] cleavage. Although comprising a separation by gel electrophoresis, zymography cannot clearly be termed an electrophoretic method, as the determination of hyaluronidase activity is based on the digestion of hyaluronan in the substrate-containing gel.[193-195] A completely different approach to the determination of hyaluronidase activity is the ELISA-like assay developed by Stern and coworkers.[196-198] Although the list presented here is not exhaustive, most methods except for electrophoresis and chromatography do not provide information on the size-distribution of the substrates and products of hyaluronidases. Especially for small oligosaccharides, powerful, sensitive, and specific analytical approaches for many scientific problems concerning hyaluronan and hyaluronidases are still lacking.

1.4 References

1. Meyer, K.; Palmer, J. W. The polysaccharide of the vitreous humor. *J. Biol. Chem.* **1934,** 107, 629-634.

2. Hascall, V. C.; Laurent, T. C. Hyaluronan: structure and physical properties. *Glycoforum* **1997**. (http://glycoforum.gr.jp/science/hyaluronan/HA01/HA01E.html)

3. Weissmann, B.; Meyer, K.; Sampson, P.; Linker, A. Isolation of oligosaccharides enzymatically produced from hyaluronic acid. *J. Biol. Chem.* **1954,** 208, 417-429.

4. Toole, B. P. Hyaluronan in morphogenesis and tissue remodeling. *Glycoforum* **1998**. (http://glycoforum.gr.jp/science/hyaluronan/HA08/HA08E.html)

5. Laurent, T. C.; Fraser, J. R. Hyaluronan. *FASEB J.* **1992,** 6, 2397-2404.

6. Taylor, K. R.; Gallo, R. L. Glycosaminoglycans and their proteoglycans: host-associated molecular patterns for initiation and modulation of inflammation. *FASEB J.* **2006,** 20, 9-22.

7. Scott, J. E. Secondary and tertiary structures of hyaluronan in aqueous solution. Some biological consequences. *Glycoforum* **1998**. (http://glycoforum.gr.jp/science/hyaluronan/HA02/HA02E.html)

8. Scott, J. E. Supramolecular organization of extracellular matrix glycosaminoglycans, *in vitro* and in the tissues. *FASEB J.* **1992,** 6, 2639-2645.

9. Scott, J. E.; Heatley, F. Biological properties of hyaluronan in aqueous solution are controlled and sequestered by reversible tertiary structures, defined by NMR spectroscopy. *Biomacromolecules* **2002,** 3, 547-553.

10. Almond, A.; DeAngelis, P. L.; Blundell, C. D. Hyaluronan: the local solution conformation determined by NMR and computer modeling is close to a contracted left-handed 4-fold helix. *J. Mol. Biol.* **2006,** 358, 1256-1269.

11. Almond, A. Hyaluronan. *Cell. Mol. Life Sci.* **2007,** 64, 1591-1596.

12. Yaffe, N. R.; Almond, A.; Blanch, E. W. A new route to carbohydrate secondary and tertiary structure using Raman spectroscopy and Raman optical activity. *J. Am. Chem. Soc.* **2010,** 132, 10654-10655.

13. Cowman, M. K.; Matsuoka, S. Experimental approaches to hyaluronan structure. *Carbohydr. Res.* **2005,** 340, 791-809.

14. Tammi, R.; Tammi, M. Hyaluronan in the epidermis. *Glycoforum* **1998**. (http://glycoforum.gr.jp/science/hyaluronan/HA04/HA04E.html)

15. Hardingham, T. E. Cartilage: Aggrecan-link protein-hyaluronan aggregates. *Glycoforum* **1998**. (http://glycoforum.gr.jp/science/hyaluronan/HA05/HA05E.html)

16. Meyer, K.; Smyth, E. M.; Dawson, M. H. The isolation of a mucopolysaccaride from synovial fluid. *J. Biol. Chem.* **1939,** 128, 319-327.

17. Sundblad, L. The chemistry of synovial fluid with special regard to hyaluronic acid. *Acta Orthop. Scand.* **1950,** 20, 105-113.

18. Sundblad, L. Determination of anomalous viscosity in pathological joint fluids. *Scand. J. Clin. Lab. Invest.* **1954,** 6, 288-294.

19. Balazs, E. A.; Watson, D.; Duff, I. F.; Roseman, S. Hyaluronic acid in synovial fluid. I. Molecular parameters of hyaluronic acid in normal and arthritic human fluids. *Arthritis Rheum.* **1967,** 10, 357-376.

20. Dahl, L. B.; Dahl, I. M.; Engstrom-Laurent, A.; Granath, K. Concentration and molecular weight of sodium hyaluronate in synovial fluid from patients with rheumatoid arthritis and other arthropathies. *Ann. Rheum. Dis.* **1985,** 44, 817-822.

21. Dunn, S.; Kolomytkin, O. V.; Marino, A. A. Pathophysiology of osteoarthritis: evidence against the viscoelastic theory. *Pathobiology* **2009,** 76, 322-328.

22. Ragan, C.; Meyer, K. The hyaluronic acid of synovial fluid in rheumatoid arthritis. *J. Clin. Invest.* **1949,** 28, 56-59.

23. Stafford, C. T.; Niedermeier, W.; Holley, H. L.; Pigman, W. Studies on the concentration and intrinsic viscosity of hyaluronic acid in synovial fluids of patients with rheumatic diseases. *Ann. Rheum. Dis.* **1964,** 23, 152-157.

24. Asari, A.; Miyauchi, S. Medical application of hyaluronan. *Glycoforum* **2000**. (http://glycoforum.gr.jp/science/hyaluronan/HA13/HA13E.html)

25. Salustri, A.; Fulop, C. Role of hyaluronan during ovulation and fertilization. *Glycoforum* **1998**. (http://glycoforum.gr.jp/science/hyaluronan/HA03/HA03E.html)

26. De Plater, G.; Martin, R. L.; Milburn, P. J. A pharmacological and biochemical investigation of the venom from the platypus (*Ornithorhynchus anatinus*). *Toxicon* **1995,** 33, 157-169.

27. Grey, C.; Edebrink, P.; Krook, M.; Jacobsson, S. P. Development of a high performance anion exchange chromatography analysis for mapping of oligosaccharides. *J. Chromatogr. B Analyt. Technol. Biomed. Life Sci.* **2009,** 877, 1827-1832.

28. Frost, G. I.; Csóka, A. B.; Stern, R. The hyaluronidases: a chemical, biological and clinical overview. *Trends Glycosci. Glycotechnol.* **1996,** 8, 419-434.

29. Nagaraju, S.; Devaraja, S.; Kemparaju, K. Purification and properties of hyaluronidase from *Hippasa partita* (funnel web spider) venom gland extract. *Toxicon* **2007,** 50, 383-393.

30. Meyer, K. Hyaluronidases. In: *The Enzymes*, Boyer, P. D. (Ed.). Academic Press: New York, **1971**, Vol. 3, pp 307-320.

31. Stern, R.; Csóka, A. B. Mammalian hyaluronidases. *Glycoforum* **2000**. (http://glycoforum.gr.jp/science/hyaluronan/HA15/HA15E.html)

32. Hofinger, E. S. A.; Hoechstetter, J.; Oettl, M.; Bernhardt, G.; Buschauer, A. Isoenzyme-specific differences in the degradation of hyaluronic acid by mammalian-type hyaluronidases. *Glycoconj. J.* **2008,** 25, 101-109.

33. Hofinger, E. S. A. Recombinant expression, purification and characterization of human hyaluronidases. PhD thesis, University of Regensburg, Regensburg, **2007**.

34. Sugahara, K.; Yamada, S.; Sugiura, M.; Takeda, K.; Yuen, R.; Khoo, H. E.; Poh, C. H. Identification of the reaction products of the purified hyaluronidase from stonefish (*Synanceja horrida*) venom. *Biochem. J.* **1992,** 283, 99-104.

35. Hofinger, E. S. A.; Bernhardt, G.; Buschauer, A. Kinetics of Hyal-1 and PH-20 hyaluronidases: comparison of minimal substrates and analysis of the transglycosylation reaction. *Glycobiology* **2007,** 17, 963-971.

36. Cramer, J. A.; Bailey, L. C.; Bailey, C. A.; Miller, R. T. Kinetic and mechanistic studies with bovine testicular hyaluronidase. *Biochim. Biophys. Acta* **1994,** 1200, 315-321.

37. Highsmith, S.; Garvin, J. H., Jr.; Chipman, D. M. Mechanism of action of bovine testicular hyaluronidase. Mapping of the active site. *J. Biol. Chem.* **1975,** 250, 7473-7480.

38. Nakatani, H. Monte Carlo simulation of hyaluronidase reaction involving hydrolysis, transglycosylation and condensation. *Biochem. J.* **2002,** 365, 701-705.

39. Saitoh, H.; Takagaki, K.; Majima, M.; Nakamura, T.; Matsuki, A.; Kasai, M.; Narita, H.; Endo, M. Enzymic reconstruction of glycosaminoglycan oligosaccharide chains using the transglycosylation reaction of bovine testicular hyaluronidase. *J. Biol. Chem.* **1995,** 270, 3741-3747.

40. Takagaki, K.; Nakamura, T.; Izumi, J.; Saitoh, H.; Endo, M.; Kojima, K.; Kato, I.; Majima, M. Characterization of hydrolysis and transglycosylation by testicular hyaluronidase using ion-spray mass spectrometry. *Biochemistry* **1994,** 33, 6503-6507.

41. Weissmann, B. The transglycosylative action of testicular hyaluronidase. *J. Biol. Chem.* **1955,** 216, 783-794.

42. Kakizaki, I.; Ibori, N.; Kojima, K.; Yamaguchi, M.; Endo, M. Mechanism for the hydrolysis of hyaluronan oligosaccharides by bovine testicular hyaluronidase. *FEBS J.* **2010,** 277, 1776-1786.

43. Yuki, H.; Fishman, W. H. Purification and characterization of leech hyaluronic acid-endo-β-glucuronidase. *J. Biol. Chem.* **1963,** 238, 1877-1879.

44. Hotez, P.; Cappello, M.; Hawdon, J.; Beckers, C.; Sakanari, J. Hyaluronidases of the gastrointestinal invasive nematodes *Ancylostoma caninum* and *Anisakis simplex*: possible functions in the pathogenesis of human zoonoses. *J. Infect. Dis.* **1994,** 170, 918-926.

45. Suzuki, S. Microbial hyaluronan lyases. *Glycoforum* **2000**. (http://glycoforum.gr.jp/science/hyaluronan/HA14/HA14E.html)

46. Baker, J. R.; Pritchard, D. G. Action pattern and substrate specificity of the hyaluronan lyase from group B streptococci. *Biochem. J.* **2000,** 348 Pt 2, 465-471.

47. Jedrzejas, M. J. Three-dimensional structures of hyaluronate lyases from *Streptococcus* species and their mechanism of hyaluronan degradation. *Glycoforum* **2002**. (http://glycoforum.gr.jp/science/hyaluronan/HA24/HA24E.html)

48. Li, S.; Jedrzejas, M. J. Hyaluronan binding and degradation by *Streptococcus agalactiae* hyaluronate lyase. *J. Biol. Chem.* **2001,** 276, 41407-41416.

49. Mello, L. V.; De Groot, B. L.; Li, S.; Jedrzejas, M. J. Structure and flexibility of *Streptococcus agalactiae* hyaluronate lyase complex with its substrate. Insights into the mechanism of processive degradation of hyaluronan. *J. Biol. Chem.* **2002,** 277, 36678-36688.

50. Pritchard, D. G.; Lin, B.; Willingham, T. R.; Baker, J. R. Characterization of the group B streptococcal hyaluronate lyase. *Arch. Biochem. Biophys.* **1994,** 315, 431-437.

51. Pritchard, D. G.; Trent, J. O.; Li, X.; Zhang, P.; Egan, M. L.; Baker, J. R. Characterization of the active site of group B streptococcal hyaluronan lyase. *Proteins* **2000,** 40, 126-134.

52. Hynes, W. L.; Walton, S. L. Hyaluronidases of Gram-positive bacteria. *FEMS Microbiol. Lett.* **2000,** 183, 201-207.

53. Hirayama, Y.; Yoshimura, M.; Ozeki, Y.; Sugawara, I.; Udagawa, T.; Mizuno, S.; Itano, N.; Kimata, K.; Tamaru, A.; Ogura, H.; Kobayashi, K.; Matsumoto, S. Mycobacteria exploit host hyaluronan for efficient extracellular replication. *PLoS Pathog.* **2009,** 5, e1000643.

54. Botzki, A.; Rigden, D. J.; Braun, S.; Nukui, M.; Salmen, S.; Hoechstetter, J.; Bernhardt, G.; Dove, S.; Jedrzejas, M. J.; Buschauer, A. L-Ascorbic acid 6-hexadecanoate, a potent hyaluronidase inhibitor. X-ray structure and molecular modeling of enzyme-inhibitor complexes. *J. Biol. Chem.* **2004,** 279, 45990-45997.

55. Csóka, A. B.; Frost, G. I.; Stern, R. The six hyaluronidase-like genes in the human and mouse genomes. *Matrix Biol.* **2001,** 20, 499-508.

56. Csóka, A. B.; Scherer, S. W.; Stern, R. Expression analysis of six paralogous human hyaluronidase genes clustered on chromosomes 3p21 and 7q31. *Genomics* **1999,** 60, 356-361.

57. Frost, G. I.; Csóka, A. B.; Wong, T.; Stern, R. Purification, cloning, and expression of human plasma hyaluronidase. *Biochem. Biophys. Res. Commun.* **1997,** 236, 10-15.

58. Gold, E. W. Purification and properties of hyaluronidase from human liver. Differences from and similarities to the testicular enzyme. *Biochem. J.* **1982,** 205, 69-74.

59. Afify, A. M.; Stern, M.; Guntenhöner, M.; Stern, R. Purification and characterization of human serum hyaluronidase. *Arch. Biochem. Biophys.* **1993,** 305, 434-441.

60. Csóka, A. B.; Frost, G. I.; Wong, T.; Stern, R. Purification and microsequencing of hyaluronidase isozymes from human urine. *FEBS Lett.* **1997,** 417, 307-310.

61. Stern, R. Devising a pathway for hyaluronan catabolism: are we there yet? *Glycobiology* **2003,** 13, 105R-115R.

62. Csóka, A. B.; Frost, G. I.; Heng, H. H.; Scherer, S. W.; Mohapatra, G.; Stern, R. The hyaluronidase gene *HYAL1* maps to chromosome 3p21.2-p21.3 in human and 9F1-F2 in mouse, a conserved candidate tumor suppressor locus. *Genomics* **1998,** 48, 63-70.

63. Frost, G. I.; Mohapatra, G.; Wong, T. M.; Csóka, A. B.; Gray, J. W.; Stern, R. *HYAL1*$^{LUCA-1}$, a candidate tumor suppressor gene on chromosome 3p21.3, is inactivated in head and neck squamous cell carcinomas by aberrant splicing of pre-mRNA. *Oncogene* **2000,** 19, 870-877.

64. Tan, J. X.; Wang, X. Y.; Li, H. Y.; Su, X. L.; Wang, L.; Ran, L.; Zheng, K.; Ren, G. S. HYAL1 overexpression is correlated with the malignant behavior of human breast cancer. *Int. J. Cancer* **2011,** 128, 1303-1315.

65. Tan, J. X.; Wang, X. Y.; Su, X. L.; Li, H. Y.; Shi, Y.; Wang, L.; Ren, G. S. Upregulation of HYAL1 expression in breast cancer promoted tumor cell proliferation, migration, invasion and angiogenesis. *PLoS One* **2011,** 6, e22836.

66. Lokeshwar, V. B.; Cerwinka, W. H.; Lokeshwar, B. L. HYAL1 hyaluronidase: a molecular determinant of bladder tumor growth and invasion. *Cancer Res.* **2005,** 65, 2243-2250.

67. Lokeshwar, V. B.; Rubinowicz, D.; Schroeder, G. L.; Forgacs, E.; Minna, J. D.; Block, N. L.; Nadji, M.; Lokeshwar, B. L. Stromal and epithelial expression of tumor markers hyaluronic acid and HYAL1 hyaluronidase in prostate cancer. *J. Biol. Chem.* **2001,** 276, 11922-11932.

68. Lokeshwar, V. B.; Cerwinka, W. H.; Isoyama, T.; Lokeshwar, B. L. HYAL1 hyaluronidase in prostate cancer: a tumor promoter and suppressor. *Cancer Res.* **2005,** 65, 7782-7789.

69. Natowicz, M. R.; Short, M. P.; Wang, Y.; Dickersin, G. R.; Gebhardt, M. C.; Rosenthal, D. I.; Sims, K. B.; Rosenberg, A. E. Clinical and biochemical manifestations of hyaluronidase deficiency. *N. Engl. J. Med.* **1996,** 335, 1029-1033.

70. Triggs-Raine, B.; Salo, T. J.; Zhang, H.; Wicklow, B. A.; Natowicz, M. R. Mutations in *HYAL1*, a member of a tandemly distributed multigene family encoding disparate hyaluronidase activities, cause a newly described lysosomal disorder, mucopolysaccharidosis IX. *Proc. Natl. Acad. Sci. U. S. A.* **1999,** 96, 6296-6300.

71. Jadin, L.; Wu, X.; Ding, H.; Frost, G. I.; Onclinx, C.; Triggs-Raine, B.; Flamion, B. Skeletal and hematological anomalies in HYAL2-deficient mice: a second type of mucopolysaccharidosis IX? *FASEB J.* **2008,** 22, 4316-4326.

72. Lepperdinger, G.; Strobl, B.; Kreil, G. *HYAL2*, a human gene expressed in many cells, encodes a lysosomal hyaluronidase with a novel type of specificity. *J. Biol. Chem.* **1998,** 273, 22466-22470.

73. Lepperdinger, G.; Müllegger, J.; Kreil, G. Hyal2 – less active, but more versatile? *Matrix Biol.* **2001,** 20, 509-514.

74. de la Motte, C.; Nigro, J.; Vasanji, A.; Rho, H.; Kessler, S.; Bandyopadhyay, S.; Danese, S.; Fiocchi, C.; Stern, R. Platelet-derived hyaluronidase 2 cleaves hyaluronan into fragments that trigger monocyte-mediated production of proinflammatory cytokines. *Am. J. Pathol.* **2009,** 174, 2254-2264.

75. Hamberger, J. Characterization of mammalian hyaluronidase-2 activity and identification of inhibitors of *Streptococcal* hyaluronan lyase. PhD thesis, University of Regensburg, Regensburg, **2012**.

76. Novak, U.; Stylli, S. S.; Kaye, A. H.; Lepperdinger, G. Hyaluronidase-2 overexpression accelerates intracerebral but not subcutaneous tumor formation of murine astrocytoma cells. *Cancer Res.* **1999,** 59, 6246-6250.

77. Chang, N. S. Transforming growth factor-β1 blocks the enhancement of tumor necrosis factor cytotoxicity by hyaluronidase Hyal-2 in L929 fibroblasts. *BMC Cell Biol.* **2002,** 3, 8.

78. Reese, K. L.; Aravindan, R. G.; Griffiths, G. S.; Shao, M.; Wang, Y.; Galileo, D. S.; Atmuri, V.; Triggs-Raine, B. L.; Martin-Deleon, P. A. Acidic hyaluronidase activity is present in mouse sperm and is reduced in the absence of SPAM1: evidence for a role for hyaluronidase 3 in mouse and human sperm. *Mol. Reprod. Dev.* **2010,** 77, 759-772.

79. Kaneiwa, T.; Mizumoto, S.; Sugahara, K.; Yamada, S. Identification of human hyaluronidase-4 as a novel chondroitin sulfate hydrolase that preferentially cleaves the galactosaminidic linkage in the trisulfated tetrasaccharide sequence. *Glycobiology* **2010,** 20, 300-309.

80. Gmachl, M.; Sagan, S.; Ketter, S.; Kreil, G. The human sperm protein PH-20 has hyaluronidase activity. *FEBS Lett.* **1993,** 336, 545-548.

81. Martin-DeLeon, P. A. Germ-cell hyaluronidases: their roles in sperm function. *Int. J. Androl.* **2011,** 34, e306-318.

82. Sabeur, K.; Cherr, G. N.; Yudin, A. I.; Primakoff, P.; Li, M. W.; Overstreet, J. W. The PH-20 protein in human spermatozoa. *J. Androl.* **1997,** 18, 151-158.

83. Cherr, G. N.; Yudin, A. I.; Overstreet, J. W. The dual functions of GPI-anchored PH-20: hyaluronidase and intracellular signaling. *Matrix Biol.* **2001,** 20, 515-525.

84. Yudin, A. I.; Vandevoort, C. A.; Li, M. W.; Overstreet, J. W. PH-20 but not acrosin is involved in sperm penetration of the macaque zona pellucida. *Mol. Reprod. Dev.* **1999,** 53, 350-362.

85. Freeman, M. E.; Anderson, P.; Oberg, M.; Dorfman, A. Preparation of purified hyaluronidase from bovine testis. *J. Biol. Chem.* **1949,** 180, 655-662.

86. Meyer, M. F.; Kreil, G.; Aschauer, H. The soluble hyaluronidase from bull testes is a fragment of the membrane-bound PH-20 enzyme. *FEBS Lett.* **1997,** 413, 385-388.

87. Fraser, J. R.; Laurent, T. C.; Pertoft, H.; Baxter, E. Plasma clearance, tissue distribution and metabolism of hyaluronic acid injected intravenously in the rabbit. *Biochem. J.* **1981,** 200, 415-424.

88. Weigel, P. H.; DeAngelis, P. L. Hyaluronan synthases: a decade-plus of novel glycosyltransferases. *J. Biol. Chem.* **2007,** 282, 36777-36781.

89. Weigel, P. H.; Hascall, V. C.; Tammi, M. Hyaluronan synthases. *J. Biol. Chem.* **1997,** 272, 13997-14000.

90. Spicer, A. P.; McDonald, J. A. Eucaryotic hyaluronan synthases. *Glycoforum* **1998**. (http://glycoforum.gr.jp/science/hyaluronan/HA07/HA07E.html)

91. Itano, N.; Sawai, T.; Yoshida, M.; Lenas, P.; Yamada, Y.; Imagawa, M.; Shinomura, T.; Hamaguchi, M.; Yoshida, Y.; Ohnuki, Y.; Miyauchi, S.; Spicer, A. P.; McDonald, J. A.; Kimata, K. Three isoforms of mammalian hyaluronan synthases have distinct enzymatic properties. *J. Biol. Chem.* **1999,** 274, 25085-25092.

92. Camenisch, T. D.; Spicer, A. P.; Brehm-Gibson, T.; Biesterfeldt, J.; Augustine, M. L.; Calabro, A., Jr.; Kubalak, S.; Klewer, S. E.; McDonald, J. A. Disruption of hyaluronan synthase-2 abrogates normal cardiac morphogenesis and hyaluronan-mediated transformation of epithelium to mesenchyme. *J. Clin. Invest.* **2000,** 106, 349-360.

93. Stern, R.; Csóka, A. B. Update on the mammalian hyaluronidases. *Glycoforum* **2004**. (http://www.glycoforum.gr.jp/science/hyaluronan/HA15a/HA15aE.html)

94. Knudson, W.; Knudson, C. B. The hyaluronan receptor, CD44. *Glycoforum* **1999**. (http://glycoforum.gr.jp/science/hyaluronan/HA10/HA10E.html)

95. Knudson, W.; Knudson, C. B. The hyaluronan receptor, CD44 -update-. *Glycoforum* **2005**. (http://glycoforum.gr.jp/science/hyaluronan/HA10a/HA10aE.html)

96. Turley, E. A.; Harrison, R. RHAMM, a member of the hyaladherins. *Glycoforum* **1999**. (http://glycoforum.gr.jp/science/hyaluronan/HA11/HA11E.html)

97. Ponta, H.; Sherman, L.; Herrlich, P. A. CD44: from adhesion molecules to signalling regulators. *Nat. Rev. Mol. Cell Biol.* **2003,** 4, 33-45.

98. Screaton, G. R.; Bell, M. V.; Jackson, D. G.; Cornelis, F. B.; Gerth, U.; Bell, J. I. Genomic structure of DNA encoding the lymphocyte homing receptor CD44 reveals at least 12 alternatively spliced exons. *Proc. Natl. Acad. Sci. U. S. A.* **1992,** 89, 12160-12164.

99. Lesley, J.; Hyman, R.; English, N.; Catterall, J. B.; Turner, G. A. CD44 in inflammation and metastasis. *Glycoconj. J.* **1997,** 14, 611-622.

100. Turley, E. A.; Noble, P. W.; Bourguignon, L. Y. Signaling properties of hyaluronan receptors. *J. Biol. Chem.* **2002,** 277, 4589-4592.

101. Hamilton, S. R.; Fard, S. F.; Paiwand, F. F.; Tolg, C.; Veiseh, M.; Wang, C.; McCarthy, J. B.; Bissell, M. J.; Koropatnick, J.; Turley, E. A. The hyaluronan receptors CD44 and Rhamm (CD168) form complexes with ERK1,2 that sustain high basal motility in breast cancer cells. *J. Biol. Chem.* **2007,** 282, 16667-16680.

102. Slevin, M.; Krupinski, J.; Gaffney, J.; Matou, S.; West, D.; Delisser, H.; Savani, R. C.; Kumar, S. Hyaluronan-mediated angiogenesis in vascular disease: uncovering RHAMM and CD44 receptor signaling pathways. *Matrix Biol.* **2007,** 26, 58-68.

103. Turley, E. A.; Belch, A. J.; Poppema, S.; Pilarski, L. M. Expression and function of a receptor for hyaluronan-mediated motility on normal and malignant B lymphocytes. *Blood* **1993,** 81, 446-453.

104. Hall, C. L.; Wang, C.; Lange, L. A.; Turley, E. A. Hyaluronan and the hyaluronan receptor RHAMM promote focal adhesion turnover and transient tyrosine kinase activity. *J. Cell Biol.* **1994,** 126, 575-588.

105. Gao, F.; Yang, C. X.; Mo, W.; Liu, Y. W.; He, Y. Q. Hyaluronan oligosaccharides are potential stimulators to angiogenesis via RHAMM mediated signal pathway in wound healing. *Clin. Invest. Med.* **2008,** 31, E106-116.

106. Jackson, D. G. The lymphatic endothelial hyaluronan receptor LYVE-1. *Glycoforum* **2004**. (http://glycoforum.gr.jp/science/hyaluronan/HA28/HA28E.html)

107. Termeer, C.; Benedix, F.; Sleeman, J.; Fieber, C.; Voith, U.; Ahrens, T.; Miyake, K.; Freudenberg, M.; Galanos, C.; Simon, J. C. Oligosaccharides of hyaluronan activate dendritic cells via toll-like receptor 4. *J. Exp. Med.* **2002,** 195, 99-111.

108. Taylor, K. R.; Trowbridge, J. M.; Rudisill, J. A.; Termeer, C. C.; Simon, J. C.; Gallo, R. L. Hyaluronan fragments stimulate endothelial recognition of injury through TLR4. *J. Biol. Chem.* **2004,** 279, 17079-17084.

109. Zhou, B.; Weigel, J. A.; Fauss, L.; Weigel, P. H. Identification of the hyaluronan receptor for endocytosis (HARE). *J. Biol. Chem.* **2000,** 275, 37733-37741.

110. Bono, P.; Cordero, E.; Johnson, K.; Borowsky, M.; Ramesh, V.; Jacks, T.; Hynes, R. O. Layilin, a cell surface hyaluronan receptor, interacts with merlin and radixin. *Exp. Cell Res.* **2005,** 308, 177-187.

111. Bono, P.; Rubin, K.; Higgins, J. M.; Hynes, R. O. Layilin, a novel integral membrane protein, is a hyaluronan receptor. *Mol. Biol. Cell* **2001,** 12, 891-900.

112. Asari, A. Novel functions of hyaluronan oligosaccharides. *Glycoforum* **2005**. (http://www.glycoforum.gr.jp/science/hyaluronan/HA12a/HA12aE.html)

113. Feinberg, R. N.; Beebe, D. C. Hyaluronate in vasculogenesis. *Science* **1983,** 220, 1177-1179.

114. West, D. C.; Hampson, I. N.; Arnold, F.; Kumar, S. Angiogenesis induced by degradation products of hyaluronic acid. *Science* **1985,** 228, 1324-1326.

115. West, D. C.; Kumar, S. The effect of hyaluronate and its oligosaccharides on endothelial cell proliferation and monolayer integrity. *Exp. Cell Res.* **1989,** 183, 179-196.

116. Cao, G.; Savani, R. C.; Fehrenbach, M.; Lyons, C.; Zhang, L.; Coukos, G.; Delisser, H. M. Involvement of endothelial CD44 during *in vivo* angiogenesis. *Am. J. Pathol.* **2006,** 169, 325-336.

117. Matou-Nasri, S.; Gaffney, J.; Kumar, S.; Slevin, M. Oligosaccharides of hyaluronan induce angiogenesis through distinct CD44 and RHAMM-mediated signalling pathways involving Cdc2 and γ-adducin. *Int. J. Oncol.* **2009,** 35, 761-773.

118. Savani, R. C.; Cao, G.; Pooler, P. M.; Zaman, A.; Zhou, Z.; DeLisser, H. M. Differential involvement of the hyaluronan (HA) receptors CD44 and receptor for HA-mediated motility in endothelial cell function and angiogenesis. *J. Biol. Chem.* **2001,** 276, 36770-36778.

119. Gao, F.; Liu, Y.; He, Y.; Yang, C.; Wang, Y.; Shi, X.; Wei, G. Hyaluronan oligosaccharides promote excisional wound healing through enhanced angiogenesis. *Matrix Biol.* **2010,** 29, 107-116.

120. Noble, P. W. Hyaluronan and its catabolic products in tissue injury and repair. *Matrix Biol.* **2002,** 21, 25-29.

121. Nakamura, K.; Yokohama, S.; Yoneda, M.; Okamoto, S.; Tamaki, Y.; Ito, T.; Okada, M.; Aso, K.; Makino, I. High, but not low, molecular weight hyaluronan prevents T-cell-mediated liver injury by reducing proinflammatory cytokines in mice. *J. Gastroenterol.* **2004,** 39, 346-354.

122. Neumann, A.; Schinzel, R.; Palm, D.; Riederer, P.; Munch, G. High molecular weight hyaluronic acid inhibits advanced glycation endproduct-induced NF-κB activation and cytokine expression. *FEBS Lett.* **1999,** 453, 283-287.

123. McKee, C. M.; Lowenstein, C. J.; Horton, M. R.; Wu, J.; Bao, C.; Chin, B. Y.; Choi, A. M.; Noble, P. W. Hyaluronan fragments induce nitric-oxide synthase in murine macrophages through a nuclear factor κB-dependent mechanism. *J. Biol. Chem.* **1997,** 272, 8013-8018.

124. McKee, C. M.; Penno, M. B.; Cowman, M.; Burdick, M. D.; Strieter, R. M.; Bao, C.; Noble, P. W. Hyaluronan (HA) fragments induce chemokine gene expression in alveolar macrophages. The role of HA size and CD44. *J. Clin. Invest.* **1996,** 98, 2403-2413.

125. Noble, P. W.; McKee, C. M.; Cowman, M.; Shin, H. S. Hyaluronan fragments activate an NF-κB/I-κBα autoregulatory loop in murine macrophages. *J. Exp. Med.* **1996,** 183, 2373-2378.

126. Xu, H.; Ito, T.; Tawada, A.; Maeda, H.; Yamanokuchi, H.; Isahara, K.; Yoshida, K.; Uchiyama, Y.; Asari, A. Effect of hyaluronan oligosaccharides on the expression of heat shock protein 72. *J. Biol. Chem.* **2002,** 277, 17308-17314.

127. Toole, B. P.; Ghatak, S.; Misra, S. Hyaluronan oligosaccharides as a potential anticancer therapeutic. *Curr. Pharm. Biotechnol.* **2008,** 9, 249-252.

128. Ghatak, S.; Misra, S.; Toole, B. P. Hyaluronan oligosaccharides inhibit anchorage-independent growth of tumor cells by suppressing the phosphoinositide 3-kinase/Akt cell survival pathway. *J. Biol. Chem.* **2002,** 277, 38013-38020.

129. Meyer, K. The biological significance of hyaluronic acid and hyaluronidase. *Physiol. Rev.* **1947,** 27, 335-359.

130. Duran-Reynals, F. Tissue permeability and the spreading factors in infection: a contribution to the host:parasite problem. *Bacteriol. Rev.* **1942,** 6, 197-252.

131. Duran-Reynals, F. The effect of extracts of certain organs from normal and immunized animals on the infecting power of vaccine virus. *J. Exp. Med.* **1929,** 50, 327-340.

132. Chain, E.; Duthie, E. S. Identity of hyaluronidase and spreading Factor. *Br. J. Exp. Pathol.* **1940,** 21, 324-338.

133. Chain, E.; Duthie, E. S. A mucolytic enzyme in testis extracts. *Nature* **1939,** 144, 977-978.

134. Jaques, R. A biological method of assay of hyaluronidase. *Biochem. J.* **1953,** 53, 56-59.

135. Humphrey, J. H.; Jaques, R. Hyaluronidase: correlation between biological assay and other methods of assay. *Biochem. J.* **1953,** 53, 59-62.

136. Fulton, J. K.; Marcus, S.; Robinson, W. D. Use of the streptococcal decapsulation test as a measure of thermolabile hyaluronidase inhibitor in serum. *Ann. N. Y. Acad. Sci.* **1950,** 52, 1133-1138.

137. Lincicome, D. R. A streptococcal decapsulation test for detection of hyaluronidase activity in animal parasites. *Exp. Parasitol.* **1953,** 2, 333-340.

138. Robertson, W. v. B.; Ropes, M. W.; Bauer, W. Mucinase: a bacterial enzyme which hydrolyses synovial fluid mucin and other mucins. *J. Biol. Chem.* **1940,** 133, 261-276.

139. McClean, D. Studies on diffusing factors: 2. Methods of assay of hyaluronidase and their correlation with skin diffusing activity. *Biochem. J.* **1943,** 37, 169-177.

140. Warren, G. H.; Durso, J. G. A synovial fluid clot prevention test for the determination of hyaluronidase activity. *Endocrinology* **1951,** 48, 408-412.

141. Gunter, G. S. The determination of "Spinnbarkeit" of synovial fluid and its destruction by enzymic activity. *Aust. J. Exp. Biol. Med. Sci.* **1949,** 27, 265-274.

142. Madinaveitia, J.; Quibell, T. H. H. Studies on diffusing factors: The action of testicular extracts on the viscosity of vitreous humour preparations. *Biochem. J.* **1940,** 34, 625-631.

143. Alburn, H. E.; Whitley, R. W. Factors affecting the assay of hyaluronidase. *J. Biol. Chem.* **1951,** 192, 379-393.

144. Hoechstetter, J. Characterisation of bovine testicular hyaluronidase and a hyaluronate lyase from *Streptococcus agalactiae*: investigations on the effect of pH on hyaluronan degradation and preclinical studies on the adjuvant administration of the enzymes in cancer chemotherapy. PhD thesis, University of Regensburg, Regensburg, **2005**.

145. Kass, E. H.; Seastone, C. V. The role of the mucoid polysaccharide (hyaluronic acid) in the virulence of group a hemolytic streptococci. *J. Exp. Med.* **1944,** 79, 319-330.

146. Dorfman, A.; Ott, M. L. A turbidimetric method for the assay of hyaluronidase. *J. Biol. Chem.* **1948,** 172, 367-375.

147. Pearce, R. H. The turbidimetric estimation of hyaluronidase. *Biochem. J.* **1953,** 55, 467-472.

148. Pearce, R. H. The turbidimetric estimation of hyaluronate. *Biochem. J.* **1953,** 55, 472-477.

149. Tolksdorf, S.; H., M. M.; McCullagh, D. R.; Schwenk, E.; Bloomfield, D. S. The turbidimetric assay of hyaluronidase. *J. Lab. Clin. Med.* **1949,** 34, 74-89.

150. Schmith, K.; Faber, V. The turbidimetric method for determination of hyaluronidase. *Scand. J. Clin. Lab. Invest.* **1950,** 2, 292-297.

151. Rapport, M. M.; Meyer, K.; Linker, A. Correlation of reductimetric and turbidimetric methods for hyaluronidase assay. *J. Biol. Chem.* **1950,** 186, 615-623.

152. Di Ferrante, N. Turbidimetric measurement of acid mucopolysaccharides and hyaluronidase activity. *J. Biol. Chem.* **1956,** 220, 303-306.

153. Bohn, R.; Dinnendahl, V.; Kalbhen, D. A. Automatisches Verfahren zur Bestimmung von sauren Mucopolysacchariden und seine Anwendung in der analytischen Biochemie. *Fresenius Z. Anal. Chem.* **1969,** 247, 312-316.

154. Elson, L. A.; Morgan, W. T. A colorimetric method for the determination of glucosamine and chondrosamine. *Biochem. J.* **1933,** 27, 1824-1828.

155. Morgan, W. T.; Elson, L. A. A colorimetric method for the determination of *N*-acetylglucosamine and *N*-acetylchrondrosamine. *Biochem. J.* **1934,** 28, 988-995.

156. Reissig, J. L.; Storminger, J. L.; Leloir, L. F. A modified colorimetric method for the estimation of *N*-acetylamino sugars. *J. Biol. Chem.* **1955,** 217, 959-966.

157. Gacesa, P.; Savitsky, M. J.; Dodgson, K. S.; Olavesen, A. H. A recommended procedure for the estimation of bovine testicular hyaluronidase in the presence of human serum. *Anal. Biochem.* **1981,** 118, 76-84.

158. Muckenschnabel, I.; Bernhardt, G.; Spruß, T.; Dietl, B.; Buschauer, A. Quantitation of hyaluronidases by the Morgan-Elson reaction: comparison of the enzyme activities in the plasma of tumor patients and healthy volunteers. *Cancer Lett.* **1998,** 131, 13-20.

159. Asteriou, T.; Deschrevel, B.; Delpech, B.; Bertrand, P.; Bultelle, F.; Merai, C.; Vincent, J. C. An improved assay for the *N*-acetyl-D-glucosamine reducing ends of polysaccharides in the presence of proteins. *Anal. Biochem.* **2001,** 293, 53-59.

160. Takahashi, T.; Ikegami-Kawai, M.; Okuda, R.; Suzuki, K. A fluorimetric Morgan-Elson assay method for hyaluronidase activity. *Anal. Biochem.* **2003,** 322, 257-263.

161. Bitter, T.; Muir, H. M. A modified uronic acid carbazole reaction. *Anal. Biochem.* **1962,** 4, 330-334.

162. Cesaretti, M.; Luppi, E.; Maccari, F.; Volpi, N. A 96-well assay for uronic acid carbazole reaction. *Carbohydr. Polym.* **2003,** 54, 59-61.

163. Kudo, K.; Tu, A. T. Characterization of hyaluronidase isolated from *Agkistrodon contortrix contortrix* (Southern Copperhead) venom. *Arch. Biochem. Biophys.* **2001,** 386, 154-162.

164. Nimptsch, K.; Süß, R.; Riemer, T.; Nimptsch, A.; Schnabelrauch, M.; Schiller, J. Differently complex oligosaccharides can be easily identified by matrix-assisted laser desorption and ionization time-of-flight mass spectrometry directly from a standard thin-layer chromatography plate. *J. Chromatogr. A* **2010,** 1217, 3711-3715.

165. Shimada, E.; Matsumura, G. Thin-layer chromatography of hyaluronate oligosaccharides. *J. Biochem.* **1984,** 96, 721-725.

166. Zhang, Z.; Xie, J.; Zhang, F.; Linhardt, R. J. Thin-layer chromatography for the analysis of glycosaminoglycan oligosaccharides. *Anal. Biochem.* **2007,** 371, 118-120.

167. Chen, F.; Kakizaki, I.; Yamaguchi, M.; Kojima, K.; Takagaki, K.; Endo, M. Novel products in hyaluronan digested by bovine testicular hyaluronidase. *Glycoconj. J.* **2009,** 26, 559-566.

168. Tawada, A.; Masa, T.; Oonuki, Y.; Watanabe, A.; Matsuzaki, Y.; Asari, A. Large-scale preparation, purification, and characterization of hyaluronan oligosaccharides from 4-mers to 52-mers. *Glycobiology* **2002,** 12, 421-426.

169. Alaniz, L.; Garcia, M. G.; Gallo-Rodriguez, C.; Agusti, R.; Sterin-Speziale, N.; Hajos, S. E.; Alvarez, E. Hyaluronan oligosaccharides induce cell death through PI3-K/Akt pathway independently of NF-κB transcription factor. *Glycobiology* **2006,** 16, 359-367.

170. Prebyl, B. S.; Kaczmarek, C.; Tuinman, A. A.; Baker, D. C. Characterizing the electrospray-ionization mass spectral fragmentation pattern of enzymatically derived hyaluronic acid oligomers. *Carbohydr. Res.* **2003,** 338, 1381-1387.

171. Price, K. N.; Al, T.; Baker, D. C.; Chisena, C.; Cysyk, R. L. Isolation and characterization by electrospray-ionization mass spectrometry and high-performance anion-exchange chromatography of oligosaccharides derived from hyaluronic acid by hyaluronate lyase digestion: observation of some heretofore unobserved oligosaccharides that contain an odd number of units. *Carbohydr. Res.* **1997,** 303, 303-311.

172. Mahoney, D. J.; Aplin, R. T.; Calabro, A.; Hascall, V. C.; Day, A. J. Novel methods for the preparation and characterization of hyaluronan oligosaccharides of defined length. *Glycobiology* **2001,** 11, 1025-1033.

173. Vercruysse, K. P.; Lauwers, A. R.; Demeester, J. M. Kinetic investigation of the degradation of hyaluronan by hyaluronidase using gel permeation chromatography. *J. Chromatogr. B, Biomed. Appl.* **1994,** 656, 179-190.

174. Cramer, J. A.; Bailey, L. C. A reversed-phase ion-pair high-performance liquid chromatography method for bovine testicular hyaluronidase digests using postcolumn derivatization with 2-cyanoacetamide and ultraviolet detection. *Anal. Biochem.* **1991,** 196, 183-191.

175. Rai, S. K.; Duh, F. M.; Vigdorovich, V.; Danilkovitch-Miagkova, A.; Lerman, M. I.; Miller, A. D. Candidate tumor suppressor HYAL2 is a glycosylphosphatidylinositol (GPI)-anchored cell-surface receptor for jaagsiekte sheep retrovirus, the envelope protein of which mediates oncogenic transformation. *Proc. Natl. Acad. Sci. U. S. A.* **2001,** 98, 4443-4448.

176. Vigdorovich, V.; Strong, R. K.; Miller, A. D. Expression and characterization of a soluble, active form of the jaagsiekte sheep retrovirus receptor, Hyal2. *J. Virol.* **2005,** 79, 79-86.

177. Min, H.; Cowman, M. K. Combined alcian blue and silver staining of glycosaminoglycans in polyacrylamide gels: application to electrophoretic analysis of molecular weight distribution. *Anal. Biochem.* **1986,** 155, 275-285.

178. Ikegami-Kawai, M.; Takahashi, T. Microanalysis of hyaluronan oligosaccharides by polyacrylamide gel electrophoresis and its application to assay of hyaluronidase activity. *Anal. Biochem.* **2002,** 311, 157-165.

179. Calabro, A.; Benavides, M.; Tammi, M.; Hascall, V. C.; Midura, R. J. Microanalysis of enzyme digests of hyaluronan and chondroitin/dermatan sulfate by fluorophore-assisted carbohydrate electrophoresis (FACE). *Glycobiology* **2000,** 10, 273-281.

180. Calabro, A.; Hascall, V. C.; Midura, R. J. Adaptation of FACE methodology for microanalysis of total hyaluronan and chondroitin sulfate composition from cartilage. *Glycobiology* **2000,** 10, 283-293.

181. Kooy, F. K.; Ma, M.; Beeftink, H. H.; Eggink, G.; Tramper, J.; Boeriu, C. G. Quantification and characterization of enzymatically produced hyaluronan with fluorophore-assisted carbohydrate electrophoresis. *Anal. Biochem.* **2009,** 384, 329-336.

182. Hong, M.; Sudor, J.; Stefansson, M.; Novotny, M. V. High-resolution studies of hyaluronic acid mixtures through capillary gel electrophoresis. *Anal. Chem.* **1998,** 70, 568-573.

183. Hutterer, K. M.; Jorgenson, J. W. Separation of hyaluronic acid by ultrahigh-voltage capillary gel electrophoresis. *Electrophoresis* **2005,** 26, 2027-2033.

184. Grimshaw, J.; Kane, A.; Trocha-Grimshaw, J.; Douglas, A.; Chakravarthy, U.; Archer, D. Quantitative analysis of hyaluronan in vitreous humor using capillary electrophoresis. *Electrophoresis* **1994,** 15, 936-940.

185. Grimshaw, J.; Trocha-Grimshaw, J.; Fisher, W.; Rice, A.; Smith, S.; Spedding, P.; Duffy, J.; Mollan, R. Quantitative analysis of hyaluronan in human synovial fluid using capillary electrophoresis. *Electrophoresis* **1996,** 17, 396-400.

186. Grimshaw, J. Analysis of glycosaminoglycans and their oligosaccharide fragments by capillary electrophoresis. *Electrophoresis* **1997,** 18, 2408-2414.

187. Pattanaargson, S.; Roboz, J. Determination of hyaluronidase activity in venoms using capillary electrophoresis. *Toxicon* **1996,** 34, 1107-1117.

188. Hayase, S.; Oda, Y.; Honda, S.; Kakehi, K. High-performance capillary electrophoresis of hyaluronic acid: determination of its amount and molecular mass. *J. Chromatogr. A* **1997,** 768, 295-305.

189. Kinoshita, M.; Okino, A.; Oda, Y.; Kakehi, K. Anomalous migration of hyaluronic acid oligomers in capillary electrophoresis: correlation to susceptibility to hyaluronidase. *Electrophoresis* **2001,** 22, 3458-3465.

190. Park, Y.; Cho, S.; Linhardt, R. J. Exploration of the action pattern of *Streptomyces* hyaluronate lyase using high-resolution capillary electrophoresis. *Biochim. Biophys. Acta* **1997,** 1337, 217-226.

191. Kühn, A. V.; Rüttinger, H. H.; Neubert, R. H.; Raith, K. Identification of hyaluronic acid oligosaccharides by direct coupling of capillary electrophoresis with electrospray ion trap mass spectrometry. *Rapid Commun. Mass Spectrom.* **2003,** 17, 576-582.

192. Blundell, C. D.; Almond, A. Enzymatic and chemical methods for the generation of pure hyaluronan oligosaccharides with both odd and even numbers of monosaccharide units. *Anal. Biochem.* **2006,** 353, 236-247.

193. Cherr, G. N.; Meyers, S. A.; Yudin, A. I.; VandeVoort, C. A.; Myles, D. G.; Primakoff, P.; Overstreet, J. W. The PH-20 protein in cynomolgus macaque spermatozoa: identification of two different forms exhibiting hyaluronidase activity. *Dev. Biol.* **1996,** 175, 142-153.

194. Miura, R. O.; Yamagata, S.; Miura, Y.; Harada, T.; Yamagata, T. Analysis of glycosaminoglycan-degrading enzymes by substrate gel electrophoresis (zymography). *Anal. Biochem.* **1995,** 225, 333-340.

195. Steiner, B.; Cruce, D. A zymographic assay for detection of hyaluronidase activity on polyacrylamide gels and its application to enzymatic activity found in bacteria. *Anal. Biochem.* **1992,** 200, 405-410.

196. Stern, M.; Stern, R. An ELISA-like assay for hyaluronidase and hyaluronidase inhibitors. *Matrix* **1992,** 12, 397-403.

197. Frost, G. I.; Stern, R. A microtiter-based assay for hyaluronidase activity not requiring specialized reagents. *Anal. Biochem.* **1997,** 251, 263-269.

198. Nawy, S. S.; Csóka, A. B.; Mio, K.; Stern, R. Hyaluronidase activity and hyaluronidase inhibitors. Assay using a microtiter-based system. *Methods Mol. Biol.* **2001,** 171, 383-389.

2 Scope and objectives

Hyaluronan and the corresponding degradation products, resulting from enzymatic cleavage of the polysaccharide by hyaluronidases, are supposed to influence various physiological and pathophysiological processes in a size-dependent manner. However, the biological relevance has not been unequivocally proven. Neither has the occurrence of the suggested hyalobiuronic acids of different degrees of polymerization in biological systems been confirmed, nor their concentration systematically determined. The hyaluronan turnover is depending on the balanced activity of both hyaluronan synthases and hyaluronidases. The enzymological characterization of hyaluronidase isoenzymes is compromised by the lack of suitable analytical methods for the determination of the polydisperse substrates as well as the reaction products.

Aiming at elucidating the molecular mechanisms and the biological relevance of hyaluronan metabolism, this work was focused on sensitive and selective methods to complement the analytical toolbox in this field. Hence, appropriate techniques had to be developed and optimized, especially with regard to the determination of hyaluronan oligosaccharides. For this purpose, the most promising approaches were hyphenated chromatographic and electrophoretic methods.

Another objective of this thesis was to explore the applicability of the new methods, in combination with conventional techniques, to (bio)analytical investigations of samples of different origin. Therefore, enzymological and biological studies of hyaluronidases and hyaluronan oligosaccharides *in vitro* and in biological matrices, e. g. synovial fluid, were envisaged. As minimal substrates were required for enzymological characterization of isoenzymes, chemically defined oligosaccharides had to be prepared and quantified. Exploring the enzymatic cleavage of hyaluronan oligosaccharides, we attempted to gain deeper insight into the catalytic mechanisms, accepted substrates, and product spectra produced by different hyaluronidase isoenzymes.

Finally, focusing on the putative (patho)physiological role of hyaluronan, hyaluronan oligosaccharides, and hyaluronidases, the developed analytical methods had to be applied to complex samples. Furthermore, biological assays were expected to shed light on size-dependent effects of hyaluronan and chemically defined hyaluronan oligosaccharides on processes such as cell migration, cell proliferation, wound healing, and angiogenesis.

3 CZE–ESI-TOF-MS for the fast analysis of small hyaluronan oligosaccharides

Note: Prior to the submission of this thesis, parts of this chapter have already been published in cooperation with partners.[1] In addition, parts of the concerted work, realized in the course of this collaboration, are already included in the PhD thesis submitted by Marco Grundmann in 2012.[2] For detailed information on the nature of this collaboration, see also "Acknowledgements and declaration of collaborations".

3.1 Introduction

Capillary electrophoresis with UV detection (CZE–UV) was used successfully by Grimshaw et al. for the analysis of different glycosaminoglycans and their degradation products[3] as well as for the quantification of hyaluronan in biological material after digestion of the polysaccharide with hyaluronidases.[4, 5] By contrast, Pattanaargson studied the action of venom hyaluronidases by capillary electrophoresis.[6] Later on, capillary electrophoresis[7-11] and the related technique of capillary gel electrophoresis[12, 13] were frequently applied to the analysis of hyaluronan. In our group, CZE–UV was previously used by Hofinger et al. for the analysis of hyaluronan oligosaccharides and hyaluronidase activity.[14, 15]

However, due to the lack of suitable chromophores, UV detection of hyaluronan oligosaccharides is extremely difficult. Therefore, on-line coupling of separation techniques to mass spectrometry is a promising approach for glycosaminoglycan analysis. Recently, a review on this topic has been published by Zaia.[16] Kühn et al. lately described methods for CE−MS analysis of hyaluronan oligosaccharides using coated capillaries and electrospray ion trap mass spectrometry.[17, 18] Nevertheless, using these methods, migration times were apparently too long for fast at-line analysis. For this purpose, total analysis time (including sample pretreatment, injection protocol, and electrophoretic separation) should not exceed 2–5 min.

Thus, we decided to develop a fast capillary zone electrophoresis separation coupled to electrospray ionization time-of-flight mass spectrometry (CZE–ESI-TOF-MS). In order to improve separation efficiency and accelerate separation, optimization aimed at the use of short capillaries and high electric field strengths. Separations at high electric field strengths, often requiring special background electrolytes and experimental setups, have already been described for different analytical problems.[13, 19-23] Additionally, other studies reported short capillaries to be of advantage.[24-28]

Finally, a method for a cationic model system, recently published by our cooperation partners, used capillaries with a length of 28 cm and inner diameters from 75 µm down to 5 µm, applying electric field strength of 1.25 kV/cm.[29] Under these conditions, extremely fast electrophoretic separations were achieved.[29] On this basis, a similar method for the anionic hyaluronan oligosaccharides had to be established. Thereby, various parameters were optimized in different combinations. The relevant steps are presented in this chapter in a logical order.

3.2 Materials and methods

3.2.1 Oligosaccharide standards and sample preparation

Standard oligosaccharides (n_2–n_4) of 2–4 hyalobiuronic acid moieties (oligoHA from Hyalose, Oklahoma City, OK, USA) were purchased from AMSBIO (Abingdon, UK). For CZE–UV a mixture of the standard analytes (100 µM each) was dissolved in 10-fold diluted background electrolyte containing the EOF marker (*cf*. Section 3.2.2). For mass spectrometric detection, water purified with a Milli-Q system (Millipore, Eschborn, Germany) was used as solvent for the analytes. In this case, the oligosaccharide concentration was 20 µM for method optimization.

Hyalo-Oligo, a low molecular weight hyaluronan oligosaccharide mixture with an average molecular weight below 10 kDa, was kindly provided by Kewpie (also named Q. P. Corp., Tokyo, Japan). Samples from incubation mixtures containing buffer salts and bovine serum albumin (Serva, Heidelberg, Germany) were diluted 1:10 with purified water or aqueous solution of internal standard (*cf*. Section 3.2.2) prior to injection. No further pretreatment was necessary.

3.2.2 EOF markers and internal standard

For UV detection, 0.1% (v/v) of benzyl alcohol (Merck, Darmstadt, Germany) was added to the sample solution as a neutral marker of the electroosmotic flow (EOF). In case of CZE–MS of hyaluronan oligosaccharides, the choice of an appropriate EOF marker is complicated by the *m/z* range of the analytes. The marker substance has to be of similar molecular weight, soluble in the aqueous electrolyte system, uncharged under the separation conditions, and suitable for electrospray ionization. Rhodamine B (Figure 3.1), with its fixed positive charge and its acidic carboxylic group, was previously reported to be applicable as EOF marker having zero net charge at a pH between 8.3 and 9.0.[30] Moreover, rhodamine B has a comparable molecular mass to small hyaluronan oligosaccharides. However, due to its structural properties, rhodamine B is ionizable only in the positive ESI mode. In contrast,

hyaluronan oligosaccharides were analyzed in the negative ESI mode. Therefore, polarity had to be changed during the run. As this step takes approximately 20 s, EOF marker and analytes could not be recorded simultaneously in one run under the optimized fast separation conditions. Nevertheless, rhodamine B was added to the oligosaccharide mixture at a final concentration of 1 µM to record the EOF when possible.

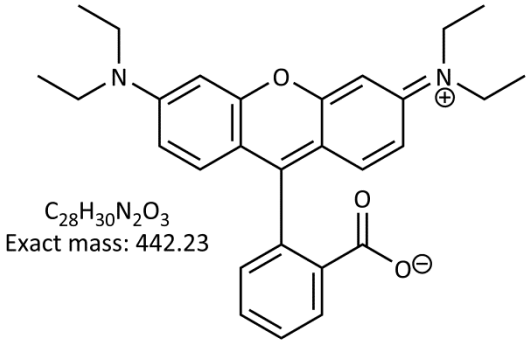

Figure 3.1: Rhodamine B in the charge state under the pH conditions used for CZE–MS. Due to the fixed positive charge and the deprotonated carboxylic group at alkaline pH, the molecule has zero net charge.

Similar difficulties affect the search for an internal standard. Aiming at short run times, the substance of choice should migrate faster towards the detector than the analytes. Otherwise, analyses would be unnecessarily prolonged. Therefore, acarbose (Bayer, Wuppertal, Germany) was used at a concentration of 90 µM. The molecule is depicted in Figure 3.2.

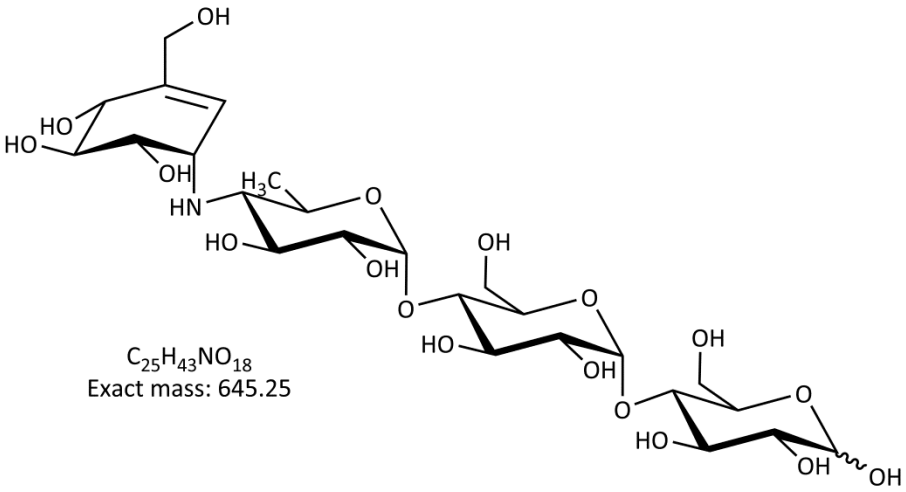

Figure 3.2: Acarbose can be used as internal standard because of its favorable migration behavior and an exact mass close to the hyaluronan oligosaccharide analytes.

More details on the use of acarbose as internal standard, especially for fast at-line analysis, are discussed below (*cf*. Section 3.3.8).

3.2.3 Preparation of the background electrolytes

Ammonium acetate solutions were used as background electrolyte. Therefore, a stock solution of 1 M ammonium acetate (Merck, Darmstadt, Germany) in water, purified by a Milli-Q system (Millipore, Eschborn, Germany), was prepared and stored at 5 °C for a maximum period of one month. The background electrolyte was always prepared freshly by dilution of this solution with purified water and addition of concentrated ammonia solution (Merck, Darmstadt, Germany) for pH adjustment. Prior to use, the solution was filtrated through a Millex-GP 0.22 µm syringe filter unit (Merck-Millipore, Darmstadt, Germany). Solutions used with the automated Bio-Rad CZE–UV system were additionally degassed by centrifugation at 13000 × *g* for 10 min.

3.2.4 Instrumentation, capillary material, and separation conditions for CZE–UV experiments

For preliminary tests on background electrolyte composition, a Bio-Rad Biofocus 3000 system (Bio-Rad, Munich, Germany) was used with UV detection at 200 nm. Separation was performed in a fused silica capillary (MicroQuartz, Munich, Germany) with an inner diameter of 50 µm, a total length of 75 cm, and an effective length (from injection position to detector window) of 70.4 cm. The apparatus was equipped with a liquid cooling system for controlling capillary temperature, operated with a mixture of water and methanol. Capillary as well as sampler carousels were always cooled to 15 °C. Prior to sample injection, the capillary was conditioned with 0.1 M sodium hydroxide solution (300 s), water (200 s), and background electrolyte (600 s). Afterwards, the oligosaccharide mixture was injected by pressure (20 psi · s) and separated at a constant voltage of 20 kV in normal polarity mode (injection at the anodic end, detector window next to the cathode).

3.2.5 Instrumentation and capillary material for CZE–ESI-TOF-MS

The general setup for CZE–ESI-TOF-MS experiments is schematically represented in Figure 3.3. The optional water bath was used to regulate the temperature of incubation mixtures when analyzing enzymatic reactions. After appropriate sample preparation (dilution, addition of standard), injection was performed using a manual injection technique (*cf*. Section 3.2.7).

Separation was carried out using a home-made CE system. A high voltage source (model HCN 7E-35000, FuG Elektronik, Rosenheim-Langenpfunzen, Germany) was linked to the vial containing the background electrolyte by an immersed platinum electrode. Equally, the proximal part of the fused silica capillary (Polymicro Technologies, Phoenix, AZ, USA), purchased from Optronis (Kehl, Germany), was dipped into the vial. Capillaries had an outer

diameter of 360 µm and inner diameters of 5, 10, 15, 20, or 50 µm, respectively. They were manually cut to appropriate lengths. High voltage was regulated with an external control unit which also served as remote control for data acquisition.

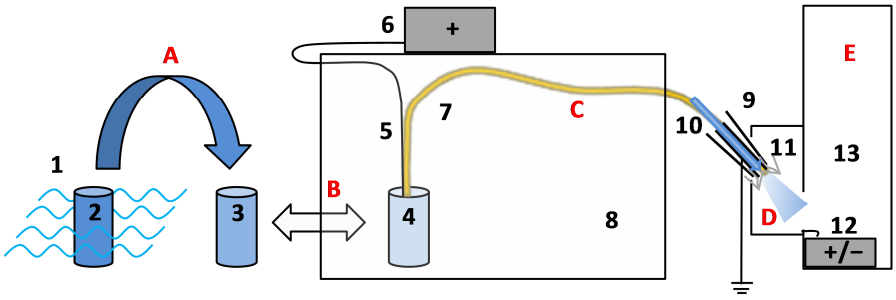

Figure 3.3: General setup for CZE–ESI-TOF-MS: water bath at 37 °C for incubation mixtures (1), incubation vial (2), sample injection vial (3), background electrolyte (4), electrode (5), separation high voltage source (6), separation capillary (7), insulating box (8), interface (9), sheath liquid flow provided by a syringe pump (10), nebulizer gas (11), ESI high voltage source (12), mass detector (13). Processes: sample preparation (A), manual injection (B), electrophoretic separation (C), ionization (D), detection (E).

An insulating box made of acrylic glass protected the operator from the high voltage. The distal part of the capillary was passed through a small notch in the acrylic glass box and coupled to a micrOTOF-MS (Bruker Daltonik, Bremen, Germany) by a coaxial sheath liquid sprayer (Agilent Technologies, Waldbronn, Germany). A constant flow of the sheath liquid (*cf*. Section 3.2.6) was provided by a syringe pump (model 601553, KD Scientific, Holliston, MA, USA) equipped with a 2.5 mL glass syringe (ILS, Stützerbach, Germany), both not depicted in Figure 3.3. It should be noted that, using the ground as part of the ESI high voltage circuit, the ESI high voltage source (number 12) depicted in Figure 3.3 was set positive for negative ionization mode and vice versa.

For long capillaries with an inner diameter of 50 µm, cooling with pressurized nitrogen (using an additional silicone tube around the capillary) was found to be advantageous to reduce Joule heating. For the short capillaries used in most of the experiments, however, cooling was neither necessary nor possible. Resistive heating was low under these conditions and a significant part of the capillary was then encased by the MS interface.

3.2.6 Sheath liquid, MS parameter settings, and mass calibration

As results of preliminary optimization experiments on ionization and sheath liquid composition, negative ionization mode and an acidic sheath liquid were chosen for MS coupling. Although for acidic analytes a basic sheath liquid seems reasonable, the addition of acid was found to be beneficial. In detail, the mixture consisted of 2-propanol (HPLC–MS grade, Carl Roth, Karlsruhe, Germany), water (purified with an Astacus system, MembraPure, Bodenheim, Germany), and formic acid (Merck, Darmstadt Germany) at a ratio of 50:50:0.2

(v/v/v). The flow rate of the sheath liquid was 8 µL/min. An overview of the instrumental settings for mass spectrometry during method optimization (standard) and later modifications is provided in Table 3.1.

Depending on the *m/z* of the respective analytes, different procedures for mass calibration were chosen. For standard calibration (analytes with *m/z* below approximately 1300), sodium formate clusters were used. Using capillaries with inner diameters of 25 µm and below, signal intensities of the clusters formed by sodium formate solution were too low for mass calibration. Therefore, the reference clusters were formed *in situ* by forced injection of 1 M sodium hydroxide solution, prepared from 50% sodium hydroxide solution (Sigma-Aldrich, Munich, Germany), in combination with the formic acid content of the sheath liquid. For single experiments focusing on oligosaccharides with higher molecular mass, cesium perfluoroheptanoic acid clusters were used.[31] For this purpose, a calibration solution was prepared from perfluoroheptanoic acid and cesium hydrogen carbonate, both from Sigma-Aldrich (Munich, Germany).

For all analytes, extracted ion traces were calculated from the recorded mass spectra. Thereby, only *m/z* values having an abundance of at least 20% of the base peak were summed up. This procedure gave reproducible results and best signal-to-noise ratios. When significant formation of adduct species, mainly sodium adducts, was observed, the signals were included in the extracted ion traces under the same rule.

Table 3.1: MS parameter settings. The standard method settings were used for optimization of CZE conditions. Later on, some parameters were modified for the analysis of large and small oligosaccharides.

	Standard method	**Modification 1 (large oligosaccharides)**	**Modification 2 (small oligosaccharides)**
Source			
Ionization, polarity	ESI, negative (positive for EOF marker)	ESI, negative	ESI, negative
Scan range (*m/z*)	300–3000	300–3000	300–1200
Capillary (V)	5000	4500	5000
End plate offset (V)	−500	−500	−500
Nebulizer (bar)	1.0	1.0	1.2
Dry heater (°C)	190	190	190
Dry gas (L/min)	4.0	4.0	4.0
Ion optics			
Capillary exit (V)	−100.0	−100.0	−100
Skimmer 1 (V)	−33.0	−33.0	−33.0
Hexapole 1 (V)	−22.5	−22.5	−22.5
Skimmer 2 (V)	−22.0	−22.0	−22.0
Hexapole 2 (V)	−20.5	−20.5	−20.5
Hexapole RF (V)	800.0	800.0	300.0
Transfer time (µs)	113.0	49.0	40.0
Pre pulse storage (µs)	20.0	10.0	10.0
Lens 1 storage (V)	−30.0	−30.0	−30.0
Lens 1 extraction (V)	−20.8	−20.8	−20.8
Lens 2 (V)	−14.0	−8.0	−8.0
Lens 3 (V)	20.0	20.0	20.0
Lens 4 (V)	−10.0	0.0	0.0
Lens 5 (V)	−5.0	28.5	28.5
Data acquisition			
Spectra rate (Hz)	5 or 10	10	10

3.2.7 Manual sample injection

Unlike the automated sample injection in CZE–UV experiments (*cf*. Section 3.2.4), a manual sample injection technique was applied with the CZE–ESI-TOF-MS assembly.[29] In summary, the proximal end of the separation capillary was manually dipped into the sample solution for a defined time interval and then removed back to the vial containing the background electrolyte. Before, the laminar flow through the capillary, which is caused by the suction pressure created at the ESI-MS interface, was determined for each capillary. From these experiments, the time of capillary immersion needed for filling an injection zone of desired length could be calculated. With capillary diameters of 15 µm or below, however, the reduced laminar flow would lead to a drastic prolongation of the injection process. Therefore, sealed sample vials were additionally pressurized by injection of a defined volume of air using a syringe.

3.3 Results and discussion

3.3.1 Preliminary tests using CZE–UV

Starting with conditions adapted from previously described CZE–UV methods for hyaluronan oligosaccharide analysis,[14, 15] the background electrolyte had to be altered to a volatile system with regard to CZE–MS coupling. Therefore, ammonium acetate solutions of various pH values (Figure 3.4) and salt concentrations (Figure 3.5) were compared using UV detection at 200 nm. The electropherograms clearly indicated an increase in migration times of the analyte peaks with decreasing pH and increasing salt concentration. At high pH, however, the separation efficiency was negatively affected. For this reason, a pH of 8.5 was chosen as starting point for further optimization as a compromise. Ammonium acetate concentration was kept below 100 mM in CZE–MS experiments, starting with 25 mM.

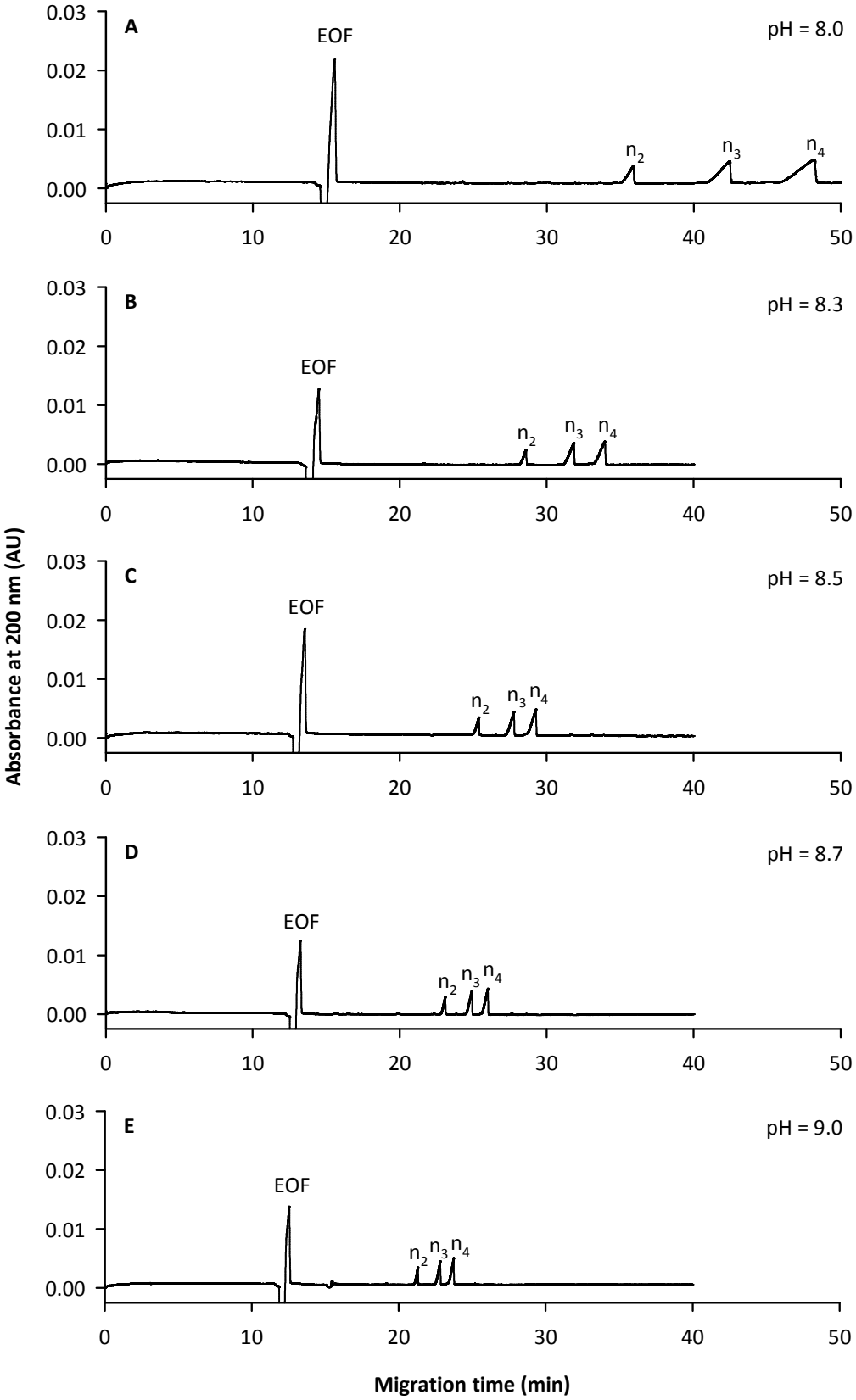

Figure 3.4: CZE–UV experiment using 100 mM ammonium acetate solutions with pH values of 8.0 (A), 8.3 (B), 8.5 (C), 8.7 (D), and 9.0 (E) as background electrolytes. Oligosaccharide standards at 100 µM, EOF marked by benzyl alcohol. Fused silica capillary with a total length of 75 cm, an effective length of 70.4 cm, and an inner diameter of 50 µm. Separation voltage: 20 kV. Capillary temperature: 15 °C. UV detection at 200 nm.

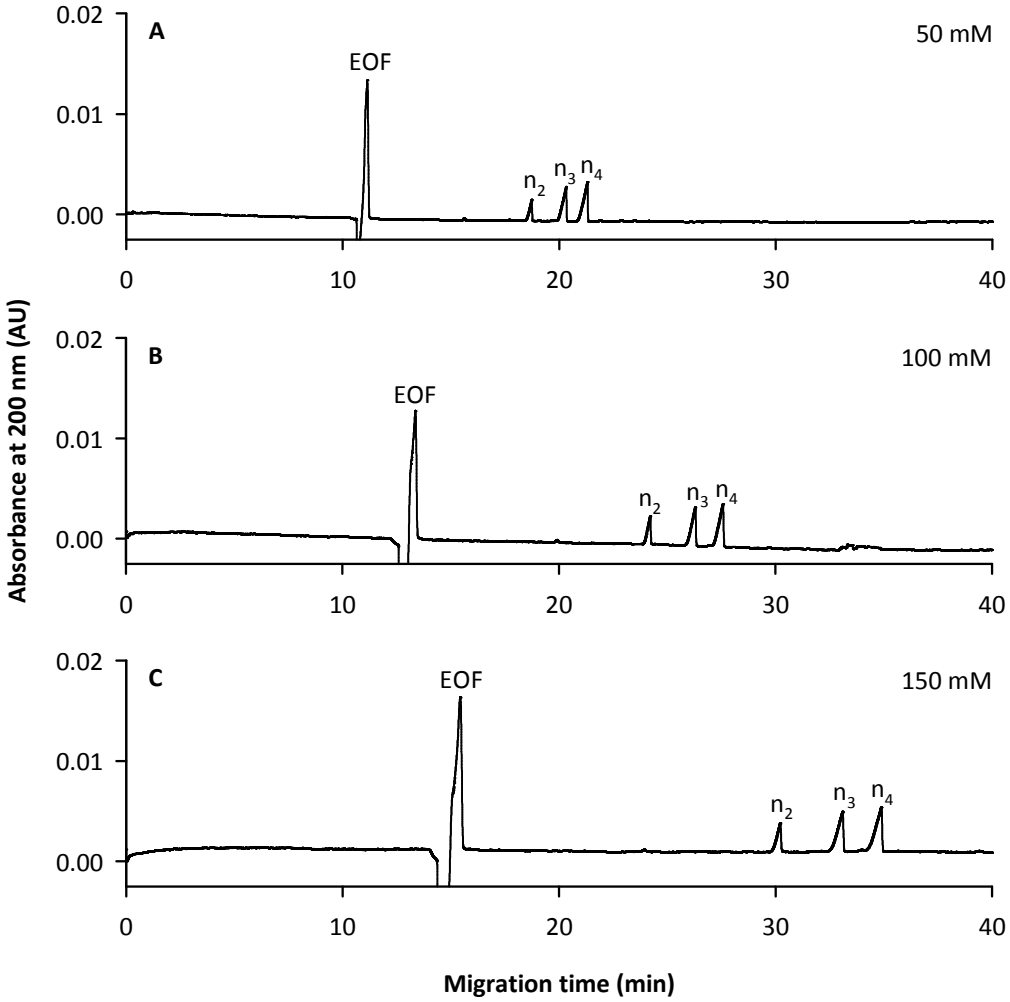

Figure 3.5: CZE–UV experiment using 50 mM (A), 100 mM (B), and 150 mM (C) ammonium acetate background electrolytes, all adjusted to a pH of 8.5. Oligosaccharide standards at 100 µM, EOF marked by benzyl alcohol. Fused silica capillary with a total length of 75 cm, an effective length of 70.4 cm, and an inner diameter of 50 µm. Separation voltage: 20 kV. Capillary temperature: 15 °C. UV detection at 200 nm.

3.3.2 Optimization of the injection zone length

The first parameter to be examined was the length of the injection zone. Using the manual injection technique described in Section 3.2.7, the capillary was dipped into the sample vial for 10, 20, or 40 s. Under the conditions of this particular experiment, these intervals corresponded to injection zones of 0.7%, 1.4%, or 2.9% of the total capillary length (Figure 3.6). The electropherograms clearly demonstrated that, within the investigated range, no adverse effects on peak shape and separation were observed when the capillary was filled with sample to a higher percentage. As injection was only driven by the suction pressure, the time interval needed for the injection process naturally increases in parallel with the desired injection zone. The effect was even more prominent when the inner diameter of the capillary was reduced. However, prolongation of the time period required for injection, was in conflict with the aim of short run times allowing for fast at-line analysis. Hence, 2% of the capillary were filled with the sample solution in the following experiments. It should be

noted at this point that, keeping this relative value (percentage of respective capillary length) constant, any change in capillary length or inner diameter affects the total volume and thus the amount of analyte injected.

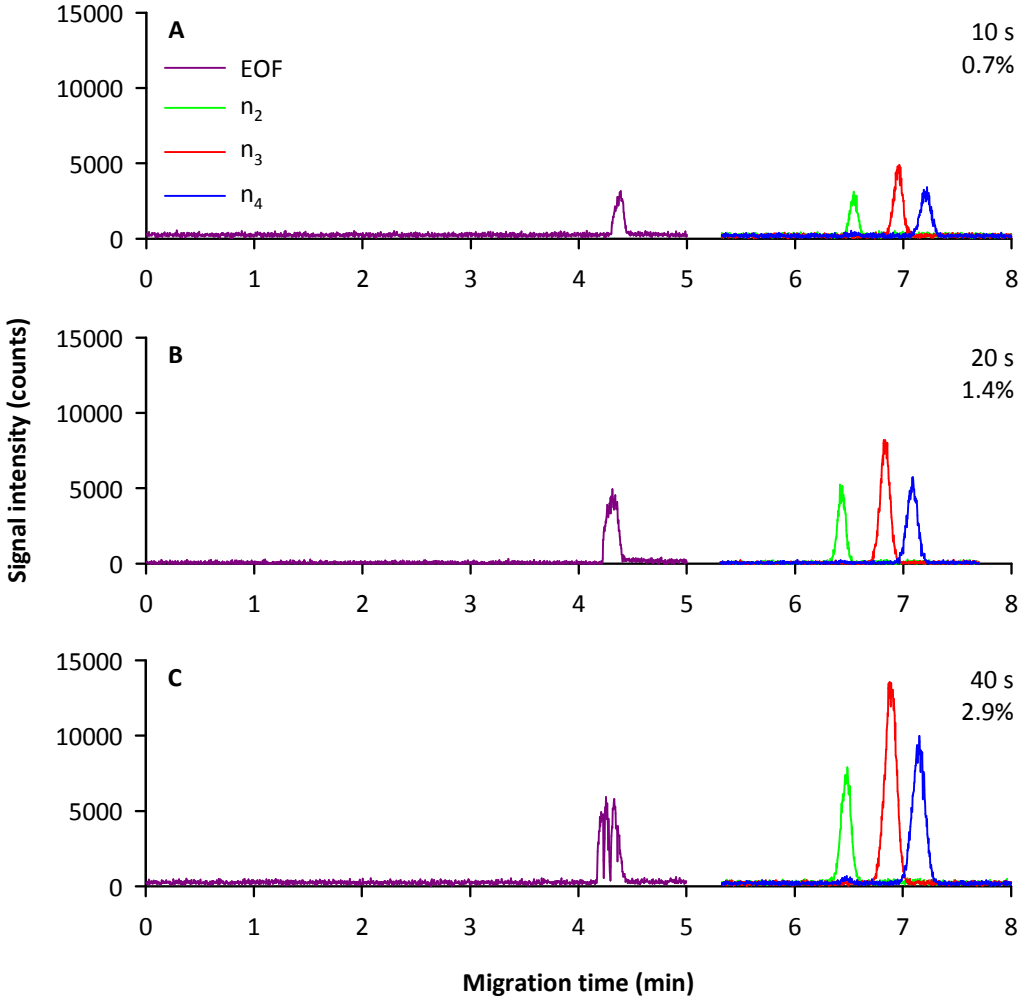

Figure 3.6: Variations in the duration of the injection interval and the corresponding sample zone lengths (given as percentage of the total capillary length). Oligosaccharide standards at 20 µM, rhodamine B (EOF marker) at 1 µM. Fused silica capillary with a total length of 75 cm and an inner diameter of 50 µm. Background electrolyte: 25 mM ammonium acetate solution, pH = 8.5. Separation voltage: 35 kV. Spectra rate: 5 Hz. Electropherograms show extracted ion traces.

3.3.3 Capillary length and electric field strength

Using special experimental setups, extremely high voltages can be applied.[13, 20, 23] However, in view of limitations in maximum voltage provided by common high voltage sources, further increase in field strength can only be achieved by reducing capillary length. Therefore, capillaries of 75, 50, 43, 30, and 28 cm, respectively, were compared, applying a constant separation voltage of 35 kV (Figure 3.7).

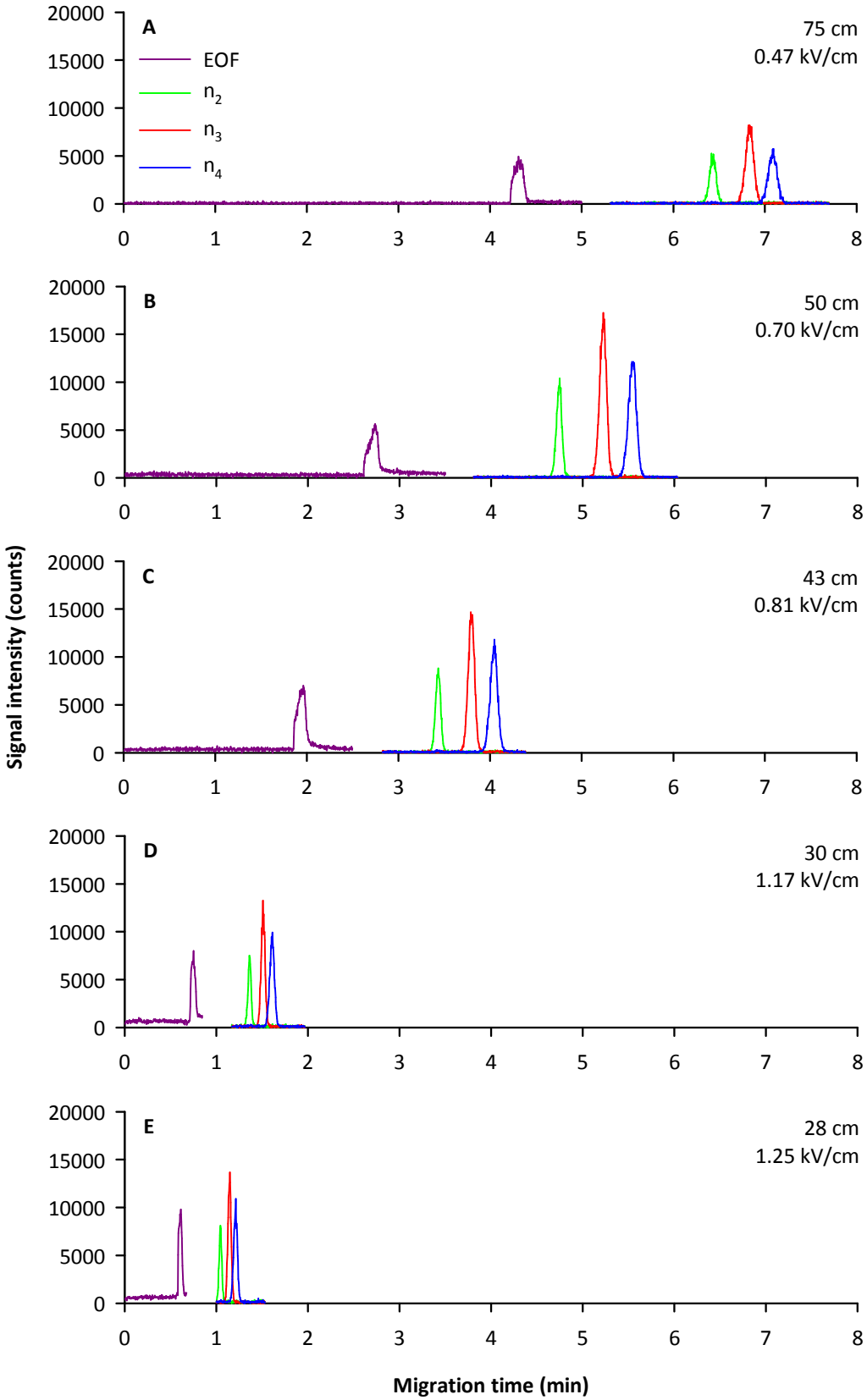

Figure 3.7: Increase in electric field strength from 0.47 kV/cm (A) to 1.25 kV/cm (E) by stepwise reduction of capillary length from 75 cm (A) to 28 cm (E). Oligosaccharide standards at 20 µM, rhodamine B (EOF marker) at 1 µM. Injection zone: 2% of the capillary. Fused silica capillaries with an inner diameter of 50 µm. Background electrolyte: 25 mM ammonium acetate solution, pH = 8.5. Separation voltage: 35 kV. Spectra rate: 5 Hz. Reproduced and adapted from Fig. 2 of the original publication[1] with kind permission from Springer Science and Business Media.

Further reduction of capillary length was not feasible using the interface for MS coupling and the manual injection technique. Otherwise, the part of the capillary outside the interface would have been too short for manual handling.

The stepwise reduction of capillary length led to considerably shorter migration times of less than 90 s instead of approximately 7 min. Moreover, peaks were sharpened by high electric field conditions. As a result, separation efficiency deteriorated only slightly. However, signal intensities were influenced in different ways when reducing the length of the capillary stepwise. Initially, peak heights increased due to peak sharpening, followed by slightly decreasing peak heights because of the reduced amount of analyte injected (*cf*. Section 3.3.2). Finally the combination of both effects led to constant peak heights.

3.3.4 Capillary inner diameter

Recent studies demonstrated the beneficial effect of reduced capillary inner diameters on separation efficiency.[29] Consequently, inner diameters of 50, 25, 15, 10, and 5 µm were compared (Figure 3.8). Peaks were sharpened, resulting in constant heights from 50 µm down to 15 µm inner diameter. Remarkably, this constancy in signal intensity was achieved despite of a reduction of the injected sample volume by a factor of 11. However, according to the quadratic correlation between radius and volume, further reduction led to considerably lower signal intensities. It should be noted that, as a consequence of the narrow and sharp peaks, a data acquisition rate of 5 Hz was insufficient for capillaries with inner diameters of 10 and 15 µm. For this reason, the spectra rate was increased to 10 Hz. By this change, signal intensities were halved at constant signal-to-noise ratio. Therefore, the scaling of the ordinate axes in Figure 3.8 was adapted for better comparability.

In summary, separation efficiency and peak resolution were improved when using capillaries of smaller inner diameters. Thereby, 15 µm was the smallest diameter showing no significant loss in sensitivity. Accordingly, capillaries with an inner diameter of 15 µm and a length of 28 cm were chosen for the following evaluation of background electrolyte composition. To obtain a sufficient number of data points for peak calculation, spectra rate of the MS detection was set to 10 Hz for future experiments.

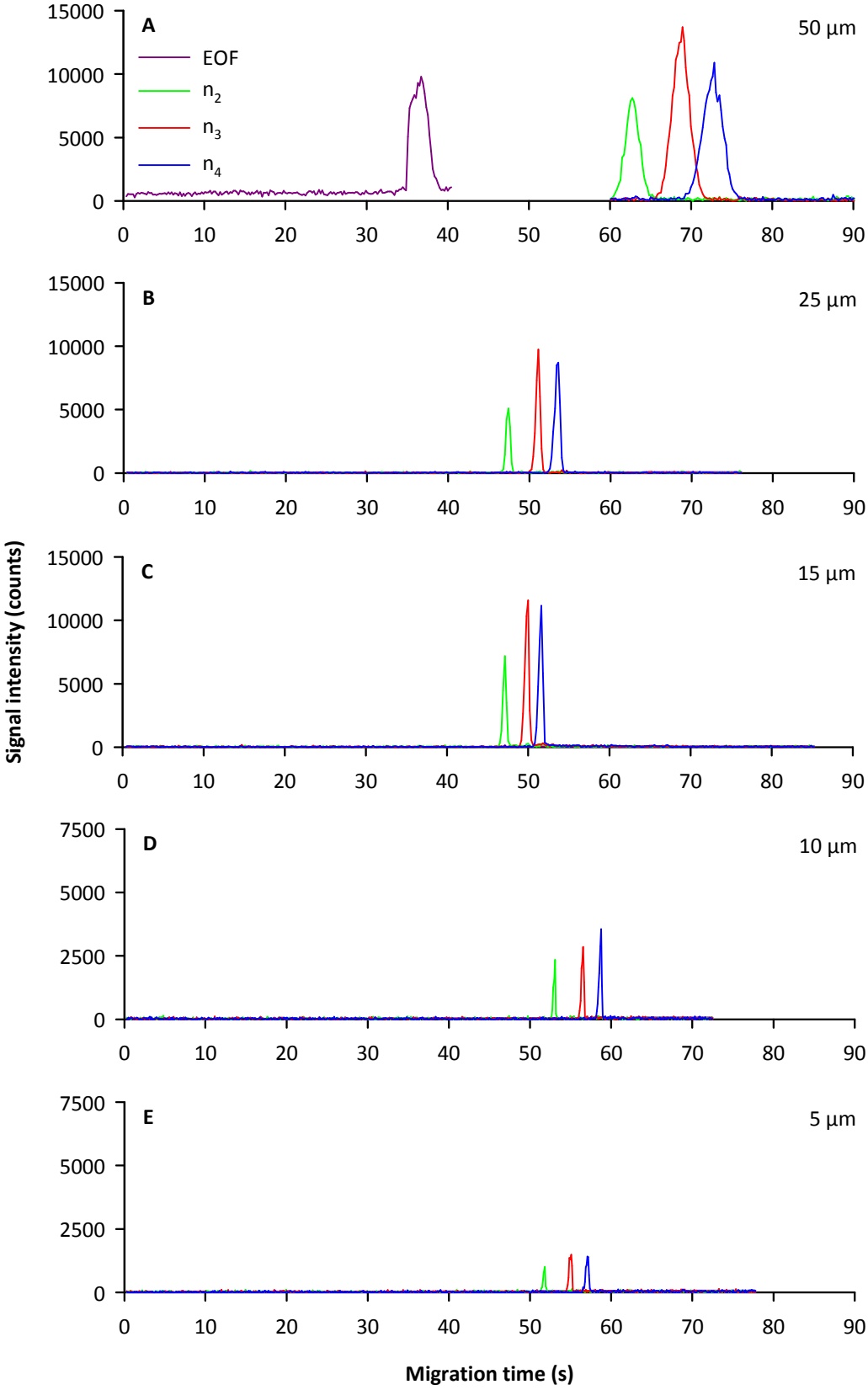

Figure 3.8: Comparison of capillaries with inner diameters of 50 µm (A), 25 µm (B), and 15 µm (C) at a spectra rate of 5 Hz. Data acquisition rate was changed to 10 Hz for 10 µm (D) and 5 µm (E) capillaries. Therefore, the ordinate axes of the electropherograms were adapted. Oligosaccharide standards at 20 µM, rhodamine B (EOF marker) at 1 µM. Injection zone: 2% of the capillary. Fused silica capillaries with a length of 28 cm. Background electrolyte: 25 mM ammonium acetate, pH = 8.5. Separation voltage: 35 kV. Reproduced and adapted from Fig. 3 of the original publication[1] with kind permission from Springer Science and Business Media.

3.3.5 Concentration and pH of the background electrolyte

Having started with experiments on the composition of the background electrolyte using CZE–UV (*cf*. Section 3.3.1), things have come full circle at this point of parameter optimization. In this section, background electrolytes of different concentrations (Figure 3.9) and pH values (Figure 3.10) are compared under CZE–MS conditions.

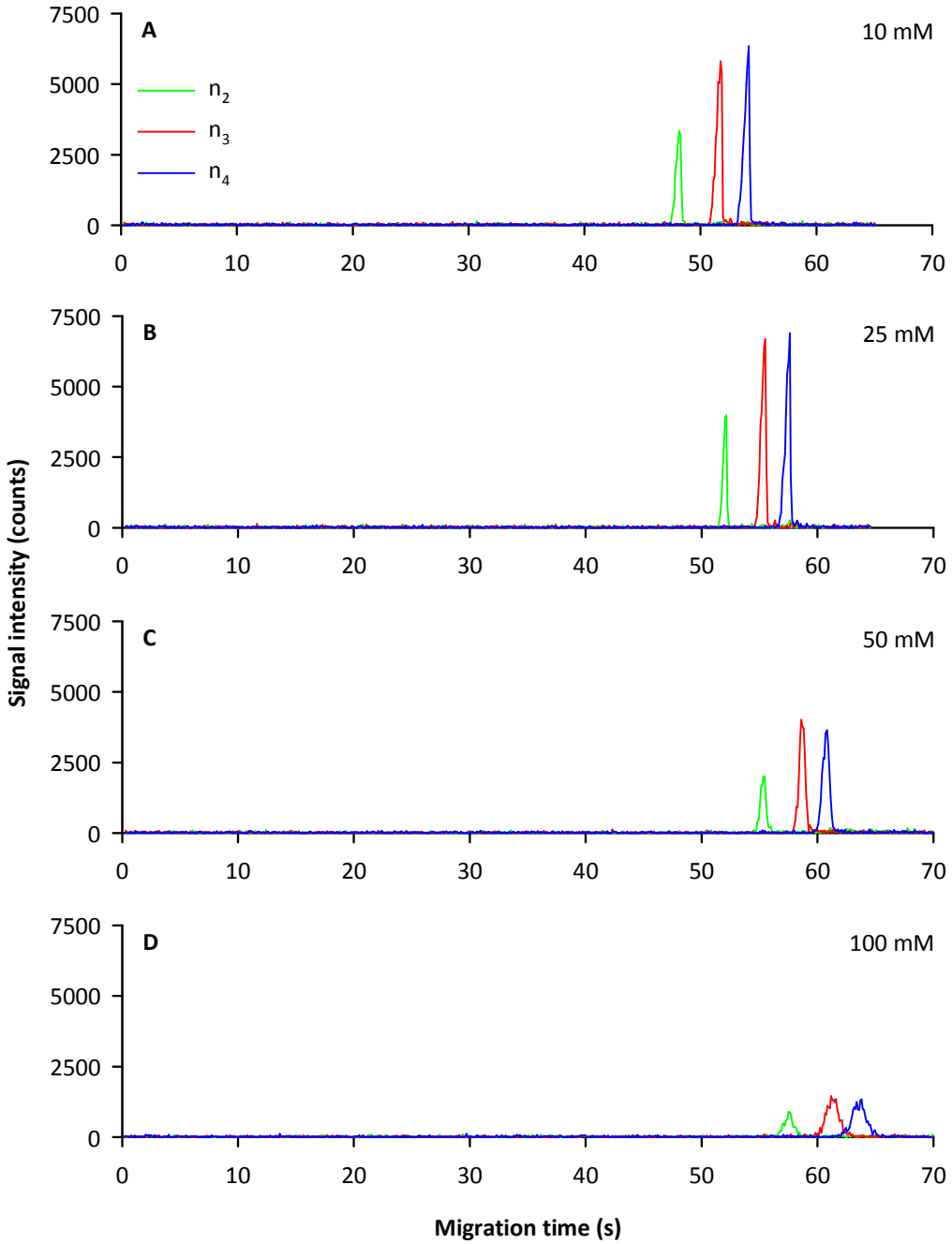

Figure 3.9: Comparison of background electrolytes of 10 mM (A), 25 mM (B), 50 mM (C), and 100 mM (E) ammonium acetate, all adjusted to a pH of 8.5 by addition of ammonia. Oligosaccharide standards at 20 µM. Injection zone: 2% of the capillary. Fused silica capillary with a length of 28 cm and an inner diameter of 15 µm. Separation voltage: 35 kV. Spectra rate: 10 Hz. Reproduced and adapted from Fig. 4 of the original publication[1] with kind permission from Springer Science and Business Media.

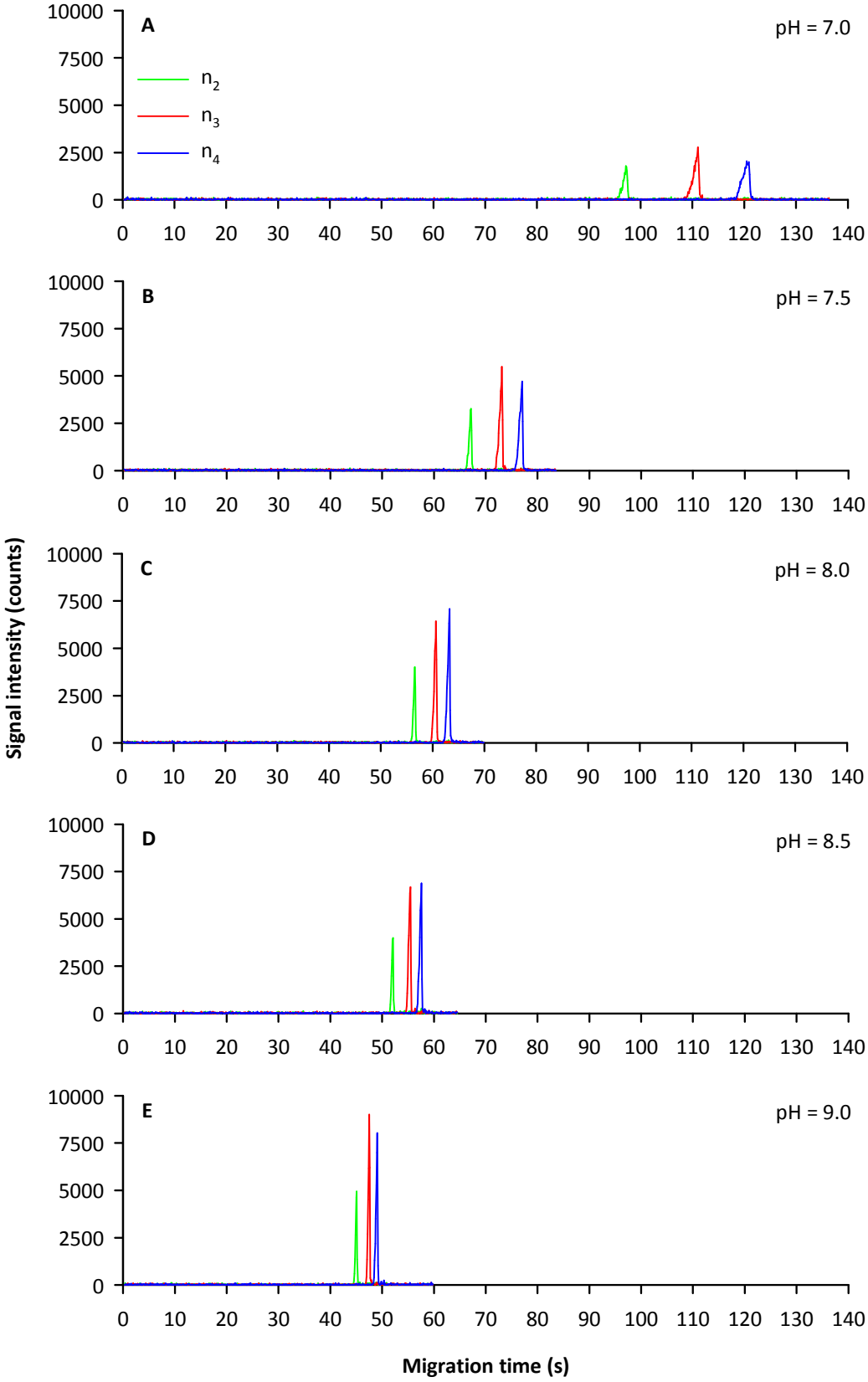

Figure 3.10: Comparison of background electrolytes adjusted to pH values of 7.0 (A), 7.5 (B), 8.0 (C), 8.5 (D), and 9.0 (E), ammonium acetate concentration was 25 mM. Oligosaccharide standards at 20 µM. Injection zone: 2% of the capillary. Fused silica capillary with a length of 28 cm and an inner diameter of 15 µm. Separation voltage: 35 kV. Spectra rate: 10 Hz. Reproduced and adapted from Fig. 5 of the original publication[1] with kind permission from Springer Science and Business Media.

Owing to low inner diameter and short length of the capillary, a broad concentration range of the background electrolyte can be used at high electric field strengths without running the risk of extensively high currents. Nevertheless, Figure 3.9 illustrates a decrease in signal intensities and significant peak broadening with 50 mM and 100 mM ammonium acetate. This unexpected effect seems to arise from resistive heating. In contrast, an interaction of ions of the background electrolyte with the mass spectrometric detection of the analyte anions seems less probable with regard to constant peak areas. At ammonium acetate concentrations of 10 mM and 25 mM, no difference in signal intensities was observed. Providing a higher buffer capacity, 25 mM ammonium acetate solution was chosen as background electrolyte.

Comparison of different pH values, depicted in Figure 3.10, confirmed the findings from the respective CE–UV experiment (*cf*. Figure 3.4). Increasing pH values resulted in higher signal intensities and shorter migration times, whereas separation efficiency was reduced. Thus, the choice of a pH value of 8.5 as compromise, already described in Section 3.3.1, was corroborated.

3.3.6 Characterization of the optimized method

According to the results of the CZE optimization, a 15 µm × 28 cm capillary and a background electrolyte of 25 mM ammonium acetate at a pH = 8.5 were chosen for further characterization. Under these conditions, mixtures containing 1, 2, 4, 10, 20, and 40 µM of each of the three standard oligosaccharides (n_2–n_4) were separated. Five consecutive separations were conducted for each concentration. As a result, linear calibration curves were obtained with coefficients of determination (R^2) in a range of 0.993–0.997 for the three standard substances. Limit of detection (LOD) and limit of quantification (LOQ) were estimated from the signal-to-noise ratio (S/N) of the lowest concentration measured. From the average S/N for 1 mM standard oligosaccharide mixture, LOD and LOQ were calculated as S/N = 3 and S/N = 10, respectively. Exact values are listed in Table 3.2.

Although concentration ranges of 0.46–0.76 µM for LOD and 1.54–2.54 µM for LOQ seem rather high at first sight, the injection volume should be considered. For an injection zone of 2% of the total capillary length and this particular capillary, the volume of the sample can be calculated as a cylinder with a radius of 7.5 µm and a height/length of 5.6 mm. Accordingly 990 pL were injected. In view of this extremely low sample volume, the concentrations for LOD and LOQ can be converted into absolute amounts of 0.46–0.75 fmol and 1.53–2.51 fmol, respectively. Hence, CZE–ESI-TOF-MS is perfectly suited for the analysis of small sample volumes but disadvantageous for the investigation of highly diluted samples.

Additionally, the repeatability of the method was examined. With regard to the migration times, values for all 30 separations performed for linearity studies were included. Mean and standard deviation for peak heights and peak areas, in contrast, were calculated from 5 consecutive measurements using a 1 µM solution of the standard analytes. These results are also shown in Table 3.2. An interesting detail is the relatively high standard deviation for peak height and peak area of n_3 in comparison to the other oligosaccharides. This can be explained by the observation of two differently charged species ($[M-H]^-$ and $[M-2H]^{2-}$ ions) for the hexasaccharide. The ratio of the two ions, which are detected with different sensitivity, shows certain variability.

Table 3.2: Limit of detection, limit of quantification, calibration parameters, and repeatability of the optimized CZE–ESI-TOF-MS method (n_x: oligosaccharides consisting of *x* hyalobiuronic acid moieties).

	n_2	**n_3**	**n_4**
LOD, LOQ, calibration parameters			
Limit of detection, LOD, S/N = 3, given as sample concentration (µM)	0.76	0.52	0.46
Limit of detection, LOD, S/N = 3, given as total amount injected (fmol)	0.75	0.51	0.46
Limit of quantification, LOQ, S/N = 10, given as sample concentration (µM)	2.54	1.72	1.54
Limit of quantification, LOQ, S/N = 10, given as total amount injected (fmol)	2.51	1.71	1.53
Linear range investigated, given as sample concentration (µM)	1–40	1–40	1–40
Coefficient of determination, R^2	0.997	0.997	0.993
Repeatability			
Migration time (s): mean ± SD (RSD), *N* = 30	44.30 ± 0.39 (0.88%)	46.69 ± 0.45 (0.96%)	48.17 ± 0.50 (1.04%)
Peak height (counts): mean ± SD (RSD), standards at 10 µM, *N* = 5	1936 ± 136 (7.02%)	2992 ± 430 (14.37%)	3727 ± 108 (2.90%)
Peak area (counts · s): mean ± SD (RSD), standards at 10 µM, *N* = 5	637.4 ± 68.5 (10.75%)	1070.3 ± 221.2 (20.67%)	1360.8 ± 79.2 (5.82%)

It should be emphasized that migration times of all three standard oligosaccharides were less than 50 s, although the anionic analytes show counter-electroosmotic migration. Therefore, the method promised to allow for high throughput as well as fast at-line analysis of hyaluronidase action.

3.3.7 Application to a complex hyaluronan oligosaccharide mixture

For optimization purposes, a mixture of three defined standard oligosaccharides of 2–4 hyalobiuronic acid moieties had been used. To assess the newly developed method for its ability for separation and detection of a broad variety of hyaluronan oligosaccharides, a complex mixture (Hyalo-Oligo) was analyzed. A concentrated solution of the mixture was injected and separated as described but using a 25 µm instead of a 15 µm capillary. For unknown samples, the expected *m/z* cannot be predicted. The most feasible approach to this problem is the visualization of the results in a density plot. Therein, mass-to-charge ratios are plotted versus migration time. The intensity of each signal is reflected by a color scale. A density plot for the oligosaccharide mixture, including assignment of the detected signals, is depicted in Figure 3.11.

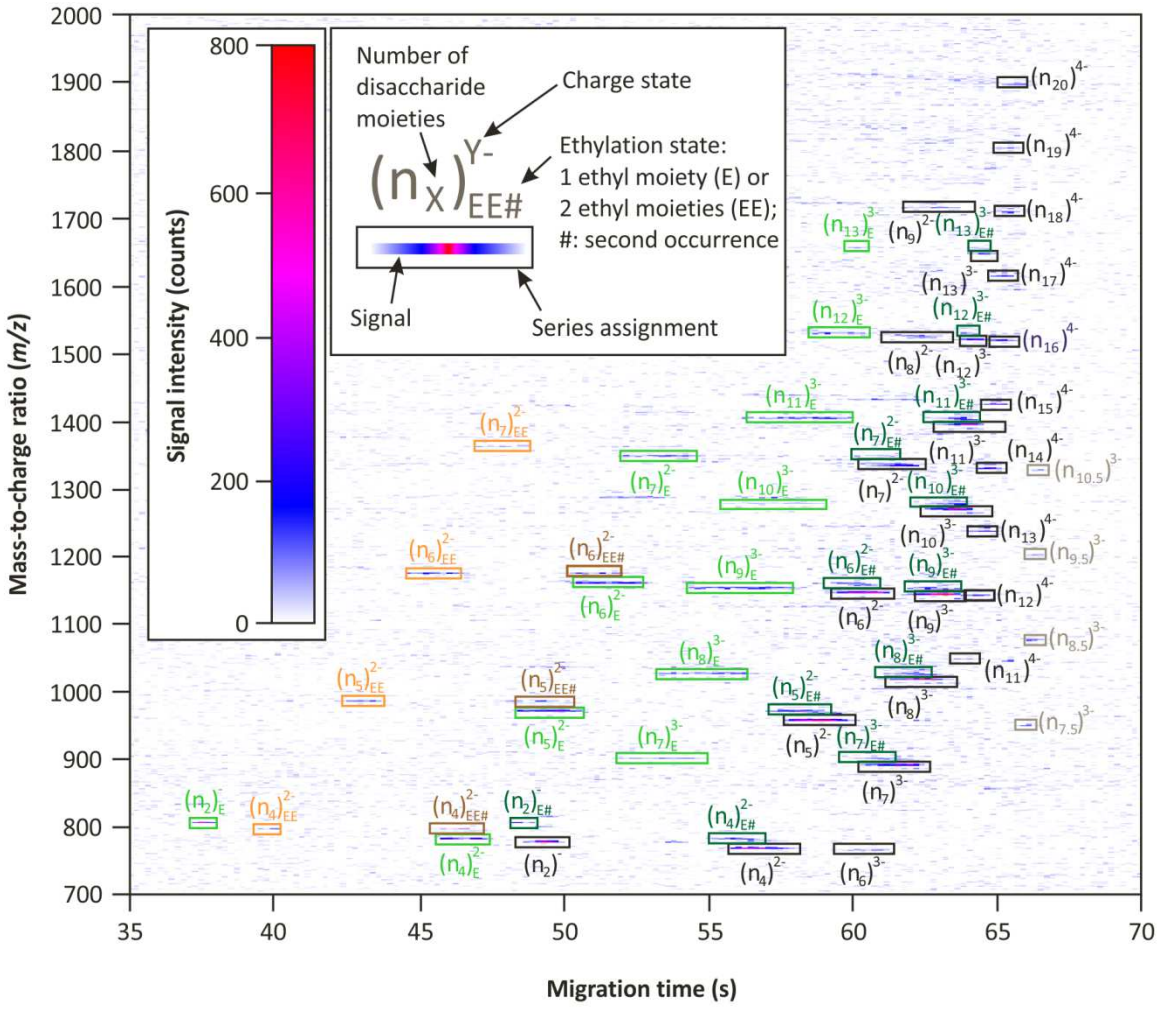

Figure 3.11: Density plot visualizing the separation of a complex mixture of hyaluronan oligosaccharides. CZE conditions: 25 µm × 28 cm capillary, ammonium acetate background electrolyte (25 mM, pH = 8.5), 35 kV. Analytes are designated according to the number of disaccharide units and charge state. Black: normal oligosaccharides consisting of an integer number of hyalobiuronic acid moieties. Grey: oligosaccharides lacking one *N*-acetyl-D-glucosamine moiety. Green: oligosaccharides with an additional ethyl substitution in two series (light and dark green). Orange and brown: two series of di-ethylated species.

In this mixture, multiple homologous series of hyaluronan oligosaccharide species were identified in charge states from −1 to −4. As expected, the most prominent signals corresponded to the normal oligosaccharides consisting of an integer number (namely 2–20) of disaccharide units (*cf.* Figure 3.11, black rectangles). However, to a certain extent, additional species were detected. Some oligosaccharides consisted of an odd number of monosaccharides, lacking an *N*-acetyl-D-glucosamine moiety (*cf.* Figure 3.11, grey rectangles). Probably due to the increased relative content of negatively charged glucuronic acid moieties, these substances showed faster migration against the electroosmotic flow, compared to the respective even-numbered oligosaccharides.

The opposite effect was observed for the mono- (*cf.* Figure 3.11, light and dark green rectangles) and di-ethylated (*cf.* Figure 3.11, orange and brown rectangles) oligosaccharides present in the mixture, possibly due to esterification. Interestingly, species of both ethylation states (mono- and di-ethylated) each gave two series of signals, marked in different colors. Mass spectra of the corresponding signals from these two series showed no differences. Consequently, it may be assumed that variations in migration times originate from different hydrodynamic radii, depending on the respective position of ethylation. In spite of many benefits of ESI-TOF-MS with regard to the challenging detection of hyaluronan oligosaccharides, this particular mass spectrometric detection is insufficient to discriminate between isomers. Nevertheless, the existence of isomers in the mixture was proven by combination with a complementary separation method (CZE). Hence, this example clearly illustrates the advantages of hyphenated techniques.

3.3.8 Acarbose as internal standard for at-line analysis

Aiming at fast qualitative and quantitative at-line monitoring of hyaluronan and hyaluronan degradation by hyaluonidases, an internal standard had to be selected. Acarbose was found to be a suitable reference (*cf*. Section 3.2.2). Preliminary experiments (not shown) suggested a 1:10 dilution of incubation mixtures with water to avoid peak broadening caused by high ionic strength of the sample. Further pretreatment of the samples containing buffer salts and bovine serum albumin (*cf*. Chapter 6 for details) was unnecessary. Therefore, the following studies explored the effect on separation when using a 100 µM solution of acarbose instead of water for the dilution of the analytes (Figure 3.12). To allow for a fast pressure-free injection protocol, a capillary with an inner diameter of 25 µm was used.

Firstly, the standard oligosaccharides were injected in aqueous solution (Figure 3.12 A). Secondly, acarbose was added at a final concentration of 90 µM (Figure 3.12 B). Thirdly, a typical incubation buffer was added at a concentration equal to a 1:10 dilution of an aliquot from a real incubation mixture (Figure 3.12 C). Finally, this experiment was repeated using MS parameter settings optimized for small oligosaccharides (Figure 3.12 D). For each series,

ten consecutive injections were carried out ($N = 10$). One representative electropherogram from each series is depicted.

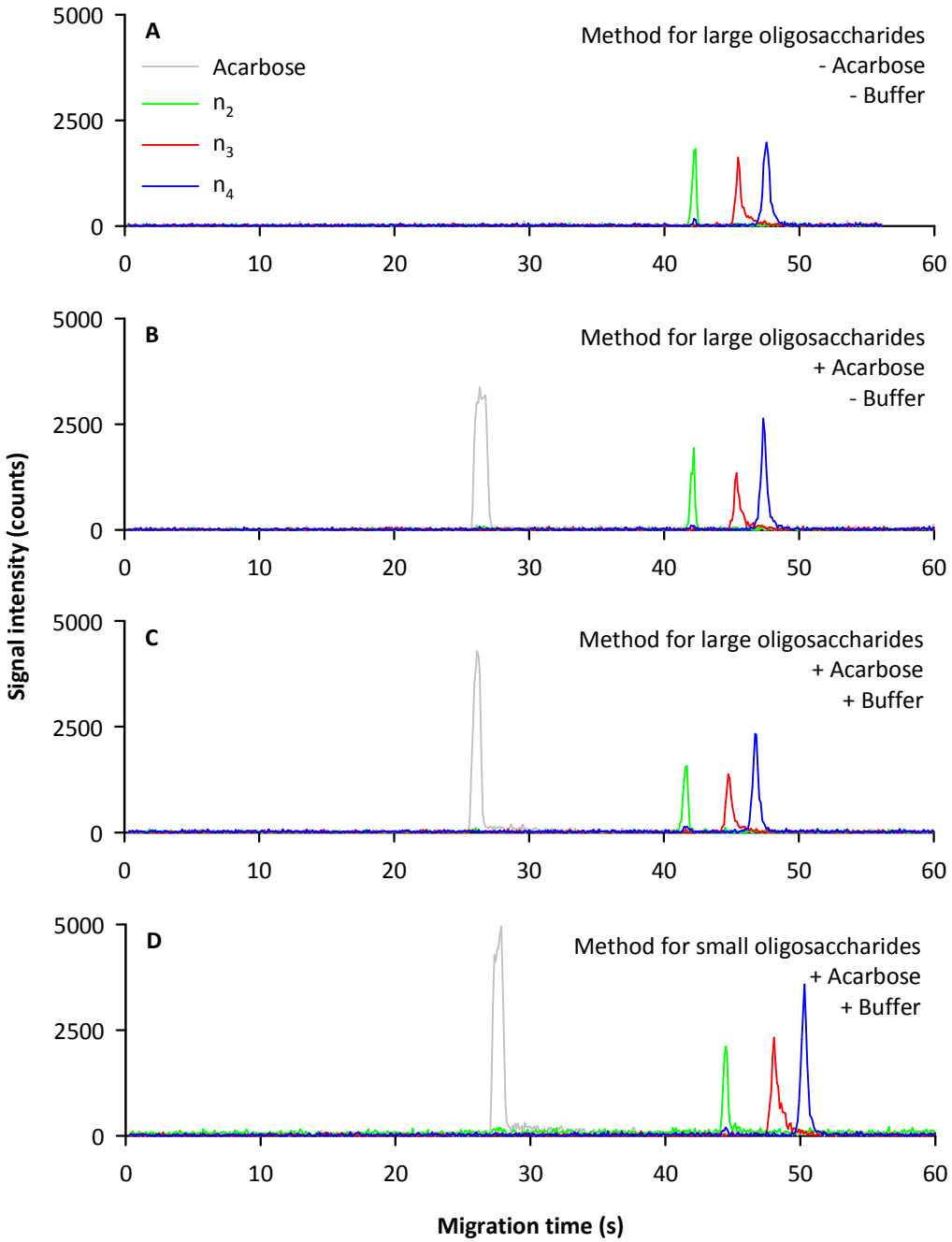

Figure 3.12: Acarbose (90 µM) as internal standard. Oligosaccharides (n_2–n_4) at a concentration of 16.7 µM. Injection (2% of capillary length): aqueous solution (A), additionally containing acarbose (B), containing both acarbose and incubation buffer (C, D). Experiment D was performed with MS parameters optimized for *m/z* values of small oligosaccharides. Separation conditions: 25 µm × 28 cm capillary, ammonium acetate background electrolyte (25 mM, pH = 8.5), 35 kV.

Apparently, neither the addition of acarbose as internal standard nor the matrix components from the incubation mixtures affected the separation and detection of the oligosaccharides. The internal standard was well separated from the analyte peaks. Moreover, the short migration time of acarbose, compared to the analytes, is of paramount importance with

regard to fast analysis. Hence, the total run time is not prolonged by using this substance as internal standard. In the following step, standardization was achieved by dividing peak heights and peak areas by the respective value for the acarbose peak. Means, standard deviations, and relative standard deviations were calculated (Table 3.3).

Table 3.3: Acarbose as internal standard. Standardization of peak height and peak area. Experiments from Figure 3.12: aqueous solution (A), additionally containing acarbose (B), containing both acarbose and incubation buffer (C, D). Experiment D was performed with MS parameters optimized for small oligosaccharides. Each series consisted of 10 consecutive injections (*N* = 10).

	A (*N* = 10)	**B (*N* = 10)**	**C (*N* = 10)**	**D (*N* = 10)**
Tetrasaccharide (n_2)				
Height (counts): mean ± SD (RSD)	1742 ± 123 (7.05%)	1705 ± 159 (9.34%)	1453 ± 84 (5.81%)	2316 ± 265 (11.42%)
Height ratio: mean ± SD (RSD)	—	0.51 ± 0.04 (8.40%)	0.34 ± 0.02 (7.19%)	0.37 ± 0.05 (12.55%)
Area (counts · s): mean ± SD (RSD)	618 ± 50 (8.07%)	612 ± 38 (6.13%)	591 ± 54 (9.18%)	1043 ± 125 (12.00%)
Area ratio: mean ± SD (RSD)	—	0.19 ± 0.01 (5.44%)	0.22 ± 0.02 (10.14%)	0.22 ± 0.02 (8.46%)
Hexasaccharide (n_3)				
Height (counts) mean ± SD (RSD)	1276 ± 372 (29.14%)	1267 ± 168 (13.27%)	1278 ± 198 (15.51%)	2719 ± 353 (12.99%)
Height ratio: mean ± SD (RSD)	—	0.38 ± 0.05 (12.57%)	0.29 ± 0.03 (10.70%)	0.43 ± 0.05 (12.33%)
Area (counts · s): mean ± SD (RSD)	772 ± 62 (8.03%)	781 ± 60 (7.74%)	748 ± 55 (7.32%)	1786 ± 231 (12.91%)
Area ratio: mean ± SD (RSD)	—	0.24 ± 0.02 (6.21%)	0.28 ± 0.02 (7.98%)	0.37 ± 0.03 (7.39%)
Octasaccharide (n_4)				
Height (counts): mean ± SD (RSD)	2075 ± 271 (13.04%)	2373 ± 211 (8.88%)	2175 ± 262 (12.03%)	4047 ± 431 (10.65%)
Height ratio: mean ± SD (RSD)	—	0.71 ± 0.07 (9.50%)	0.50 ± 0.06 (11.14%)	0.65 ± 0.07 (10.54%)
Area (counts · s): mean ± SD (RSD)	1248 ± 136 (10.92%)	1330 ± 102 (7.69%)	1201 ± 90 (7.53%)	2063 ± 243 (11.79%)
Area ratio: mean ± SD (RSD)	—	0.41 ± 0.03 (6.04%)	0.44 ± 0.03 (7.08%)	0.43 ± 0.03 (8.06%)

From the relative standard deviations it becomes obvious that, within a series of consecutive injections (under identical conditions), standardization is beneficial with regard to repeatability. Moreover, comparison of the different sets of experiments (under different conditions) also revealed well comparable results for the area ratios. The only exception was observed for n_3, comparing MS settings optimized for different *m/z* ranges. As already described in Section 3.3.6, this oligosaccharide was observed in two differently charged states. Obviously, a method detecting both species with high sensitivity (D) leads to higher signals for the n_3 than a method which is less efficient in detecting the $[M-2H]^{2-}$ ion with its lower *m/z* ratio (A–C).

3.4 Summary and conclusion

A fast capillary zone electorophoresis (CZE) method coupled to electrospray ionization time-of-flight mass spectrometry (ESI-TOF-MS) was established for the analysis of oligosaccharide fragments derived from hyaluronan. Best results were achieved using fused silica capillaries with an inner diameter of 15 µm and a length of 28 cm, the shortest length possible with the experimental setup used. Applying a constant voltage of 35 kV, an electric field strength of 1.25 kV/cm was achieved. As background electrolyte, a 25 mM solution of ammonium acetate was adjusted to a pH of 8.5 to allow for fast separations with good separation efficiency. The method was further characterized, revealing an LOD of 0.46–0.76 µM and an LOQ of 1.54–2.54 µM with regard to aqueous solutions of the different standard oligosaccharides. These values correspond to absolute amounts in the fmol range because a volume of only 990 pL (2% of the capillary length) had been injected.

Standard analytes consisting of 2–4 hyalobiuronic acid moieties and even a complex mixture of hyaluronan oligosaccharides were separated within less than 70 s. The benefit of the hyphenation was demonstrated by analysis of this complex mixture. Probably, no detection method would have been able to provide as much information on the identity of the different oligosaccharides in the mixture as mass spectrometry. However, the used ESI-TOF-MS has its limits with regard to discrimination between isomers (due to identical *m/z* ratio). In this case, additional information on the composition of the oligosaccharide mixture was obtained in combination with CZE. Thus, hyphenation of two complementary analytical methods makes CZE–ESI-TOF-MS a very powerful tool for the determination of these challenging analytes. In preparation of later at-line analysis, capillary inner diameter was increased to 25 µm to allow for a faster manual injection. Acarbose was established as internal standard. As samples from incubation mixtures can be injected directly after 1:10 dilution with an aqueous solution of the internal standard, this protocol allows for fast at-line monitoring of hyaluronidase activity. Moreover, recent developments in injection

procedures for small sample volumes are very promising for further acceleration and future automation.[32]

3.5 References

1. Grundmann, M.; Rothenhöfer, M.; Bernhardt, G.; Buschauer, A.; Matysik, F. M. Fast counter-electroosmotic capillary electrophoresis–time-of-flight mass spectrometry of hyaluronan oligosaccharides. *Anal. Bioanal. Chem.* **2012,** 402, 2617-2623.

2. Grundmann, M. Concepts for the analysis of very small samples and fast capillary electrophoresis coupled to mass spectrometry. PhD thesis, University of Regensburg, Regensburg, **2012**.

3. Grimshaw, J. Analysis of glycosaminoglycans and their oligosaccharide fragments by capillary electrophoresis. *Electrophoresis* **1997,** 18, 2408-2414.

4. Grimshaw, J.; Kane, A.; Trocha-Grimshaw, J.; Douglas, A.; Chakravarthy, U.; Archer, D. Quantitative analysis of hyaluronan in vitreous humor using capillary electrophoresis. *Electrophoresis* **1994,** 15, 936-940.

5. Grimshaw, J.; Trocha-Grimshaw, J.; Fisher, W.; Rice, A.; Smith, S.; Spedding, P.; Duffy, J.; Mollan, R. Quantitative analysis of hyaluronan in human synovial fluid using capillary electrophoresis. *Electrophoresis* **1996,** 17, 396-400.

6. Pattanaargson, S.; Roboz, J. Determination of hyaluronidase activity in venoms using capillary electrophoresis. *Toxicon* **1996,** 34, 1107-1117.

7. Hayase, S.; Oda, Y.; Honda, S.; Kakehi, K. High-performance capillary electrophoresis of hyaluronic acid: determination of its amount and molecular mass. *J. Chromatogr. A* **1997,** 768, 295-305.

8. Kinoshita, M.; Okino, A.; Oda, Y.; Kakehi, K. Anomalous migration of hyaluronic acid oligomers in capillary electrophoresis: correlation to susceptibility to hyaluronidase. *Electrophoresis* **2001,** 22, 3458-3465.

9. Matsuno, Y. K.; Kakoi, N.; Kinoshita, M.; Matsuzaki, Y.; Kumada, J.; Kakehi, K. Electrophoresis studies on the contaminating glycosaminoglycans in commercially available hyaluronic acid products. *Electrophoresis* **2008,** 29, 3628-3635.

10. Park, Y.; Cho, S.; Linhardt, R. J. Exploration of the action pattern of *Streptomyces* hyaluronate lyase using high-resolution capillary electrophoresis. *Biochim. Biophys. Acta* **1997,** 1337, 217-226.

11. Volpi, N.; Maccari, F.; Linhardt, R. J. Capillary electrophoresis of complex natural polysaccharides. *Electrophoresis* **2008,** 29, 3095-3106.

12. Hong, M.; Sudor, J.; Stefansson, M.; Novotny, M. V. High-resolution studies of hyaluronic acid mixtures through capillary gel electrophoresis. *Anal. Chem.* **1998,** 70, 568-573.

13. Hutterer, K. M.; Jorgenson, J. W. Separation of hyaluronic acid by ultrahigh-voltage capillary gel electrophoresis. *Electrophoresis* **2005,** 26, 2027-2033.

14. Hofinger, E. S. A.; Bernhardt, G.; Buschauer, A. Kinetics of Hyal-1 and PH-20 hyaluronidases: comparison of minimal substrates and analysis of the transglycosylation reaction. *Glycobiology* **2007,** 17, 963-971.

15. Hofinger, E. S. A.; Hoechstetter, J.; Oettl, M.; Bernhardt, G.; Buschauer, A. Isoenzyme-specific differences in the degradation of hyaluronic acid by mammalian-type hyaluronidases. *Glycoconj. J.* **2008,** 25, 101-109.

16. Zaia, J. On-line separations combined with MS for analysis of glycosaminoglycans. *Mass Spectrom. Rev.* **2009,** 28, 254-272.

17. Kühn, A. V.; Ozegowski, J. H.; Peschel, G.; Neubert, R. H. Complementary exploration of the action pattern of hyaluronate lyase from *Streptococcus agalactiae* using capillary electrophoresis, gel-permeation chromatography and viscosimetric measurements. *Carbohydr. Res.* **2004,** 339, 2541-2547.

18. Kühn, A. V.; Rüttinger, H. H.; Neubert, R. H.; Raith, K. Identification of hyaluronic acid oligosaccharides by direct coupling of capillary electrophoresis with electrospray ion trap mass spectrometry. *Rapid Commun. Mass Spectrom.* **2003,** 17, 576-582.

19. Hjertén, S.; Valtcheva, L.; Elenbring, K.; Liao, J. L. Fast, high-resolution (capillary) electrophoresis in buffers designed for high field strengths. *Electrophoresis* **1995,** 16, 584-594.

20. Hutterer, K. M.; Jorgenson, J. W. Ultrahigh-voltage capillary zone electrophoresis. *Anal. Chem.* **1999,** 71, 1293-1297.

21. Palonen, S.; Jussila, M.; Porras, S. P.; Hyötyläinen, T.; Riekkola, M. L. Extremely high electric field strengths in non-aqueous capillary electrophoresis. *J. Chromatogr. A* **2001,** 916, 89-99.

22. Palonen, S.; Jussila, M.; Porras, S. P.; Hyötyläinen, T.; Riekkola, M. L. Nonaqueous capillary electrophoresis with alcoholic background electrolytes: separation efficiency under high electrical field strengths. *Electrophoresis* **2002,** 23, 393-399.

23. Henley, W. H.; Jorgenson, J. W. Ultra-high voltage capillary electrophoresis >300kV: Recent advances in instrumentation and analyte detection. *J. Chromatogr. A* **2012,** 1261, 171-178.

24. Kennedy, R. T. Bioanalytical applications of fast capillary electrophoresis. *Anal. Chim. Acta* **1999,** 400, 163-180.

25. Matysik, F. M. Capillary batch injection – a new approach for sample introduction into short-length capillary electrophoresis with electrochemical detection. *Electrochem. Commun.* **2006,** 8, 1011-1015.

26. Matysik, F. M.; Neusüß, C.; Pelzing, M. Fast capillary electrophoresis coupled with time-of-flight mass spectrometry under separation conditions of high electrical field strengths. *Analyst* **2008,** 133, 1764-1766.

27. Müller, O.; Minarik, M.; Foret, F. Ultrafast DNA analysis by capillary electrophoresis/laser-induced fluorescence detection. *Electrophoresis* **1998,** 19, 1436-1444.

28. Opekar, F.; Coufal, P.; Štulík, K. Rapid capillary zone electrophoresis along short separation pathways and its use in some hyphenated systems: a critical review. *Chem. Rev.* **2009,** 109, 4487-4499.

29. Grundmann, M.; Matysik, F. M. Fast capillary electrophoresis−time-of-flight mass spectrometry using capillaries with inner diameters ranging from 75 to 5 µm. *Anal. Bioanal. Chem.* **2011,** 400, 269-278.

30. Pittman, J. L.; Schrum, K. F.; Gilman, S. D. On-line monitoring of electroosmotic flow for capillary electrophoretic separations. *Analyst* **2001,** 126, 1240-1247.

31. König, S.; Fales, H. M. Calibration of mass ranges up to *m/z* 10,000 in electrospray mass spectrometers. *J. Am. Soc. Mass Spectrom.* **1999,** 10, 273-276.

32. Grundmann, M.; Matysik, F. M. Analyzing small samples with high efficiency: capillary batch injection–capillary electrophoresis–mass spectrometry. *Anal. Bioanal. Chem.* **2012,** 404, 1713-1721.

4 HPAEC–PAD for sensitive determination of hyaluronan oligosaccharides up to 10 kDa

4.1 Introduction

High performance anion exchange chromatography (HPAEC), sometimes also termed high pH anion exchange chromatography, is commonly used for the analysis of saccharides in food and beverage[1-8] as well as for the elucidation of protein glycosylation patterns.[9-11] Moreover, the method was reported to be a useful tool for studies on saccharide-metabolizing enzymes.[12-14] The first separation of hyaluronan oligosaccharides by ion exchange was described by Weissmann et al. in 1954.[15] Since then, various liquid chromatography conditions, using UV absorbance[16-20] or pulsed amperometric[21-23] detection (PAD), were reported for hyaluronan oligosaccharides.

UV detection of hyaluronan oligosaccharides, especially those produced by mammalian hyaluronidases (*cf*. Chapter 1), is only possible at very short wavelengths. PAD enables more sensitive analytical studies of such compounds. Separation of the acidic oligosaccharides can be achieved by anion exchange chromatography under alkaline conditions (Figure 4.1 A–D). The particularity of the following pulsed amperomety is the sequential application of different potentials. In case of the triple pulse sequence, the detection potential is followed by oxidative cleaning and reductive electrode regeneration (Figure 4.1 E).

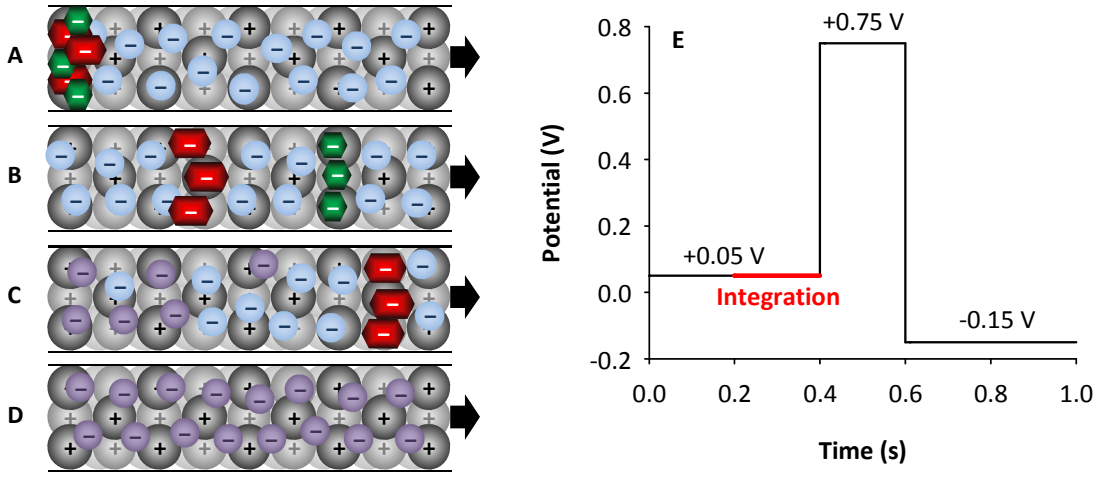

Figure 4.1: Principle of HPAEC–PAD. Column containing cationic solid phase material is preconditioned with anionic (alkaline) eluent when sample is injected (A). Analytes are then separated due to differences in ionic interaction with the stationary phase (B). A gradient from weak to strong eluent is applied to elute all the analytes from the column (C). At the end of the separation, all analytes have been eluted and the column is filled with the strong eluent (D). Detection is achieved by a pulsed amperometric method (E). The potential used for oxidation of the analytes (signal integration) is followed by an oxidative cleaning step and reductive regeneration of the electrode surface.

Previously reported conditions for ion exchange chromatography often required long run times.[16-18, 21] Hence, based on the reported methods we systematically studied the influence of various parameters on separation, aiming at optimization for qualitative and quantitative analysis of small oligosaccharides. In addition, method development was also directed towards the determination of the size distribution of hyaluronan oligosaccharide mixtures. Both aspects are necessary for the characterization of different hyaluronidases with regard to substrate and product spectra, cleavage mechanisms, and kinetic parameters.

4.2 Materials and methods

4.2.1 Oligosaccharide standards and sample preparation

Oligosaccharide standards (oligoHA from Hyalose, Oklahoma City, OK, USA) were purchased from AMSBIO (Abingdon, UK). A standard mixture containing 20 µM (5 µM for comparison of columns) of each oligosaccharide was used. Hyalo-Oligo, a low molecular weight hyaluronan oligosaccharide mixture with an average molecular weight below 10 kDa, was kindly provided by Kewpie (also named Q. P. Corp., Tokyo, Japan). Standards were dissolved in water, purified with a Milli-Q system (Millipore, Eschborn, Germany). From incubation mixtures (*cf*. Chapter 6, Section 6.2.2 for exact composition), protein was removed by boiling for 15 min, centrifugation at 13000 × *g* for 10 min, and filtration through a Phenex-NY 4 mm syringe filter 0.2 µm (Phenomenex, Aschaffenburg, Germany).

4.2.2 Preparation and storage of eluents

A 1 M sodium hydroxide solution was freshly prepared, using water purified with a Milli-Q system (Millipore, Eschborn, Germany) and a 50% (w/v) sodium hydroxide solution (Mallinckrodt Baker, Griesheim, Germany). For the second eluent, solid sodium acetate (electrochemical grade, Dionex/Thermo Fisher Scientific, Idstein, Germany) was dissolved in purified water and filtrated through an Express^{TM} PLUS 0.22 µm bottle top filter (Merck-Millipore, Darmstadt, Germany). Afterwards, a suitable amount of 50% (w/v) sodium hydroxide solution (Mallinckrodt Baker, Griesheim, Germany) was added to reach a final concentration of 1 M sodium acetate and 100 mM sodium hydroxide. Purified water served as third component for different eluent compositions. Prior to usage, all eluents were degassed with helium and, during chromatography, always kept under helium to avoid dissolution of oxygen and carbon dioxide.

4.2.3 Instrumentation and chromatography conditions

Chromatography was carried out on a Dionex DX-600 system, consisting of an AS50 autosampler (temperature set to 10 °C) and column compartment, GS50 gradient pump, and ED50 electrochemical detector for pulsed amperometric detection (Dionex/Thermo Fisher Scientific, Idstein, Germany). The chromatography system was equipped with a CarboPac™ PA100 guard (2 mm × 50 mm) and analytical column (2 mm × 250 mm) or a CarboPac™ PA200 guard (3 mm × 50 mm) and analytical column (3 mm × 250 mm), respectively. All columns were from Dionex/Thermo Fisher Scientific (Idstein, Germany). Chromatograms were evaluated with the included software PeakNet 6.30 SP1 Build 587.

Prior to sample application, the column was equilibrated for 10 min. In general, injection volumes were 5 µL or 10 µL. For all separations, constant concentrations of sodium hydroxide and various linear sodium acetate gradients of 20 min were used. The final eluent composition was kept constant for additional 10 min. Detailed information on the separation parameters are given with the chromatograms.

4.2.4 Electrochemical detector settings

A gold electrode served as working electrode and potentials were measured against a silver/silver chloride reference electrode. Data were acquired at a rate of 1 Hz with a standard triple pulse sequence (Figure 4.1 E) for carbohydrates, characterized by the following electric potentials and durations: E_1 = +0.05 V for 0.4 s (integrating from 0.2 s to 0.4 s), E_2 = +0.75 V (0.2 s), and E_3 = −0.15 V (0.4 s).

4.2.5 Assessment of analyte stability by CZE–ESI-TOF-MS

Studies on analyte stability and formation of chemical degradation products under alkaline conditions were performed by dissolution of the standard oligosaccharides in sodium hydroxide solution, prepared from 50% sodium hydroxide solution (HPLC–MS grade, Sigma-Aldrich, Munich, Germany). Samples were analyzed by HPAEC–PAD and in part by the CZE–ESI-TOF-MS method described in Chapter 3.

4.2.6 Size-dependent precipitation of hyaluronan fragments

Precipitation experiments were performed according to the turbidimetric hyaluronidase assay described by Di Ferrante.[24] Solutions of the low molecular weight hyaluronan (HA < 10 kDa) preparation Hyalo-Oligo (Kewpie/Q. P. Corp., Tokyo, Japan) and hyaluronan from *Streptococcus zooepidemicus* (Aqua Biochem, Dessau, Germany) were prepared to yield concentrations of 2 mg/mL. 50 µL of the respective solution (water for blank) were

added to 200 µL of incubation buffer (*cf*. Chapter 6 for details). 100 µL of a solution (0.2 mg/mL) of bovine serum albumin (BSA, Serva, Heidelberg, Germany) were added to samples without enzyme. Otherwise, half of the BSA was replaced by bovine testicular hyaluronidase (BTH, Neopermease®, kindly provided by Sanabo, Vienna, Austria). The enzyme solution had been adjusted to 400 IU/mL (based on the declaration by the supplier) by addition of an appropriate portion of the BSA solution.

The mixtures were incubated at 37 °C for 30 min. 1200 µL of 2.5% (m/v) cetyltrimethylammonium bromide (CTAB, Merck, Darmstadt, Germany), dissolved in 0.5 M sodium hydroxide solution (Carl Roth, Karlsruhe, Germany), were added. Water instead of CTAB was added to the control sample. Turbidity was complete within 20 min at 25 °C and was quantified by measurement of extinction at 600 nm using a CARY 100 photometer (Agilent Technologies, Darmstadt, Germany).

Prior to chromatography, the precipitate was removed by short centrifugation (5 min at 13000 × *g*). Additionally, samples were cleaned from protein by boiling for 5 min, centrifugation for 15 min, and filtration as described (*cf*. Section 4.2.1). Afterwards, the solution was directly injected for HPAEC. Thereby, low temperatures should be avoided to prevent precipitation of residual CTAB and clogging of the chromatography system.

4.3 Results and discussion

4.3.1 Optimization of the sodium hydroxide concentration

Standard eluents for the columns used in this study, recommended by the manufacturer, consist of constant concentration of sodium hydroxide and an additional gradient of sodium acetate. For the analysis of acidic substances, post-column addition of the basic component is often performed alternatively.[22, 23, 25, 26] However, the latter procedure was not possible with the given instrumentation. Therefore, we decided to use a solvent system of sodium hydroxide and sodium acetate.

Figure 3.4 indicates that variation of the sodium hydroxide content from 100 mM to 200 mM did not influence separation, when using the same sodium acetate gradient. However, the sensitivity of the detection decreased with increasing sodium hydroxide concentration. Consequently, a concentration of 100 mM sodium hydroxide was chosen for further method development.

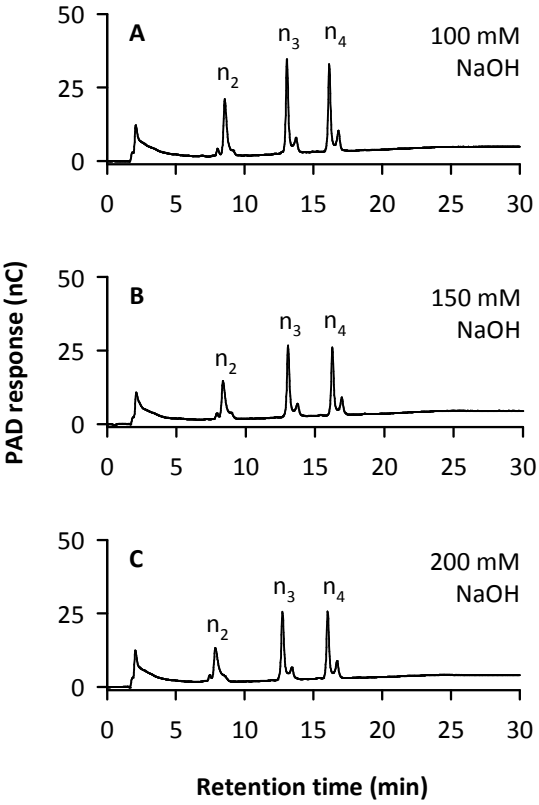

Figure 4.2: Comparison of eluents containing 100 mM (A), 150 mM (B), and 200 mM (C) sodium hydroxide. 5 µL of 20 µM standard mixture (n_2–n_4) injected. Column: CarboPac™ PA100. Gradient: 200–700 mM sodium acetate. Flow: 0.25 mL/min. Temperature: not regulated.

4.3.2 Sodium acetate gradient

With increasing chain length, oligosaccharides show higher affinity to the stationary phase. To elute these strongly bound analytes in an acceptable run time, gradients of the strong eluent sodium acetate are necessary. Keeping the duration of the gradient program constant, the end point composition (Figure 4.3) as well as the initial composition of the eluent (Figure 4.4) was varied.

Increasing the final concentration of the gradient from 700 mM to 900 mM gave sharper peaks. Consequently, the separation was not negatively affected, although retention times were reduced. In contrast, variation of the starting conditions was not beneficial. When chromatography was started with 0 mM sodium acetate, retention times increased without improvement of resolution. With a higher content of sodium acetate (300 mM) in the initial eluent, significant broadening was observed for the tetrasaccharide (n_2) peak. Moreover, this peak was very poorly separated from the signal associated with the void volume under these conditions. A gradient from 200 mM to 900 mM sodium acetate proved to be the optimum.

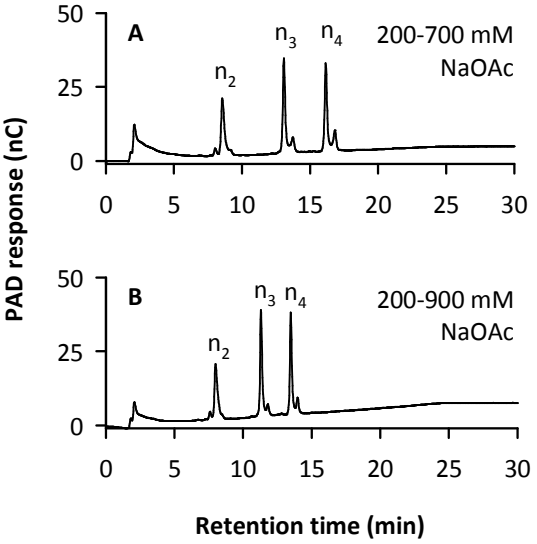

Figure 4.3: Sodium acetate gradients of 200–700 mM (A) and 200–900 mM (B). 5 µL of 20 µM standard mixture (n_2–n_4) injected. Column: CarboPac™ PA100. Sodium hydroxide: 100 mM. Flow: 0.25 mL/min. Temperature: not regulated.

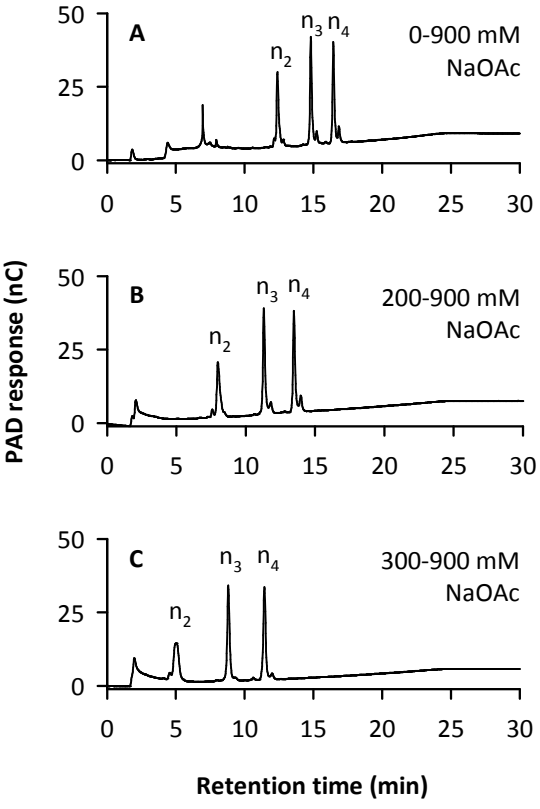

Figure 4.4: Sodium acetate gradients of 0–900 mM (A), 200–900 mM (B), and 300–900 mM (C). 5 µL of 20 µM standard mixture (n_2–n_4) injected. Column: CarboPac™ PA100. Sodium hydroxide: 100 mM. Flow: 0.25 mL/min. Temperature: not regulated.

4.3.3 Column temperature

To this point, all experiments on eluent optimization were performed at ambient temperature without regulation by the column oven. To investigate the influence of the column temperature on separation and analyte stability, chromatography was performed at different temperatures, varied from 15 °C to 40 °C, while all other conditions were kept constant. The resulting chromatograms are depicted in Figure 4.5.

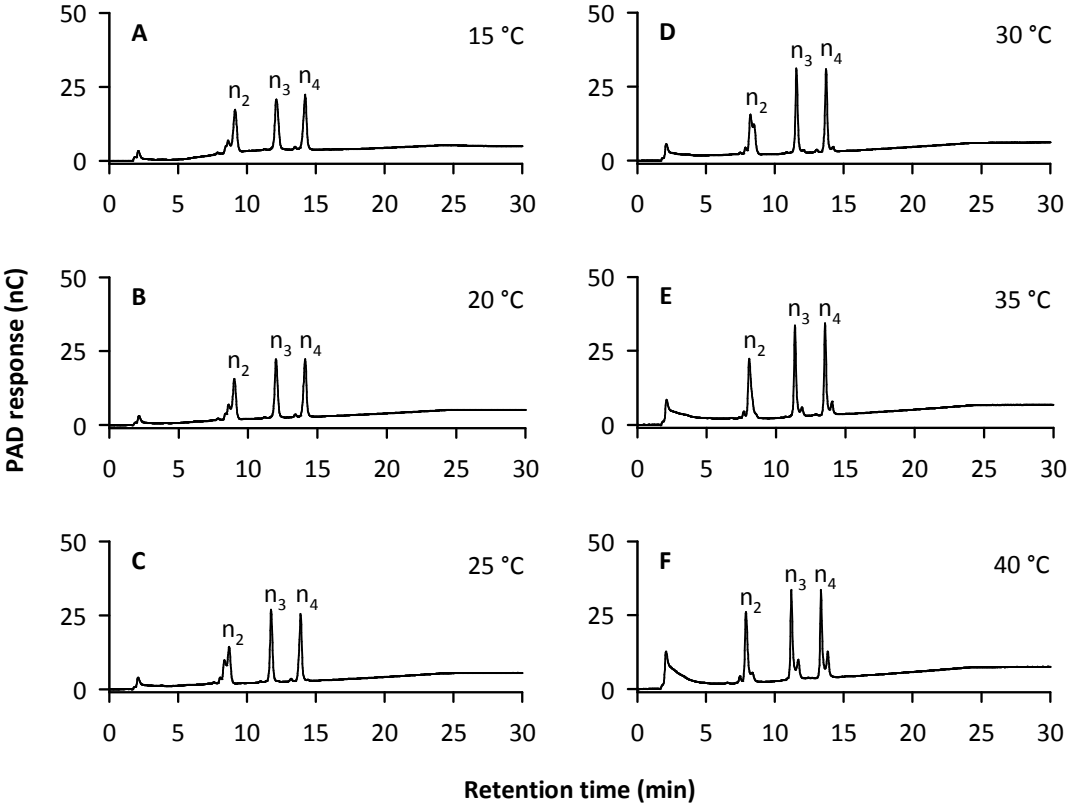

Figure 4.5: Stepwise increase of column temperature from 15 °C (A) to 40 °C (F). 5 µL of 20 µM standard mixture (n_2–n_4) injected. Column: CarboPac™ PA100. Sodium hydroxide: 100 mM. Sodium acetate gradient: 200–900 mM. Flow: 0.25 mL/min.

With increasing column temperature, peaks became sharper. However, the area of the void volume peak increased, and minor peaks, eluting after the main peaks, were detected. Recently, this phenomenon was observed under chromatography conditions different from those used in this work.[16] By mass spectrometry, the authors assigned the minor peaks to *N*-deacetylation products of the standard oligosaccharides, suggesting an enzymatic deacetylation by bovine testicular hyaluronidase.[16]

Although, regarding the study by Chen et al.,[16] an enzymatic mechanism cannot be completely ruled out, the significant increase in the minor peaks at higher temperature (in the present work) strongly suggested a non-enzymatic mechanism resulting in the

corresponding degradation products. Provided that deacetylation occurs, it might be speculated that the increase in the void volume signal resulted from liberated acetate.

In addition, the formation of odd-numbered oligosaccharides was previously described in literature.[18, 20, 23] Only minor changes of the chromatographic properties are to be expected after removal of an *N*-acetyl-D-glucosamine moiety from the oligosaccharide, as the influence of the negatively charged glucuronic acids is probably predominating under the conditions of anion exchange chromatography. Therefore, the oligosaccharides resulting from degradation are expected to elute close to the corresponding even-numbered sugars. Monosaccharides, cleaved off from oligosaccharides, elute with the void volume under the conditions used. Thus, formation of odd-numbered oligosaccharides would equally lead to an increase of the void volume signal.

To scrutinize the formation of minor peaks, stability experiments were performed. The results are discussed in Section 4.3.7.

4.3.4 Comparison of the CarboPac™ PA100 and the CarboPac™ PA200 column at different flow and temperature conditions

In the following optimization step, the CarboPac™ PA100 was compared to the CarboPac™ PA200 column as stationary phase. Separations on CarboPac™ PA100 were thereby conducted at a flow rate of 0.25 mL/min and at low (20 °C) and high (40 °C) temperature. In contrast, the CarboPac™ PA200 column was, in accordance with the manufacturer's specifications, operated at 0.50 mL/min and 40 °C. Due to the occurrence of high pressure, comparative analysis at 20 °C was not possible with the latter column material. Probably, this finding relates to the increasing viscosity of the sodium hydroxide eluent at low temperature. Resolution was enhanced by changing the column from CarboPac™ PA100 to CarboPac™ PA200 as well as by increasing the temperature. Figure 4.6 illustrates these results for the standard oligosaccharides (Figure 4.6 A–C) and a low molecular weight hyaluronan preparation (Figure 4.6 D–F). With this complex mixture of hyaluronan oligosaccharides, the beneficial effect of the change in stationary phase material is even more pronounced than for the standard analytes. A detailed discussion on the analysis of the respective saccharide mixture is provided in Section 4.3.6.

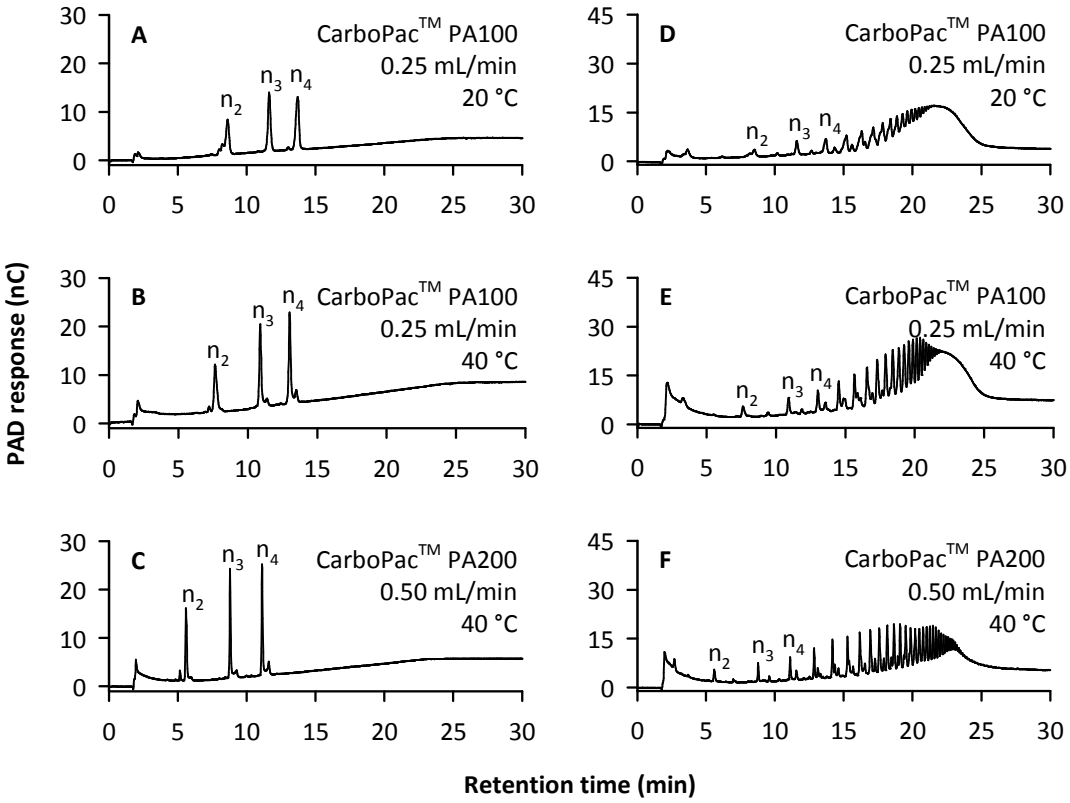

Figure 4.6: Variation of column, flow, and temperature. 10 µL of 5 µM standard mixture (A–C) or 10 µL of an aqueous solution of 0.5 mg/mL Hyalo-Oligo oligosaccharide mixture (D–F) injected. CarboPac™ PA100 column operated at 0.25 mL/min and 20 °C (A, D) or 40 °C (B, E), CarboPac™ PA200 column operated at 0.50 mL/min and 40 °C (C, F). Eluent: 100 mM sodium hydroxide, gradient of 200–900 mM sodium acetate.

4.3.5 Characterization of the optimized method

Best results were achieved using the CarboPac™ PA200 column at a temperature of 40 °C and a flow rate of 0.50 mL/min. The sodium hydroxide concentration of the mobile phase was kept constant at 100 mM, a 20 min linear gradient of 200–900 mM sodium acetate was applied, and final conditions kept constant for additional 10 min. In summary, including an equilibration phase of 10 min prior to injection, total run duration was 40 min.

From the baseline noise, signal-to-noise ratio (S/N) was calculated for a low concentration of the standard analytes. Subsequently, the limit of detection (LOD, S/N = 3) and the limit of quantification (LOQ, S/N = 10) were deduced from the S/N values. Injecting 10 µL of the sample, the limit of detection for the standard oligosaccharides was 20–30 nM or, expressed as total amount of the analyte, 0.2–0.3 pmol. A chromatogram for an amount of the standard analytes close to the LOD (0.5 pmol each) is depicted in Figure 4.7.

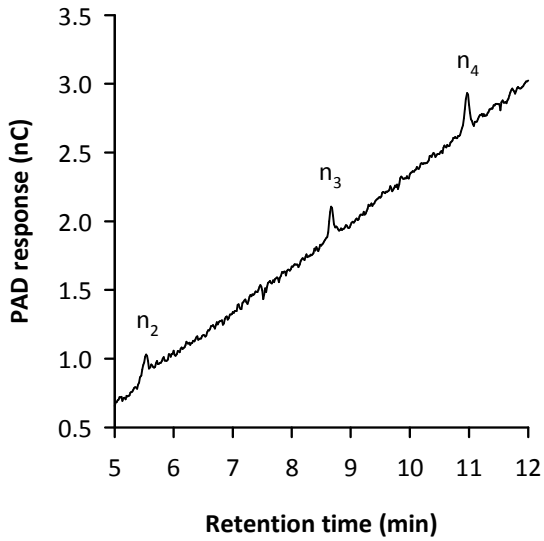

Figure 4.7: HPAEC–PAD at very low analyte concentrations. 10 µL of 0.05 µM (0.5 pmol) standard mixture (n_2–n_4) injected. Column: CarboPac™ PA200. Sodium hydroxide: 100 mM. Sodium acetate gradient: 200–900 mM. Flow: 0.50 mL/min. Temperature: 40 °C.

Linearity was examined by injecting 10 µL of standard mixtures (n_2–n_4) at concentrations of 0.1, 0.25, 0.5, 0.75, 1.0, 2.5, 5.0, 7.5, 10, 25, 50, 75, and 100 µM. For each concentration three independent samples prepared from the same stock solution were used. Plotting the area of the main peaks versus sample concentration revealed a linear correlation from 0.1 to 10 µM with coefficients of correlation in the range of 0.9977 to 0.9987. It is noteworthy that comparable values were obtained when using the sum of the areas of main and corresponding satellite peak (not shown). These findings suggest that the formation of the minor peaks is due to an equilibrium process and does not affect the applicability of the method for quantitative analysis.

Average migration time was calculated from all 39 injections performed to determine the linearity of the method. In contrast, repeatability of the main peak area was determined using standards at a concentration of 0.5 µM (N = 3). All values regarding sensitivity, linearity, and repeatability are summarized in Table 4.1.

Table 4.1: Limit of detection, limit of quantification, calibration parameters, and repeatability of the optimized HPAEC–PAD method (n_x: oligosaccharides consisting of *x* hyalobiuronic acid moieties).

	n_2	n_3	n_4
LOD, LOQ, calibration parameters			
Limit of detection, LOD, S/N = 3, given as sample concentration (nM), 10 µL injected	30	20	20
Limit of detection, LOD, S/N = 3, given as total amount injected (pmol)	0.3	0.2	0.2
Limit of quantification, LOQ, S/N = 10, given as sample concentration (nM), 10 µL injected	110	70	60
Limit of quantification, LOQ, S/N = 10, given as total amount injected (pmol)	1.1	0.7	0.6
Linear range investigated, given as sample concentration (µM), 10 µL injected	0.1–10	0.1–10	0.1–10
Coefficient of determination, R^2	0.9981	0.9977	0.9987
Sample concentration showing deviation from linearity (µM), 10 µL injected	25	25	25
Repeatability			
Average retention time (min): mean ± SD (RSD), *N* = 39	5.598 ± 0.017 (0.31%)	8.786 ± 0.023 (0.26%)	11.105 ± 0.026 (0.23%)
Main peak areas (nC · min): mean ± SD (RSD), 0.5 µM, 10 µL injected, *N* = 3	0.171 ± 0.010 (5.70%)	0.215 ± 0.021 (9.69%)	0.214 ± 0.009 (4.35%)

4.3.6 Analysis of a complex mixture of hyaluronan oligosaccharides

Figure 4.6 already showed chromatograms obtained by separation of a complex mixture of hylauronan oligosaccharides, marketed as Hyalo-Oligo. To further characterize this mixture, an aqueous solution and an incubation mixture, both containing the Hyalo-Oligo preparation, were analyzed (Figure 4.8). The sample, containing buffer salts and bovine serum albumin, was prepared as described in Section 4.2.1. It becomes obvious from Figure 4.8 that, after deproteinization, the matrix components from the incubation mixtures did not interfere with the chromatographic separation. The void volume signal increased, whereas detection of the analytes was not hampered in any way. The oligosaccharides of the mixture were separated from 2 (n_2) up to at least 25–30 disaccharide units (n_{25}–n_{30}), corresponding to a molecular weight of 9.5–11.4 kDa. The disaccharide (n_1), however, could not be separated from the void volume signal. The observed size distribution confirmed that the low molecular weight hyaluronan preparation Hyalo-Oligo has an average molecular weight

below 10 kDa as specified by the manufacturer. The small peaks detected in between the main substance peaks probably correspond to ethylated derivatives, which have previously been identified by CZE–ESI-TOF-MS of the same oligosaccharide mixture (*cf*. Chapter 3, Section 3.3.7).

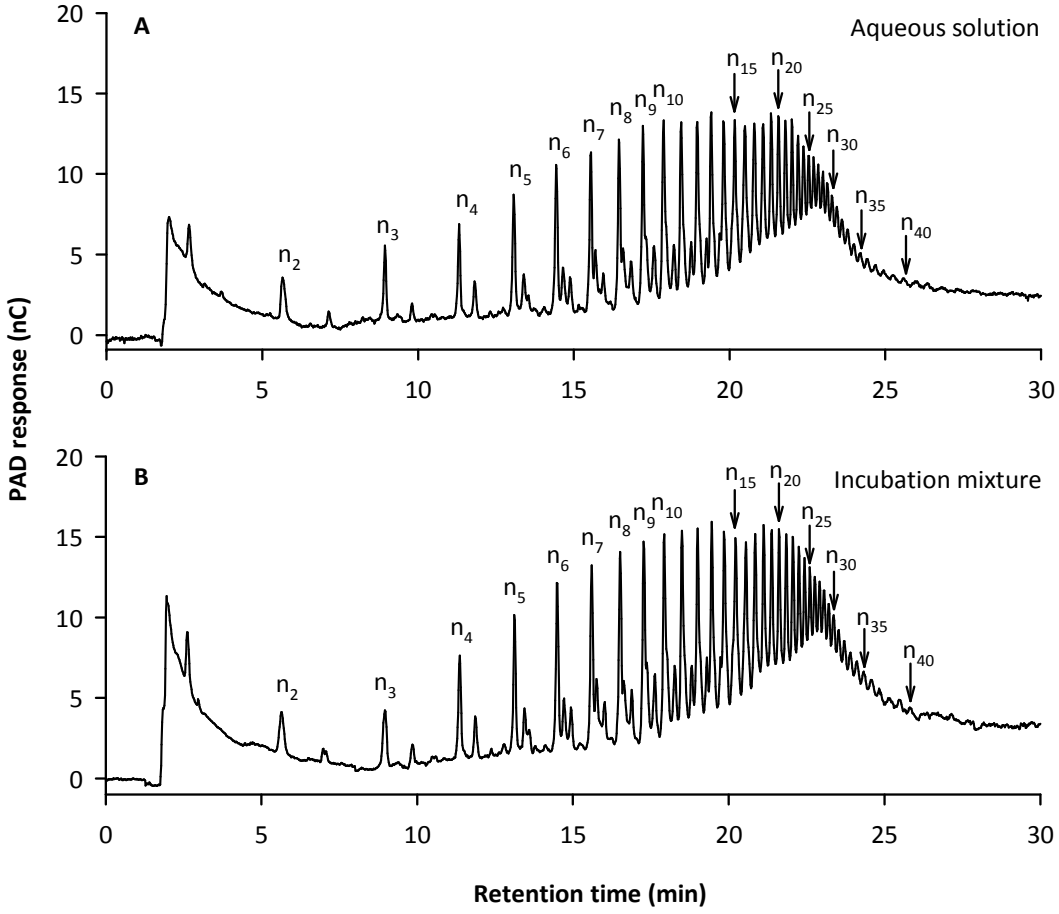

Figure 4.8: Separation of a complex mixture of hyaluronan oligosaccharides from aquaeous solution (A) and from an incubation mixture (B). Oligosaccharides are labeled as n_x according to the number (*x*) of disaccharide units. 10 µL of 0.5 mg/mL Hyalo-Oligo injected. Chromatography conditions: CarboPac™ PA200, 100 mM sodium hydroxide, gradient of 200–900 mM sodium acetate, 40 °C, 0.5 mL/min.

4.3.7 Formation of odd-numbered oligosaccharides under strongly alkaline conditions

In general, the oligosaccharides derived from hyaluronan are even-numbered oligosaccharides, consisting of an integer number of hyalobiuronic acid (disaccharide) moieties. Nevertheless, some authors also reported the occurrence of odd-numbered oligosaccharides.[18, 20, 23] These odd-numbered sugars might be the reason for additional peaks under the alkaline conditions of HPAEC, especially observed at higher temperature (*cf*. Figure 4.5). To study this phenomenon, the standard oligosaccharides were dissolved in 20 mM sodium hydroxide solution. Under these conditions, the formation of odd-numbered oligosaccharides, even at ambient temperature of 22 °C, was proven by CZE–ESI-TOF-MS

analysis (Figure 4.9). The detected odd-numbered oligosaccharides are formed from the corresponding even-numbered oligosaccharides by cleavage of one *N*-acetyl-D-glucosamine moiety. The loss of a glucuronic acid moiety was not observed. As already suggested by Hoechstetter,[20] the mechanism of this alkaline cleavage is presumably similar to the proposed mechanism[27] of the Morgan-Elson reaction.

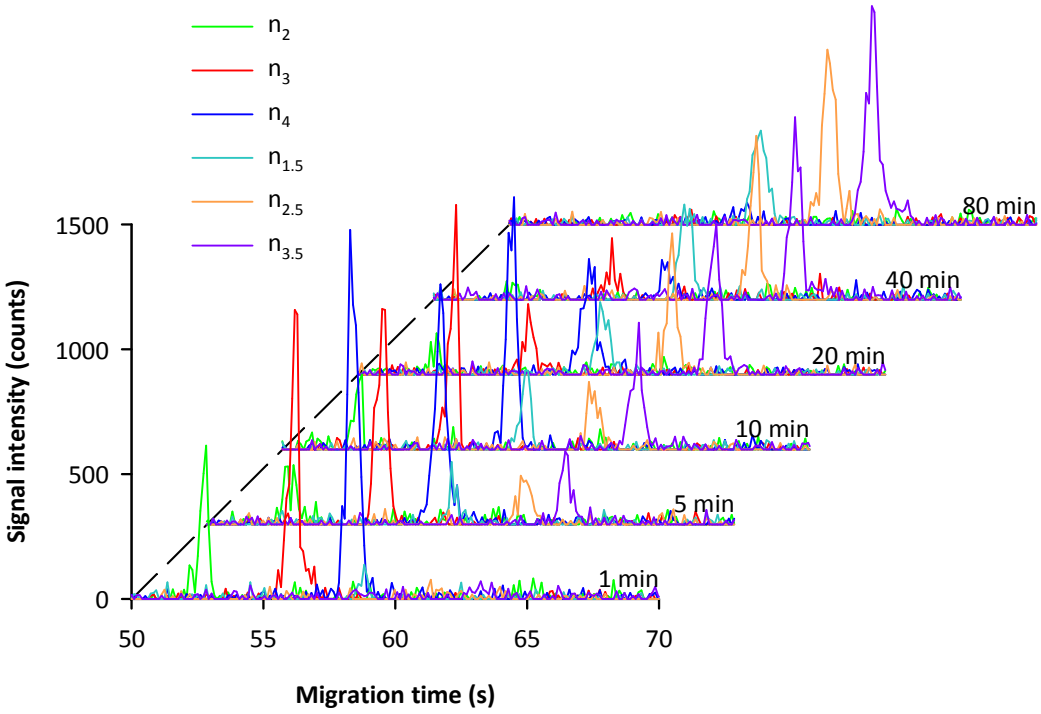

Figure 4.9: Formation of odd-numbered oligosaccharides ($n_{1.5}$, $n_{2.5}$, $n_{3.5}$) in 20 mM sodium hydroxide solution at 22 °C. Initial concentration of each even-numbered standard oligosaccharide (n_2, n_3, n_4) was 4 µM. CZE conditions: 15 µm × 28 cm capillary, ammonium acetate background electrolyte (25 mM, pH = 8.5), 35 kV. Signals are extracted ion traces from CZE–ESI-TOF-MS coupling.

The impact of high pH values and elevated temperature on the chemical conversion of the analytes was studied by means of HPAEC–PAD. Even-numbered standard oligosaccharides were dissolved in water or 100 mM sodium hydroxide solution, simulating the eluent conditions. Chromatograms were recorded immediately and after different periods of heating at 100 °C (Figure 4.10). Neither the heated aqueous solution (Figure 4.10 B) nor the directly injected alkaline solution (Figure 4.10 C) revealed any significant change in peak appearance. After incubation under alkaline conditions at 10 °C for 24 h, two peaks, with a very small third peak in between, became visible (Figure 4.10 D). The same phenomenon was seen after heating of the alkaline solution. Thereby, total peak area dramatically decreased, probably due to complete degradation of the oligosaccharides (Figure 4.10 E). After 15 min of heating, the peaks had entirely disappeared (Figure 4.10 F).

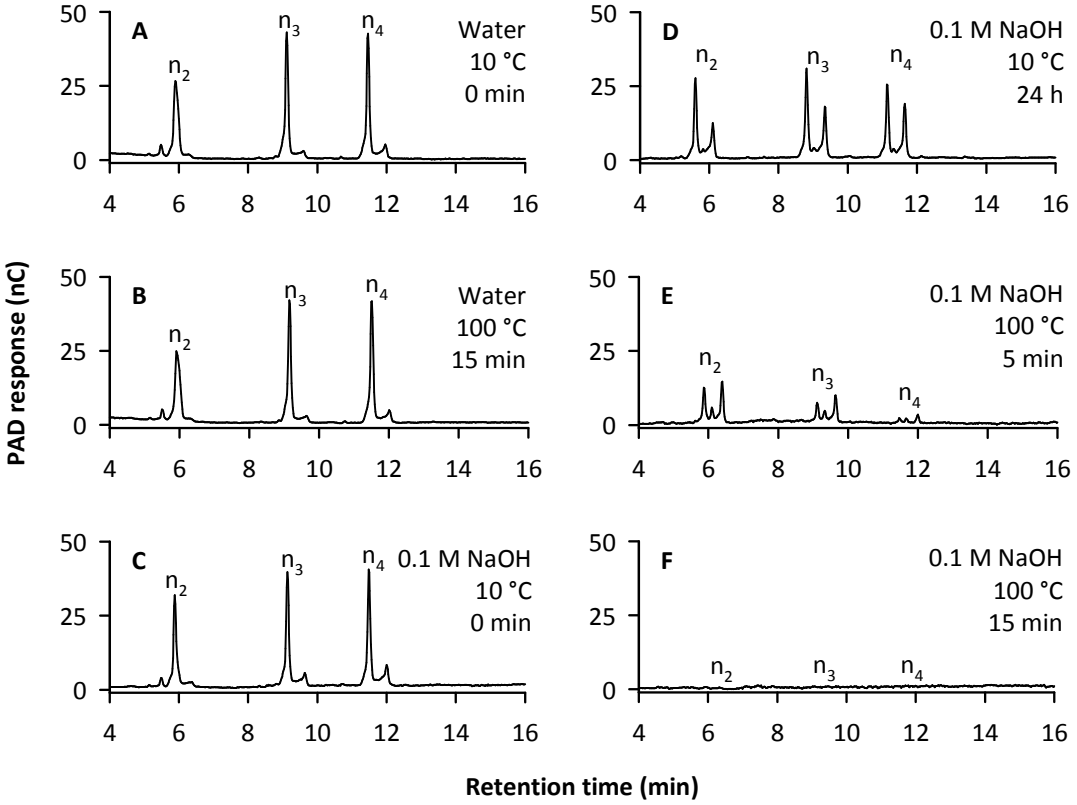

Figure 4.10: Stability of hyaluronan oligosaccharides (n_2-n_4, 20 µM) against heating and under alkaline conditions. 10 µL of sample injected. Chromatography conditions: CarboPac™ PA200, 100 mM sodium hydroxide, gradient of 200–900 mM sodium acetate, 40 °C, 0.5 mL/min.

In contrast to the chromatogram obtained by HPAEC–PAD of the alkaline solution stored at 10 °C for 24 h (Figure 4.10 D), CZE–ESI-TOF-MS analysis of the same sample revealed only signals from the three odd-numbered oligosaccharides and their corresponding sodium adducts. Neither oligosaccharides resulting from cleavage of glucuronic acid nor residual even-numbered sugars were detected. This finding was in good accordance with the fast degradation observed at room temperature. Probably, the distinct peaks correspond to isomers of the odd-numbered oligosaccharides, which give the same *m/z* signal and cannot be separated by the CZE method. It is known from recent NMR experiments that elimination of *N*-acetyl-D-glucosamine moieties from hyaluronan oligosaccharides under strongly alkaline conditions leads to high amounts (ca. 30%) of stereoisomers by keto-enol tautomerizations (Lobry de Bruyn–van Ekenstein transformations).[28] We heated the oligosaccharides in a 100 mM solution of sodium hydroxide. These harsh conditions are expected to cause isomerization to a considerable extent. It might further be assumed that the small third peak of each triplet corresponds to residual even-numbered oligosaccharide, which could not be observed in CZE–ESI-TOF-MS due to very low concentration.

Within the recorded *m/z* range from 300 to 3000 (no detection of monosaccharides possible) an additional signal at *m/z* = 405.03 and corresponding sodium adducts were observed. This signal was not detected in the kinetic experiment shown in Figure 4.9. The

corresponding chemical entity, probably a reaction product with reduced molecular mass, showed a single charge in the negative ESI mode. Due to its migration behavior, however, this molecular species should be uncharged under the conditions of the CZE, hence not containing a glucuronic acid moiety. Assuming a dimeric adduct of the anhydro-derivative of *N*-acetyl-D-glucosamine proposed by Muckenschnabel et al. (Figure 4.11),[27] the calculated *m/z* of 405.15 for $[M-H]^-$ does not fit exactly the measured value. However, this discrepancy of 0.12 might lie within the limits of the experimental errors. The signal for the disaccharide would be expected at *m/z* = 396.12 ($[M-H]^-$).

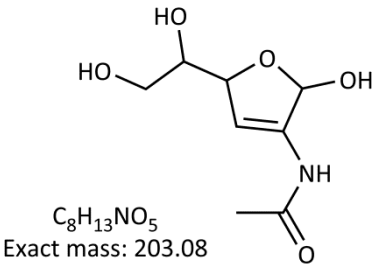

Figure 4.11: The anhydro-derivative of *N*-acetyl-D-glucosamine (proposed by Muckenschnabel et al.)[27] probably occurs when hyaluronan oligosaccharides are destructed under strongly alkaline conditions.

4.3.8 Studies on the size-dependent precipitation of hyaluronan fragments in the turbidimetric hyaluronidase activity assay

For the turbidimetric hyaluronidase assay described by Meyer,[29] the size limit for precipitation of hyaluronan is supposed to be in a molecular weight range of 6–8 kDa.[30] Assuming a similar behavior in the assay according to Di Ferrante,[24] the HPAEC–PAD should be able to detect a decrease in the corresponding oligosaccharide peaks. Therefore, the oligosaccharide preparation Hyalo-Oligo (molecular weight < 10 kDa) as well as high molecular weight hyaluronan were precipitated with cetyltrimethylamonium bromide (CTAB). The results from the precipitation experiments are depicted in Figure 4.12.

For the Hyalo-Oligo mixture, peaks in the respective region of the chromatogram disappeared after addition of the CTAB reagent (red circles in Figure 4.12 B, C). Precipitation was also confirmed by the corresponding extinction at 600 nm. Enzymatic cleavage by bovine testicular hyaluronidase led to a reduction in molecular weight, disabling precipitation (Figure 4.12 D). No turbidity occured in this case. The small oligosaccharides were not removed and could still be detected by HPAEC–PAD. The same effect was observed using high molecular weight hyaluronan of bacterial origin. Prior to digestion, hyaluronan was precipitated by CTAB leading to high turbidity. Enzymatic action resulted in the formation of products with low molecular weight which had not been detected without addition of enzyme (green rectangles in Figure 4.12 E, F). Turbidity after addition of CTAB was thereby reduced to a level comparable to control. The tetrasaccharide (n_2) and

hexasaccharide (n_3), produced by the action of bovine testicular hyaluronidase, clearly showed the characteristic two peaks (blue arrows in Figure 4.12 D, F), discussed in Section 4.3.7, due to the treatment with alkaline CTAB reagent and boiling for deproteinization.

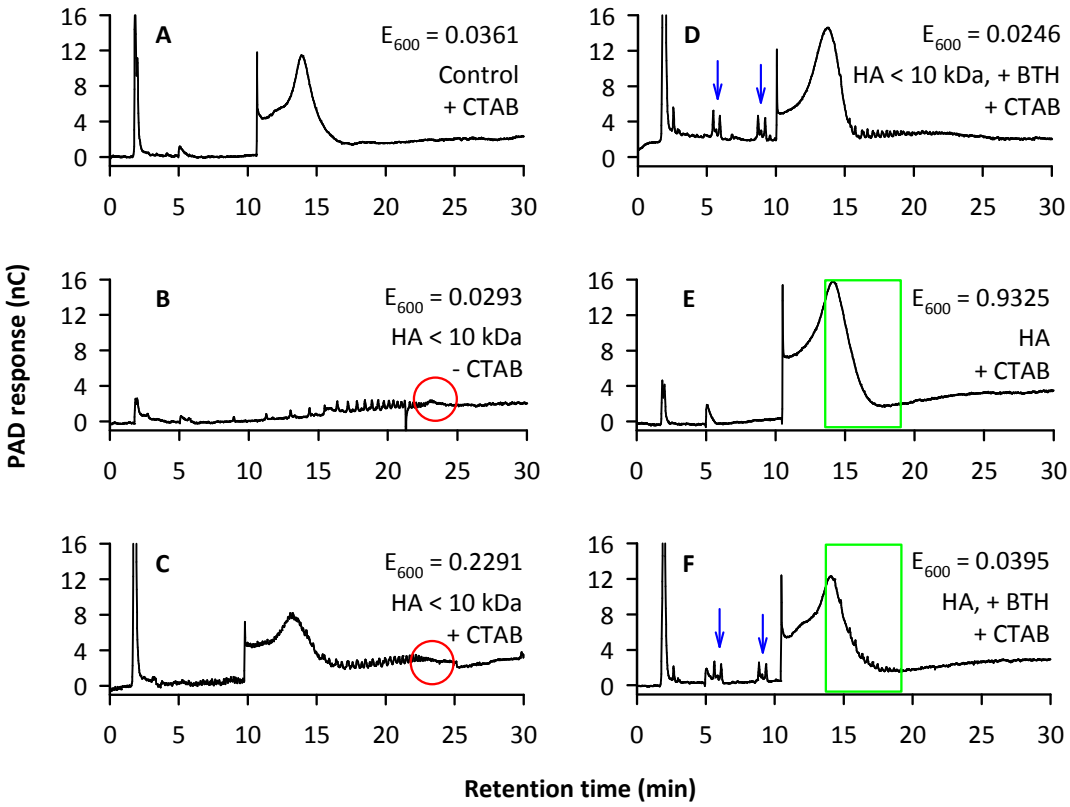

Figure 4.12: Chromatograms of supernatants after precipitation of hyaluronan with cetyltrimethylammonium bromide (CTAB). High molecular weight hyaluronan (HA) or the oligosaccharide mixture Hyalo-Oligo (HA < 10 kDa) were used. Addition of bovine testicular hyaluronidase (BTH) led to enzymatic degradation (D, F). For each sample, the extinction at 600 nm (E_{600}) is given as turbidity value. Red circles: region of precipitation. Green rectangles: undigested versus digested hyaluronan, formation of oligosaccharides. Blue arrows: two peaks due to instability during boiling in alkaline solution.

In summary, the results confirm that precipitation with CTAB only occurs for hyaluronan oligosaccharides and polysaccharides beyond a molecular weight of approximately 6–8 kDa. Smaller oligosaccharides are still present in the supernatant after removing the precipitate by centrifugation.

4.4 Summary and conclusion

Parameters for high performance anion exchange chromatography with pulsed amperometric detection (HPAEC–PAD) were optimized with regard to the analysis of hyaluronan oligosaccharides. For PAD, a standard triple pulse sequence for carbohydrates (E_1 = +0.05 V, E_2 = +0.75 V, and E_3 = −0.15 V) was applied. Using a CarboPac™ PA200 column at 40 °C and a flow rate of 0.50 mL/min, 100 mM sodium hydroxide eluents with an

additional gradient of 200–900 mM sodium acetate were chosen. With 10 min of equilibration, a gradient duration of 20 min, and additional 10 min at 900 mM sodium acetate concentration, each run lasted 40 min. Under these conditions, the separation of oligosaccharides of 2 (n_2, molecular weight: ca. 0.8 kDa) up to 25–30 (n_{25}–n_{30}, molecular weight: ca. 9.5–11.4 kDa) hyalobiuronic acid moieties was successful. For small oligosaccharides (n_2–n_4), LOD was 0.2–0.3 pmol (depending on the oligosaccharide), expressed as absolute amounts injected.

Buffer components from incubation mixtures did not interfere with the analysis of a hyaluronan oligosaccharide mixture, recommending HPAEC–PAD for mechanistic and enzymological studies on hyaluronidases. Moreover, HPAEC–PAD together with additional CZE–ESI-TOF-MS analysis provided deeper insight into the chemical formation of odd-numbered oligosaccharides under alkaline conditions. Finally, HPAEC–PAD was successfully used to elucidate the size-dependent precipitation of hyaluronan oligosaccharide in the turbidimetric assay by Di Ferrante.[24]

4.5 References

1. Borromei, C.; Cavazza, A.; Corradini, C.; Vatteroni, C.; Bazzini, A.; Ferrari, R.; Merusi, P. Validated HPAEC-PAD method for prebiotics determination in synbiotic fermented milks during shelf life. *Anal. Bioanal. Chem.* **2010,** 397, 127-135.

2. Borromei, C.; Cavazza, A.; Merusi, C.; Corradini, C. Characterization and quantitation of short-chain fructooligosaccharides and inulooligosaccharides in fermented milks by high-performance anion-exchange chromatography with pulsed amperometric detection. *J. Sep. Sci.* **2009,** 32, 3635-3642.

3. Bruggink, C.; Maurer, R.; Herrmann, H.; Cavalli, S.; Hoefler, F. Analysis of carbohydrates by anion exchange chromatography and mass spectrometry. *J. Chromatogr. A* **2005,** 1085, 104-109.

4. Cordella, C. B.; Militão, J. S.; Clément, M. C.; Cabrol-Bass, D. Honey characterization and adulteration detection by pattern recognition applied on HPAEC-PAD profiles. 1. Honey floral species characterization. *J. Agric. Food Chem.* **2003,** 51, 3234-3242.

5. Der Agopian, R. G.; Soares, C. A.; Purgatto, E.; Cordenunsi, B. R.; Lajolo, F. M. Identification of fructooligosaccharides in different banana cultivars. *J. Agric. Food Chem.* **2008,** 56, 3305-3310.

6. Liu, Y.; Jiang, X. L.; Cui, H.; Guan, H. S. Analysis of oligomannuronic acids and oligoguluronic acids by high-performance anion-exchange chromatography and electrospray ionization mass spectrometry. *J. Chromatogr. A* **2000,** 884, 105-111.

7. Verspreet, J.; Pollet, A.; Cuyvers, S.; Vergauwen, R.; Van den Ende, W.; Delcour, J. A.; Courtin, C. M. A simple and accurate method for determining wheat grain fructan content and average degree of polymerization. *J. Agric. Food Chem.* **2012,** 60, 2102-2107.

8. Zook, C. M.; LaCourse, W. R. Pulsed amperometric detection of carbohydrates in fruit juices following high performance anion exchange chromatography. *Curr. Sep.* **1995,** 14, 48-52.

9. Behan, J. L.; Smith, K. D. The analysis of glycosylation: a continued need for high pH anion exchange chromatography. *Biomed. Chromatogr.* **2011,** 25, 39-46.

10. Stadheim, T. A.; Li, H.; Kett, W.; Burnina, I. N.; Gerngross, T. U. Use of high-performance anion exchange chromatography with pulsed amperometric detection for *O*-glycan determination in yeast. *Nat. Protoc.* **2008,** 3, 1026-1031.

11. Grey, C.; Edebrink, P.; Krook, M.; Jacobsson, S. P. Development of a high performance anion exchange chromatography analysis for mapping of oligosaccharides. *J. Chromatogr. B Analyt. Technol. Biomed. Life Sci.* **2009,** 877, 1827-1832.

12. Radva, D.; Knutsen, S. H.; Kosáry, J.; Ballance, S. Application of high-performance anion-exchange chromatography with pulsed amperometric detection to compare the kinetic properties of β-glucosidase on oligosaccharides from lichenase digested barley beta-glucan. *Carbohydr. Res.* **2012,** 358, 56-60.

13. Rodriguez-Colinas, B.; Poveda, A.; Jimenez-Barbero, J.; Ballesteros, A. O.; Plou, F. J. Galacto-oligosaccharide synthesis from lactose solution or skim milk using the β-galactosidase from *Bacillus circulans*. *J. Agric. Food Chem.* **2012,** 60, 6391-6398.

14. Iqbal, S.; Nguyen, T. H.; Nguyen, T. T.; Maischberger, T.; Haltrich, D. β-Galactosidase from *Lactobacillus plantarum* WCFS1: biochemical characterization and formation of prebiotic galacto-oligosaccharides. *Carbohydr. Res.* **2010,** 345, 1408-1416.

15. Weissmann, B.; Meyer, K.; Sampson, P.; Linker, A. Isolation of oligosaccharides enzymatically produced from hyaluronic acid. *J. Biol. Chem.* **1954,** 208, 417-429.

16. Chen, F.; Kakizaki, I.; Yamaguchi, M.; Kojima, K.; Takagaki, K.; Endo, M. Novel products in hyaluronan digested by bovine testicular hyaluronidase. *Glycoconj. J.* **2009,** 26, 559-566.

17. Kakizaki, I.; Ibori, N.; Kojima, K.; Yamaguchi, M.; Endo, M. Mechanism for the hydrolysis of hyaluronan oligosaccharides by bovine testicular hyaluronidase. *FEBS J.* **2010,** 277, 1776-1786.

18. Mahoney, D. J.; Aplin, R. T.; Calabro, A.; Hascall, V. C.; Day, A. J. Novel methods for the preparation and characterization of hyaluronan oligosaccharides of defined length. *Glycobiology* **2001,** 11, 1025-1033.

19. Tawada, A.; Masa, T.; Oonuki, Y.; Watanabe, A.; Matsuzaki, Y.; Asari, A. Large-scale preparation, purification, and characterization of hyaluronan oligosaccharides from 4-mers to 52-mers. *Glycobiology* **2002,** 12, 421-426.

20. Hoechstetter, J. Characterisation of bovine testicular hyaluronidase and a hyaluronate lyase from *Streptococcus agalactiae*: investigations on the effect of pH on hyaluronan degradation and preclinical studies on the adjuvant administration of the enzymes in cancer chemotherapy. PhD thesis, University of Regensburg, Regensburg, **2005**.

21. Alaniz, L.; Garcia, M. G.; Gallo-Rodriguez, C.; Agusti, R.; Sterin-Speziale, N.; Hajos, S. E.; Alvarez, E. Hyaluronan oligosaccharides induce cell death through PI3-K/Akt pathway independently of NF-κB transcription factor. *Glycobiology* **2006,** 16, 359-367.

22. Prebyl, B. S.; Kaczmarek, C.; Tuinman, A. A.; Baker, D. C. Characterizing the electrospray-ionization mass spectral fragmentation pattern of enzymatically derived hyaluronic acid oligomers. *Carbohydr. Res.* **2003,** 338, 1381-1387.

23. Price, K. N.; Al, T.; Baker, D. C.; Chisena, C.; Cysyk, R. L. Isolation and characterization by electrospray-ionization mass spectrometry and high-performance anion-exchange chromatography of oligosaccharides derived from hyaluronic acid by hyaluronate lyase digestion: observation of some heretofore unobserved oligosaccharides that contain an odd number of units. *Carbohydr. Res.* **1997,** 303, 303-311.

24. Di Ferrante, N. Turbidimetric measurement of acid mucopolysaccharides and hyaluronidase activity. *J. Biol. Chem.* **1956,** 220, 303-306.

25. Clarke, A. J.; Sarabia, V.; Keenleyside, W.; MacLachlan, P. R.; Whitfield, C. The compositional analysis of bacterial extracellular polysaccharides by high-performance anion-exchange chromatography. *Anal. Biochem.* **1991,** 199, 68-74.

26. Hotchkiss, A. T., Jr.; Hicks, K. B. Analysis of oligogalacturonic acids with 50 or fewer residues by high-performance anion-exchange chromatography and pulsed amperometric detection. *Anal. Biochem.* **1990,** 184, 200-206.

27. Muckenschnabel, I.; Bernhardt, G.; Spruß, T.; Dietl, B.; Buschauer, A. Quantitation of hyaluronidases by the Morgan-Elson reaction: comparison of the enzyme activities in the plasma of tumor patients and healthy volunteers. *Cancer Lett.* **1998,** 131, 13-20.

28. Blundell, C. D.; Almond, A. Enzymatic and chemical methods for the generation of pure hyaluronan oligosaccharides with both odd and even numbers of monosaccharide units. *Anal. Biochem.* **2006,** 353, 236-247.

29. Meyer, K. The biological significance of hyaluronic acid and hyaluronidase. *Physiol. Rev.* **1947,** 27, 335-359.

30. Rapport, M. M.; Meyer, K.; Linker, A. Correlation of reductimetric and turbidimetric methods for hyaluronidase assay. *J. Biol. Chem.* **1950,** 186, 615-623.

5 Preparation of purified hyaluronan oligosaccharides and planar chromatography for quality control

Note: As stated in the list of publications, major parts of this chapter have already been published (in cooperation with partners from the Department of Pharmaceutical Biology) prior to the submission of this thesis.[1] For detailed information on the nature of this collaboration, see also "Acknowledgements and declaration of collaborations".

5.1 Introduction

Purified oligosaccharides derived from hyaluronan are indispensable tools for proper enzymological characterization of hyaluronidase isoenzymes and for pharmacological experiments. Consequently, convenient methods for quality control of these substances are required. Historically, hyaluronan oligosaccharides were separated by paper chromatography.[2] However, more recently, mainly high performance liquid chromatography (HPLC) and related techniques were used for chromatographic analysis and quality control of these saccharides.[3-5]

Nevertheless, owing to the development of high performance thin layer chromatography (HPTLC),[6] automating approaches, and hyphenation techniques,[7] planar chromatography has gained more attention in recent years. As sugars are difficult analytes for reversed phase HPLC, planar chromatography and its versatile derivatization options are an especially promising alternative. Moreover, planar chromatography enables the convenient and cost-effective analysis of multiple samples in parallel. Thin layer chromatography (TLC) on normal phase standard silica plates in combination with manifold post-chromatographic derivatization methods[8-11] or direct matrix assisted laser desorption ionization time-of-flight mass spectrometry (MALDI-TOF-MS)[9] was also previously reported for hyaluronan oligosaccharides. However, a quantitative HPTLC method had not been described in literature until publication of the results of the present project.[1]

A convenient quantitative HPTLC method with reagent-free derivatization on amino-modified silica was developed and validated. Coupling of normal phase standard TLC to electrospray ionization quadrupole time-of-flight mass spectrometry (ESI-Q-TOF-MS) additionally allowed for unambiguous identification of the oligosaccharides. Whereas MALDI-TOF-MS requires an electrically conductive aluminum back[9] and cannot be applied to glass-backed HPTLC plates, ESI-MS can be easily coupled to HPTLC.

5.2 Materials and methods

5.2.1 Standard analytes and preparation of oligosaccharides

Commercially available oligosaccharides (oligoHA from Hyalose, Oklahoma City, OK, USA) of 2–4 hyalobiuronic acid moieties (n_2–n_4), purchased from AMSBIO (Abingdon, UK), served as standard analytes. In-house digestion of hyaluronan (HA) from *Streptococcus zooepidemicus* (Aqua Biochem, Dessau, Germany) and subsequent purification, both essentially performed according to Hofinger et al.,[12] yielded sufficient amounts of these oligosaccharides for further studies. In detail, the preparation was carried out as follows.

The incubation buffer for the enzymatic digestion was prepared by dissolving 0.77 g of ammonium acetate (Merck, Darmstadt, Germany) and 0.58 g of sodium chloride (VWR, Haasrode, Belgium) in 100 mL of water purified with a Milli-Q system (Millipore, Eschborn, Germany). Buffer pH was then adjusted to a value of 5.0 by addition of concentrated hydrochloric acid (Merck, Darmstadt, Germany). Bovine testicular hyaluronidase (BTH, Neopermease®, kindly provided by Sanabo, Vienna, Austria) was diluted with bovine serum albumin (BSA, Serva, Heidelberg, Germany) solution (0.2 mg/mL) to the desired enzyme concentration. An activity to 10000 IU/mL (based on the declaration by the supplier) was found to be optimal for the preparation of n_2, n_3, and n_4. 50 mL of aqueous HA solution (5 mg/mL), 25 mL of bovine serum albumin solution, and 74 mL of purified water were mixed with 50 mL of the incubation buffer. Finally, addition of 1 mL of the prepared enzyme solution started the reaction. The mixture was incubated at 37 °C in a water bath for 72 h before the digestion process was stopped by boiling for 10 min.

In a first purification step, precipitated protein was removed by centrifugation at 5000 × *g* for 20 min. Aliquots of 100 mL were lyophilized and the obtained lyophilisate was dissolved in 2 mL of purified water. After filtration through a Millex-GV 0.22 µm syringe filter (Merck-Millipore, Darmstadt, Germany), the solution was injected into a gel filtration system, equipped with a HiLoad 16/60 Superdex™ 30 prep grade column (GE-Healthcare Bio-Sciences AB, Uppsala, Sweden). A 0.1 M solution of ammonium acetate (Merck, Darmstadt, Germany), filtrated through an Express™ PLUS 0.22 µm bottle top filter (Merck-Millipore, Darmstadt, Germany), was used as volatile mobile phase with regard to subsequent lyophilization. The chromatographic system was operated using a Pharmacia LKB Gradient pump 2249 (Amersham Pharmacia Biotech, Freiburg, Germany) at a flow rate of 0.5 mL/min. Elution of the oligosaccharides was monitored at 210 nm with a Shimadzu SPD-6AV UV detector (Shimadzu, Kyoto, Japan). Fractions were collected, pooled, lyophilized, and finally dissolved in 200 µL of purified water. Purity and identity of the hylauronan oligosaccharides were controlled by CZE–ESI-TOF-MS[13] (detailed description in Chapter 3) and oligosaccharide solutions were stored at −80 °C.

5.2.2 HPAEC–PAD of HA oligosaccharide mixtures from enzymatic digestion

For control and optimization of the digestion conditions, aliquots of the boiled and filtrated incubation mixture were analyzed by high performance anion exchange chromatography with pulsed amperometric detection (HPAEC–PAD) as described in Chapter 4. Prior to injection, the samples were diluted 1:10 with purified water.

5.2.3 Colorimetric estimation of oligosaccharide concentration

Oligosaccharide concentrations of the samples from in-house preparation were estimated by a colorimetric analysis.[14-17] The concentrated stock solution (*cf*. Section 5.2.1) was diluted 1:900 with purified water, and 450 µL of the dilution were mixed with alkaline borate solution. After 4.5 min of boiling and subsequent cooling on ice for additional 2 min, 1500 µL of *p*-dimethylaminobenzaldehyde solution were added. Both reagents were prepared as reported in literature.[14] *p*-Dimethylaminobenzaldehyde was from Sigma-Aldrich (Munich, Germany), all other chemicals were from Merck (Darmstadt, Germany). During 20 min of incubation at 37 °C the characteristic purple color of the reaction product developed. *N*-Acetyl-D-glucosamine at the reducing ends was determined by measuring absorbance of the colored product at 586 nm with a CARY 100 photometer (Agilent Technologies, Darmstadt, Germany). *N*-Acetyl-D-glucosamine (Fluka, Buchs, Switzerland) was used as calibration standard. The molar "concentration of reducing ends" equals the molar concentration of the (purified) oligosaccharides. Based on the results from the colorimetric quantification, samples for HPTLC experiments were diluted to reach a concentration of approximately 50 µM.

5.2.4 Stationary and mobile phases

TLC plates (aluminum-backed) and HPTLC plates (glass-backed) coated with silica 60 F_{254} (Merck, Darmstadt, Germany) were used to explore post-chromatographic staining or hyphenation to mass spectrometry. By contrast, for reagent-free derivatization, amino-modified silica Nano-SIL NH_2/UV_{254} (Macherey-Nagel, Düren, Germany) served as stationary phase. Square Nano-SIL NH_2 HPTLC plates (10 cm × 10 cm), used for the comparison of detection methods (*cf*. Section 4.3.3) and 2D chromatography (*cf*. Section 5.3.4), did not contain a UV indicator.

The mobile phases for all separations consisted of 1-butanol (Sigma-Aldrich, Munich, Germany), formic acid 98–100% (Merck, Darmstadt, Germany), and water. Ratios of 3:5:2 (v/v/v) for unmodified silica and 3:4:1 (v/v/v) for amino-modified silica gave the best results.

5.2.5 Sample application technique and chromatography conditions

The highly polar oligosaccharides were dissolved in water. The solution was sprayed on the chromatography plates with a Linomat 5 (CAMAG, Muttenz, Switzerland) in bands (length: 8 mm), 10 mm from the bottom edge of the plate. The application volume for both, samples and references, was 10 µL per band. To avoid band broadening during application, the settings for sample solvent type were adjusted to aqueous solution. Nitrogen was used as spray gas.

Chromatographic development was performed in a saturated automatic ADC2 Chamber (Twin Trough Chamber, CAMAG, Muttenz, Switzerland) to a distance of 70 mm from the bottom edge of the plate. Accordingly, considering the application position, the chromatogram was developed over a path of 60 mm. A saturated solution of magnesium chloride (Merck, Darmstadt, Germany) was used for adjustment of air humidity.

5.2.6 Post-chromatographic derivatization

With the hyaluronan oligosaccharides lacking suitable chromophores, visualization of the bands on the plates can only be achieved by post-chromatographic derivatization methods. A widely used technique is the orcinol/sulfuric acid staining.[8, 9] The derivatization reagent for this reaction was prepared by dissolving 0.2 g of orcinol (Fluka, Buchs, Switzerland) in 100 mL of sulfuric acid (10% or 75%), which was carefully prepared from concentrated sulfuric acid (Merck, Darmstadt, Germany) and water at a ratio of 3:1 (v/v), according to literature,[18] or 1:9 (v/v). With a reagent sprayer, the acidic staining reagent was sprayed on the plates. Alternatively, the plates were dipped into the reagent using a home-made dipping device. Upon heating on a plate heater (Desaga, Sarstedt group, Nümbrecht, Germany) at 100 °C for 15 min, colored bands developed. Immediately after heating, the plates were scanned for densitometric quantification. Scanning time was only 2 min. No fading of the color was observed during measurement.

Another classical post-chromatographic staining method for hyaluronan oligosaccharides is the Morgan-Elson reaction,[2, 19] performed in two steps.[19] Reagent 1 was prepared from a solution of 0.5 mL acetylacetone (Fluka, Buchs, Switzerland) in 50 mL of 1-butanol (Sigma-Aldrich, Munich, Germany) and an alkaline solution, namely a mixture of 1 part of an aqueous potassium hydroxide (Merck, Darmstadt, Germany) solution 50% (m/v) and 4 parts of ethanol (Carl Roth, Karlsruhe, Germany). 0.5 ml of the alkaline solution and 10 mL of the acetylacetone solution were mixed to give reagent 1. For reagent 2, 1 g of *p*-dimethylamino-benzaldehyde (Sigma-Aldrich, Munich, Germany) was dissolved in a mixture of 30 mL of ethanol (Carl Roth, Karlsruhe, Germany) and 30 mL of concentrated hydrochloric acid (Merck, Darmstadt, Germany), followed by dilution with 180 mL of 1-butanol (Sigma-Aldrich,

Munich, Germany). Plates then were dipped into reagent 1, heated at approximately 100 °C for 5 min, subsequently treated with reagent 2, and finally heated again for 5 min. As a result, this procedure revealed characteristic red bands on yellow background.

Reagent-free derivatization on amino-modified silica plates was achieved by heating the plate at approximately 200 °C for 15 min. Carbohydrates thereby probably undergo a Maillard-like reaction to form high-molecular products, which emit bright blue fluorescence when the plate is illuminated with UV light at a wavelength of 366 nm.[20-22] This phenomenon has also been previously described for other analytes, such as catecholamines, on amino-modified TLC plates.[23]

5.2.7 Documentation, measurement of absorbance spectra, densitometric quantification, and data processing

Images of the plates at 254 nm, 366 nm, and white light were recorded on a Reprostar 3 (CAMAG, Muttenz, Switzerland). Absorbance spectra were determined with a TLC Scanner 3 (CAMAG, Muttenz, Switzerland) in reflection mode. Densitometric quantification was performed by reflectance scan at the respective UV–VIS absorbance maximum for each derivatization procedure. All data were analyzed with winCATS 1.4.6 (CAMAG, Muttenz, Switzerland). In contrast, quadratic curve fitting was conducted with SigmaPlot for Windows 11.2.0.5 (Systat Software Inc., San Jose, CA, USA).

5.2.8 Coupling to mass spectrometry

TLC was directly coupled to mass spectrometry using the TLC–MS interface (Figure 5.1) from CAMAG (Muttenz, Switzerland). Desorption of the analytes from the plates was achieved by an HPLC pump (Agilent 1260 Infinity Quaternary Pump, Agilent technologies, Waldbronn, Germany) driven solvent stream of acetonitrile/water/formic acid (90:10:0.1). High resolution mass spectra of the extracted substances were recorded in negative ionization mode ($[M-H]^-$ and $[M-2H]^{2-}$) with an Agilent 6540 ultra-high definition (UHD) accurate-mass-TOF LC/MS (Agilent technologies, Waldbronn, Germany). The internal mass calibration standard was hexakis(2,2,3,3-tetrafluoropropoxy)phosphazine. Exact masses of the analytes were calculated with Agilent MassHunter Workstation Software B.04.06.

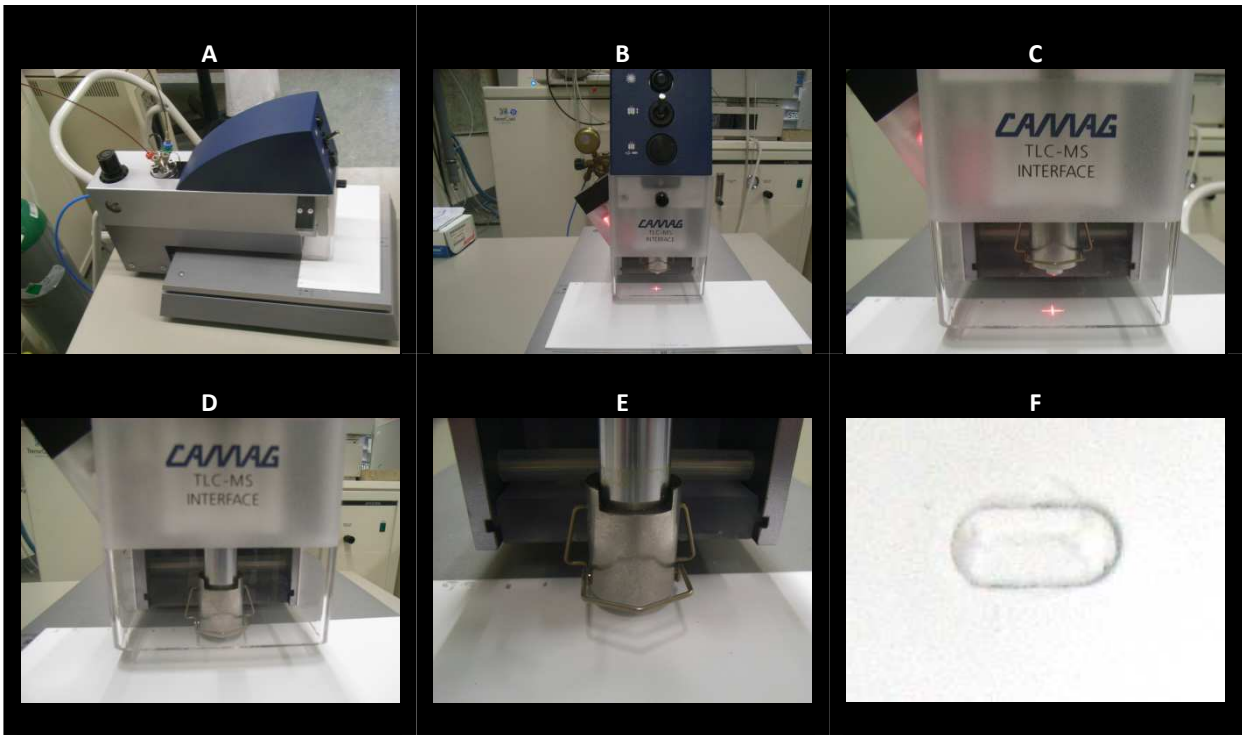

Figure 5.1: The CAMAG TLC–MS interface. Device seen slanted from above (A), frontal view (B), laser cross hairs for positioning (C), extraction process (D), detailed view of the elution head (E), and trace left on the plate by the oval elution head (F).

5.3 Results and discussion

5.3.1 Optimization of oligosaccharide preparation by enzymatic digestion

With regard to high yields of the small oligosaccharides comprising 2–4 disaccharide units (n_2–n_4), different enzyme concentrations were tested for optimization of the digestion of hyaluronan. HPAEC–PAD chromatograms of the obtained oligosaccharide mixtures are depicted in Figure 3.4.

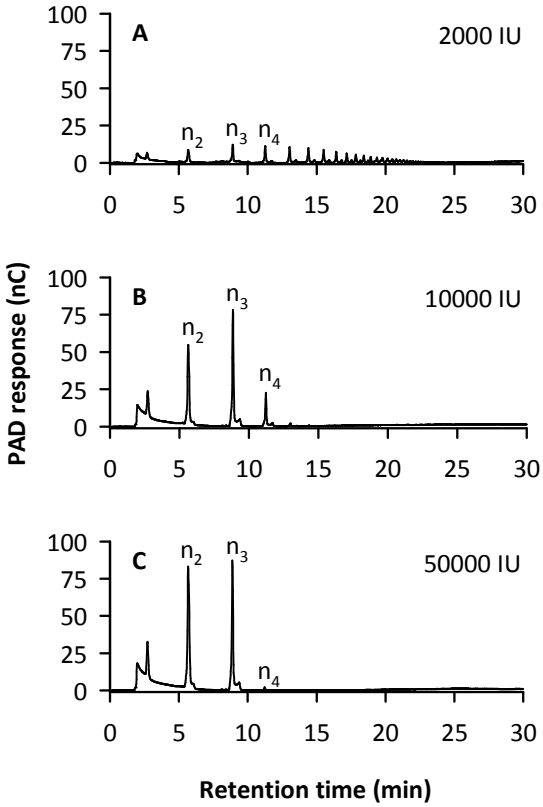

Figure 5.2: HPAEC–PAD chromatograms of incubation mixtures (diluted 1:10) from preparation of small hyaluronan oligosaccharides (n_2, n_3, and n_4). Incubation buffer for digestion: ammonium acetate, pH = 5.0 (containing BSA and NaCl). Activity of bovine testicular hyaluronidase: 2000 IU (A), 10000 IU (B), or 50000 IU (C) per 200 mL. Incubation for 72 h. Chromatography: CarboPac™ PA200, 100 mM sodium hydroxide, gradient of 200–900 mM sodium acetate, 40 °C, 0.5 mL/min.

Under the given conditions and after an incubation time of 72 h, 10000 IU of the enzyme preparation in a total volume of 200 mL incubation mixture were found to be the optimum for the preparation of the desired size range of oligosaccharides. Lower enzyme concentrations led to high content of larger oligosaccharides, which, in addition, were difficult to purify. Inversely, with higher concentration of the enzyme the amount of the octasaccharide n_4 was very low.

5.3.2 Choice and optimization of mobile phase for HPTLC

Articles dealing with TLC of hyaluronan oligosaccharides can roughly be divided into two groups according to the solvent system used. The older publications describe a 2-propanol/water (66:34) mixture containing 0.05 M sodium chloride,[8, 10] whereas more recently reported procedures use 1-butanol/formic acid/water at a ratio of 4:8:1[11] or 3:4:1[9] as mobile phase. The latter system was chosen, because, with respect to TLC–MS coupling, salt contamination should be avoided. Therefore, various mixtures of 1-butanol, formic acid, and water were initially tested on TLC plates. As a result, a composition of 3:4:1 was found to be ideal for amino-modified silica, whereas in case of unmodified silica the ratio was slightly changed to 3:5:2 in order to increase R_f values.

5.3.3 Comparison of stationary phase materials and post-chromatographic derivatization methods

Having determined the ideal composition of the mobile phase, the stationary phases (normal phase and amino-modified silica) and derivatization methods (orcinol/sulfuric acid staining, Morgan-Elson reaction, and thermal derivatization on amino-modified phase) had to be compared in the next step. For this purpose, the n_2 standard oligosaccharide at concentrations of 10, 25, 50, 100, 250, and 500 µM and a 75 µM mixture of n_2, n_3, and n_4 standard (10 µL per band) were used. As derivatization by spraying is not ideal for densitometry, the content of sulfuric acid in the orcinol reagent had to be reduced from 75% to 10% for a dipping procedure. As shown in Figure 5.3, this modification of the reagent did not affect the detection.

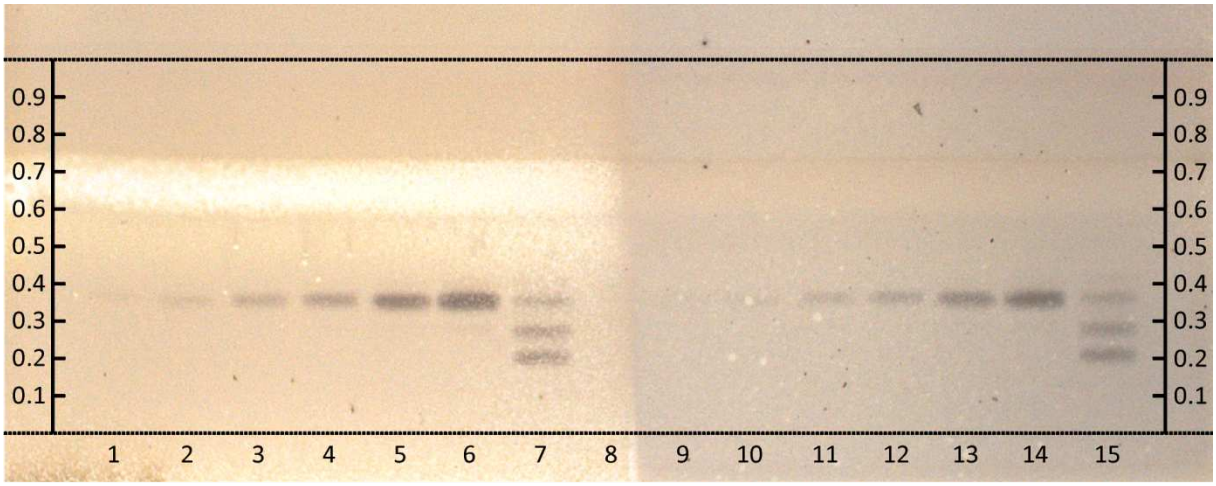

Figure 5.3: Effect of the sulfuric acid content of the orcinol reagent on the detection of the analytes. Silica high performance thin layer chromatography (HPTLC) plate after spraying with orcinol in 10% (left) and 75% (right) H_2SO_4. Tetrasaccharide (n_2) 100, 250, 500, 1000, 2500, and 5000 pmol/band (lanes 1–6, 9–14), standard oligosaccharide mixture (n_2–n_4) 750 pmol/band (lanes 7, 15), blank (lane 8). Mobile phase: 1-butanol/formic acid/water (3:5:2). Developing distance: 6 cm (7 cm from the bottom edge). Vertical axis indicates the R_f scale. Reproduced from Fig. 2 of the original publication[1] with kind permission from Elsevier.

Figure 5.4 compares the different stationary phases and derivatization methods. Both stationary phases allowed for efficient separation of the standard oligosaccharides. With regard to derivatization, however, the pictures clearly indicate the superiority of the orcinol staining method on silica and the thermal derivatization on amino-modified silica in comparison to the Morgan-Elson reaction.

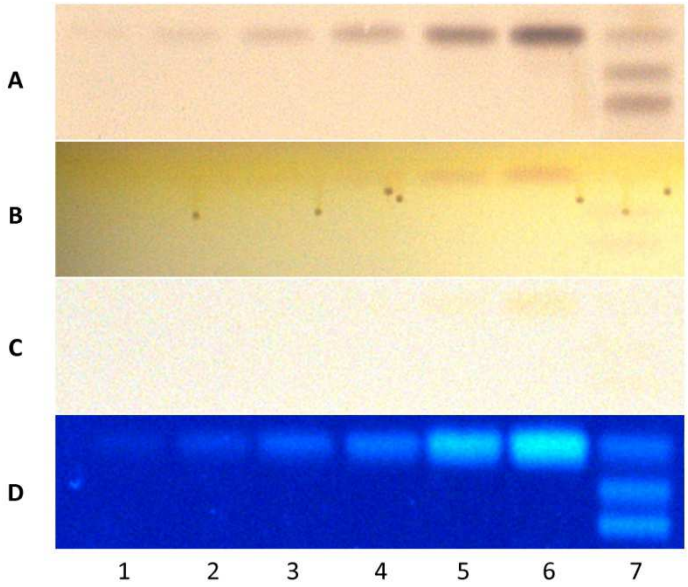

Figure 5.4: Separation of hyaluronan oligosaccharides by high performance thin layer chromatography (HPTLC) on silica or amino-modified silica and visualization by different detection methods. Silica HPTLC plates after dipping into orcinol/10% H_2SO_4 reagent (A) and Morgan-Elson reagent (B). Amino-modified silica HPTLC plate after heating, illuminated with white (C) and UV light at 366 nm (D). Tetrasaccharide (n_2) 100, 250, 500, 1000, 2500, and 5000 pmol/band (lanes 1–6), oligosaccharide mixture (n_2–n_4) 750 pmol/band (lane 7). Mobile phase: 1-butanol/formic acid/water (silica (A, B): 3:5:2, amino-modified silica (C, D): 3:4:1). Developing distance: 6 cm (7 cm from the bottom edge). Reproduced from Fig. 3 of the original publication[1] with kind permission from Elsevier.

To pinpoint the differences in sensitivity for the tested derivatization methods, densitometric scans in the measured UV–VIS absorbance maxima after visualization were conducted in reflectance mode. As for coupling to MS the position of the unmodified analytes on the plate must be localized, the plates were additionally scanned at 205 nm prior to any treatment with derivatization reagents. Peak heights were then plotted versus the total amount of n_2 (Figure 5.5).

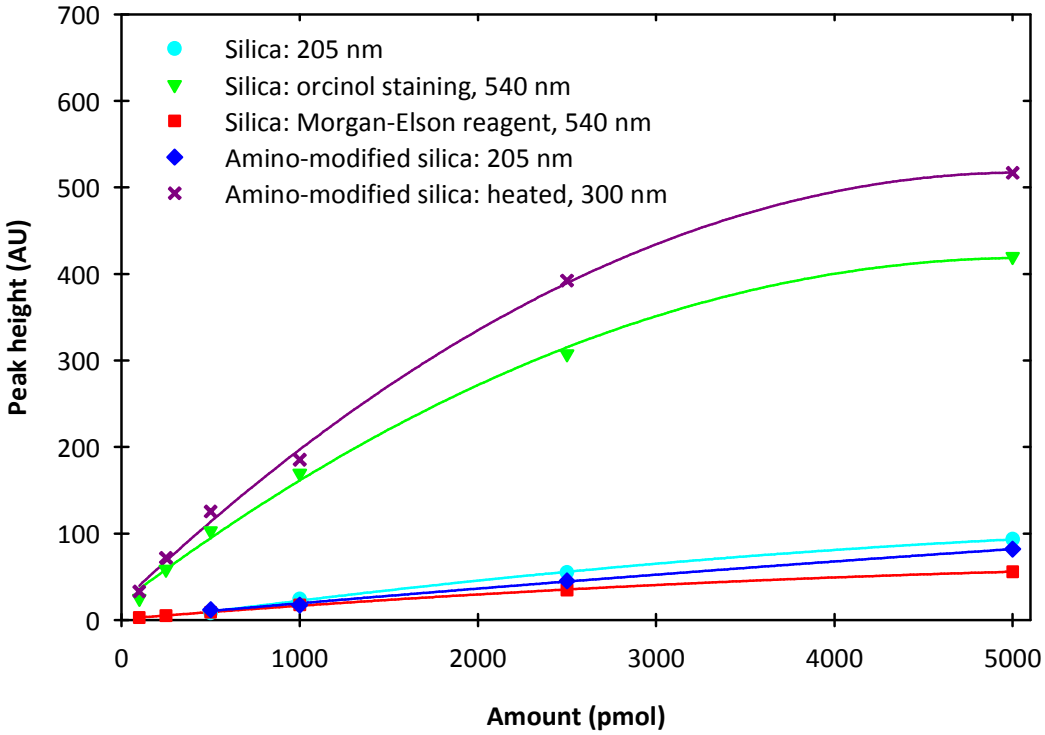

Figure 5.5: Sensitivity of different derivatization modes for the tetrasaccharide (n_2). Calibration curves for densitometric scans (reflectance mode) of the plates from Figure 5.4. Silica plate prior to derivatization scanned at 205 nm (circle, cyan), after orcinol staining at 540 nm (triangle, green), and after Morgan-Elson staining (square, red). Amino-modified silica plate untreated at 205 nm (diamond, blue) and after heating at 300 nm (x, dark pink). Peak heights expressed as arbitrary units (AU). Reproduced in a colored version from Fig. 4 of the original publication[1] with kind permission from Elsevier.

It should be noted that the amino-modified silica phase allows for the most powerful detection by a fast and simple thermal *in situ* derivatization method at retained band resolution, when compared to unmodified silica. Localization of the underivatized oligosaccharides at 205 nm was also successful although the detection limits were high.

By analogy with paper chromatography, one could also think of cellulose as stationary phase. Due to the sulfuric acid content of the orcinol reagent and the absence of amino-groups required for the reagent-free derivatization, the use of this phase, however, is incompatible with the preferred detection modes.

5.3.4 Stability of the analytes

Stability of the analytes during separation was investigated on a square (10 cm × 10 cm) HPTLC plate by two-dimensional (2D) chromatography. After spot application of a mixture of the three oligosaccharide standards (75 µM each, 5 µL), 10 mm from the bottom edge and 20 mm from the left edge, the plate was developed twice under identical conditions to a distance of 70 mm from the edge. Afterwards, all three bands were located on a diagonal between the application point and the intersection of the solvent front lines (Figure 5.6). Thus, the stability and constant chromatographic properties of the analytes were proven.

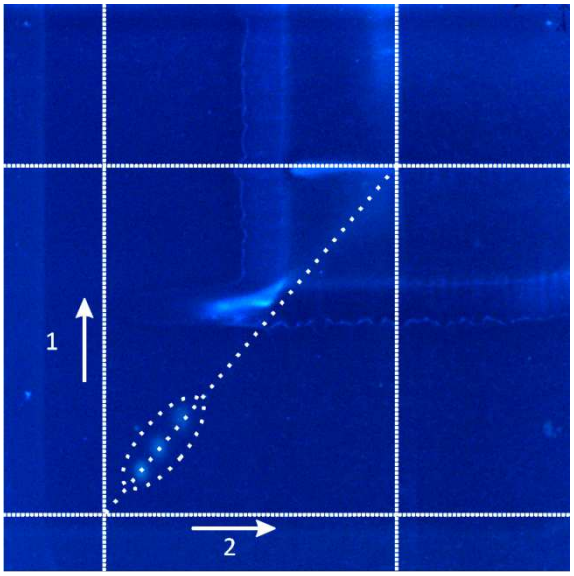

Figure 5.6: Stability of the analytes proven by 2D high performance thin layer chromatography (HPTLC) on amino-modified silica. Bands visualized after heating at 366 nm. Standard oligosaccharides (n_2–n_4, spot application, 75 µM each, 5 µL). Mobile phase: 1-butanol/formic acid/water (3:4:1). Developing distance: 6 cm (direction 1) and 5 cm (direction 2), each 7 cm from the edge of the plate. Reproduced from Fig. 5 of the original publication[1] with kind permission from Elsevier.

5.3.5 Optimization of the quantitative detection method

For densitometric quantification using amino-modified silica HPTLC plates, standard mixtures of the three oligosaccharides (n_2–n_4) were applied at amounts of 2500, 1000, 750, 500, 250, 100, 75, 50, 25, 10, and 5 pmol per band together with three samples of purified oligosacchariedes produced in-house. Chromatography was conducted as described in Section 4.2.5. When the plates were illuminated with visible light, weak brownish bands became obvious (Figure 5.7 A) upon thermal treatment. At 254 nm, however, dark bands were detected on the blue fluorescent background of the F_{254} plate (Figure 5.7 B), whereas a bright blue fluorescent was observed at 366 nm (Figure 5.7 C).

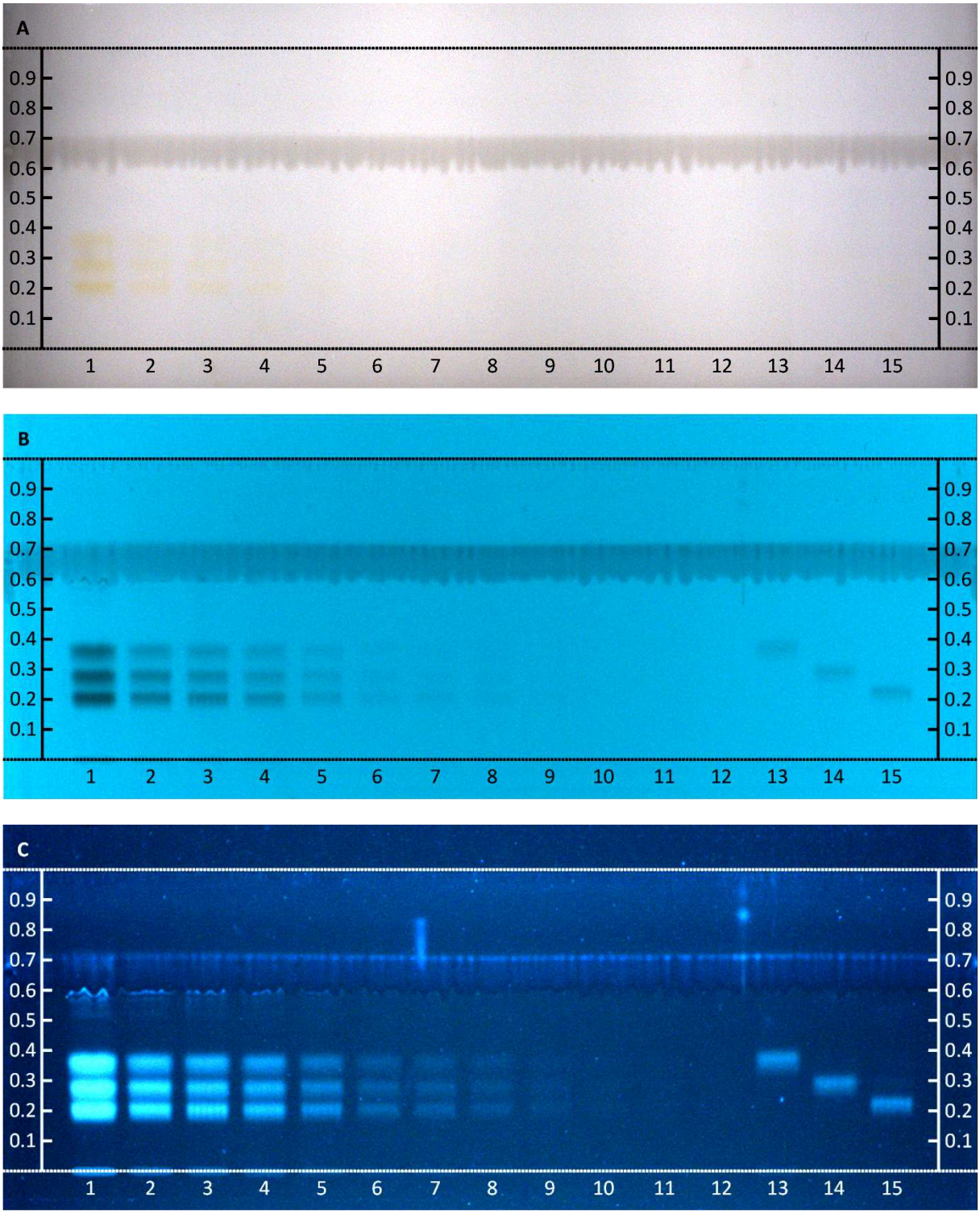

Figure 5.7: Amino-modified silica high performance thin layer chromatography (HPTLC) plate visualized with white light (A), 254 nm UV (B), and 366 nm UV (C). Standard mixture (n_2–n_4) 2500, 1000, 750, 500, 250, 100, 75, 50, 25, 10, and 5 pmol/band (lanes 1–12), n_2 sample (lane 13), n_3 sample (lane 14), n_4 sample (lane 15). Mobile phase: 1-butanol/formic acid/water (3:4:1). Developing distance: 6 cm (7 cm from the bottom edge). Vertical axes indicate the R_f scale. Reproduced from Fig. 6 and Supplementary Material 2 of the original publication[1] with kind permission from Elsevier.

Fluorescence measurement was taken into consideration for quantification, but showed relatively low signal-to-noise ratio compared to absorbance. Therefore, UV–VIS absorbance spectra (Figure 5.8) were recorded to determine the absorbance maxima.

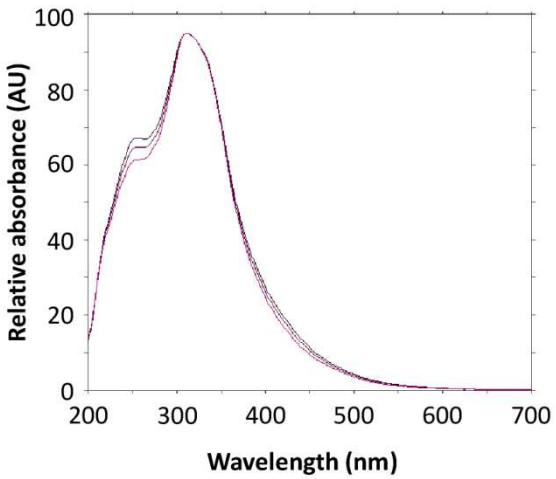

Figure 5.8: Overlay of the normalized UV–VIS absorbance spectra for the standard oligosaccharides n_2, n_3, and n_4 after heating on amino-modified silica HPTLC plate. Maximum value is set as 95 arbitrary units (AU). Reproduced from Fig. 7 of the original publication[1] with kind permission from Elsevier.

In contrast to plates without a fluorescence indicator (λ_{max} = 300 nm, not shown), λ_{max} on Nano-SIL NH_2/UV_{254} was 310 nm. Thus, this wavelength was used for quantification.

5.3.6 Characterization of the optimized quantitative method

Densitograms of the plate from Figure 5.7 were recorded at 205 nm prior to derivatization (Figure 5.9 A) and at 310 nm after thermal derivatization (Figure 5.9 B).

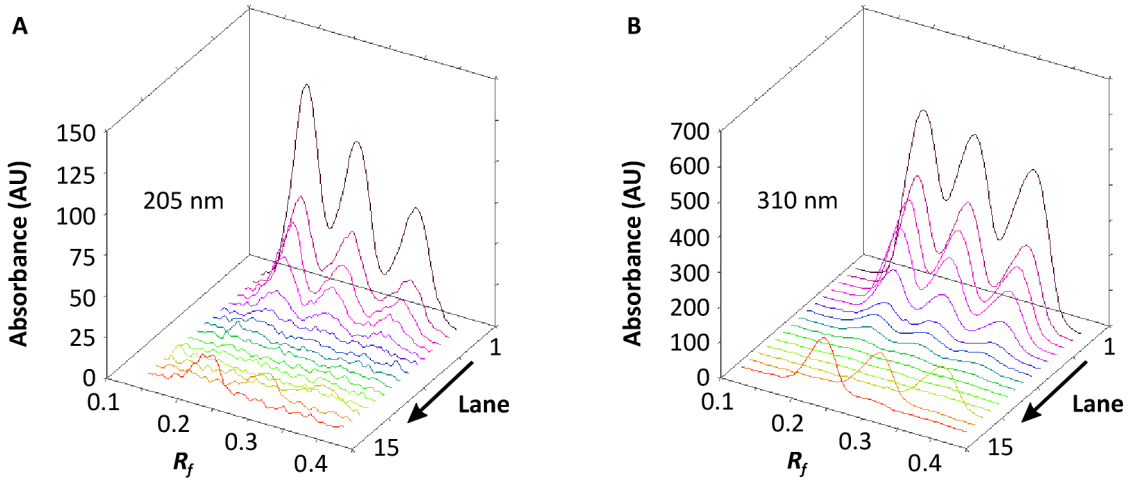

Figure 5.9: Densitograms (reflectance mode) of the plate from Figure 5.7 at 205 nm prior to derivatization (A) and at 310 nm after derivatization (B). Absorbance expressed as arbitrary units (AU). Reproduced from Fig. 8 of the original publication[1] with kind permission from Elsevier.

Limit of detection (LOD, signal-to-noise ratio 3:1) and limit of quantification (LOQ, signal-to-noise ratio 10:1) were determined from the densitogram at 310 nm as described.[24, 25] LOD was calculated by extrapolation. In contrast, LOQ was determined by interpolation of the linear lower part of the calibration curves (25–100 pmol). Depending on the oligosaccharide, LOD was 7–19 pmol per band and LOQ 37–71 pmol per band.

Compared to the LOD of 7.4 pmol for a recently published study using fluorophore-assisted carbohydrate electrophoresis (FACE),[26] the established HPTLC is a powerful and competitive alternative. Even the CZE–ESI-TOF-MS method presented in Chapter 3 revealed comparable or slightly lower LOD, considering analyte concentrations and the differences in applied sample volumes (10 µL for HPTLC, 990 pL for CZE).

Subsequently, quadratic calibration curves were constructed in the range between the respective LOQ and 2500 nm per band for the three oligosaccharides (Figure 5.10).

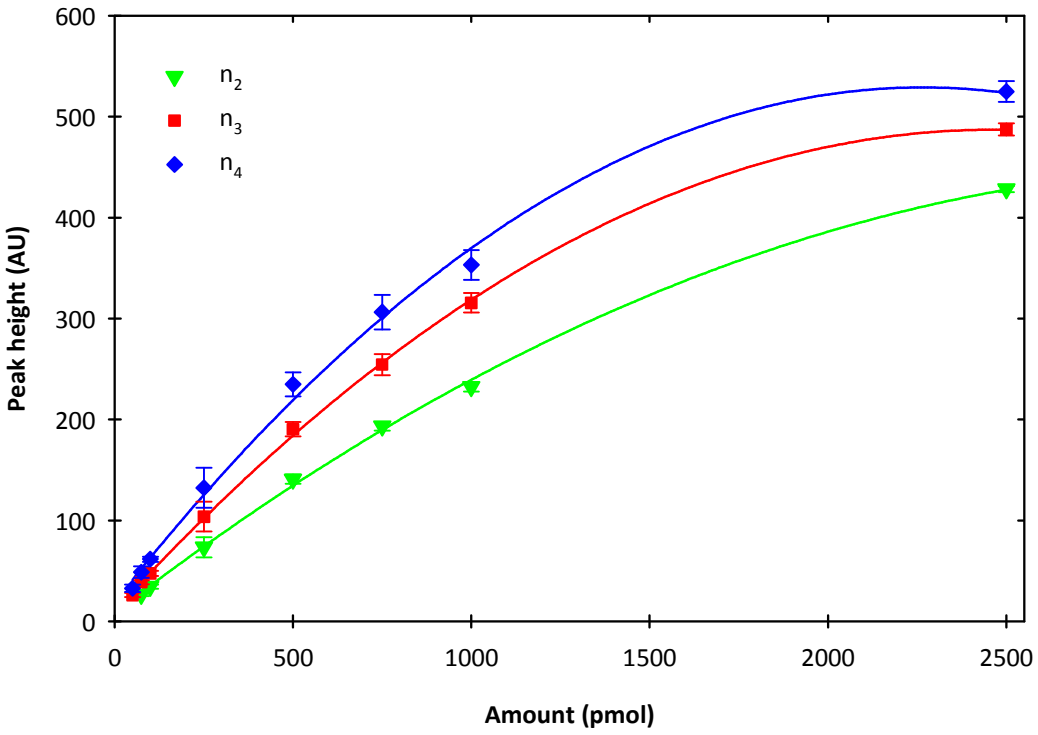

Figure 5.10: Quadratic calibration curves from absorbance scans at 310 nm (reflectance mode) of five individual plates. Tetrasaccharide (n_2, triangle, green), hexasaccharide (n_3, square, red) and octasaccharide (n_4, diamond, blue). Data presented as mean ± standard deviation. Peak heights expressed as arbitrary units (AU). Reproduced in a colored version from Fig. 9 of the original publication[1] with kind permission from Elsevier.

Correlation coefficients R^2 for the fitted curves ranged from 0.9968 to 0.9996. An overview of the quantification parameters is provided by Table 5.1. To further validate and characterize the method, the precision of the quantification was determined by intra-day and inter-day analysis. Analyses ($N = 5$) were conducted three times on the same day (repeatability) and on two following days (intermediate precision) by different

experimentators. The calculated amounts of the analytes, R_f values, and the corresponding precision parameters are listed in Table 5.2.

Table 5.1: Sensitivity of quantitative analysis (n_x: oligosaccharides consisting of *x* hyalobiuronic acid moieties). Content reproduced from Table 1 of the original publication[1] with kind permission from Elsevier.

	n_2	n_3	n_4
LOD, LOQ, calibration parameters			
Limit of detection (pmol), LOD, S/N = 3	19	10	7
Limit of quantification (pmol), LOQ, S/N = 10	71	48	37
Calibration range investigated (pmol)	75–2500	50–2500	50–2500
Coefficient of determination, R^2	0.9991	0.9996	0.9968
Quadratic calibration curve $y = ax^2 + bx + c$			
a	$-4.2104 \cdot 10^{-6}$	$-7.8426 \cdot 10^{-5}$	$-9.9323 \cdot 10^{-5}$
b	0.2730	0.3868	0.4501
c	8.4472	10.1879	18.9139

Table 5.2: Precision of R_f values and quantification for the optimized HPTLC method on amino-modified silica (n_x: oligosaccharides consisting of *x* hyalobiuronic acid moieties). Content reproduced from Table 2 of the original publication[1] with kind permission from Elsevier.

	n_2	n_3	n_4
R_f value: mean ± SD (RSD)			
Intra-day, *N* = 3	0.31 ± 0.03 (7.78%)	0.24 ± 0.03 (12.91%)	0.17 ± 0.03 (17.65%)
Inter-day, *N* = 3	0.35 ± 0.04 (10.20%)	0.26 ± 0.04 (15.81%)	0.20 ± 0.05 (22.91%)
Overall, *N* = 5	0.34 ± 0.03 (9.11%)	0.25 ± 0.03 (12.94%)	0.19 ± 0.03 (18.19%)
Calculated amount (pmol): mean ± SD (RSD)			
Intra-day, *N* = 3	445 ± 30 (6.82%)	286 ± 23 (8.10%)	330 ± 30 (8.98%)
Inter-day, *N* = 3	432 ± 18 (4.15%)	289 ± 35 (12.13%)	320 ± 20 (6.30%)
Overall, *N* = 5	440 ± 26 (5.86%)	292 ± 27 (9.37%)	331 ± 21 (6.47%)

5.3.7 Robustness

To evaluate robustness of the analytical method, the developing distance was increased, and the chromatography material was changed from HPTLC plates (glass-backed) to TLC plates (aluminum-backed). The former change simulates inadvertent exceeding of the validated developing distance in case of a device lacking automatic front detection. The latter variation explores a simplification, which might be relevant for screening purposes without the need of special HPTLC material. R_f values were determined for both variations. In addition, the amount of the oligosaccharides was calculated from the calibration standards on the respective plate. Mean, standard deviation, and relative standard deviation of all data from this experiment are summarized in Table 5.3.

Table 5.3: Robustness of separation and thermal derivatization (n_x: oligosaccharides consisting of *x* hyalobiuronic acid moieties). Content reproduced from Table 3 of the original publication[1] with kind permission from Elsevier.

	n_2	n_3	n_4
Robustness of separation			
Initial R_f	0.37	0.27	0.20
R_f upon extension of developing distance to 80 mm	0.41	0.34	0.27
R_f on aluminum-backed TLC plate	0.35	0.24	0.16
R_f: mean ± SD (RSD)	0.38 ± 0.03 (8.11%)	0.28 ± 0.05 (18.11%)	0.21 ± 0.06 (26.51%)
Calculated amount (pmol): mean ± SD (RSD)	444 ± 34 (7.59%)	288 ± 20 (6.94%)	347 ± 13 (3.70%)
Robustness of derivatization			
Initial peak height (AU)	129.4	115.6	166.7
Peak height (AU) after 5 d	125.4	112.3	161.7
Peak height (AU) after 5 d + 1 h heating	126.1	121.9	188.0
Peak height (AU): mean ± SD (RSD)	127.0 ± 2.1 (1.68%)	116.6 ± 4.9 (4.18%)	172.1 ± 14.0 (8.11%)
Calculated amount (pmol): mean ± SD (RSD)	449 ± 4 (0.86%)	272 ± 4 (1.37%)	339 ± 8 (2.30%)

When developing distance was 80 mm (from the bottom edge) instead of 70 mm, R_f values slightly increased, whereas the use of TLC material led to reduced R_f values. The range of standard deviations (0.03–0.06 R_f units), however, is comparable to that between different runs (Table 5.2). Peak heights were reduced in both cases due to peak broadening and, in

the case of the slim and flexible aluminum-backed TLC plate, probably also owing to the less tight contact between the TLC plate and the heater. Nevertheless, quantification is not affected, as it becomes obvious from the low relative standard deviations (3.70–7.59%).

Additionally, the detection procedure was modified with respect to the time from heating to scanning and the heating period itself. To evaluate the effect on peak heights and quantification, the same plate was re-scanned after 5 days, heated again for 1 h, and scanned for a third time. It turned out that band intensities were stable over at least 5 days. Although absolute peak heights increase with the heating period, the quantification is not affected (Table 5.3) because the calibration standards on the plate are always treated the same way as the sample. It should be noted that the signal-to-noise ratio can be improved by prolonged heating, enabling the quantification of low amounts of hyaluronan oligosaccharides. To increase throughput, however, 15 min of heating may be considered adequate for routine analysis.

In view of the optimal application, band length was varied between 4 and 12 mm (4, 6, 8, 10, and 12 mm) with an application volume of 5 or 10 µL (Figure 5.11). In this experiment, the validated conditions of 8 mm and 10 µL proved to be ideal.

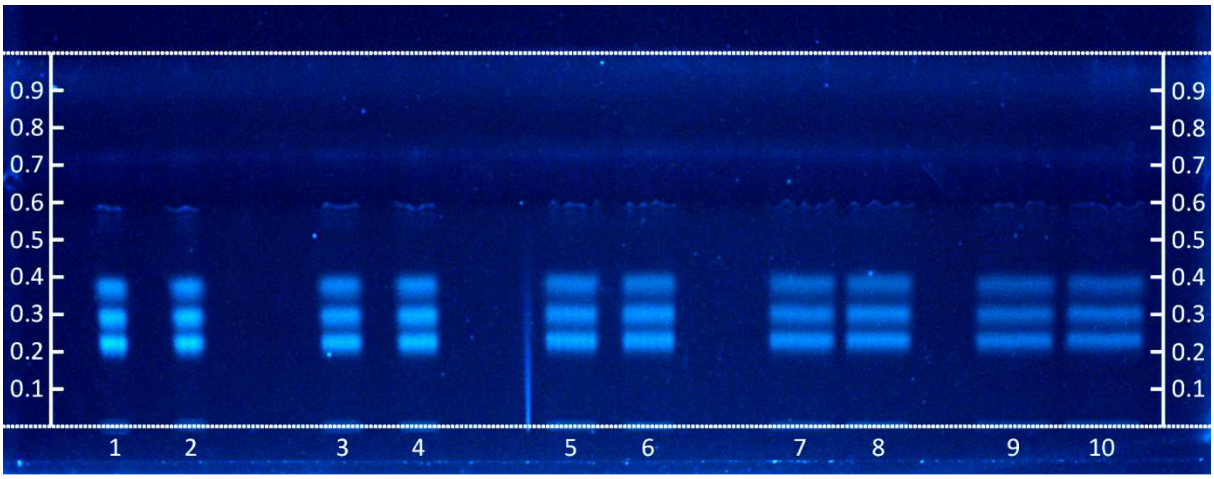

Figure 5.11: Variation of band length and spray volume. Amino-modified silica high performance thin layer chromatography (HPTLC) plate illuminated with UV light at 366 nm. Standard oligosaccharide mixture (n_2–n_4) 500 pmol/band. Band length: 4 mm (lanes 1, 2), 6 mm (lanes 3, 4), 8 mm (lanes 5, 6), 10 mm (lanes 7, 8), 12 mm (lanes 9, 10). Application volume: 10 µL (lanes 1, 3, 5, 7, and 9) or 5 µL (lanes 2, 4, 6, 8, and 10). Mobile phase: 1-butanol/formic acid/water (3:4:1). Developing distance: 6 cm (7 cm from the bottom edge). Vertical axes indicate the R_f scale. Reproduced from Supplementary Material 3 of the original publication[1] with kind permission from Elsevier.

5.3.8 Thin layer chromatography coupled to mass spectrometry

Hyphenation of thin layer chromatography and mass spectrometry (TLC–MS) with an appropriate interface broadens the applicability of planar chromatography for quality control of hyaluronan oligosaccharides. In this study, as proof of concept, ESI-Q-TOF-MS was used with standard silica TLC plates. In contrast to MALDI,[9] ESI is compatible with aluminum and glass as carrier material for the stationary phase and can be applied on both, normal TLC and HPTLC material.

A mixture (10 µL) of the purified oligosaccharide samples (250 µM each) was separated by normal phase TLC. Bands were located by densitometric scans at 205 nm. MS coupling in negative ionization mode revealed high resolution mass spectra with $[M-H]^-$ and $[M-2H]^{2-}$ ions as characteristic peaks. Full scan mass spectra obtained for the three oligosaccharides are depicted in Figure 5.12. The respective bands are marked in the inserted densitograms at 205 nm.

To identify the unknown peak at a mass-to-charge ratio of 982.99, the isotope pattern (Figure 5.13) was compared to the calculated and the experimental isotope pattern of the hyaluronan tetrasaccharide (n_2) $[M-H]^-$ ion (Figure 5.14). Calculated and experimentally observed isotope pattern for the sugar were in good accordance. The isotope pattern of the unidentified peak, however, suggested very low carbon content. Therefore, the signal probably corresponds to a highly fluorinated reaction product of the calibration standard hexakis(2,2,3,3-tetrafluoropropoxy)phosphazine.

As a result from TLC–MS, the identity and purity of the oligosaccharides prepared by enzymatic digestion and column chromatographic purification were confirmed. In particular, no odd-numbered oligosaccharides or other sugar impurities could be detected. Regardless of the relatively high amounts of analytes required, hyphenation of automated HPTLC to ESI-Q-TOF-MS represents an attractive tool for both, quantitative and unequivocal qualitative analysis of small hyaluronan oligosaccharides.

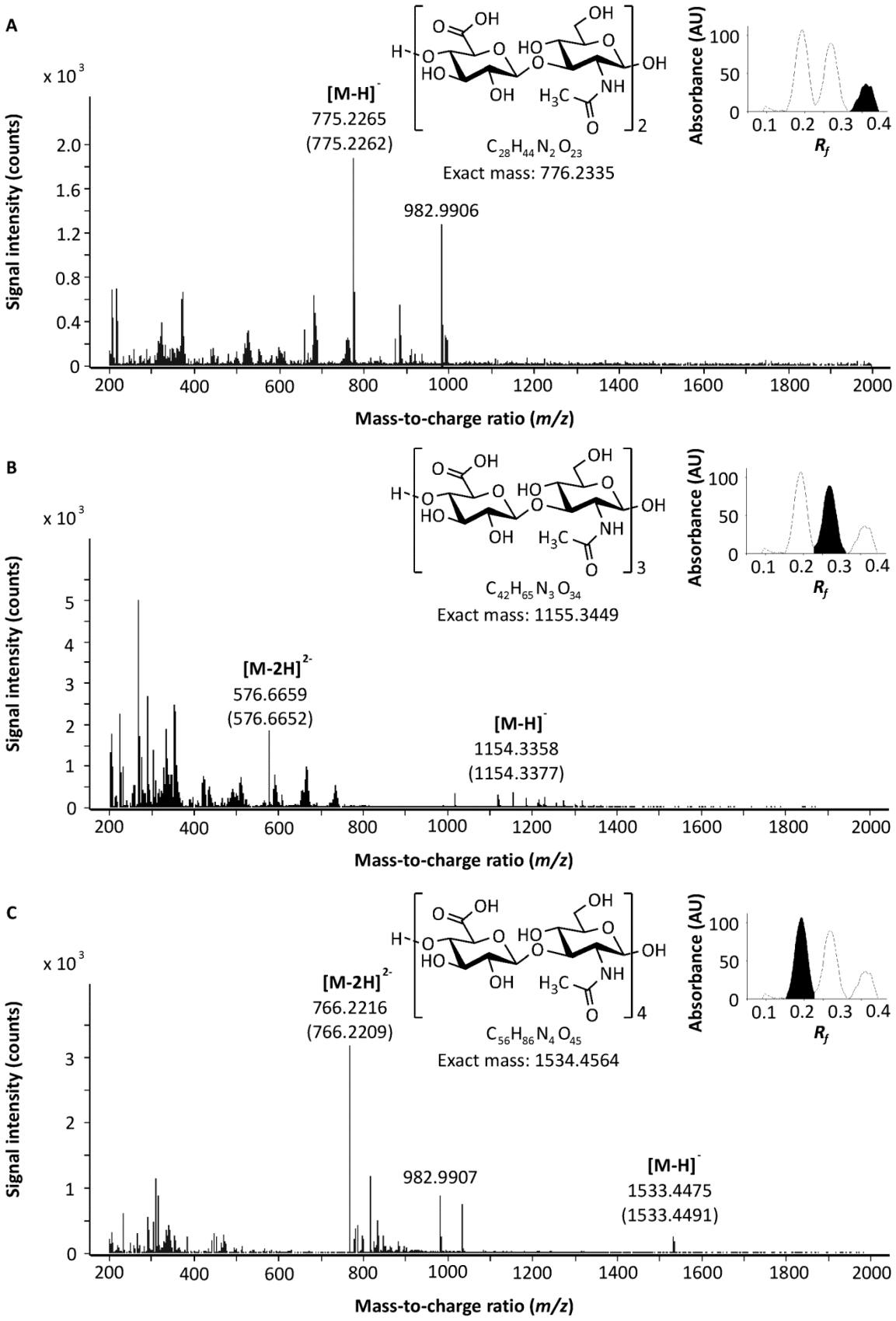

Figure 5.12: Full scan high resolution mass spectra of the hyaluronan oligosaccharides n_2 (A), n_3 (B), and n_4 (C) obtained by direct TLC–MS coupling (calculated masses in parentheses, densitograms from localization of underivatized analytes at 205 nm). Each oligosaccharide 2.5 nmol/band. Stationary phase: silica. Mobile phase: 1-butanol/formic acid/water (3:5:2). Developing distance: 6 cm (7 cm from the bottom edge). Reproduced from Supplementary Material 4 of the original publication[1] with kind permission from Elsevier.

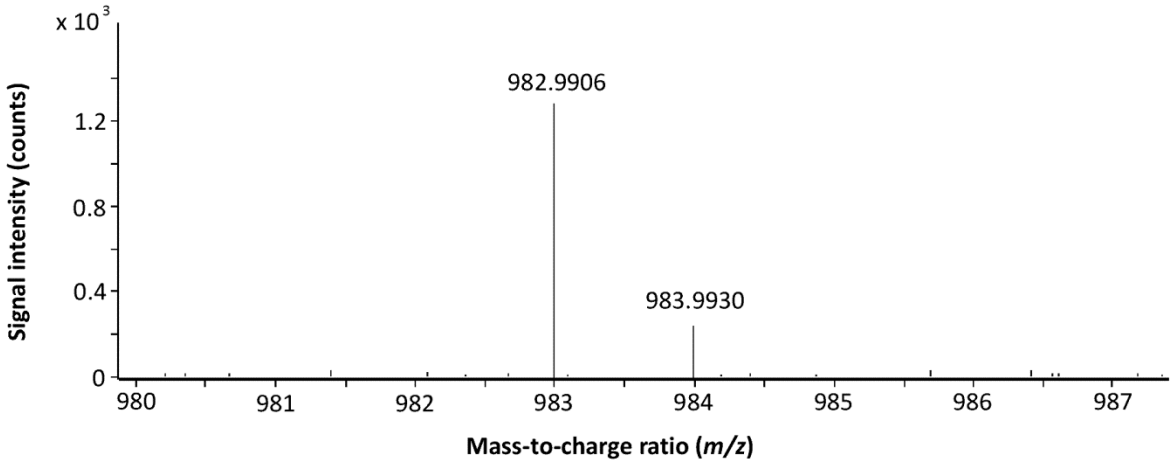

Figure 5.13: Isotope pattern of the signal at *m/z* = 982.9906 indicating the presence of a compound with a very low carbon content, probably corresponding to a reaction product of the highly fluorinated mass calibration standard hexakis(2,2,3,3-tetrafluoropropoxy)phosphazine. Reproduced from Supplementary Material 5 of the original publication[1] with kind permission from Elsevier.

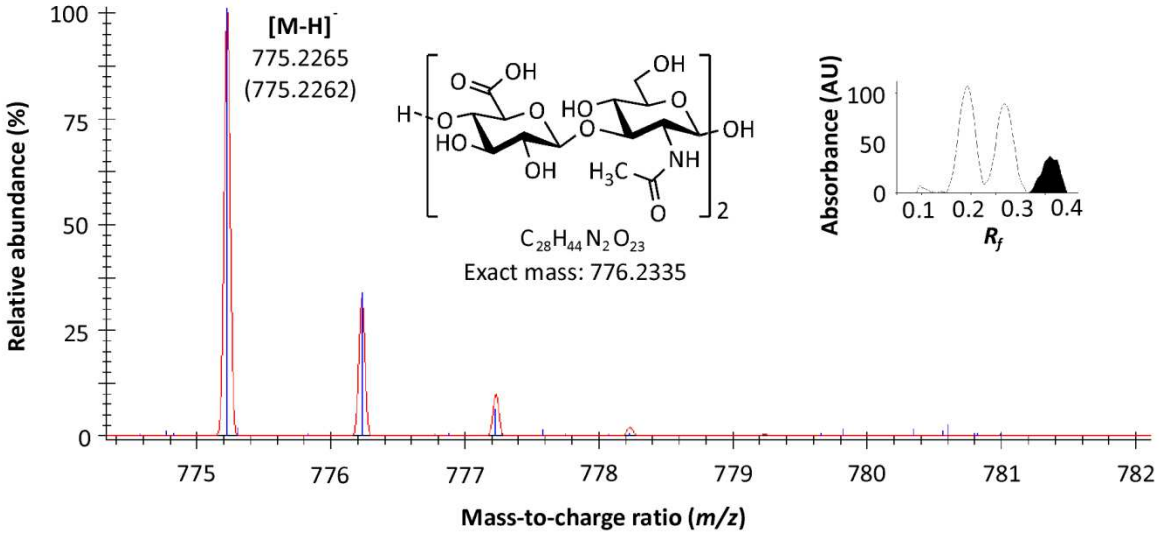

Figure 5.14: Overlay of experimental (blue) and calculated (red) isotope pattern of the tetrasaccharide (n_2) $[M-H]^-$ ion (calculated mass in parentheses, densitogram: underivatized analytes scanned at 205 nm). Reproduced from Supplementary Material 6 of the original publication[1] with kind permission from Elsevier.

5.4 Summary and conclusion

In addition to the fast CZE–ESI-TOF-MS method (*cf*. Chapter 3) and the sensitive electrochemical detection used in HPAEC–PAD (*cf*. Chapter 4), a convenient and cost-effective HPTLC method for the analysis of small saturated hyaluronan oligosaccharides consisting of 2–4 hyalobiuronic acid moieties (n_2–n_4) was established, allowing for qualitative as well as quantitative determination. The separation on amino-modified silica plates and subsequent label-free detection is superior to classical colorimetric reactions like orcinol or

Morgan-Elson reagent staining. Furthermore, unequivocal identification of the hyaluronan oligosaccharides from normal phase TLC plates is enabled by direct ESI-Q-TOF-MS coupling. Quantitative HPTLC is comparable to sophisticated methods like fluorophore-assisted carbohydrate electrophoresis[26] and CZE–ESI-TOF-MS (*cf*. Chapter 3) in terms of sensitivity. Although not reaching the excellent LOD values of HPAEC–PAD (*cf*. Chapter 4), in view of the low costs, the qualitative and quantitative analysis of multiple samples in parallel makes HPTLC an extremely interesting alternative, especially for quality control of hyaluronan oligosaccharides.

5.5 References

1. Rothenhöfer, M.; Scherübl, R.; Bernhardt, G.; Heilmann, J.; Buschauer, A. Qualitative and quantitative analysis of hyaluronan oligosaccharides with high performance thin layer chromatography using reagent-free derivatization on amino-modified silica and electrospray ionization-quadrupole time-of-flight mass spectrometry coupling on normal phase. *J. Chromatogr. A* **2012,** 1248, 169-177.

2. Weissmann, B.; Meyer, K.; Sampson, P.; Linker, A. Isolation of oligosaccharides enzymatically produced from hyaluronic acid. *J. Biol. Chem.* **1954,** 208, 417-429.

3. Prebyl, B. S.; Kaczmarek, C.; Tuinman, A. A.; Baker, D. C. Characterizing the electrospray-ionization mass spectral fragmentation pattern of enzymatically derived hyaluronic acid oligomers. *Carbohydr. Res.* **2003,** 338, 1381-1387.

4. Price, K. N.; Al, T.; Baker, D. C.; Chisena, C.; Cysyk, R. L. Isolation and characterization by electrospray-ionization mass spectrometry and high-performance anion-exchange chromatography of oligosaccharides derived from hyaluronic acid by hyaluronate lyase digestion: observation of some heretofore unobserved oligosaccharides that contain an odd number of units. *Carbohydr. Res.* **1997,** 303, 303-311.

5. Tawada, A.; Masa, T.; Oonuki, Y.; Watanabe, A.; Matsuzaki, Y.; Asari, A. Large-scale preparation, purification, and characterization of hyaluronan oligosaccharides from 4-mers to 52-mers. *Glycobiology* **2002,** 12, 421-426.

6. Reich, E.; Widmer, V. Plant analysis 2008 − planar chromatography. *Planta Med.* **2009,** 75, 711-718.

7. Morlock, G.; Schwack, W. Hyphenations in planar chromatography. *J. Chromatogr. A* **2010,** 1217, 6600-6609.

8. Kudo, K.; Tu, A. T. Characterization of hyaluronidase isolated from *Agkistrodon contortrix contortrix* (Southern Copperhead) venom. *Arch. Biochem. Biophys.* **2001,** 386, 154-162.

9. Nimptsch, K.; Süß, R.; Riemer, T.; Nimptsch, A.; Schnabelrauch, M.; Schiller, J. Differently complex oligosaccharides can be easily identified by matrix-assisted laser desorption and ionization time-of-flight mass spectrometry directly from a standard thin-layer chromatography plate. *J. Chromatogr. A* **2010,** 1217, 3711-3715.

10. Shimada, E.; Matsumura, G. Thin-layer chromatography of hyaluronate oligosaccharides. *J. Biochem.* **1984,** 96, 721-725.

11. Zhang, Z.; Xie, J.; Zhang, F.; Linhardt, R. J. Thin-layer chromatography for the analysis of glycosaminoglycan oligosaccharides. *Anal. Biochem.* **2007,** 371, 118-120.

12. Hofinger, E. S. A.; Bernhardt, G.; Buschauer, A. Kinetics of Hyal-1 and PH-20 hyaluronidases: comparison of minimal substrates and analysis of the transglycosylation reaction. *Glycobiology* **2007,** 17, 963-971.

13. Grundmann, M.; Rothenhöfer, M.; Bernhardt, G.; Buschauer, A.; Matysik, F. M. Fast counter-electroosmotic capillary electrophoresis−time-of-flight mass spectrometry of hyaluronan oligosaccharides. *Anal. Bioanal. Chem.* **2012,** 402, 2617-2623.

14. Muckenschnabel, I.; Bernhardt, G.; Spruß, T.; Dietl, B.; Buschauer, A. Quantitation of hyaluronidases by the Morgan-Elson reaction: comparison of the enzyme activities in the plasma of tumor patients and healthy volunteers. *Cancer Lett.* **1998,** 131, 13-20.

15. Gacesa, P.; Savitsky, M. J.; Dodgson, K. S.; Olavesen, A. H. A recommended procedure for the estimation of bovine testicular hyaluronidase in the presence of human serum. *Anal. Biochem.* **1981,** 118, 76-84.

16. Reissig, J. L.; Storminger, J. L.; Leloir, L. F. A modified colorimetric method for the estimation of *N*-acetylamino sugars. *J. Biol. Chem.* **1955,** 217, 959-966.

17. Morgan, W. T.; Elson, L. A. A colorimetric method for the determination of *N*-acetylglucosamine and *N*-acetylchrondrosamine. *Biochem. J.* **1934,** 28, 988-995.

18. Müthing, J. TLC in structure and recognition studies of glycosphingolipids. *Methods Mol. Biol.* **1998,** 76, 183-195.

19. Partridge, S. M.; Westall, R. G. Filter-paper partition chromatography of sugars; general description and application to the qualitative analysis of sugars in apple juice, egg white and foetal blood of sheep. *Biochem. J.* **1948,** 42, 238-250.

20. Klaus, R.; Fischer, W.; Hauck, H. E. Use of a new adsorbent in the separation and detection of glucose and fructose by HPTLC. *Chromatographia* **1989,** 28, 364-366.

21. Klaus, R.; Fischer, W.; Hauck, H. E. Application of a thermal *in situ* reaction for fluorimetric detection of carbohydrates on NH_2-layers. *Chromatographia* **1990,** 29, 467-472.

22. Morlock, G. E.; Prabha, S. Analysis and stability of sucralose in a milk-based confection by a simple planar chromatographic method. *J. Agric. Food Chem.* **2007,** 55, 7217-7223.

23. Klaus, R.; Fischer, W.; Hauck, H. E. Extension of the application of the thermal *in-situ* reaction on NH_2 layers to the detection of catecholamines in biological materials. *Chromatographia* **1993,** 37, 133-143.

24. Kandler, H.; Bleisch, M.; Widmer, V.; Reich, E. A validated HPTLC method for the determination of illegal dyes in spices and spice mixtures. *J. Liq. Chromatogr. Relat. Technol.* **2009,** 32, 1273-1288.

25. Bazylko, A.; Kiss, A. K.; Kowalski, J. High-performance thin-layer chromatography method for quantitative determination of oenothein B and quercetin glucuronide in aqueous extract of Epilobii angustifolii herba. *J. Chromatogr. A* **2007,** 1173, 146-150.

26. Kooy, F. K.; Ma, M.; Beeftink, H. H.; Eggink, G.; Tramper, J.; Boeriu, C. G. Quantification and characterization of enzymatically produced hyaluronan with fluorophore-assisted carbohydrate electrophoresis. *Anal. Biochem.* **2009,** 384, 329-336.

6 Product spectra of hyaluronidases from bovine testes and from *Streptococcus agalactiae*

6.1 Introduction

In our lab, bovine testicular hyaluronidase (BTH) and hyaluronidase from *Streptococcus agalactiae*, strain 4755, are used to identify hyaluronidase inhibitors. In addition, a lot of work was done on the characterization and comparison of these enzymes and respective preparations.[1-3] Both of them are representative examples of mammalian type hyaluronidases and those of bacterial origin, respectively. Mammalian and bacterial hyaluronidases are of particular medical and pharmacological interest and are known to exhibit fundamentally different mechanisms of hyaluronan degradation (*cf*. Chapter 1, Section 1.2.1).[4]

Testicular hyaluronidase is an endolytic enzyme, randomly hydrolyzing the β-1,4 glycosidic bonds of the hyaluronan chains.[4, 5] Thereby, oligosaccharide mixtures, mainly containing the tetrasaccharide (n_2) and the hexasaccharide (n_3), are yielded after exhaustive digestion of hyaluronan.[6-8] In addition, the enzymatic process is characterized by the parallel occurrence of hydrolysis and transglycosylation reactions, both contributing to the observed product formation.[6-14]

Hyaluronidase from *Streptococcus agalactiae* catalyzes β-elimination with unsaturated disaccharides accumulating as end products.[4, 15] A simplified reaction, assuming the theoretical minimal substrate (tetrasaccharide, n_2), and the use of abbreviations for the oligosaccharides are illustrated in Figure 6.1. Oligosaccharides are abbreviated as n_x according to the number of disaccharide units (*x*), asterisks indicate molecules with double bonds in the ring. Having observed no other oligosaccharides in partially digested hyaluronan, Pritchard et al. suggested a mechanism consisting of an initial random cleavage step followed by processive release of unsaturated disaccharides (n_1*) from the end of the hyaluronan chain.[15] Thereby, the enzyme is assumed to move along the polysaccharide chain.[15] The processive mode of action was confirmed later by digestion studies[16] as well as structural information of the enzyme in complex with substrate molecules of varying chain length.[17-19] Nevertheless, the models differ with regard to the direction of enzymatic action. While Li and Jedrzejas propose degradation from the reducing to the non-reducing end,[18] Baker and Pritchard suggest the opposite direction.[16]

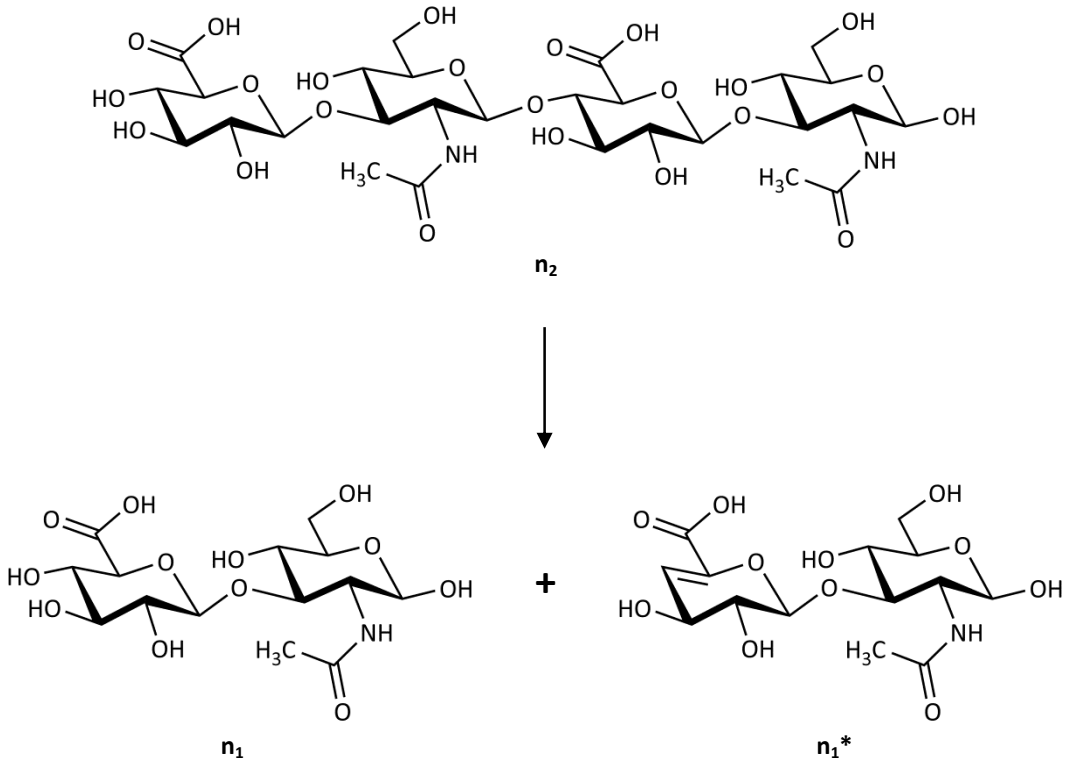

Figure 6.1: Formation of saturated (n_x) and unsaturated (n_x*) oligosaccharides by hyaluronidase from *Streptococcus agalactiae*, assuming the tetrasaccharide n_2 as substrate. Oligosaccharides are abbreviated according to the number of disaccharide units (*x*). Asterisks indicate molecules with double bonds in the ring.

Using hyaluronan and hyaluronan oligosaccharides of various molecular weights as substrates, this work aimed at deeper insight into the mechanisms of enzymatic action. Thereby, the focus was set on small oligosaccharides as these products of hyaluronan degradation are supposed to play important roles in physiological and pathophysiological processes.[20] Moreover, enzymological characterization, which is only possible when minimal substrates are used, was carried out for the bacterial enzyme using HPAEC–PAD.

6.2 Materials and methods

6.2.1 Enzymes and substrates

Bovine testicular hyaluronidase (BTH, Neopermease®) was kindly provided by Sanabo (Vienna, Austria). Bacterial hyaluronidase from *Streptococcus agalactiae*, strain 4755, was a gift from id-Pharma (Jena, Germany). Hyaluronan and hyaluronan oligosaccharides of various chain lengths were used as substrates. High molecular weight hyaluronan of bacterial origin (*Streptococcus zooepidemicus*) was purchased from Aqua Biochem (Dessau, Germany). Hyalo-Oligo, kindly provided by Kewpie (also named Q. P. Corp., Tokyo, Japan), served as low molecular weight hyaluronan oligosaccharide mixture with an average molecular weight

below 10 kDa. Purified oligosaccharides of 2–4 hyalobiuronic acid moieties (n_2–n_4) were prepared from high molecular weight hyaluronan as described in Chapter 5. For quantification, the colorimetric method was used (*cf*. Chapter 5, Section 5.2.3).

6.2.2 Incubation mixtures

The protocol for hyaluronan digestion was based on the conditions previously used in the colorimetric assay for the determination of hyaluronidase activity[21, 22] and in studies by Hofinger et al.[7, 10] on hyaluronan degradation by different hyaluronidases. A 0.2 M solution of disodium hydrogen phosphate (Merck, Darmstadt, Germany) was mixed with a 0.1 M solution of citric acid (Merck, Darmstadt, Germany), both containing 0.1 M sodium chloride (VWR, Haasrode, Belgium), to yield the desired pH value of 5.0. In general, incubation mixtures consisted of 4 parts of the incubation buffer, 2 parts of water (purified with a Milli-Q system, Millipore, Eschborn, Germany), 1 part of a 0.2 mg/mL solution of bovine serum albumin (Serva, Heidelberg, Germany), and 1 part of an aqueous solution of hyaluronan or hyaluronan oligosaccharides. For high molecular weight hyaluronan and the Hyalo-Oligo mixture, this solution contained 5 mg/mL of the respective hyaluronan preparation. The purified oligosaccharides were adjusted to the desired molarity using the concentration values calculated from colorimetric determination.

Enzyme solutions were diluted by addition of bovine serum albumin solution to yield an activity of 500 or 400 IU/mL (BTH) and 500, 400, or 20 IU/mL (bacterial enzyme), based on the activity declaration by the supplier. 1 part of this enzyme solution was added to 8 parts of the incubation mixtures to start the enzymatic reaction, resulting in final activities of 55.56, 44.44, and 2.22 IU/mL. The respective value is given with each experiment. To reference samples, bovine serum albumin solution was added instead.

6.2.3 HPAEC–PAD

After incubation at 37 °C for appropriate periods of time, the reaction was stopped by boiling. Precipitated protein was removed by centrifugation and filtration as described in Chapter 4 (Section 4.2.1). Prior to injection, samples were diluted 1:10 with purified water. Chromatography was then carried out as described (*cf*. Chapter 4), using the CarboPac™ PA200 column (Dionex/Thermo Fisher Scientific, Idstein, Germany) at an eluent flow rate of 0.5 mL/min at 40 °C, 100 mM sodium hydroxide, and a gradient of 200–900 mM sodium acetate. In contrast to at-line CZE–ESI-TOF-MS (*cf*. Section 6.2.4), an additional sample (t = 0 min) was boiled immediately after addition of enzyme.

6.2.4 Fast at-line CZE–ESI-TOF-MS

CZE–ESI-TOF-MS analysis was basically carried out according to the description in Chapter 3. For at-line experiments, a water bath (heated to 37 °C) was placed next to the CE system. The exact setup, including the water bath, was already presented in Section 3.2.5. To allow for pressure-free injection, a 25 µm × 28 cm capillary was used. The background electrolyte was ammonium acetate (25 mM, pH = 8.5). Aliquots from the incubation mixtures (*cf*. Section 6.2.2) in the water bath were taken after defined time intervals. After dilution with 9 parts (1:10 dilution) of a 100 µM aqueous solution of acarbose (Bayer, Wuppertal, Germany) and short mixing, a 30 s pressure-free injection (using the suction from ESI-MS) was performed. For the first short time intervals, only single injections could be performed. Multiple consecutive injections were conducted for the later measurements. Control with bovine serum albumin instead of enzyme was measured at t = 0 min.

6.2.5 Saturation experiment

To determine enzymological parameters for the hyaluronidase from *Streptococcus agalactiae*, a saturation experiment was performed. Incubation mixtures were prepared as described (*cf*. Section 6.2.2), containing the tetrasaccharide (n_2) at concentrations of 1, 2, 5, 10, 20, 50, 100, 200, 500, 1000, and 2000 µM (determined by colorimetry). The enzyme was diluted to yield an activity of 5 IU/mL (according to the specification by the supplier) in the incubation mixture. Bovine serum albumin was added to control (t = 0 min) instead of enzyme. After 5, 10, 20, 30, 40, and 60 min of incubation at 37 °C, the reaction was stopped by 10 min of boiling, and protein was removed by centrifugation and filtration (*cf*. Chapter 4, Section 4.2.1). Samples with initial concentrations above 10 µM were diluted with purified water to a concentration of 10 µM to ensure linearity of the following HPAEC–PAD analysis. Chromatography conditions were the same as listed in Section 6.2.3. For each incubation period, the substrate concentrations were calculated from the initial concentration and the ratio of peak areas compared to control. Curves were fitted with SigmaPlot for Windows 11.2.0.5 (Systat Software Inc., San Jose, CA, USA).

6.3 Results and discussion

6.3.1 Degradation of a low molecular weight hyaluronan oligosaccharide mixture by bovine testicular hyaluronidase

The bacterial enzyme shows maximum activity at a pH value of 5.0.[1] In addition, this value lies in between the different maxima of the activity curves obtained for bovine testicular hyaluronidase (BTH) by turbidimetric and colorimetric determination[7] as well as for the different fractions from size exclusion chromatography of the BTH preparation.[1, 7] Consequently, reactions were carried out at pH = 5.0.

The time-dependent degradation of a mixture of hyaluronan oligosaccharides of low molecular weight by bovine testicular hyaluronidase was analyzed by HPAEC–PAD (Figure 6.2). Thereby, a series of oligosaccharides was observed, exhibiting a time-dependent decrease in molecular weight. These findings and the accumulation of n_2 and n_3 as end products were consistent with the degradation of high molecular weight hyaluronan (at pH = 5.5) followed by CZE analysis.[7] Moreover, the proposed random endolytic mechanism of bovine testicular hyaluronidase[4, 5] was supported. In addition, Deschrevel et al. recently reported that the most stable enzyme–substrate complexes were formed with oligosaccharides of 8–20 hyalobiuronic acid moieties (n_8–n_{20}).[23] In agreement with this data, we observed fast degradation of the oligosaccharides of this size range at the beginning of the incubation. The formed fragments seemed to be much poorer substrates, resulting in only very slow further cleavage.

After 72 h, the tetrasaccharide (n_2) and the hexasaccharide (n_3) were the main products. Nevertheless, n_3 was produced much faster than n_2. Within the first 24 h, more n_3 than n_2 was present in the mixture (Figure 6.2 B). Hence, the time-dependent curves were in very good accordance to the results reported by Cramer et al. for the degradation of the decasaccharide (n_5) who obtained basically identical curve shapes for n_2, n_3, and n_4.[6] The formation of relatively high amounts of n_2 seemed to correlate with the disappearance of n_4 (Figure 6.2 B), which might be cleaved into two molecules of n_2. Another possible reason for the increased amount of n_2 after prolonged incubation is the additional contribution of transglycosylation to the formation of this saccharide from n_3,[6, 9] becoming more relevant with increasing concentrations of n_3. To study the turnover of small oligosaccharides in detail, additional CZE–ESI-TOF-MS experiments were performed. The results are discussed in Section 6.3.3.

A

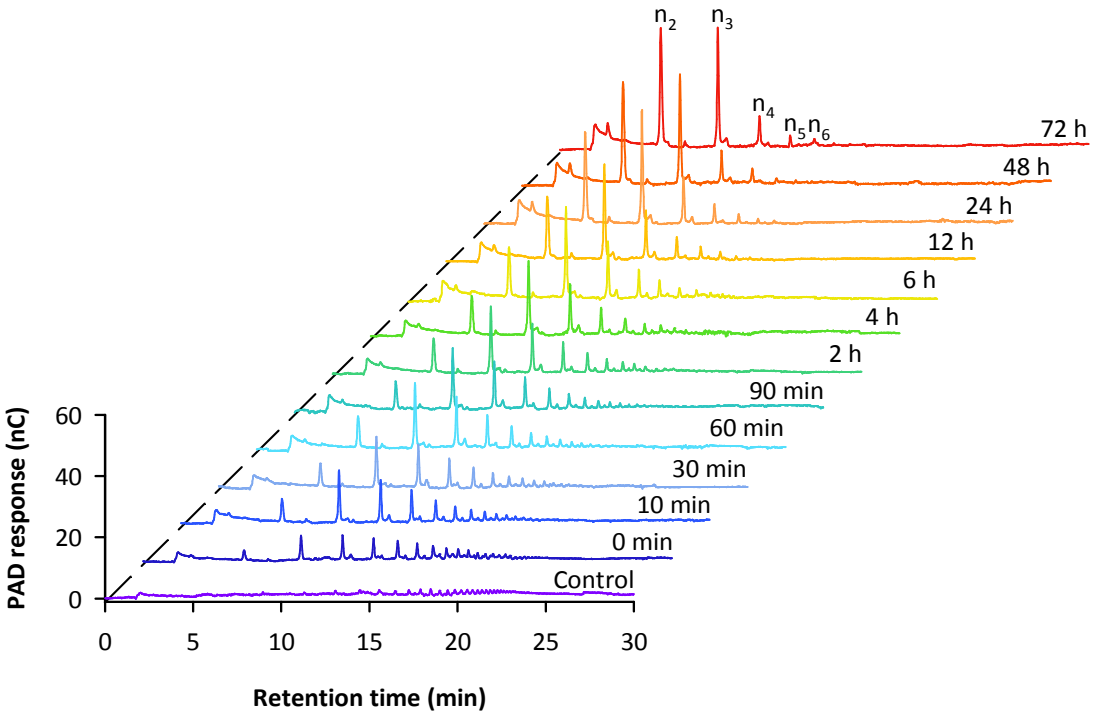

B

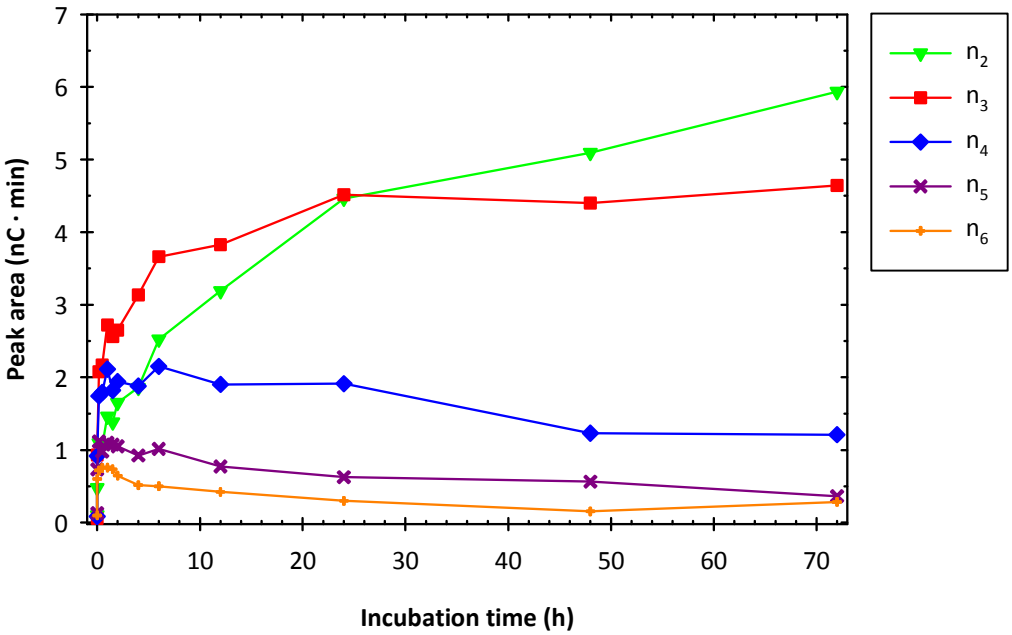

Figure 6.2: Time-dependent degradation of a low molecular weight hyaluronan oligosaccharide mixture by bovine testicular hyaluronidase (44.44 IU/mL) at pH = 5.0. Chromatograms (A) and peak areas (B). HPAEC–PAD: 10 µL of diluted (1:10) sample injected, CarboPac™ PA200, 100 mM sodium hydroxide, gradient of 200–900 mM sodium acetate, 40 °C, 0.5 mL/min.

6.3.2 Size-dependent degradation of hyaluronan by bovine testicular hyaluronidase

The incubation of both, high molecular weight hyaluronan (HMW HA) and low molecular weight hyaluronan (LMW HA), led to the intermediate formation of multiple oligosaccharides and accumulation of n_2, n_3, and n_4 after 24 h (Figure 6.3). Hence, no principal differences in the mechanism and the formed main products were observed for HMW and LMW substrates. As the enzyme acts randomly,[5] higher amounts of small oligosaccharides were observed after 1 h for the LMW mixture (Figure 6.3 E), compared to the long chains providing more possible positions for endolytic attack (Figure 6.3 B). As already discussed in Section 6.3.1, the small oligosaccharides are relatively poor substrates to the enzyme. For this reason and due to their increased formation from LMW hyaluronan, significant amounts of residual oligosaccharides n_5, n_6, and n_7 were still present after 24 h in Figure 6.3 F, but not in Figure 6.3 C. In summary, this is in agreement with the mechanism proposed in Section 6.3.1.

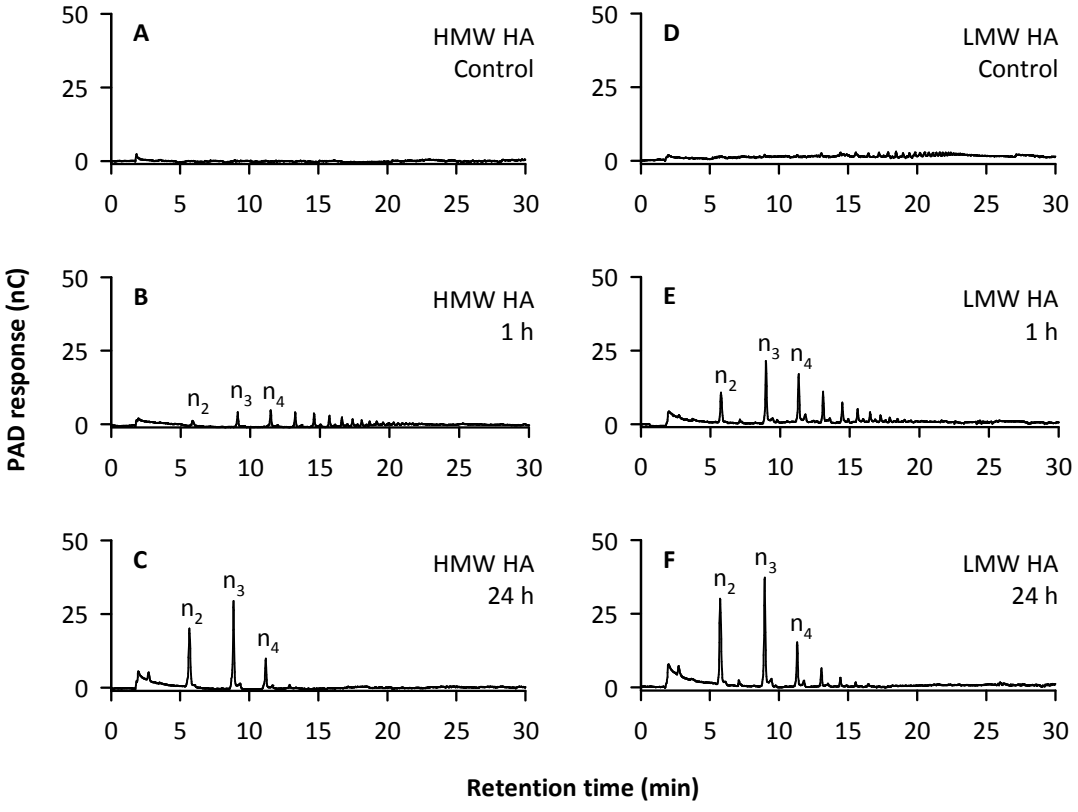

Figure 6.3: Incubation of high molecular weight hyaluronan (HMW HA, A–C) and a low molecular weight hyaluronan oligosaccharide mixture (LMW HA, D–F) with bovine testicular hyaluronidase (44.44 IU/mL) at pH = 5.0 for 1 h (B, E) and 24 h (C, F). Controls (A, D) contained bovine serum albumin instead of enzyme. HPAEC–PAD: 10 µL of diluted (1:10) sample injected, CarboPac™ PA200, 100 mM sodium hydroxide, gradient of 200–900 mM sodium acetate, 40 °C, 0.5 mL/min.

6.3.3 Fast at-line analysis of hyaluronan oligosaccharide degradation by bovine testicular hyaluronidase

In an at-line CZE–ESI-TOF-MS experiment, 500 µM of the octasaccharide (n_4, Figure 6.4), the hexasaccharide (n_3, Figure 6.5), and the tetrasaccharide (n_2, Figure 6.6) were incubated with 55.56 IU/mL bovine testicular hyaluronidase. Although signals of different analytes cannot be compared quantitatively due to differences in ionizability and MS sensitivity at the respective *m/z* ratio, qualitative and semi-quantitative conclusions are possible.

Interestingly, the disappearance of n_4 was accompanied by an almost parallel formation of n_2 and n_3 (Figure 6.4 B). Hence, the mechanism cannot be described by simple hydrolysis. Otherwise, significant amounts of n_1 would have been expected from the formation of n_3. Moreover, the formation of two molecules of n_2 out of one molecule of n_4 should have led to higher amounts of n_2 compared to n_3, assuming comparable contribution of both reactions. However, the findings are absolutely consistent with recent results by Kakizaki et al. and their mechanistic model.[11] The authors suggested the intermediate formation of a disaccharide unit (n_1) which is immediately transferred to the non-reducing end of a second oligosaccharide.[11] However, free n_1 was only detected in their incubation mixtures at trace concentrations using mass spectrometry.[11] By CZE–ESI-TOF-MS we were able to confirm the occurrence of only traces of n_1 (Figure 6.4, insets, light blue). Additionally, the formation of the decasaccharide (n_5) as product of transglycosylation was proven by Kakizaki et al.[11] as well as by our own experiments (Figure 6.4, insets, violet). We could even detect traces of the dodecasaccharide (n_6) after approximately 60–120 min of incubation (Figure 6.4, insets, orange). Assuming the described mechanism, the parallel formation of n_2 and n_3 can be explained by the transfer of intermediately formed n_1 to n_4, followed by the hydrolysis of the resulting n_5 yielding n_2 and n_3.

Neither n_3 (Figure 6.5) nor n_2 (Figure 6.6) showed any degradation. Although n_3 is known to be the minimal substrate of bovine testicular hyaluronidase,[6, 8-11] the hexasaccharide is reported to be an extremely poor substrate of the enzyme.[10, 11] Kakizaki et al. reported the degradation of approximately 10% of n_3 after 24 h.[11] In addition, Hofinger et al. described an inhibitory effect of n_3 on enzyme activity at concentrations of 200–800 µM (depending on pH).[10] With regard to the 1:10 dilution step, necessary for at-line CZE–ESI-TOF-MS, a relatively high oligosaccharide concentration of 500 µM had been chosen. Thus, substrate inhibition may explain why n_3 was not degraded.

A

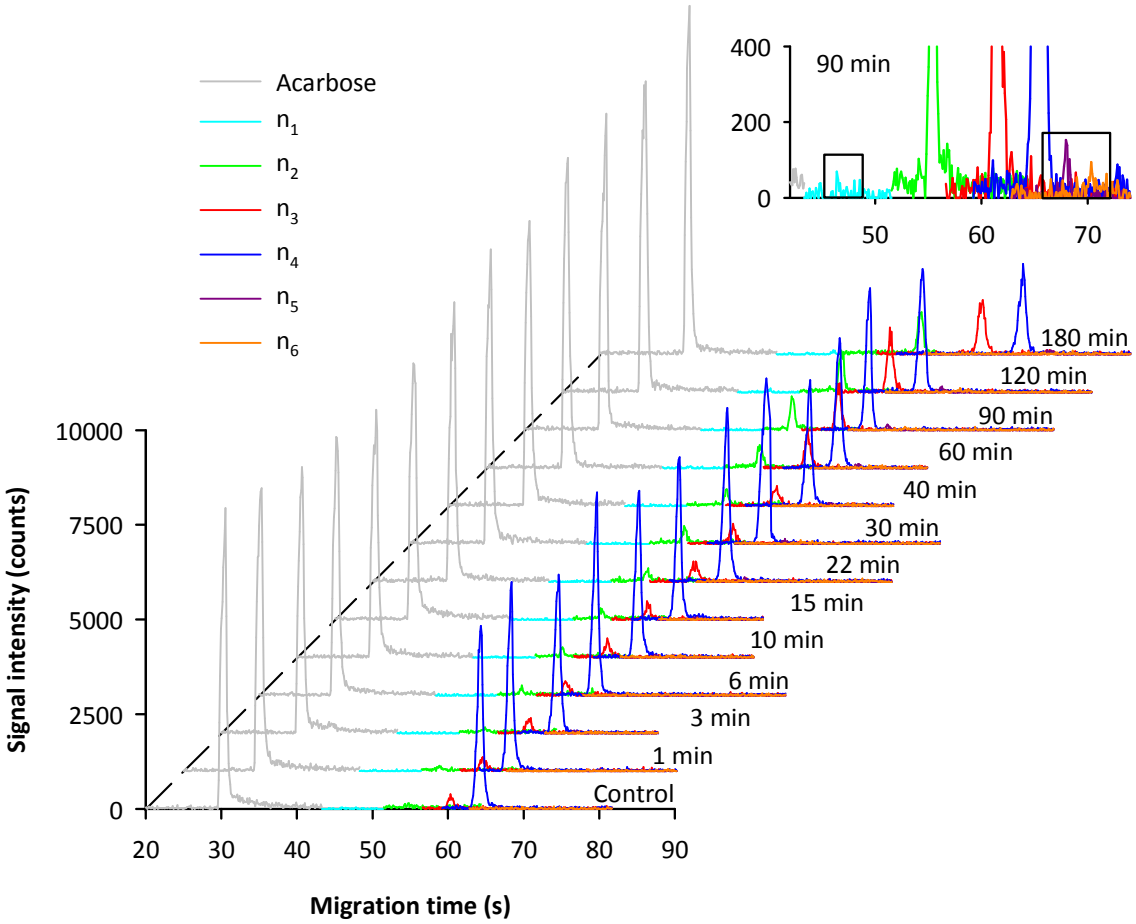

B

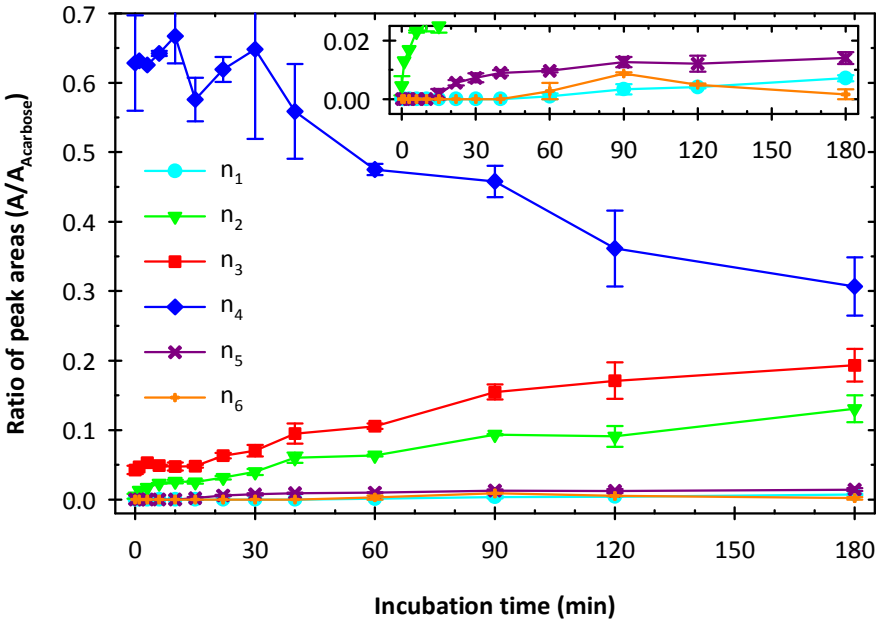

Figure 6.4: Incubation of the octasaccharide (n_4, 500 µM) with bovine testicular hyaluronidase (55.56 IU/mL) at pH = 5.0. Electropherograms (A) and standardized peak areas (B). Mean ± SEM for multiple injections. CZE: 1:10 sample dilution, 30 s injection, 25 µm × 28 cm capillary, ammonium acetate (25 mM, pH = 8.5), 35 kV.

A

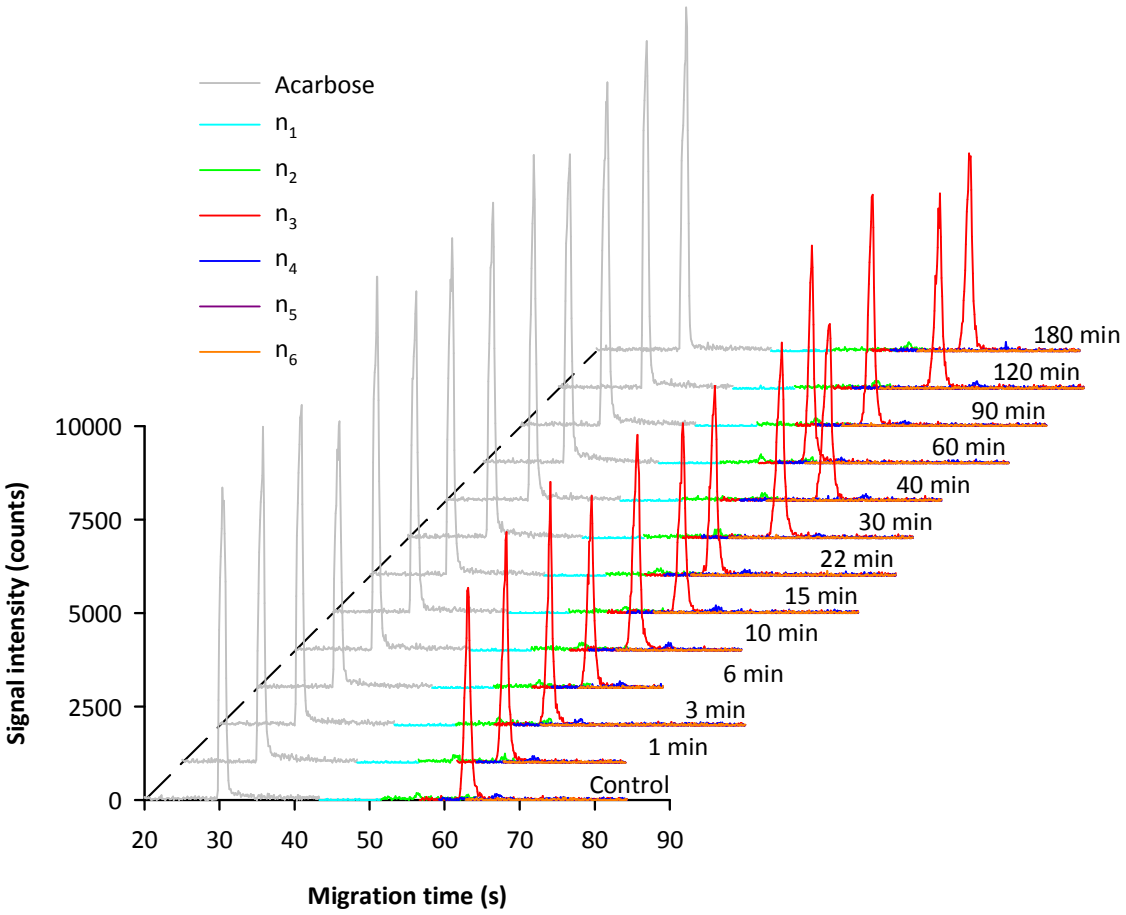

B

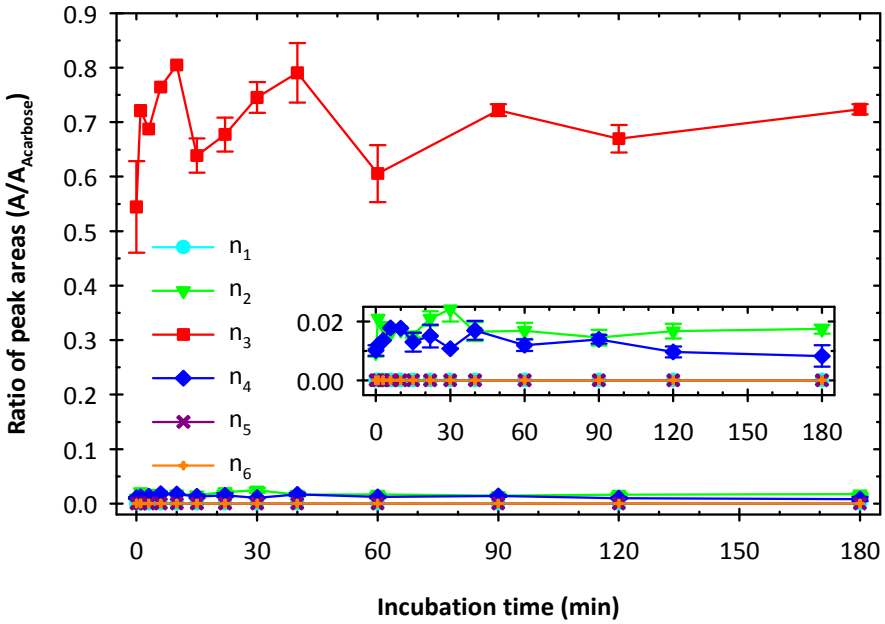

Figure 6.5: Incubation of the hexasaccharide (n_3, 500 µM) with bovine testicular hyaluronidase (55.56 IU/mL) at pH = 5.0. Electropherograms (A) and standardized peak areas (B). Mean ± SEM for multiple injections. CZE: 1:10 sample dilution, 30 s injection, 25 µm × 28 cm capillary, ammonium acetate (25 mM, pH = 8.5), 35 kV.

A

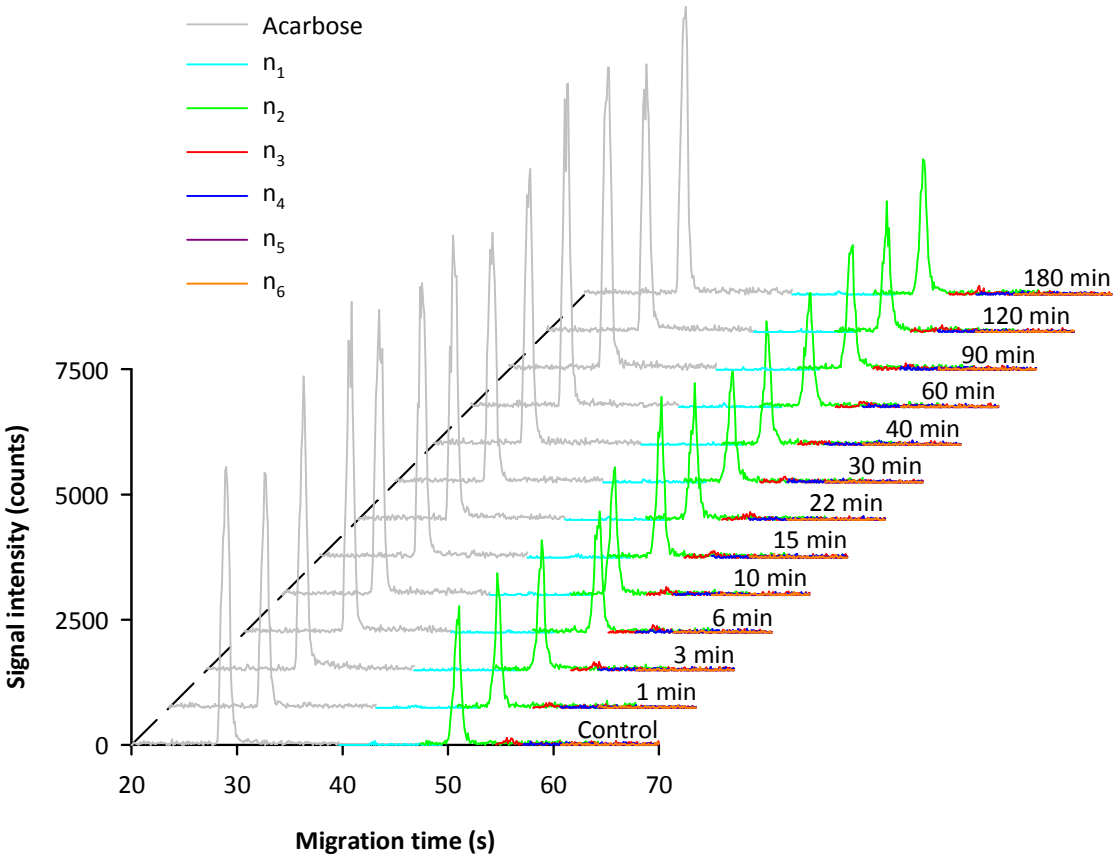

B

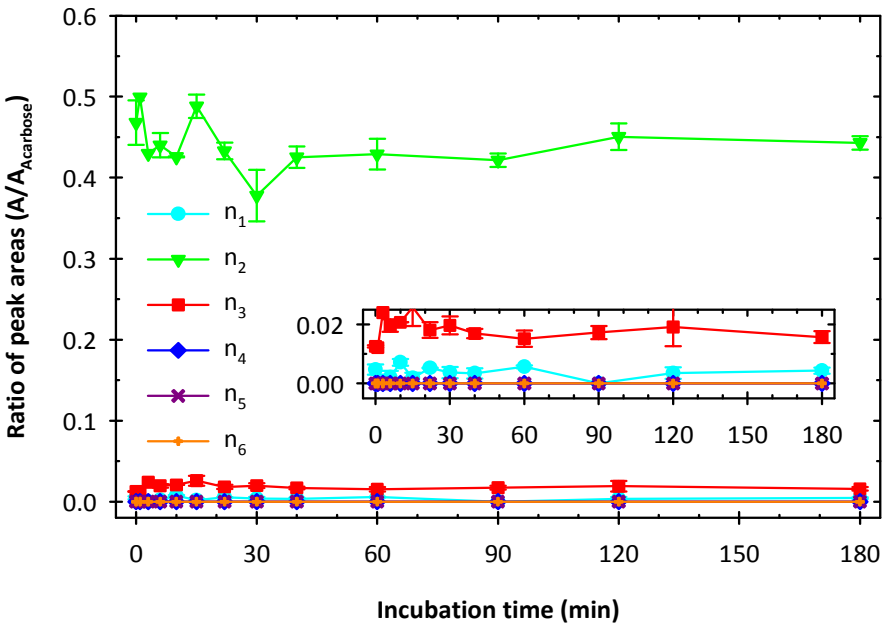

Figure 6.6: Incubation of the tetrasaccharide (n_2, 500 µM) with bovine testicular hyaluronidase (55.56 IU/mL) at pH = 5.0. Electropherograms (A) and standardized peak areas (B). Mean ± SEM for multiple injections. CZE: 1:10 sample dilution, 30 s injection, 25 µm × 28 cm capillary, ammonium acetate (25 mM, pH = 8.5), 35 kV.

6.3.4 Degradation of a low molecular weight hyaluronan oligosaccharide mixture by hyaluronidase from *Streptococcus agalactiae*

HPAEC–PAD of the time-dependent degradation of a low molecular weight hyaluronan oligosaccharide mixture by hyaluronidase from *Streptococcus agalactiae* (2.22 IU/mL) revealed a significant increase in the void volume signal (Figure 6.7). Additionally, considerable amounts of an intermediate product (with a retention time of approximately 7.2 min) were formed. This peak was followed by a series of small peaks eluting at retention times in between those observed for the standard oligosaccharides (n_2–n_4, grey arrows in Figure 6.7 A). By additional CZE–ESI-TOF-MS analysis, the unsaturated tetrasaccharide (n_2*) was proven to be the major intermediate product. Consequently, the peak at a retention time of 7.2 min was assigned to n_2*. Hence, the unsaturated oligosaccharides (n_x*) are eluted after the respective saturated equivalents (n_x) under the given chromatography conditions. The observation of additional unsaturated (apart from n_1*), but no saturated oligosaccharides, was in accordance with previous reports.[3, 16] Nevertheless, to our knowledge the intermediate formation of such remarkable amounts of n_2* has not been described so far.

Hyaluronidase from *Streptococcus agalactiae* is supposed to act via an initial random cleavage step, followed by processive exolytic degradation of the residual hyaluronan chains.[15-19, 24] Our observations support the assumption by Hoechstetter that every initial attack leads to the liberation of an unsaturated oligosaccharide,[3] predominantly the tetrasaccharide (n_2*). In this case, the relatively high number of single molecules in a low molecular weight hyaluronan oligosaccharide mixture, compared to native hyaluronan, should promote the formation of these intermediate products. This aspect will be discussed in Section 6.3.5. After prolonged periods of incubation, the intermediately formed oligosaccharides were also accepted as substrates and further degraded (Figure 6.7 B). Hence, this result raised the question if small saturated oligosaccharides were substrates of *Streptococcus agalactiae* hyaluronidase as well. Further studies on this subject are discussed in Section 6.3.6.

A

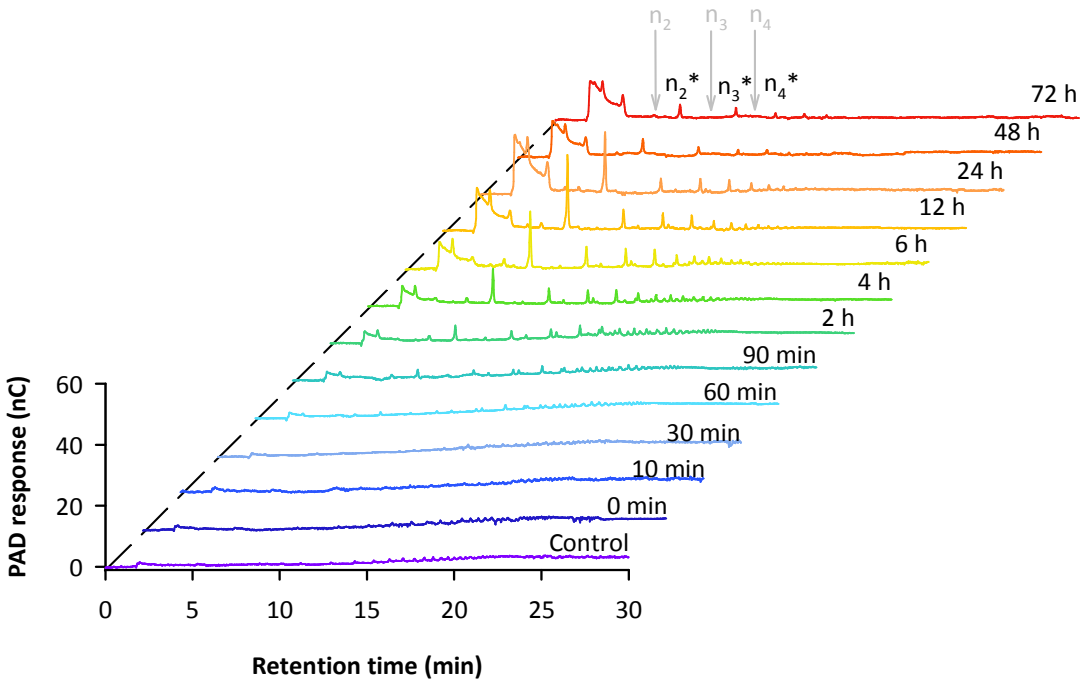

B

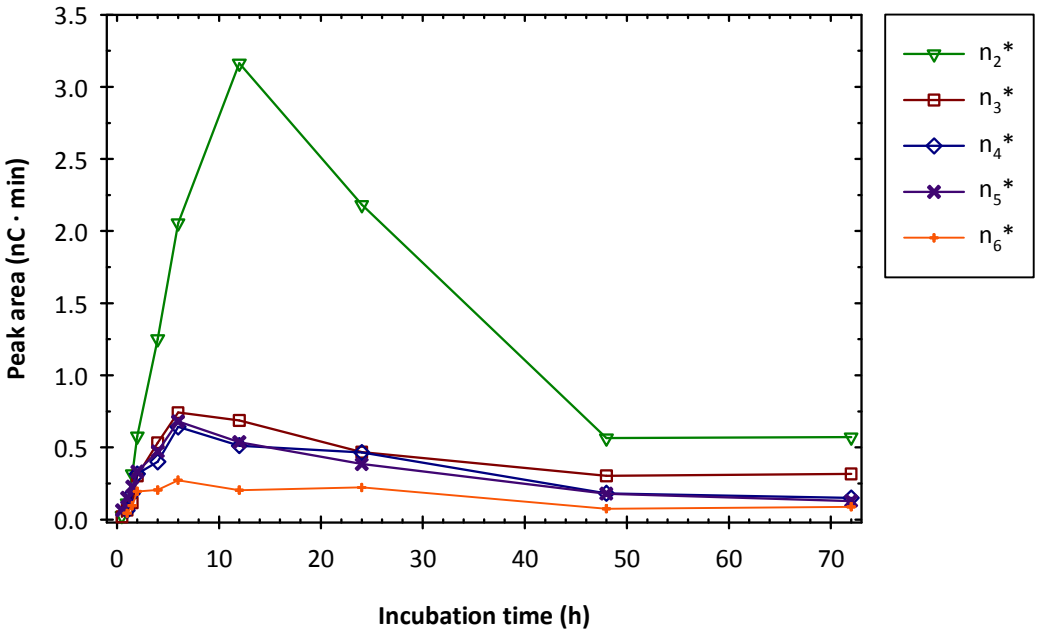

Figure 6.7: Time-dependent degradation of a low molecular weight hyaluronan oligosaccharide mixture by hyaluronidase from *Streptococcus agalactiae* (2.22 IU/mL) at pH = 5.0. Chromatograms (A) and peak areas (B). HPAEC–PAD: 10 µL of diluted (1:10) sample injected, CarboPac™ PA200, 100 mM sodium hydroxide, gradient of 200–900 mM sodium acetate, 40 °C, 0.5 mL/min.

6.3.5 Size-dependent degradation of hyaluronan by hyaluronidase from *Streptococcus agalactiae*

The theoretical considerations from Section 6.3.4 were supported by the size-dependent degradation of hyaluronan. If high molecular weight hyaluronan (HMW HA) was used as substrate for hyaluronidase from *Streptococcus agalactiae*, the amount and variety of oligosaccharides accumulating after 24 h was significantly lower than for a low molecular weight oligosaccharide mixture (Figure 6.8). As the number of individual molecules per mass unit is much higher for the oligosaccharide mixture than for native hyaluronan, the liberation of oligosaccharides by the initial random attack becomes more probable.

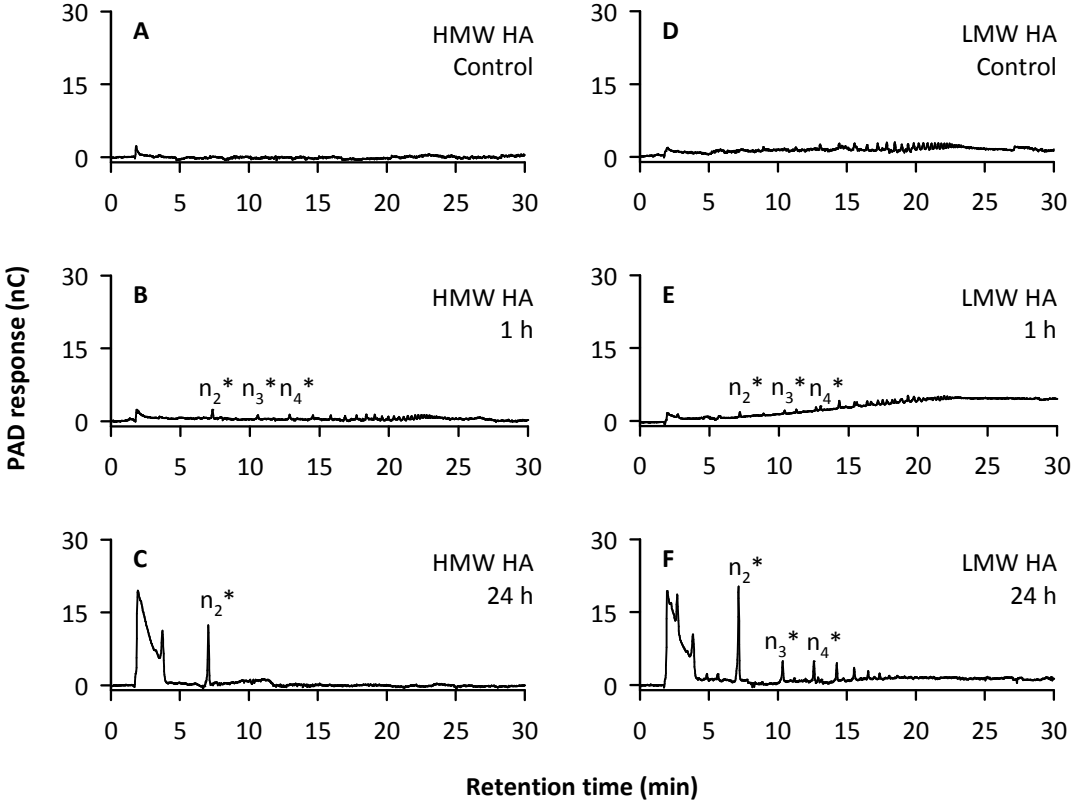

Figure 6.8: Incubation of high molecular weight hyaluronan (HMW HA, A–C) and a low molecular weight hyaluronan oligosaccharide mixture (LMW HA, D–F) with hyaluronidase from *Streptococcus agalactiae* (2.22 IU/mL) at pH = 5.0 for 1 h (B, E) and 24 h (C, F). Controls (A, D) contained bovine serum albumin instead of enzyme. HPAEC–PAD: 10 µL of diluted (1:10) sample injected, CarboPac™ PA200, 100 mM sodium hydroxide, gradient of 200–900 mM sodium acetate, 40 °C, 0.5 mL/min. Asterisks indicate the presence of double bonds in the oligosaccharides.

When the enzyme activity in the incubation mixture was increased (44.44 IU/mL instead of 2.22 IU/mL), the reaction was much faster. After 1 h, considerable amounts of n_2* were detectable. However, after 24 h it had completely disappeared, thus proving that n_2* is only an intermediate product of the reaction (Figure 6.9).

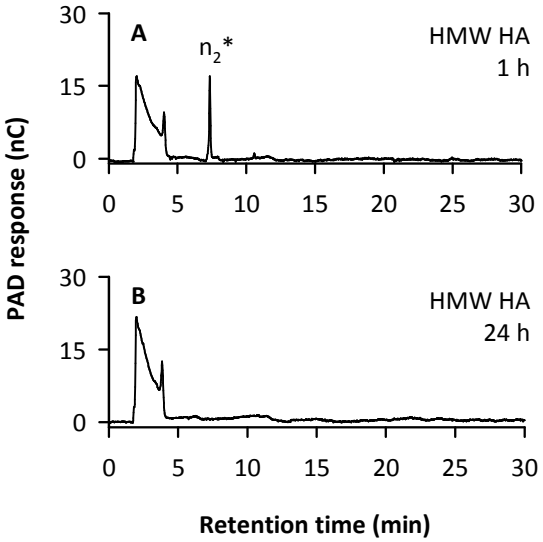

Figure 6.9: Incubation of high molecular weight hyaluronan (HMW HA) with hyaluronidase from *Streptococcus agalactiae* (44.44 IU/mL) at pH = 5.0 for 1 h (A) and 24 h (B). HPAEC–PAD: 10 µL of diluted (1:10) sample injected, CarboPac™ PA200, 100 mM sodium hydroxide, gradient of 200–900 mM sodium acetate, 40 °C, 0.5 mL/min. The intermediately formed unsaturated tetrasaccharide is abbreviated as n_2*.

6.3.6 Fast at-line analysis of hyaluronan oligosaccharide degradation by hyaluronidase from *Streptococcus agalactiae*

By analogy with Section 6.3.3, 500 µM of the octasaccharide (n_4, Figure 6.10), the hexasaccharide (n_3, Figure 6.11), and the tetrasaccharide (n_2, Figure 6.12) were incubated with 55.56 IU/mL hyaluronidase from *Streptococcus agalactiae*.

Degradation of n_4 yielded a complex mixture of saturated (n_x) and unsaturated (n_x*) intermediate products with n_1 and n_1* accumulating at the end of the incubation (Figure 6.10). Interestingly, the direct formation of n_1* and n_3 from n_4 was not observed. By contrast, both of the two other possible reactions ($n_4 \rightarrow n_2 + n_2$* and $n_4 \rightarrow n_1 + n_3$*) were catalyzed by the enzyme. Again, n_2* seemed to be the preferred intermediate product. Assuming a roughly comparable ionizability of both, the maximum concentration of n_2 was much lower than that of n_2*. Therefore, it may be concluded that n_2 tends to be retained in the active site of the enzyme and to be further degraded faster than n_2*. At first sight, the presence of free saturated oligosaccharides in the mixture seemed to contradict a processive mode of action.[15-19, 24] Nevertheless, the affinity of small oligosaccharides for the active site of the enzyme may be considerably lower compared to highly polymeric hyaluronan. As a consequence, saturated oligosaccharides would be liberated to a certain extent after the initial attack of the enzyme. As the intermediate products disappeared from the incubation mixture, the concentration of n_1* increased continuously. Both disaccharides (n_1 and n_1*) were not accepted as substrates, leading to accumulation of these molecules.

In the next step, the enzyme was provided with n_3 as substrate to further investigate if n_2* or n_1* was the predominant reaction product at the beginning of the incubation (Figure 6.11). The results were in good accordance with the previous experiments. Initially, the formation of n_2* ($n_3 \rightarrow n_1 + n_2$*) prevailed over n_1* ($n_3 \rightarrow n_1$* + n_2). As n_1 was produced in parallel to n_2*, more n_1 accumulated when compared to Figure 6.10. It should be noted again that the sensitivity of ESI-TOF-MS differs, depending on the respective oligosaccharides. For this reason the sum of the standardized peak areas of the end products was lower than expected from the stoichiometric relation of educt (n_3) to products (n_1, n_1*).

Finally, n_2 was proven to be the minimal substrate of hyaluronidase from *Streptococcus agalactiae* (Figure 6.12). Although an equimolar mixture of n_1 and n_1* was expected as end products, the standardized peak areas were not equal. As discussed above, this can be explained by differences in ionization and sensitivity of ESI-TOF-MS. Both disaccharides were not further degraded.

A

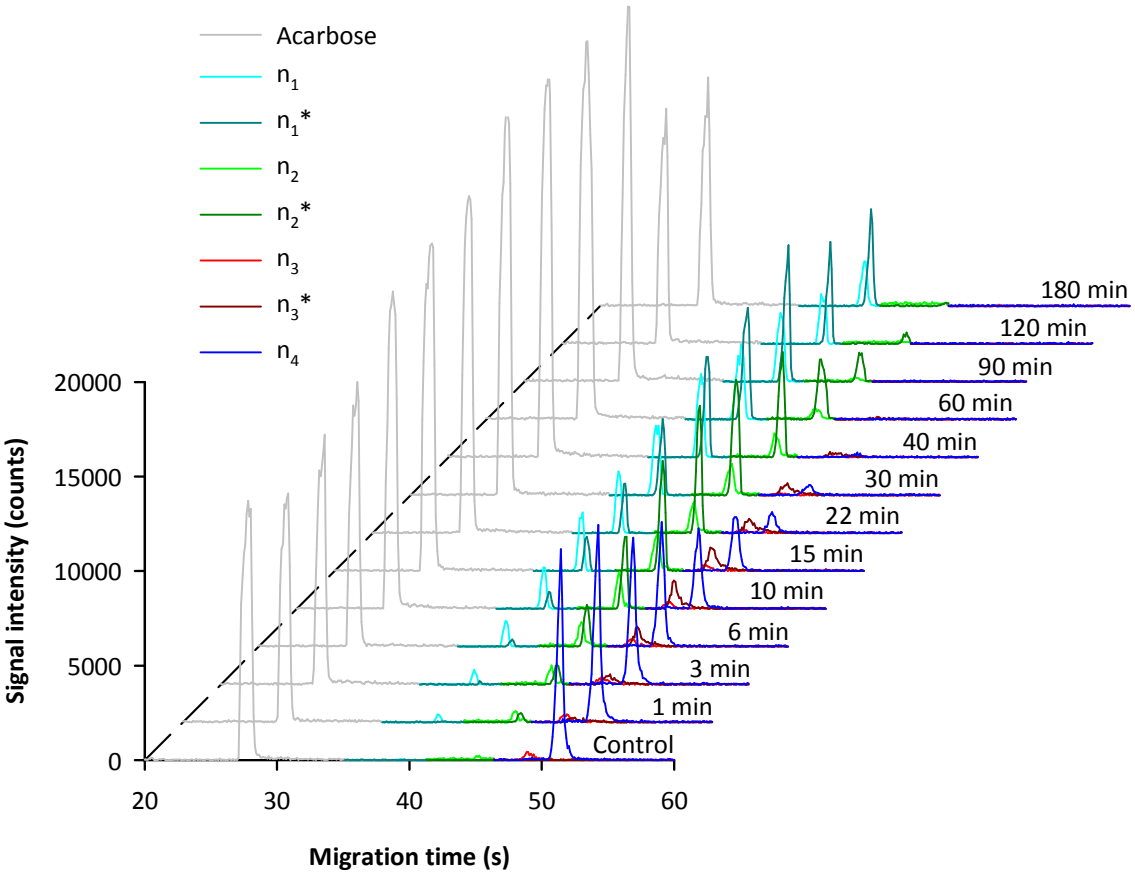

B

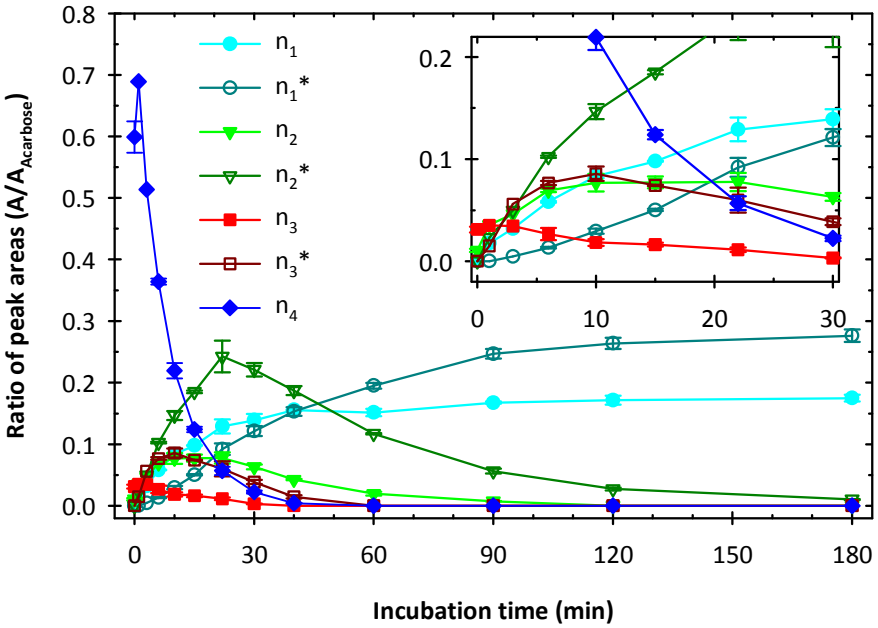

Figure 6.10: Incubation of the octasaccharide (n_4, 500 µM) with hyaluronidase from *Streptococcus agalactiae* (55.56 IU/mL) at pH = 5.0. Electropherograms (A) and standardized peak areas (B). Mean ± SEM for multiple injections. Asterisks indicate unsaturated oligosaccharides (containing a double bond). CZE: 1:10 sample dilution, 30 s injection, 25 µm × 28 cm capillary, ammonium acetate (25 mM, pH = 8.5), 35 kV.

A

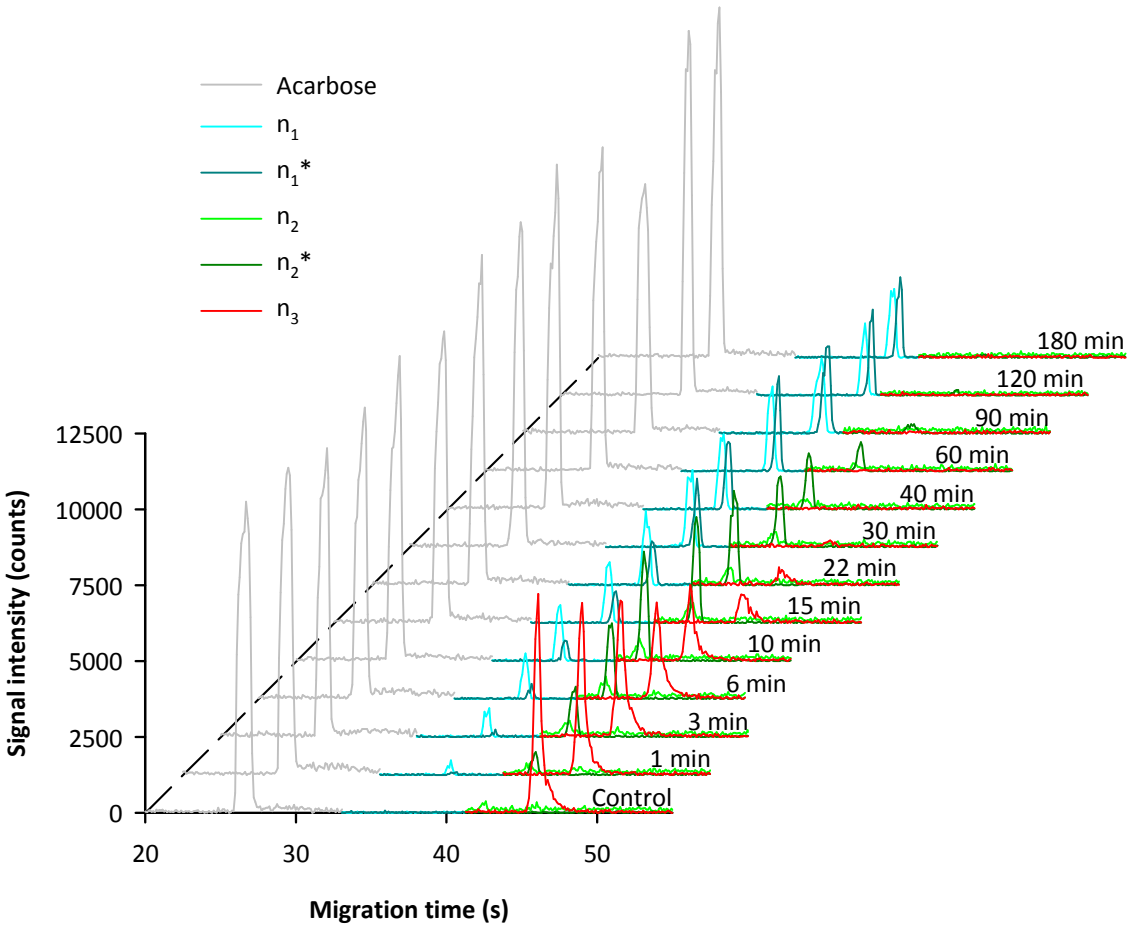

B

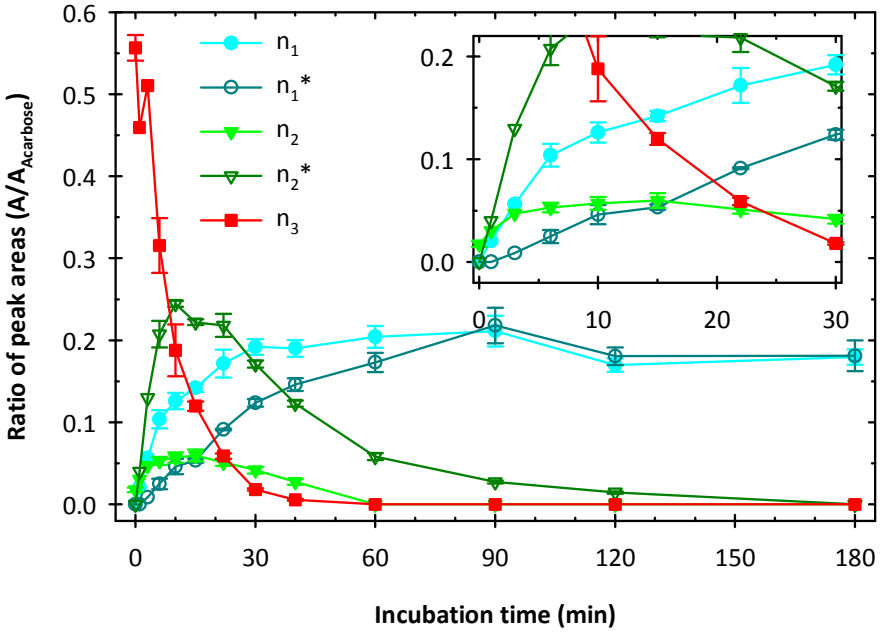

Figure 6.11: Incubation of the hexasaccharide (n_3, 500 µM) with hyaluronidase from *Streptococcus agalactiae* (55.56 IU/mL) at pH = 5.0. Electropherograms (A) and standardized peak areas (B). Mean ± SEM for multiple injections. Asterisks indicate unsaturated oligosaccharides (containing a double bond). CZE: 1:10 sample dilution, 30 s injection, 25 µm × 28 cm capillary, ammonium acetate (25 mM, pH = 8.5), 35 kV.

A

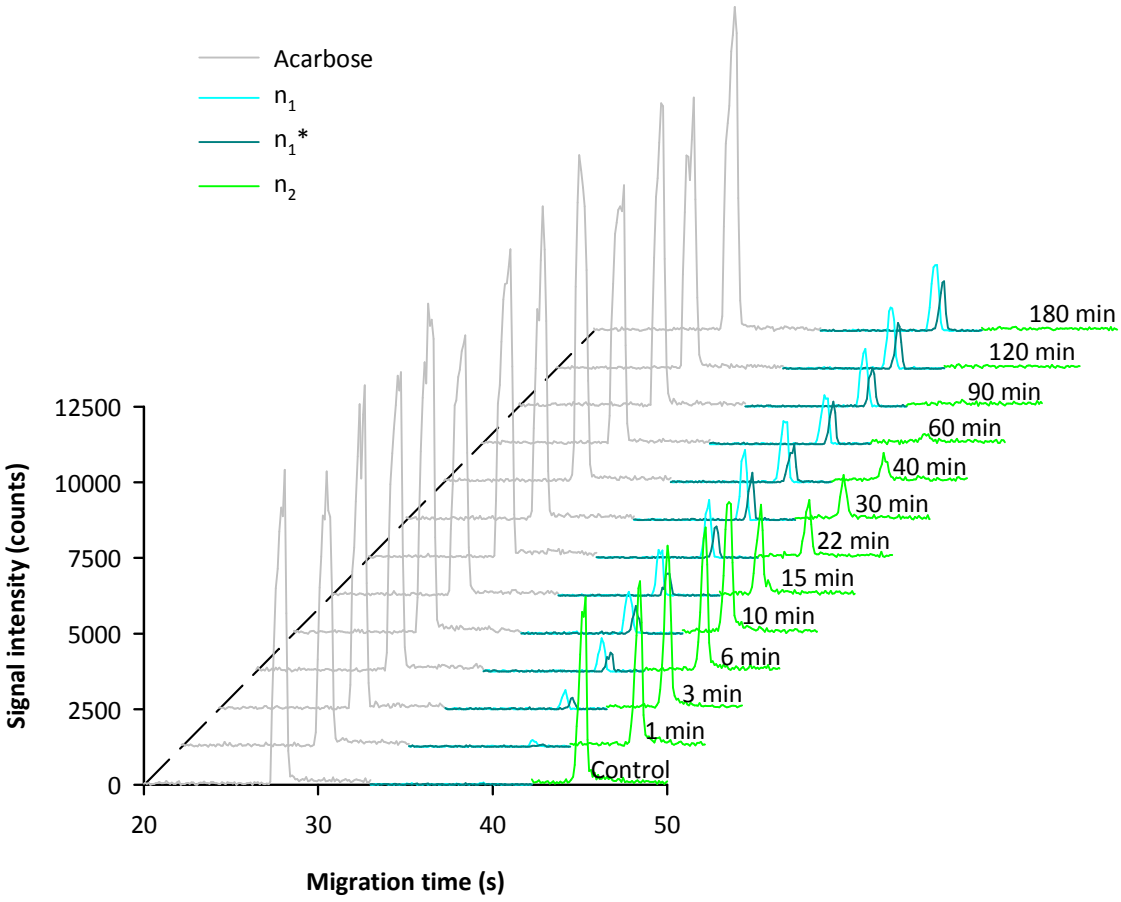

B

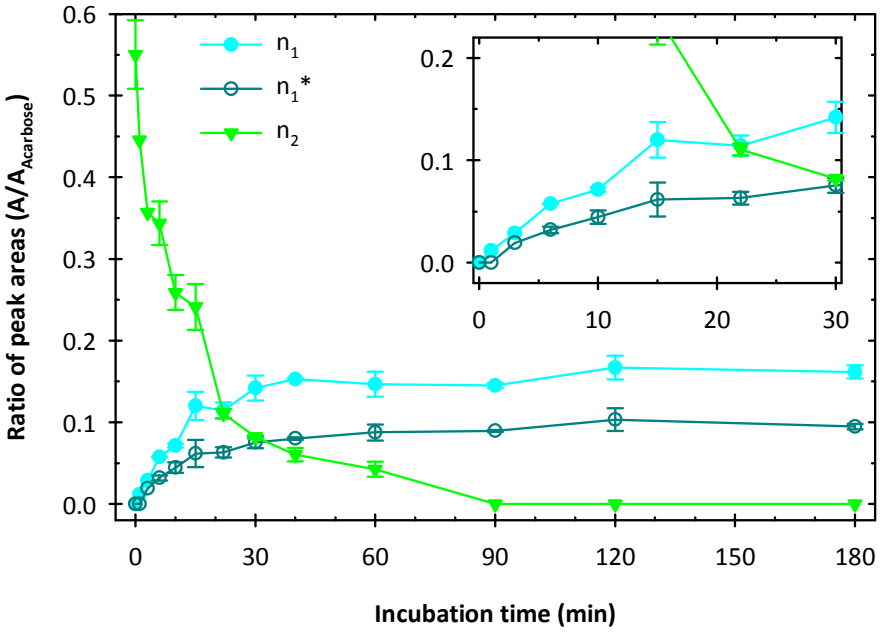

Figure 6.12: Incubation of the tetrasaccharide (n_2, 500 µM) with hyaluronidase from *Streptococcus agalactiae* (55.56 IU/mL) at pH = 5.0. Electropherograms (A) and standardized peak areas (B). Mean ± SEM for multiple injections. Asterisks indicate unsaturated oligosaccharides (containing a double bond). CZE: 1:10 sample dilution, 30 s injection, 25 µm × 28 cm capillary, ammonium acetate (25 mM, pH = 8.5), 35 kV.

6.3.7 Saturation experiment using the minimal substrate (n_2) for *Streptococcus agalactiae* hyaluronidase

Having identified the tetrasaccharide (n_2) as minimal substrate of hyaluronidase from *Streptococcus agalactiae*, strain 4755, this molecule was used for the determination of Michaelis-Menten kinetics. 5 IU/mL of the enzyme were incubated with increasing concentrations of n_2. Time-dependent reduction of the n_2 peak area was determined by HPAEC–PAD. Concentration of n_2 was plotted versus incubation time (Figure 6.13 A). From quadratic curve fits, the initial degradation velocities were calculated as slope of the tangent line at an incubation time of 0 min (derivative of the curve).

The absolute values of the initial degradation velocity were plotted versus substrate concentration (Figure 6.13 B). Hyperbolic curve fitting was carried out according to the Michaelis-Menten equation. From the curve, maximum velocity (v_{max}) and Michaelis constant (K_m) were calculated. Given as calculated values ± standard error from the fit, K_m was 923 ± 106 µM, v_{max} was 3.68 ± 0.20 nmol/min. Hence, K_m was considerably higher (by a factor of 6) than the apparent K_m values reported by Hofinger for mammalian testicular hyaluronidases and their respective minimal substrates but comparable to recombinant human Hyal-1.[25] In conclusion, the affinity of the tetrasaccharide (n_2) for the bacterial enzyme was relatively low. This finding confirmed the theoretical considerations with regard to affinity and liberation of saturated oligosaccharides in Section 6.3.6.

A

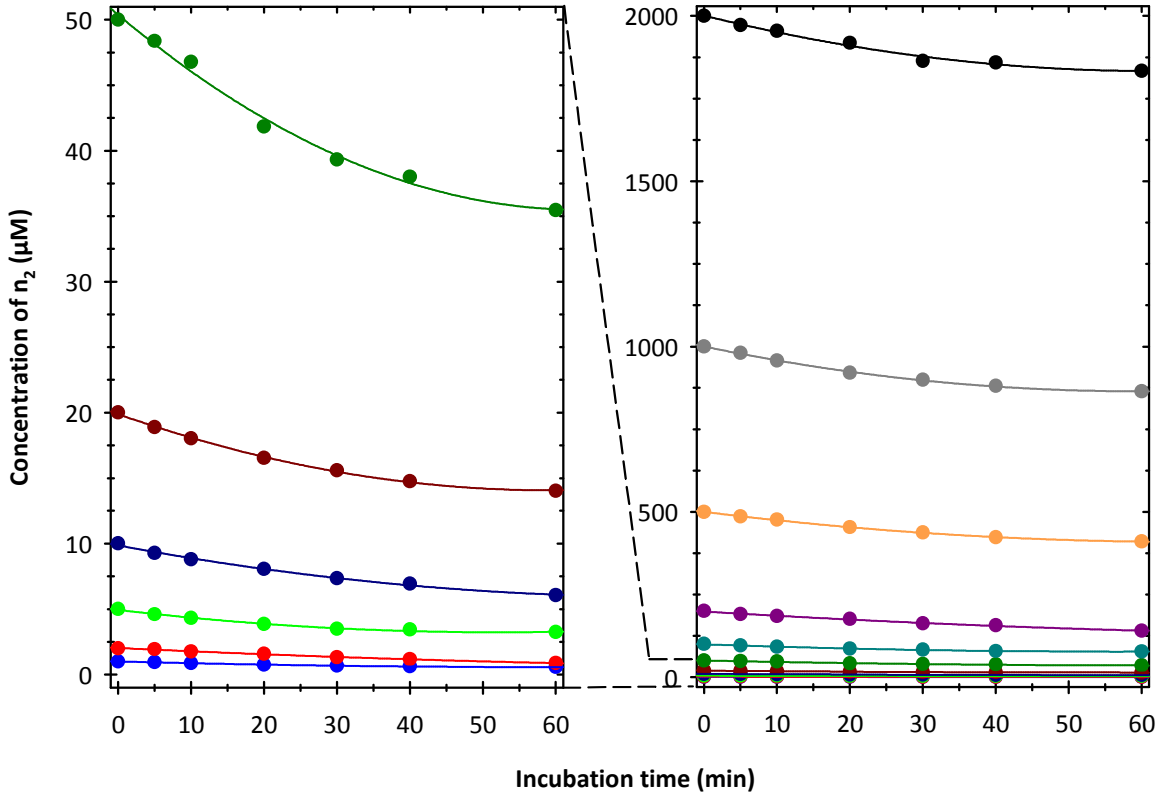

B

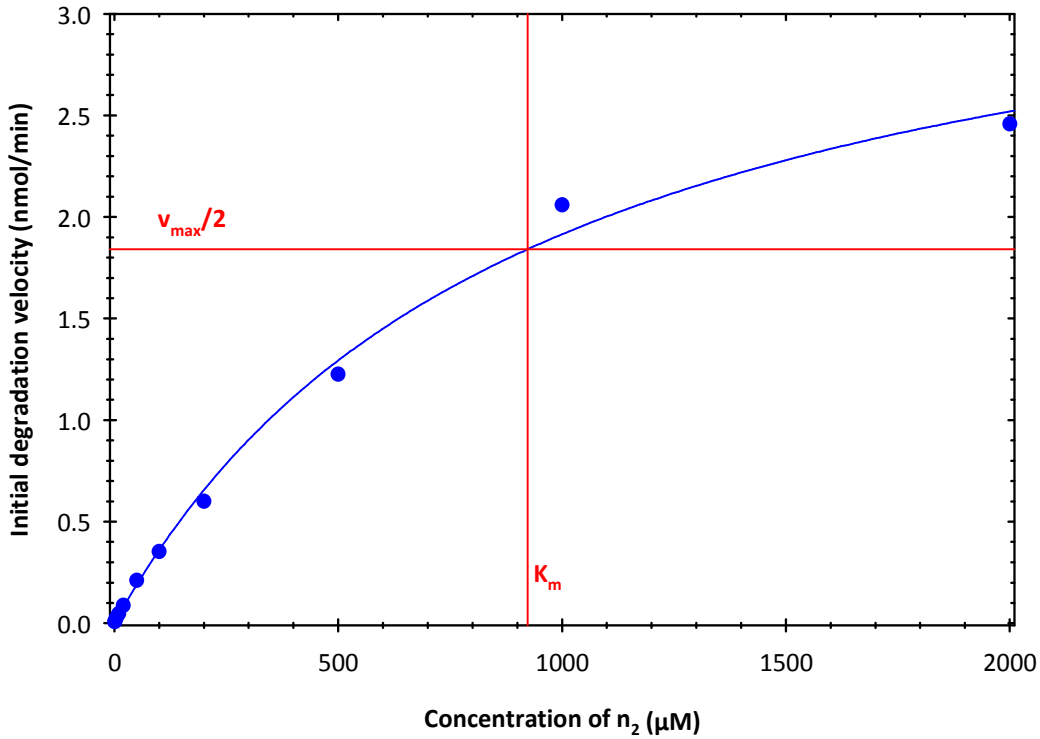

Figure 6.13: Determination of Michaelis-Menten kinetics for hyaluronidase (5 IU/mL) from *Streptococcus agalactiae*, strain 4755, at pH = 5.0. Time-dependent degradation of the tetrasaccharide (n_2) with quadratic curve fits (A) and initial degradation velocity plotted versus substrate concentration (B). Concentrations were calculated from the relative reduction of the educt peak in HPAEC–PAD chromatograms. K_m and $v_{max}/2$ were determined by hyperbolic curve fitting according to the Michaelis-Menten theory.

6.4 Summary and conclusion

A combination of HPAEC–PAD and fast at-line CZE–ESI-TOF-MS provided new insights into the enzymatic mechanisms of hyaluronidases from bovine testes and *Streptococcus agalactiae*, strain 4755. Thereby, we focused mainly on the turnover of hyaluronan oligosaccharides. Bovine testicular hyaluronidase was confirmed to attack the hyaluronan chains randomly. Moreover, a degradation study for the octasaccharide (n_4) supported the mechanism recently suggested by Kakizaki et al. after similar studies.[11]

With the bacterial enzyme, unsaturated disaccharide (n_1*) accumulated as end product. Among the intermediately liberated unsaturated oligosaccharides, the tetrasaccharide (n_2*) seemed to play a predominant role. Therefore, we suggested that n_2* is preferably cleaved off during the initial step of enzymatic action of *Streptococcus agalactiae* hyaluronidase. When small saturated oligosaccharides were used as substrates, saturated and unsaturated oligosaccharides were liberated. By contrast, saturated intermediate products are usually not observed upon the degradation of high molecular weight hyaluronan. As the saturated disaccharide (hyalobiuronic acid, n_1) was not accepted as substrate, n_1 accumulated together with n_1*.

The saturated tetrasaccharide (n_2) was identified as minimal substrate of the *Streptococcus agalactiae* hyaluronidase. Hence, it was used at increasing concentrations for a saturation experiment with 5 IU/mL of the enzyme. Kinetic parameters according to the Michaelis-Menten theory (K_m = 923 ± 106 µM, v_{max} = 3.68 ± 0.20 nmol/min) were determined.

By analogy with BTH and hyaluronidase from *Streptococcus agalactiae*, the presented experimental protocols can easily be applied to the characterization of human enzymes as well as hyaluronidases from different pathogens or animal venoms. HPAEC–PAD and CZE–ESI-TOF-MS allow for the determination of product spectra, minimal substrates, and kinetic parameters. Moreover, analysis of the enzymatic degradation of other glycosaminoglycans (e. g. chondroitin sulfate) is conceivable.

6.5 References

1. Oettl, M.; Hoechstetter, J.; Asen, I.; Bernhardt, G.; Buschauer, A. Comparative characterization of bovine testicular hyaluronidase and a hyaluronate lyase from *Streptococcus agalactiae* in pharmaceutical preparations. *Eur. J. Pharm. Sci.* **2003,** 18, 267-277.

2. Oettl, M. Biochemische Charakterisierung boviner testikulärer Hyaluronidase und Untersuchungen zum Einfluß von Hyaluronidase und Hyaluronsäure auf das Wachstum von Tumoren. PhD thesis, University of Regensburg, Regensburg, **2000**.

3. Hoechstetter, J. Characterisation of bovine testicular hyaluronidase and a hyaluronate lyase from *Streptococcus agalactiae*: investigations on the effect of pH on hyaluronan degradation and

preclinical studies on the adjuvant administration of the enzymes in cancer chemotherapy. PhD thesis, University of Regensburg, Regensburg, **2005**.

4. Meyer, K. Hyaluronidases. In: *The Enzymes*, Boyer, P. D. (Ed.). Academic Press: New York, **1971**, Vol. 3, pp 307-320.

5. Vercruysse, K. P.; Lauwers, A. R.; Demeester, J. M. Kinetic investigation of the degradation of hyaluronan by hyaluronidase using gel permeation chromatography. *J. Chromatogr. B, Biomed. Appl.* **1994,** 656, 179-190.

6. Cramer, J. A.; Bailey, L. C.; Bailey, C. A.; Miller, R. T. Kinetic and mechanistic studies with bovine testicular hyaluronidase. *Biochim. Biophys. Acta* **1994,** 1200, 315-321.

7. Hofinger, E. S. A.; Hoechstetter, J.; Oettl, M.; Bernhardt, G.; Buschauer, A. Isoenzyme-specific differences in the degradation of hyaluronic acid by mammalian-type hyaluronidases. *Glycoconj. J.* **2008,** 25, 101-109.

8. Takagaki, K.; Nakamura, T.; Izumi, J.; Saitoh, H.; Endo, M.; Kojima, K.; Kato, I.; Majima, M. Characterization of hydrolysis and transglycosylation by testicular hyaluronidase using ion-spray mass spectrometry. *Biochemistry* **1994,** 33, 6503-6507.

9. Highsmith, S.; Garvin, J. H., Jr.; Chipman, D. M. Mechanism of action of bovine testicular hyaluronidase. Mapping of the active site. *J. Biol. Chem.* **1975,** 250, 7473-7480.

10. Hofinger, E. S. A.; Bernhardt, G.; Buschauer, A. Kinetics of Hyal-1 and PH-20 hyaluronidases: comparison of minimal substrates and analysis of the transglycosylation reaction. *Glycobiology* **2007,** 17, 963-971.

11. Kakizaki, I.; Ibori, N.; Kojima, K.; Yamaguchi, M.; Endo, M. Mechanism for the hydrolysis of hyaluronan oligosaccharides by bovine testicular hyaluronidase. *FEBS J.* **2010,** 277, 1776-1786.

12. Nakatani, H. Monte Carlo simulation of hyaluronidase reaction involving hydrolysis, transglycosylation and condensation. *Biochem. J.* **2002,** 365, 701-705.

13. Saitoh, H.; Takagaki, K.; Majima, M.; Nakamura, T.; Matsuki, A.; Kasai, M.; Narita, H.; Endo, M. Enzymic reconstruction of glycosaminoglycan oligosaccharide chains using the transglycosylation reaction of bovine testicular hyaluronidase. *J. Biol. Chem.* **1995,** 270, 3741-3747.

14. Weissmann, B. The transglycosylative action of testicular hyaluronidase. *J. Biol. Chem.* **1955,** 216, 783-794.

15. Pritchard, D. G.; Lin, B.; Willingham, T. R.; Baker, J. R. Characterization of the group B streptococcal hyaluronate lyase. *Arch. Biochem. Biophys.* **1994,** 315, 431-437.

16. Baker, J. R.; Pritchard, D. G. Action pattern and substrate specificity of the hyaluronan lyase from group B streptococci. *Biochem. J.* **2000,** 348 Pt 2, 465-471.

17. Jedrzejas, M. J. Three-dimensional structures of hyaluronate lyases from *Streptococcus* species and their mechanism of hyaluronan degradation. *Glycoforum* **2002**. (http://glycoforum.gr.jp/science/hyaluronan/HA24/HA24E.html)

18. Li, S.; Jedrzejas, M. J. Hyaluronan binding and degradation by *Streptococcus agalactiae* hyaluronate lyase. *J. Biol. Chem.* **2001,** 276, 41407-41416.

19. Mello, L. V.; De Groot, B. L.; Li, S.; Jedrzejas, M. J. Structure and flexibility of *Streptococcus agalactiae* hyaluronate lyase complex with its substrate. Insights into the mechanism of processive degradation of hyaluronan. *J. Biol. Chem.* **2002,** 277, 36678-36688.

20. Asari, A. Novel functions of hyaluronan oligosaccharides. *Glycoforum* **2005**. (http://www.glycoforum.gr.jp/science/hyaluronan/HA12a/HA12aE.html)

21. Muckenschnabel, I.; Bernhardt, G.; Spruß, T.; Dietl, B.; Buschauer, A. Quantitation of hyaluronidases by the Morgan-Elson reaction: comparison of the enzyme activities in the plasma of tumor patients and healthy volunteers. *Cancer Lett.* **1998,** 131, 13-20.

22. Reissig, J. L.; Storminger, J. L.; Leloir, L. F. A modified colorimetric method for the estimation of *N*-acetylamino sugars. *J. Biol. Chem.* **1955,** 217, 959-966.

23. Deschrevel, B.; Tranchepain, F.; Vincent, J. C. Chain-length dependence of the kinetics of the hyaluronan hydrolysis catalyzed by bovine testicular hyaluronidase. *Matrix Biol.* **2008,** 27, 475-486.

24. Pritchard, D. G.; Trent, J. O.; Li, X.; Zhang, P.; Egan, M. L.; Baker, J. R. Characterization of the active site of group B streptococcal hyaluronan lyase. *Proteins* **2000,** 40, 126-134.

25. Hofinger, E. S. A. Recombinant expression, purification and characterization of human hyaluronidases. PhD thesis, University of Regensburg, Regensburg, **2007**.

7 *In vitro* studies on recombinant human PH-20, PEG-PH-20, and Hyal-1

7.1 Introduction

In Chapter 6, bovine testicular hyaluronidase (BTH) has been presented as a typical mammalian hyaluronidase. With their catalytic domains being highly conserved, the different mammalian hyaluronidase isoenzymes are supposed to exhibit very similar catalytic mechanisms.[1] Nevertheless, it is known from previous studies that these isoenzymes vary with regard to degradation of hyaluronan[2] and hyaluronan oligosaccharides.[3] Understanding the particularities of the human hyaluronidases is a prerequisite for elucidating the physiological and pathophysiological role of these enzymes.

The human counterpart of BTH is the sperm protein PH-20, which was identified as hyaluronidase in 1993.[4] By analogy with the physiological role of PH-20,[5] pharmaceutical preparations of recombinant human PH-20 (rhPH-20) were successfully applied to intracytoplasmic sperm injection (ICSI).[6, 7] Furthermore, co-administered rhPH-20 has been reported to increase subcutaneous bioavailability of drugs.[8, 9]

Human plasma hyaluronidase (Hyal-1) was also successfully cloned and expressed using different expression systems.[10, 11] Independent from the expression system, recombinant human Hyal-1 (rhHyal-1) exhibited maximum activity at pH values of 3.5–4.0,[10, 11] comparable to hyaluronidases isolated from human plasma,[10] serum,[12] liver,[13] and urine.[14] By contrast, BTH and rhPH-20 showed completely different pH profiles with maximum activity at pH > 4.0.[2, 10]

Both human hyaluronidases, Hyal-1 and PH-20, have previously been cloned, expressed, purified, and comparatively characterized in our group.[2, 3, 11, 15] Now, additional recombinant enzyme preparations from a different source became available. Hence, these enzymes had to be characterized in terms of pH profiles, mode of action, and potential inhibitors. By analogy with Chapter 6, we focused especially on the degradation of hyaluronan oligosaccharides, which not only promised best insight into the mechanisms of the enzymatic cleavage but are also supposed to play an important biological role.[16]

7.2 Materials and methods

7.2.1 Enzymes, activity units, substrates, and putative inhibitors

Recombinant human PH-20 (rhPH-20), PEGylated PH-20 (PEG-rhPH-20), and Hyal-1 (rhHyal-1) preparations from Halozyme Therapeutics (San Diego, CA, USA) were a kind gift from Gregory I. Frost, PhD. Bovine testicular hyaluronidase (BTH, Neopermease®), kindly provided by Sanabo (Vienna, Austria), was additionally used for comparison of product spectra.

The activities of the recombinant human enzymes were determined by a colorimetric assay (*cf*. Section 7.2.4). To fit the calibration range, rhPH-20 and PEG-rhPH-20 were diluted by addition of histidine buffer (10 mM histidine, 130 mM sodium chloride, pH = 6.5), the solvent of these enzymes. By contrast, rhHyal-1 was diluted by addition of incubation buffer. Activity was determined at pH = 5.0 for rhPH-20 and PEG-rhPH-20 (for better comparability to BTH) or at pH = 3.5 for rhHyal-1. According to Oettl, a formation rate of 0.1 nmol *N*-acetyl-D-glucosamine equivalents per minute (0.1 mU) is equivalent to approximately 1 IU for bovine testicular hyaluronidase (using hyaluronan from rooster comb).[17] Although hyaluronan from *Streptococcus zooepidemicus* (Aqua Biochem, Dessau, Germany) was used in this work, all activities of the recombinant human hyaluronidases are given as IU using this conversion factor. Activities for BTH are based on the specification by the supplier.

By analogy with Chapter 6, Hyalo-Oligo (Kewpie/Q. P. Corp., Tokyo, Japan), and purified oligosaccharides (prepared and quantified by colorimetry according to Chapter 5) were used as substrates in addition to hyaluronan from a bacterial source. For inhibition studies, diclofenac, indomethacin, and L-ascorbic acid-6-*O*-hexadecanoate (vitamin C palmitate) were purchased from Sigma-Aldrich (Munich, Germany).

7.2.2 Determination of protein content

Protein content of the enzyme preparations was determined by the Bradford method.[18] Human serum albumin (Behringwerke, Marburg, Germany) was used for calibration at concentrations of 50–600 µg/mL. The determination was carried out in a miniaturized version of the Bio-Rad protein assay. Different dilutions of the rhPH-20 (1:100, 1:10), the PEG-rhPH-20 (1:50, 1:10), and the rhHyal-1 (1:10, 1:5, 1:2) preparations were made. 10 µL of the calibration standards and the sample dilutions were transferred to a 96-well plate (in duplicate). 200 µL of the 1:5 diluted Bio-Rad protein assay dye reagent concentrate (Bio-Rad, Munich, Germany) were added. After 5 min of incubation, absorbance at 580 nm (slit 10 nm) was measured with a Tecan GENios Pro plate reader (Tecan, Crailsheim, Germany). Data were recorded with the corresponding XFluor GENios Pro software V.4.55. Apart from the

1:2 dilution of the rhHyal-1 preparation, all other dilutions were within the calibrated concentration range and therefore used for calculation of protein content.

7.2.3 Incubation mixtures

The composition of incubation mixtures was essentially the same as in the experiments of Chapter 6 (Section 6.2.2.). However, incubation buffers of different pH values were used in this chapter. Thereby, adjustment of pH was achieved by mixing the two buffer components in appropriate ratios. By analogy with Chapter 6, enzymes were diluted with a 0.2 mg/mL solution of bovine serum albumin (BSA, Serva, Heidelberg, Germany), which was also added to the negative (enzyme-free) controls instead of the enzyme-containing samples.

7.2.4 Colorimetric hyaluronidase activity assay

The incubation mixture was placed in a water bath at 37 °C for 30 min. The reaction was stopped by addition of alkaline borate solution and boiling for 4.5 min. The formation of oligosaccharides with *N*-acetyl-D-glucosamine at the reducing end was measured by the Morgan-Elson reaction.[19-22] Details were already described in Chapter 5 (Section 5.2.3).

7.2.5 Turbidimetric hyaluronidase activity assay

The turbidimetric hyaluronidase activity assay was a modification of the method by Di Ferrante[23] adapted for 96-well plates. Incubation mixtures were prepared as described (*cf*. Chapter 6, Section 6.2.2), except for the hyaluronan solution (2 mg/mL instead of 5 mg/mL). For the determination of pH dependency, pH of the buffer was adjusted to values of 2.0–9.0. Inhibition was determined at pH = 5.0 for rhPH-20 and PEG-rhPH-20, at pH = 3.5 for rhHyal-1. 3 µL of the putative inhibitor, dissolved in DMSO (Merck, Darmstadt, Germany), or pure solvent as control were pipetted into the wells of the 96-well plate. 60 µL of a prepared mixture (containing 31 µL of buffer, 8.1 µL of BSA solution, 12.8 µL of water, and 8.1 µL of hyaluronan solution) were added. Reaction was started by addition of 10 µL of enzyme solution (diluted with BSA solution). Control A contained no inhibitor and BSA solution instead of enzyme (no activity, equivalent to 100% inhibition). Control B also contained no inhibitor, but the respective amount of enzyme (maximum activity, 0% inhibition).

After incubation at 37 °C (30 min for pH profile, different time intervals for inhibitor testing), 200 µL of 2.5% (m/v) cetyltrimethylammonium bromide (CTAB, Merck, Darmstadt, Germany), dissolved in 0.5 M sodium hydroxide solution (Carl Roth, Karlsruhe, Germany), were added to each well. Plates were kept for additional 20 min at room temperature. Afterwards, turbidity was determined by measurement of extinction at 580 nm with a Tecan GENios Pro plate reader (Tecan, Crailsheim, Germany). Activity was expressed as relative

enzymatic activity compared to control A (0% activity) and control B (100% activity). SigmaPlot for Windows 11.2.0.5 (Systat Software Inc., San Jose, CA, USA) was used for fitting of inhibition curves (ligand binding, sigmoidal concentration-response curve, variable slope).

7.2.6 HPAEC–PAD and fast at-line CZE–ESI-TOF-MS

HPAEC–PAD and fast at-line CZE–ESI-TOF-MS protocols were the same as described in Chapter 6 (Sections 6.2.3 and 6.2.4). In detail, the methods were presented in Chapter 3 (CZE–ESI-TOF-MS) and Chapter 4 (HPAEC–PAD), respectively. For CZE–ESI-TOF-MS, control with BSA instead of enzyme was measured at t = 0 min. For HPAEC–PAD, an additional measurement of an immediately boiled sample was performed.

7.3 Results and discussion

7.3.1 Protein content and activity

Protein content and activities of the rhPH-20, PEG-rhPH-20, and rhHyal-1 preparations are listed in Table 7.1.

Table 7.1: Protein content (Bradford assay) and activity (Morgan-Elson assay) of the recombinant human hyaluronidases rhPH-20, PEG-rhPH-20, and rhHyal-1. Activities expressed as IU (marked with $^{\#}$) were calculated from the activity unit U using a factor of 10000 by analogy with BTH[17] as discussed in Section 7.2.1.

Enzyme	pH of activity determination	Protein content (µg/mL)	Activity per mL (µmol/min)	Specific activity (U/mg)
rhPH-20	5.0 (!)	10.1	44.6 (≈ 446000 IU)$^{\#}$	4.4 (≈ 44000 IU/mg)$^{\#}$
PEG-rhPH-20	5.0 (!)	5.2	9.0 (≈ 90000 IU)$^{\#}$	1.7 (≈ 17000 IU/mg)$^{\#}$
rhHyal-1	3.5	1.3	4.7 (≈ 47000 IU)$^{\#}$	3.6 (≈ 36000 IU/mg)$^{\#}$

Although pH optima of rhPH-20 and PEG-rhPH-20 later were found to be at more acidic pH of 4.0 (*cf*. Section 7.3.2), activity values listed in Table 7.1 were determined at pH = 5.0. This value lies in between the different maxima of the activity curves obtained for a previously described preparation of rhPH-20 by turbidimetric and colorimetric determination.[2] Moreover, for comparison with BTH (*cf*. Chapter 6), experiments on oligosaccharide degradation were carried out at pH = 5 (*cf*. Section 7.3.4). However, activity at the optimum (pH = 4.0) can be calculated considering the pH profiles (Figure 7.1) of rhPH-20 (75% of maximum activity at pH = 5.0, colorimetric assay) and PEG-rhPH-20 (71% of maximum activity at pH = 5.0, colorimetric assay).

7.3.2 Influence of pH on enzymatic activity

The enzymatic activity of the recombinant human hyaluronidase preparations depending on pH was determined using both the colorimetric and the turbidimetric assay (Figure 7.1). In previous studies, the pH optima of BTH and a different rhPH-20 preparation were assay-dependent.[2, 24] By contrast, the curves obtained from both assays were equivalent for the enzyme preparations discussed in this chapter. The variants of the testicular enzyme (rhPH-20 and PEG-rhPH20) showed maximum activity at a pH of 4.0 (Figure 7.1 A, B). Thus, the optimum was slightly shifted towards more acidic pH values compared to the study of Hofinger et al., who reported optima of pH = 4.5 (colorimetric assay) and pH = 5.5 (turbidimetric assay) for their preparations of rhPH-20.[2] However, for rhHyal-1 the optimum at an acidic pH of 3.5 (Hofinger et al.: pH = 3.5–4.0)[2] with a very fast decrease in activity at higher pH was confirmed (Figure 7.1 C).

Apart from the enzymes, the composition of the incubation mixtures was identical to the conditions by Hofinger et al.,[2] whereas incubation time was reduced to 30 min. As the pH optimum of BTH is known to depend on buffer type and composition,[20, 25] identical parameters were chosen for the colorimetric assay and the turbidimetric assay. According to previous protocols, only the concentration of hyaluronan differed by a factor of 2.5 to guarantee linearity in the turbidimetric assay.[2]

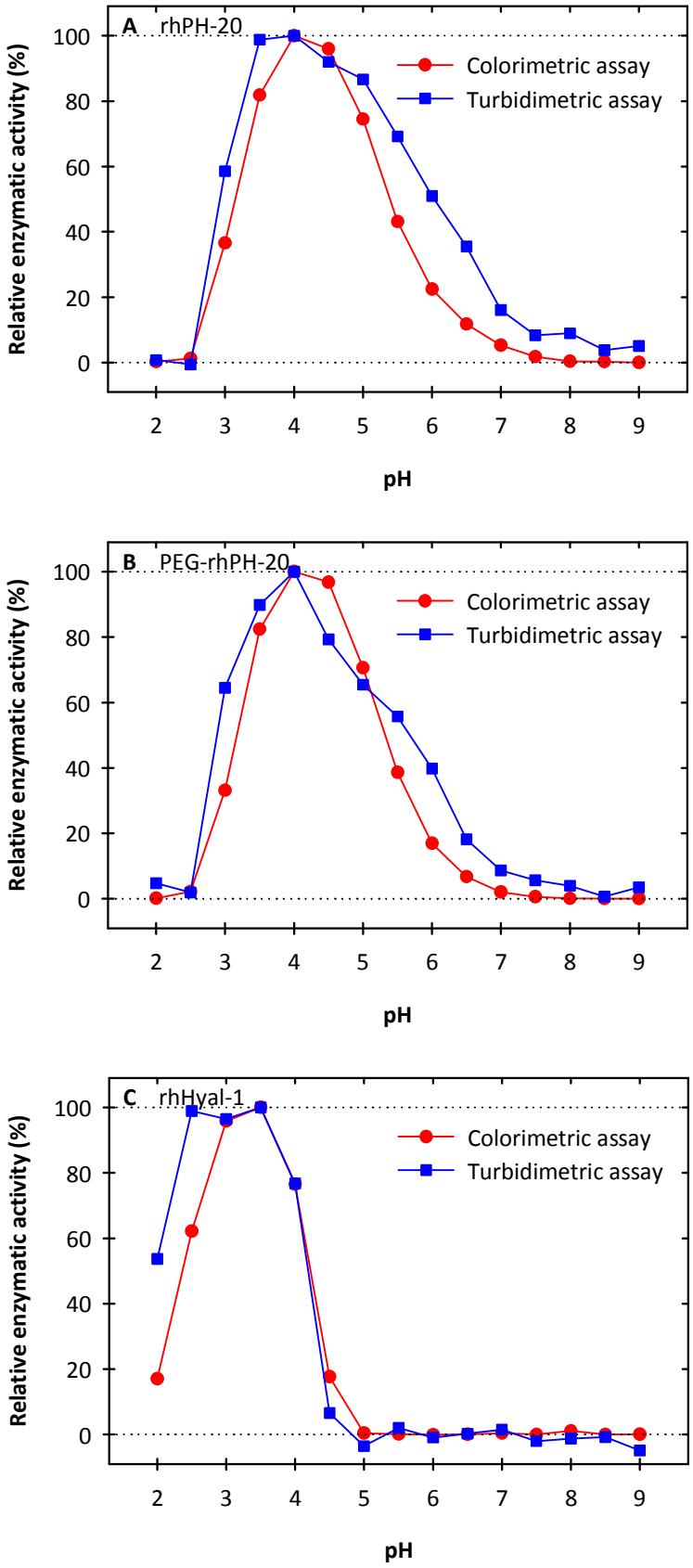

Figure 7.1: Enzymatic activity of the rhPH-20 (A), PEG-rhPH-20 (B), and rhHyal-1 (C) preparations as a function of pH. Activities were determined by colorimetric (circle, red) and turbidimetric (square, blue) assay. Data presented as mean of three independent experiments (additionally performed in duplicate for the turbidimetric assay). Maximum values set as 100%.

7.3.3 Degradation of a low molecular weight hyaluronan oligosaccharide mixture by rhPH-20, PEG-rhPH-20, and BTH

A low molecular weight hyaluronan oligosaccharide mixture was incubated with BTH (Figure 7.2 and Figure 7.3), rhPH-20 (Figure 7.4 and Figure 7.5), and PEG-rhPH-20 (Figure 7.6 and Figure 7.7) and analyzed by HPAEC–PAD. By analogy with the CZE experiments on the degradation of high molecular weight hyaluronan described in an article by Hofinger et al., incubation buffers of pH = 4.5 and pH = 5.5 were chosen in view of the reported pH-dependent differences.[2]

Neither from the chromatograms (Figure 7.2) nor from the areas of the peaks for the oligosaccharides n_2–n_6 (Figure 7.3), pH-dependent differences in product formation became obvious for BTH. The results at pH = 4.5 as well as pH = 5.5 were comparable to digestion at pH = 5.0, discussed in Chapter 6 (Section 6.3.1). After initial formation of mainly n_3, n_2 became the main product after prolonged incubation. This is in agreement with the observation discussed in detail in Chapter 6 (Section 6.3.1). Using the same concentration of BTH, product formation was generally faster at pH = 4.5 (Figure 7.3 A) compared to pH = 5.5 (Figure 7.3 B). This outcome correlates with the pH profile of BTH as determined by colorimetry.[24] From comparison of the colorimetric and the turbidimetric activity assay in combination with CZE analysis, Hofinger et al. concluded that the degradation of native hyaluronan and fragments consisting of more than 20 disaccharide units (> n_{20}) was preferred at pH = 5.5.[2] In this study, a mixture of hyaluronan oligosaccharides was used. Therefore, degradation of high molecular weight hyaluronan did not contribute to the measured velocity of product formation. Additionally, transglycosylation, competing with hydrolysis, is known to play an increasing role at higher pH.[25, 26] Both aspects may explain why the degradation of low molecular weight hyaluronan by BTH was faster at pH = 4.5.

When high molecular weight hyaluronan was used as substrate, pH-dependent differences in enzymatic activity and product spectra were reported to be much more pronounced with BTH than rhPH-20.[2] The opposite was observed for the oligosaccharide mixture. While product spectra from digestion by BTH were almost identical at pH = 4.5 and pH = 5.5, the portion of n_2 within the product mixture after incubation with rhPH-20 was considerably higher at pH = 5.5 (Figure 7.4 B and Figure 7.5 B) compared to pH = 4.5, at which n_3 remained the main product (Figure 7.4 A and Figure 7.5 A). The profile at pH = 4.5 resembles the characteristics of rhHyal-1 at pH = 3.5 (*cf*. Section 7.3.5). Thus, the product spectrum of rhPH-20 was rhHyal-1-like at pH = 4.5 and more BTH-like at pH = 5.5. This may be due to increased transglycosylation activity at pH = 5.5, which is also known to be much more pronounced for BTH than for rhHyal-1.[2, 3] Previous studies suggested that the hexasaccharide (n_3), which is the minimal substrate for BTH, is not degraded by both rhPH-20 and rhHyal-1.[3] Consequently, the binding mode of hyaluronan was assumed to be

different at the human enzymes and BTH, respectively.[3] Thus, the prevailing formation of n_3 instead of n_2 might be a consequence of different catalytic mechanisms. However, permanent intermediate formation of n_5 from transglycosylation and subsequent cleavage ($n_5 \rightarrow n_2 + n_3$) at pH = 5.5 may provide an explanation for the liberation of considerable amounts of n_2 under these conditions.

Chromatograms (Figure 7.6) and time-dependent curves (Figure 7.7) for the PEGylated variant (PEG-rhPH-20) were well comparable to unmodified rhPH-20. Taking also the pH profiles into consideration (*cf*. Section 7.3.2), PEGylation does not have an appreciable influence on the activity of rhPH-20. Hence, further studies were performed with rhPH-20.

Like BTH, both rhPH-20 and PEG-rhPH-20 produced a continuous decrease in the average molecular weight of low molecular weight hyaluronan, yielding complex mixtures of small oligosaccharides. Hence, observations from previous studies on the digestion of high molecular weight hyaluronan by mammalian type hyaluronidases were confirmed.[2]

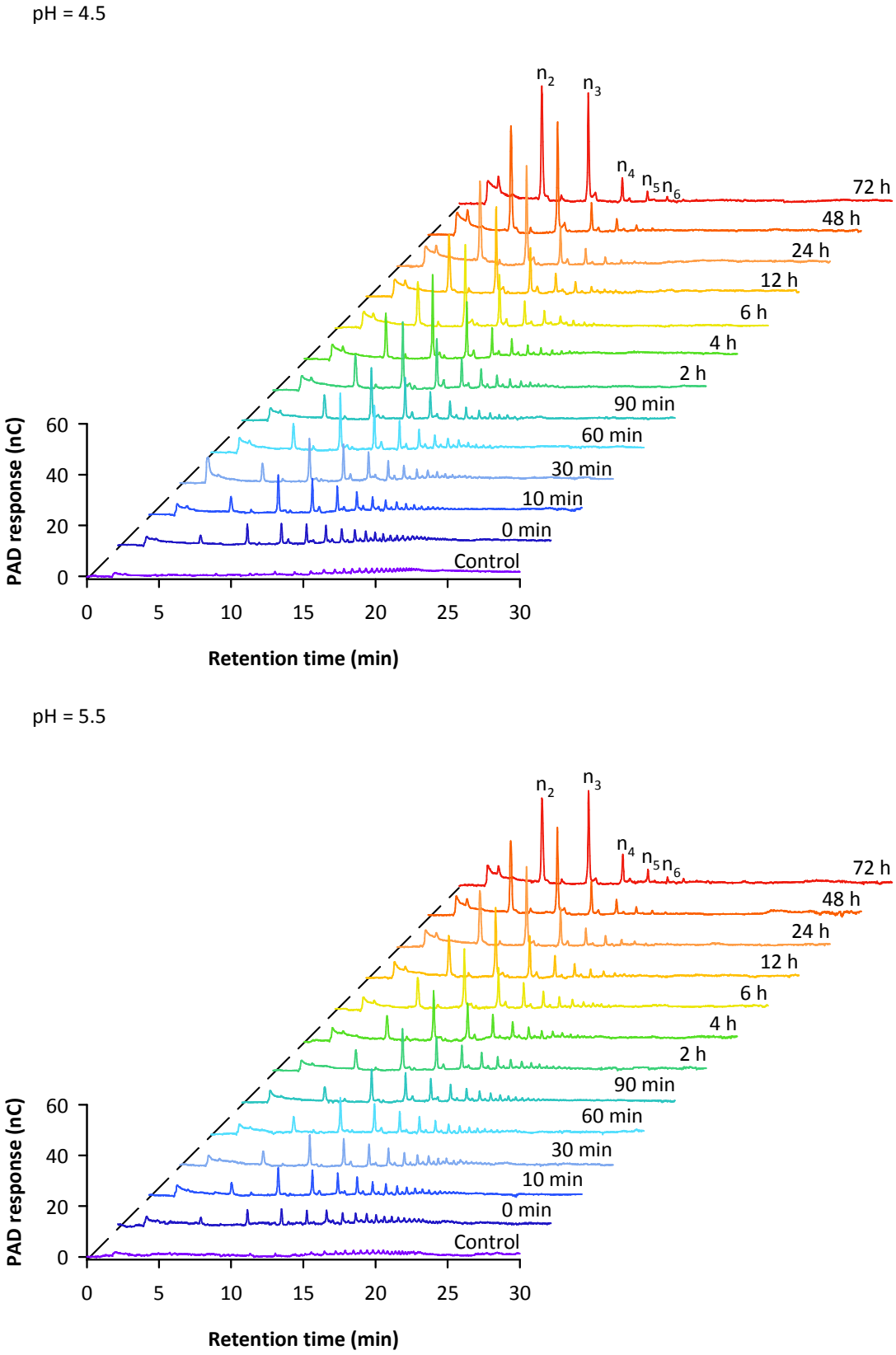

Figure 7.2: Time-dependent degradation of a low molecular weight hyaluronan oligosaccharide mixture by BTH (44.44 IU/mL) at pH = 4.5 (A) and pH = 5.5 (B). HPAEC–PAD chromatograms: 10 µL of diluted (1:10) sample injected, CarboPac™ PA200, 100 mM sodium hydroxide, gradient of 200–900 mM sodium acetate, 40 °C, 0.5 mL/min.

A pH = 4.5

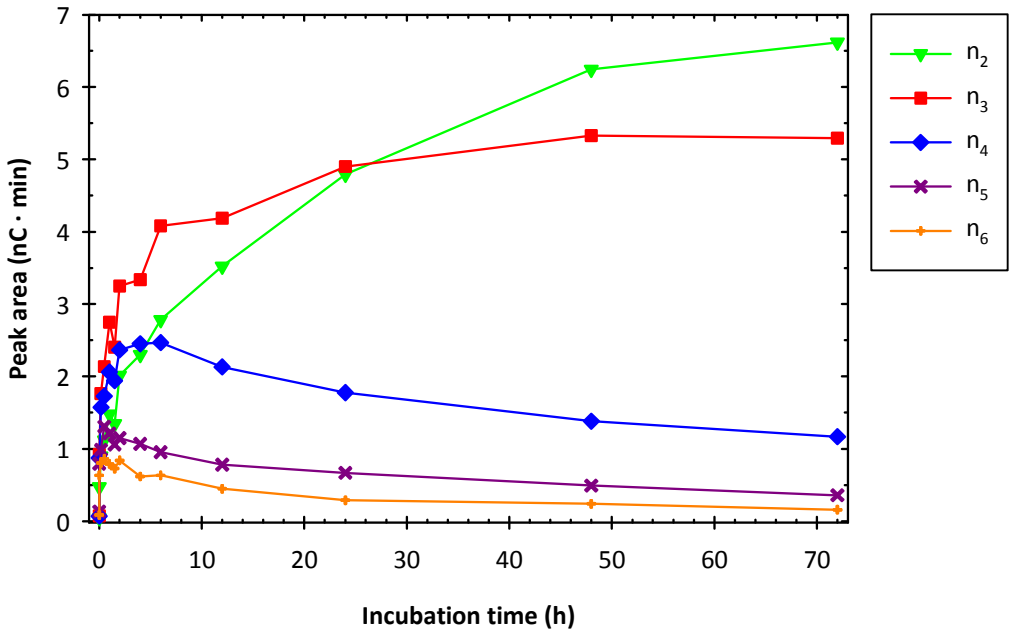

B pH = 5.5

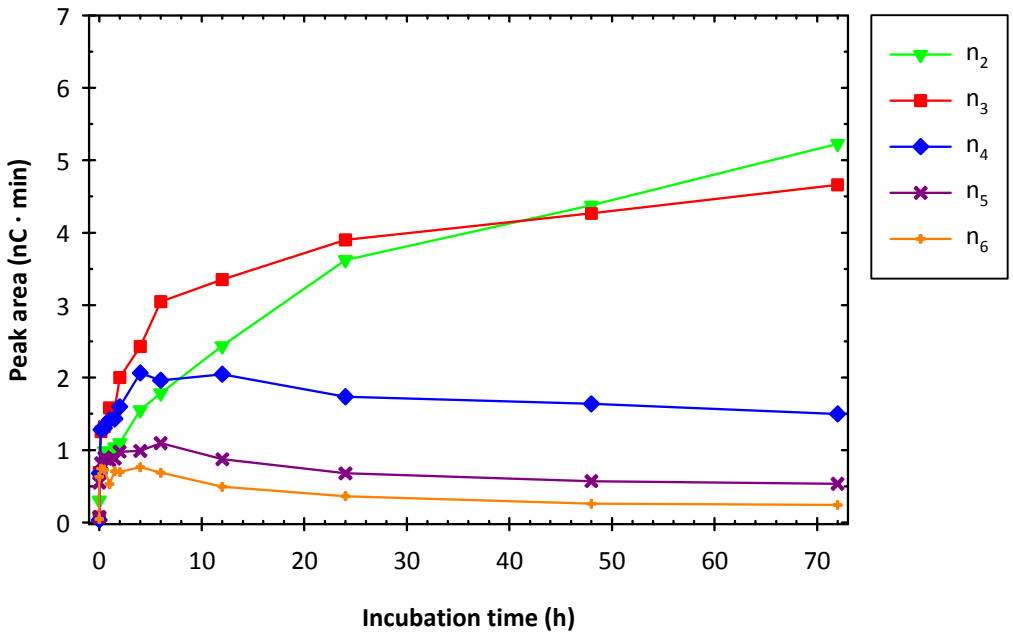

Figure 7.3: Time course of peak areas for the oligosaccharides n_2–n_6 from the chromatograms of Figure 7.2. Degradation of a low molecular weight hyaluronan oligosaccharide mixture by BTH (44.44 IU/mL) at pH = 4.5 (A) and pH = 5.5 (B). HPAEC–PAD: 10 µL of diluted (1:10) sample injected, CarboPac™ PA200, 100 mM sodium hydroxide, gradient of 200–900 mM sodium acetate, 40 °C, 0.5 mL/min.

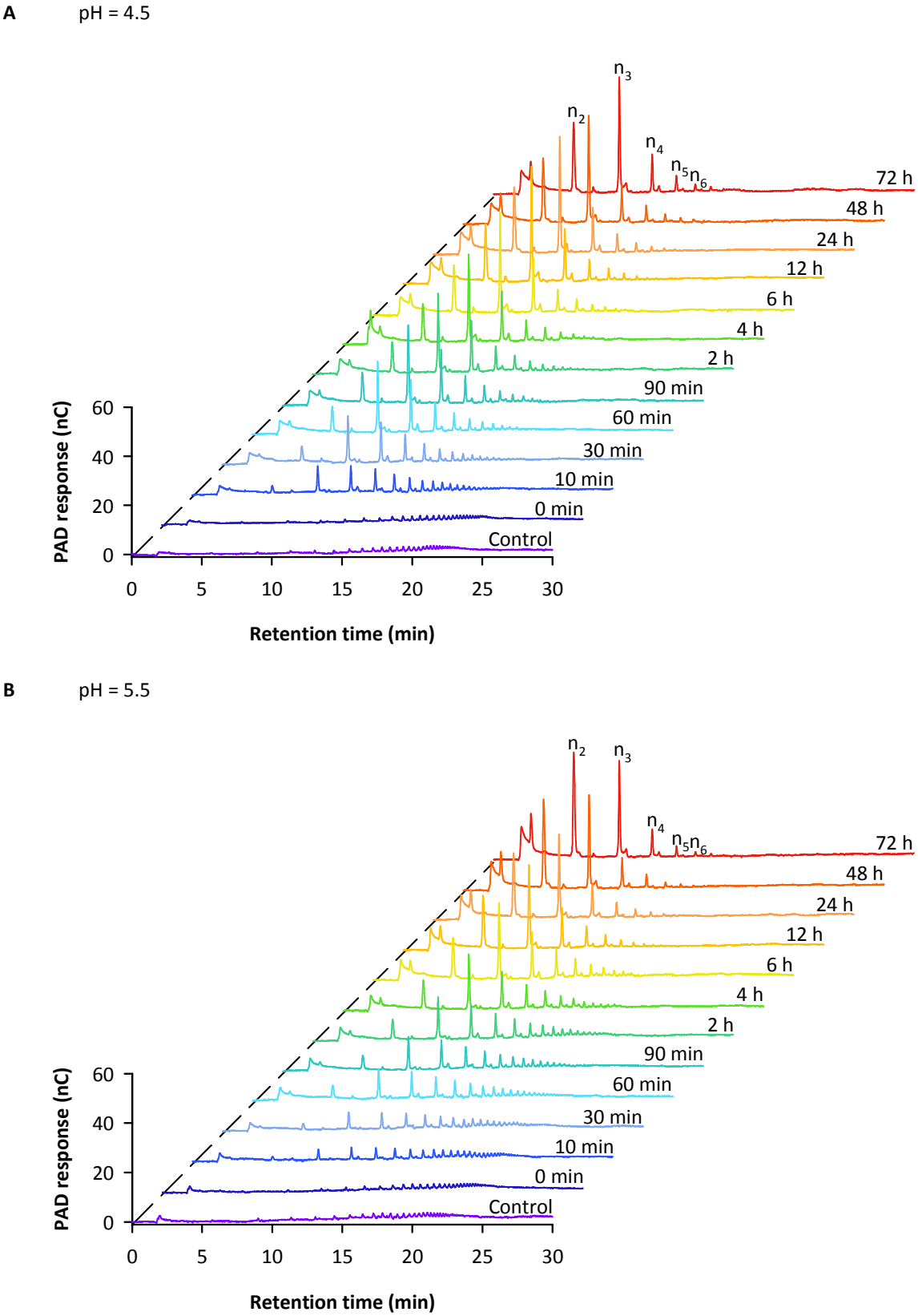

Figure 7.4: Time-dependent degradation of a low molecular weight hyaluronan oligosaccharide mixture by rhPH-20 (44.44 IU/mL) at pH = 4.5 (A) and pH = 5.5 (B). HPAEC–PAD chromatograms: 10 µL of diluted (1:10) sample injected, CarboPac™ PA200, 100 mM sodium hydroxide, gradient of 200–900 mM sodium acetate, 40 °C, 0.5 mL/min.

A pH = 4.5

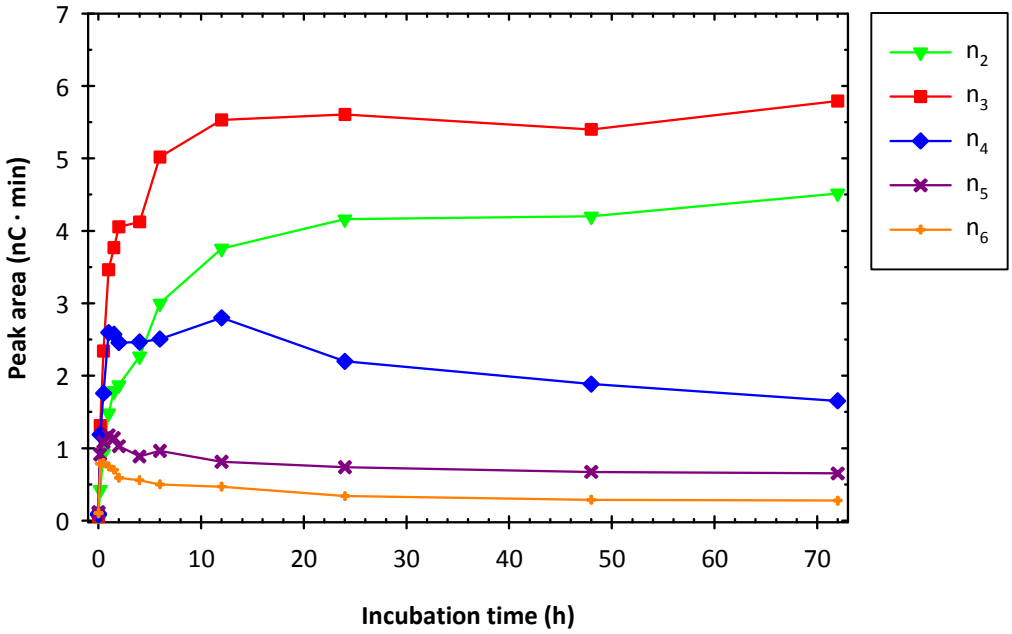

B pH = 5.5

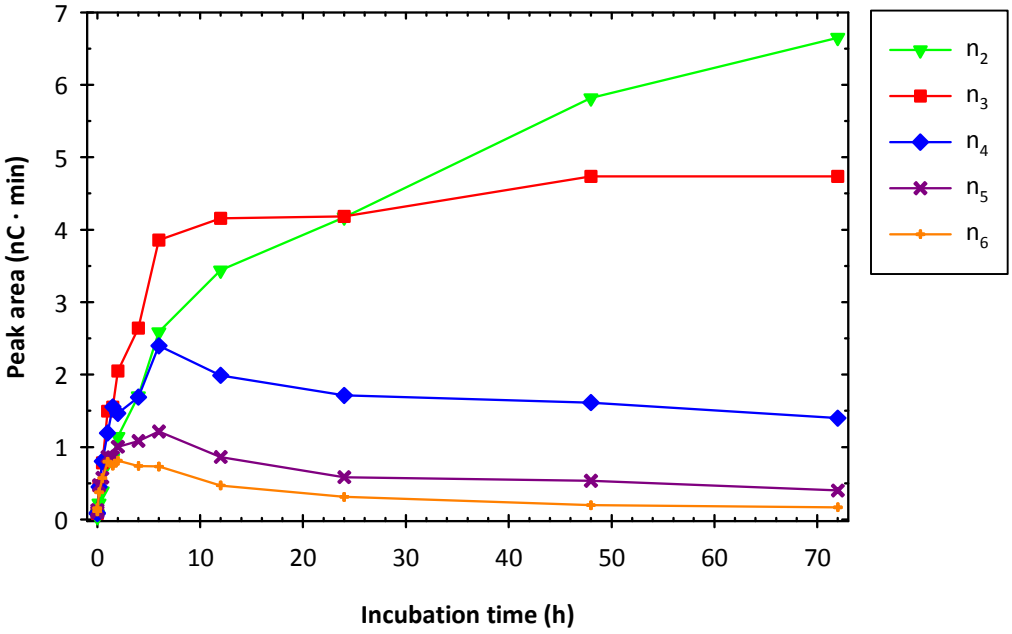

Figure 7.5: Time course of peak areas for the oligosaccharides n_2–n_6 from the chromatograms of Figure 7.4. Degradation of a low molecular weight hyaluronan oligosaccharide mixture by rhPH-20 (44.44 IU/mL) at pH = 4.5 (A) and pH = 5.5 (B). HPAEC–PAD: 10 µL of diluted (1:10) sample injected, CarboPac™ PA200, 100 mM sodium hydroxide, gradient of 200–900 mM sodium acetate, 40 °C, 0.5 mL/min.

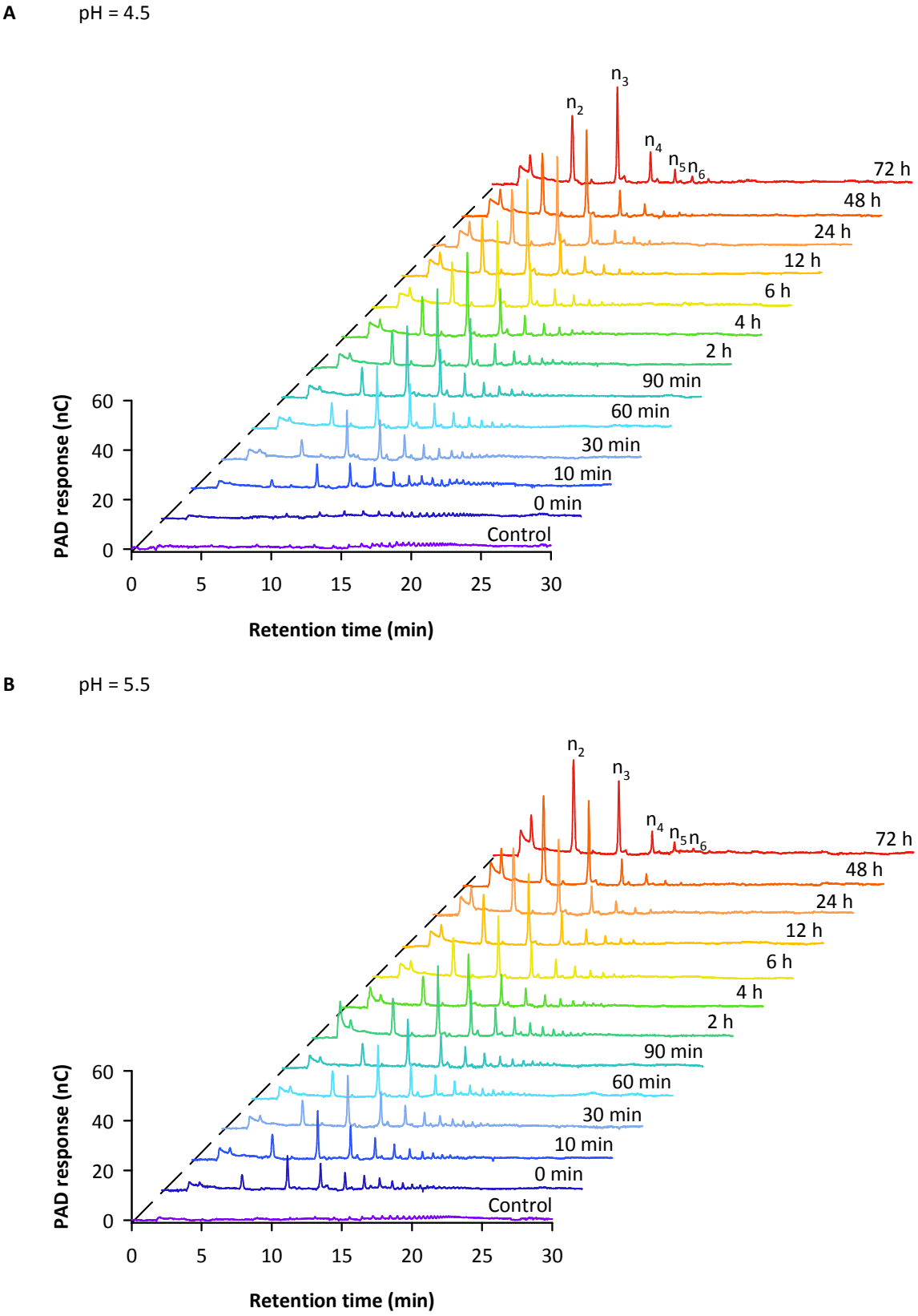

Figure 7.6: Time-dependent degradation of a low molecular weight hyaluronan oligosaccharide mixture by PEG-rhPH-20 (44.44 IU/mL) at pH = 4.5 (A) and pH = 5.5 (B). HPAEC–PAD chromatograms: 10 µL of diluted (1:10) sample injected, CarboPac™ PA200, 100 mM sodium hydroxide, gradient of 200–900 mM sodium acetate, 40 °C, 0.5 mL/min.

A pH = 4.5

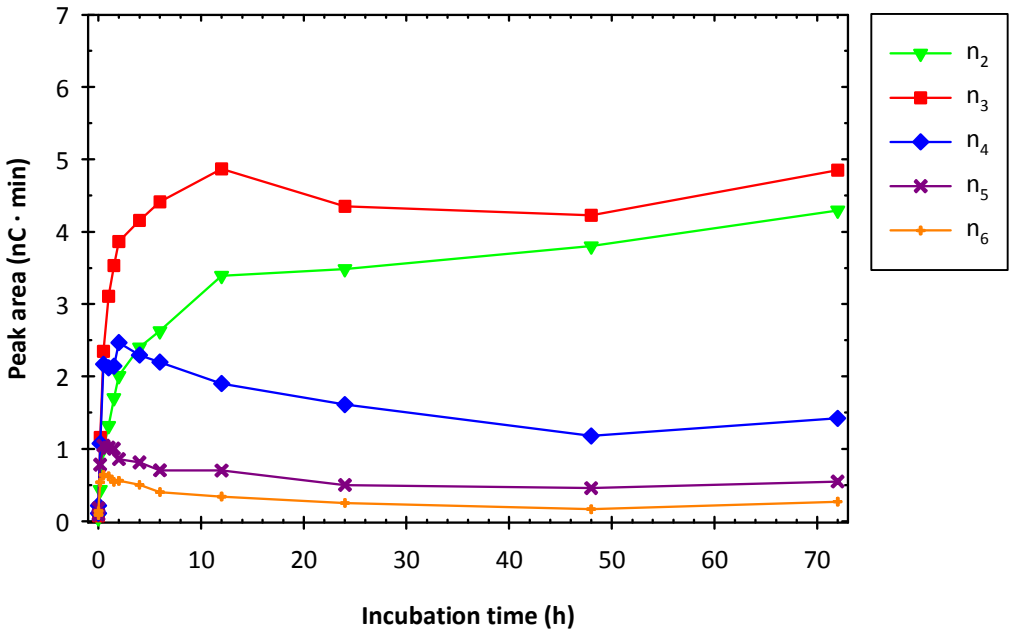

B pH = 5.5

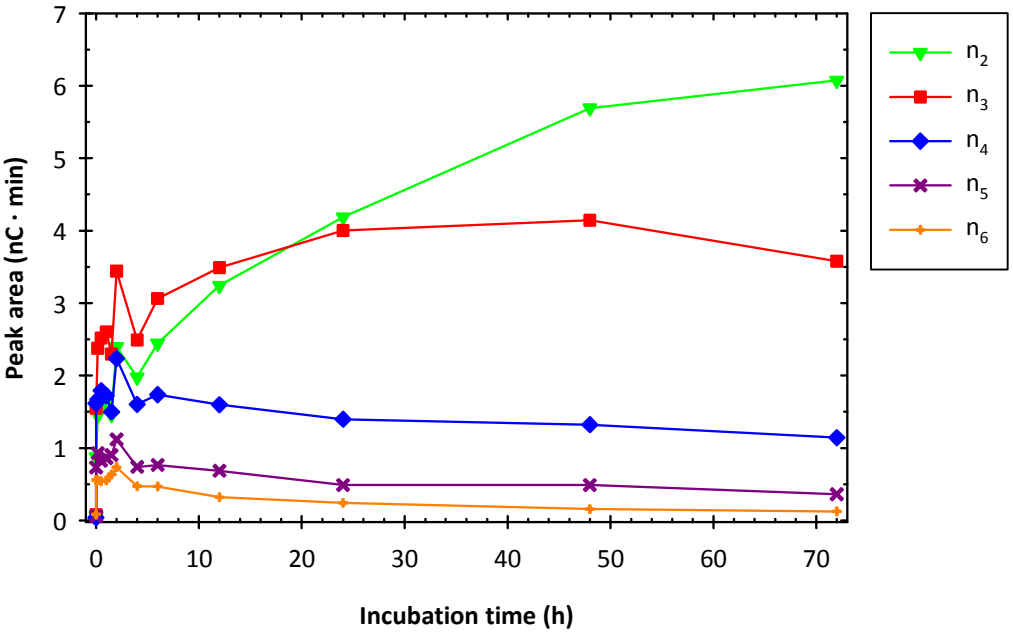

Figure 7.7: Time course of peak areas for the oligosaccharides n_2–n_6 from the chromatograms of Figure 7.6. Degradation of a low molecular weight hyaluronan oligosaccharide mixture by PEG-rhPH-20 (44.44 IU/mL) at pH = 4.5 (A) and pH = 5.5 (B). HPAEC–PAD: 10 µL of diluted (1:10) sample injected, CarboPac™ PA200, 100 mM sodium hydroxide, gradient of 200–900 mM sodium acetate, 40 °C, 0.5 mL/min.

7.3.4 Fast at-line analysis of hyaluronan oligosaccharide degradation by recombinant human PH-20

For fast at-line CZE–ESI-TOF-MS analysis of oligosaccharide degradation by recombinant human PH-20 in comparison with BTH (*cf*. Chapter 6, Section 6.3.3), 500 µM of the octasaccharide (n_4, Figure 7.8), the hexasaccharide (n_3, Figure 7.9), or the tetrasaccharide (n_2, Figure 7.10) were incubated with 55.56 IU/mL rhPH-20 under identical conditions at pH = 5.0.

Degradation of n_4 yielded n_3 as main product. By analogy with Figure 7.5 A, the portion of n_2 was considerably lower than observed for BTH under identical conditions (*cf*. Chapter 6, Section 6.3.3). Previously, similar studies using a different preparation of recombinant human PH-20 revealed the formation of mainly n_3 and smaller amounts of n_2 from n_4.[3] Moreover, the presence of n_1 and n_5 in the incubation mixtures was reported.[3] The present study confirmed the occurrence of both products (Figure 7.8, insets, light blue and violet). Taking together these observations, the prevailing reaction for n_4 was hydrolysis yielding n_1 and n_3. While n_3 accumulated, n_1 seemed to be preferably transferred to residual n_4 resulting in n_5. However, n_1 was partially liberated and could be proven by CZE–ESI-TOF-MS. In this regard, the probable mechanism resembles that proposed for BTH.[27] Nevertheless, the low amounts of n_2 and the simultaneous accumulation of n_5 suggested that both the symmetric cleavage of n_4 ($n_4 \rightarrow n_2 + n_2$) and the degradation of the newly formed n_5 ($n_5 \rightarrow n_2 + n_3$) were much slower.

In line with the results by Hofinger et al.,[3] neither n_3 (Figure 7.9) nor n_2 (Figure 7.10) were accepted as substrates by rhPH-20. Thus, neither hydrolysis nor transglycosylation reactions were observed for these oligosaccharides.

A

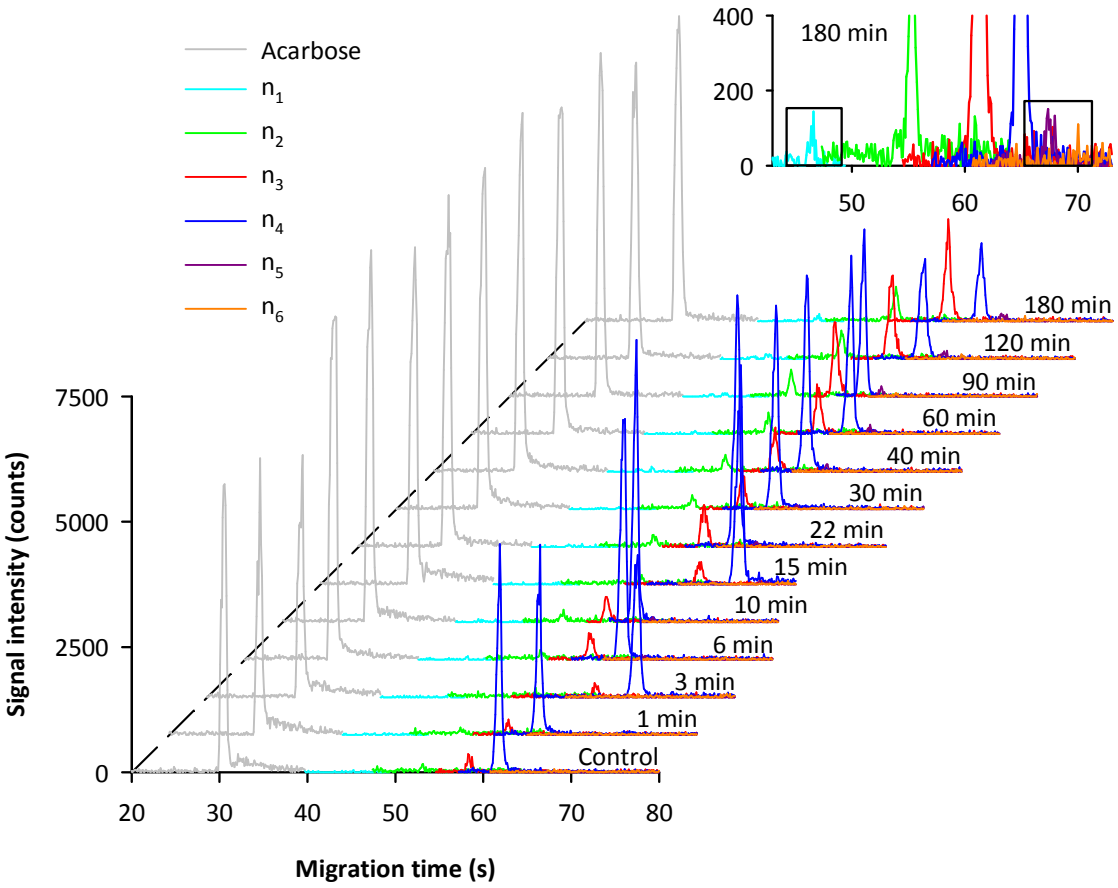

B

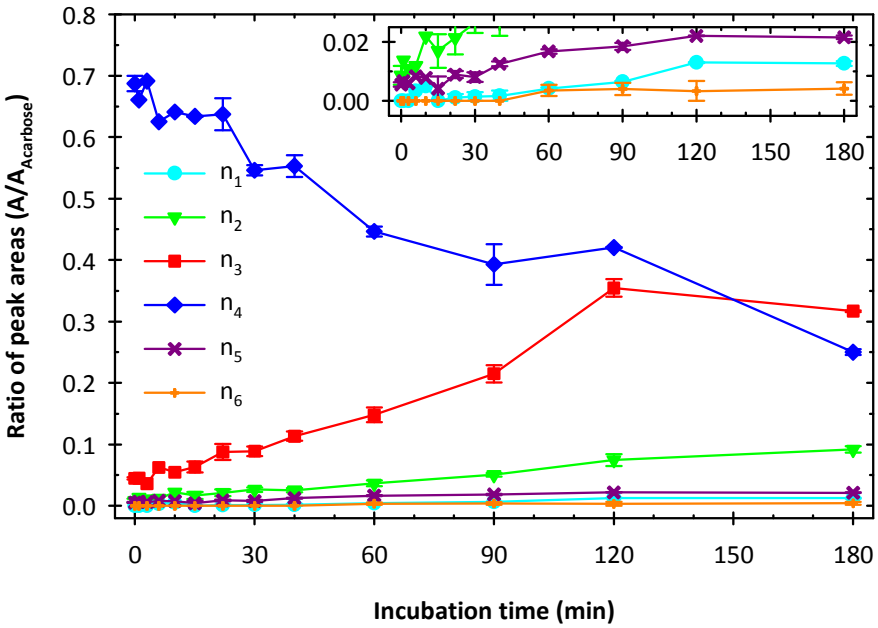

Figure 7.8: Incubation of the octasaccharide (n_4, 500 µM) with rhPH-20 (55.56 IU/mL) at pH = 5.0. Electropherograms (A) and standardized peak areas (B). Mean ± SEM for multiple injections. CZE: 1:10 sample dilution, 30 s injection, 25 µm × 28 cm capillary, ammonium acetate (25 mM, pH = 8.5), 35 kV.

A

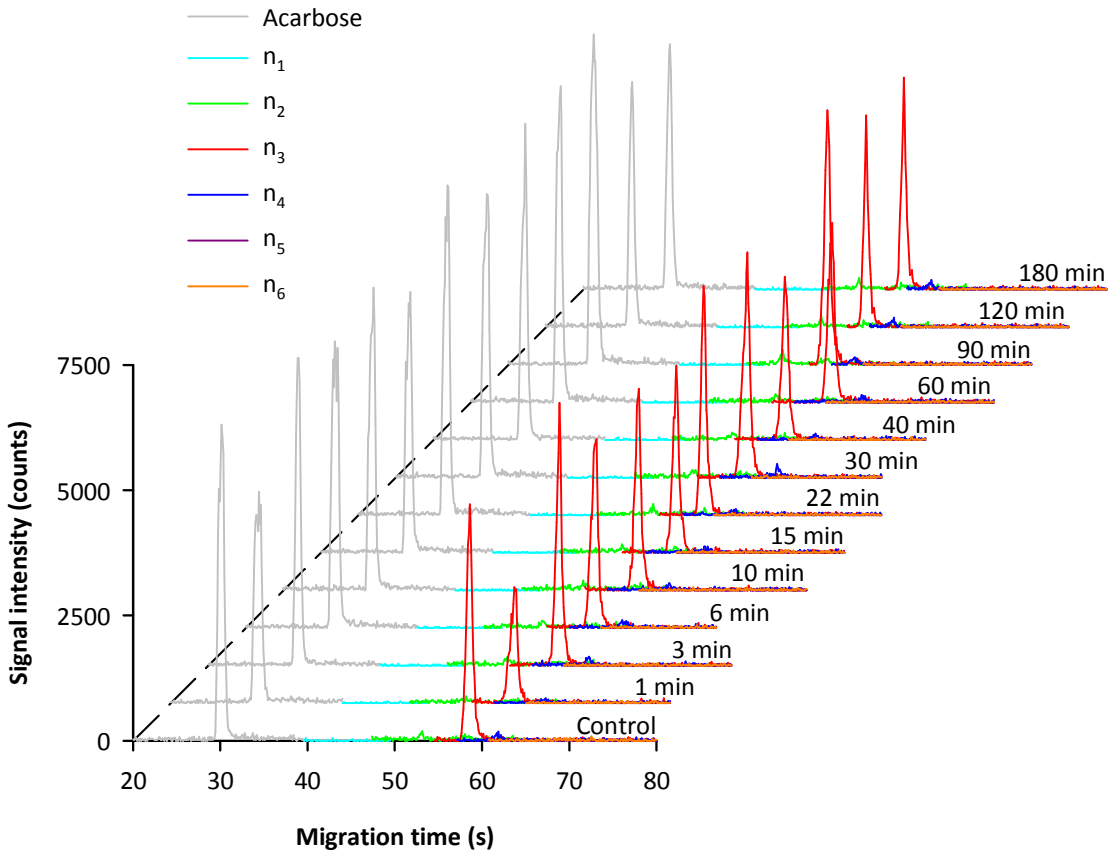

B

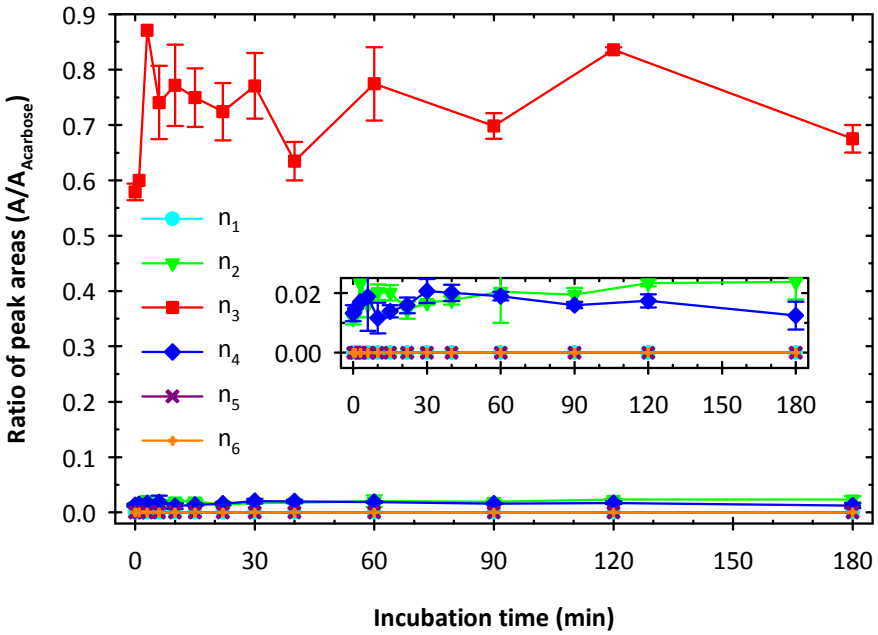

Figure 7.9: Incubation of the hexasaccharide (n_3, 500 µM) with rhPH-20 (55.56 IU/mL) at pH = 5.0. Electropherograms (A) and standardized peak areas (B). Mean ± SEM for multiple injections. CZE: 1:10 sample dilution, 30 s injection, 25 µm × 28 cm capillary, ammonium acetate (25 mM, pH = 8.5), 35 kV.

A

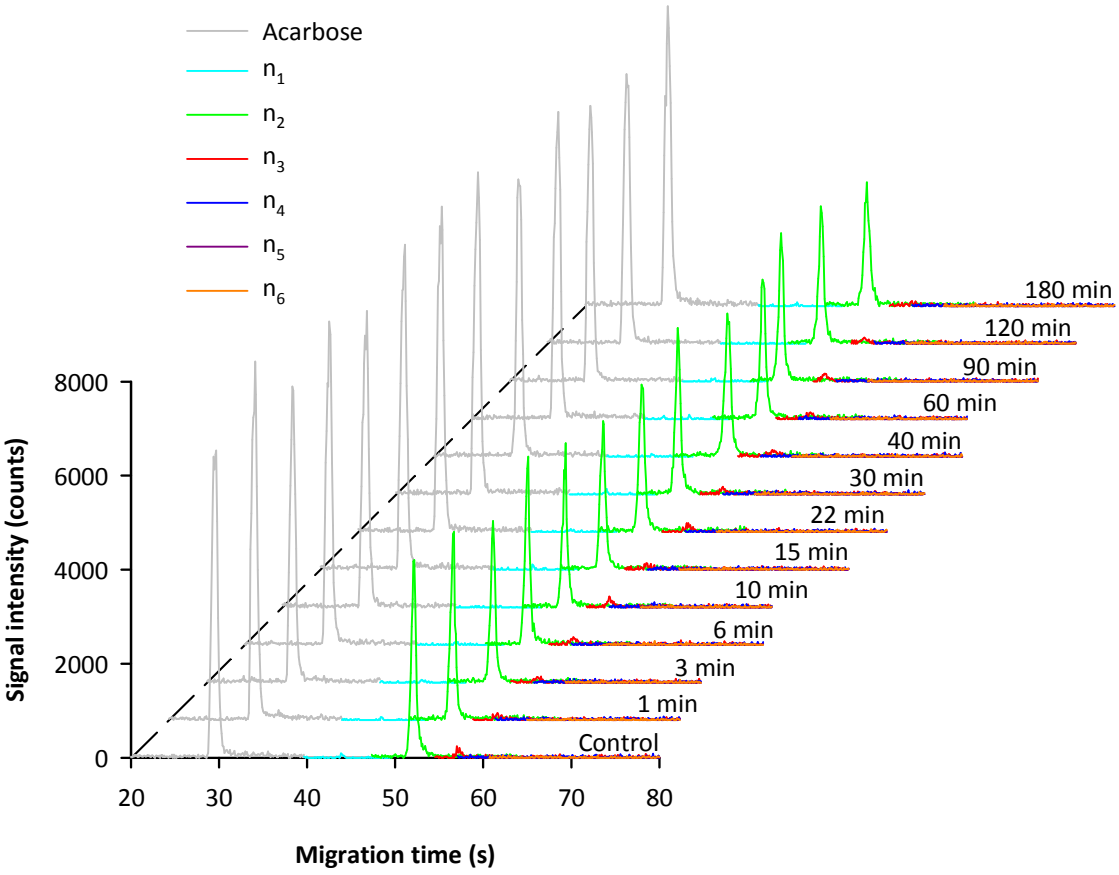

B

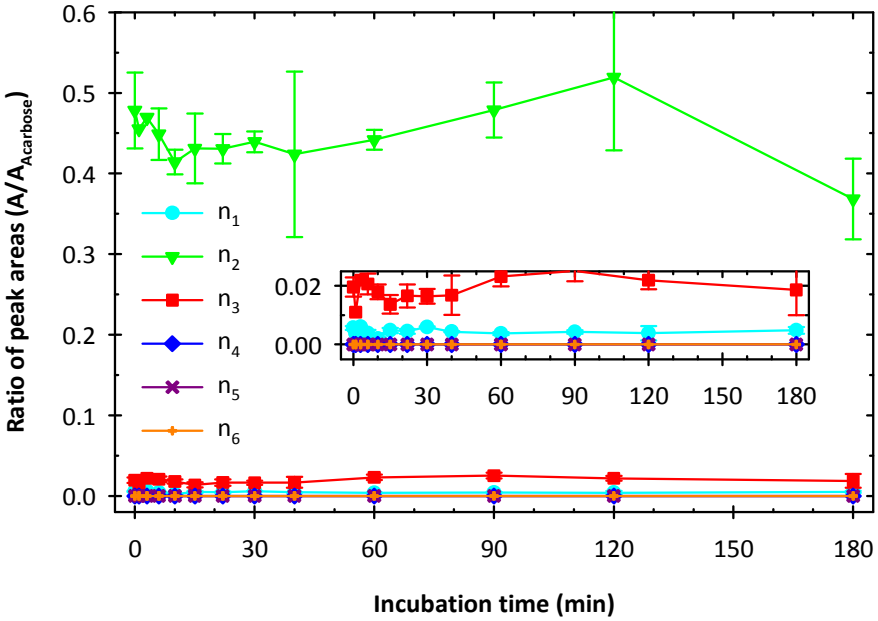

Figure 7.10: Incubation of the tetrasaccharide (n_2, 500 µM) with rhPH-20 (55.56 IU/mL) at pH = 5.0. Electropherograms (A) and standardized peak areas (B). Mean ± SEM for multiple injections. CZE: 1:10 sample dilution, 30 s injection, 25 µm × 28 cm capillary, ammonium acetate (25 mM, pH = 8.5), 35 kV.

7.3.5 Degradation of a low molecular weight hyaluronan oligosaccharide mixture by recombinant human Hyal-1

Like the other mammalian type hyaluronidases (BTH, rhPH-20, and PEG-rhPH-20) discussed in this work, rhHyal-1 continuously reduced the average molecular mass of a hyaluronan oligosaccharide mixture (Figure 7.11 A). Hence, the random endolytic mode of action, typical for this group of hyaluronidases,[2, 28, 29] was confirmed. Thereby, the product spectrum and the time-dependent formation of small oligosaccharides (Figure 7.11 B) by rhHyal-1 at a pH of 3.5 (the pH optimum of the enzyme) were similar to the degradation by rhPH-20 at pH = 4.5 (*cf*. Figure 7.4 A and Figure 7.5 A). A comparative investigation of rhHyal-1 at pH = 4.5 was impossible due to the lack of activity at this pH value (*cf*. Figure 7.1 C).

The tetrasaccharide (n_2) and the hexasaccharide (n_3) accumulated as end products with n_3 being the main component of the product mixture. Other oligosaccharides (n_4–n_6) were also present after 72 h. However, due to the shape of the time-dependent concentration curves, these molecules can be considered as intermediate products. The end products and their relative occurrence were congruent with the results from incubation of high molecular weight hyaluronan with a different preparation of rhHyal-1.[2] As discussed above (*cf*. Section 7.3.3), the predominant formation of n_3, which is different from the results with BTH, may result from an altered catalytic mechanism of the human enzymes, also reflected by their different minimal substrates.[3]

A

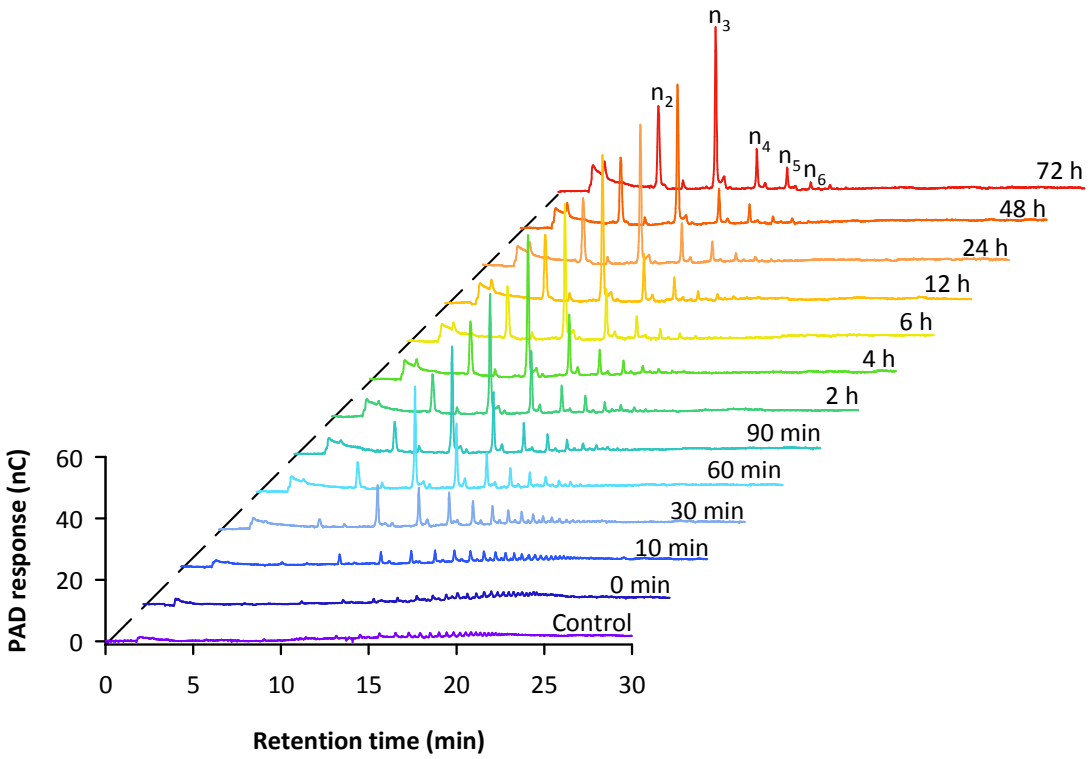

B

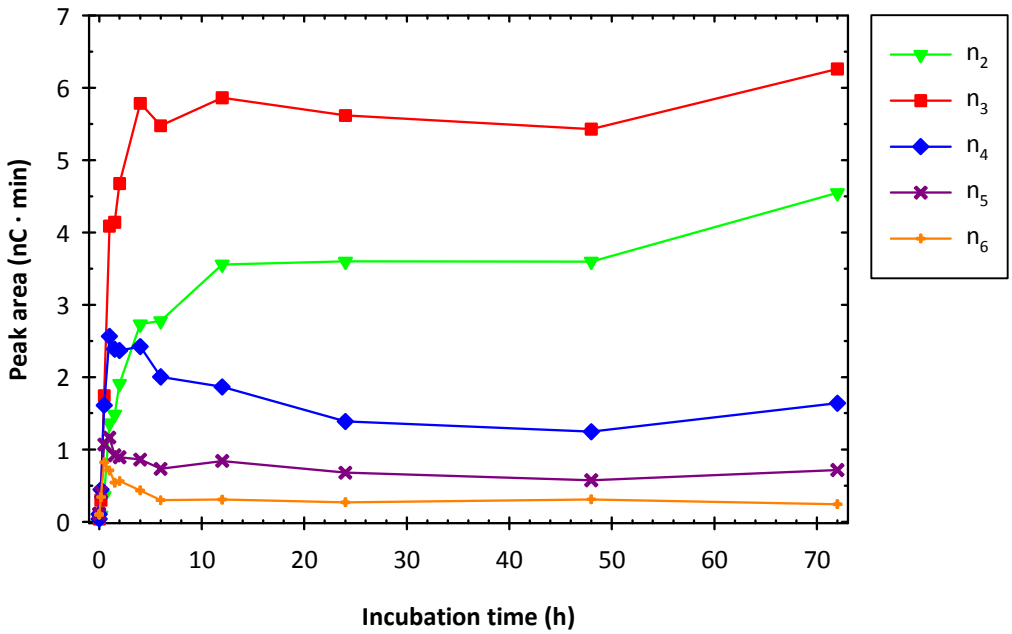

Figure 7.11: Time-dependent degradation of a low molecular weight hyaluronan oligosaccharide mixture by rhHyal-1 (44.44 IU/mL) at pH = 3.5. Chromatograms (A) and peak areas (B). HPAEC–PAD: 10 µL of diluted (1:10) sample injected, CarboPac™ PA200, 100 mM sodium hydroxide, gradient of 200–900 mM sodium acetate, 40 °C, 0.5 mL/min.

7.3.6 Fast at-line analysis of hyaluronan oligosaccharide degradation by recombinant human Hyal-1

500 µM of the octasaccharide (n_4, Figure 7.12 and Figure 7.13), the hexasaccharide (n_3, Figure 7.14), and the tetrasaccharide (n_2, Figure 7.15) were incubated with 55.56 IU/mL rhHyal-1 at the pH optimum of the enzyme (pH = 3.5). Substrates and products were analyzed at-line by CZE–ESI-TOF-MS.

During the first 180 min of incubation, enzymatic conversion of n_4 into n_2 and n_3 was proven (Figure 7.12). However, the reaction was relatively slow. Hence, the incubation period was extended up to 9 h (Figure 7.13). Taking advantage of at-line measurement, this amendment could easily be implemented while the experiment was performed. Analytical methods not allowing for at-line monitoring of the enzymatic process would have required an additional experiment to answer the problem. In contrast to BTH and rhPH-20, in the presence of rhHyal-1 the liberation of n_5 was not observed. Although n_3 was the main product, the relative amount of n_2 was higher than that produced by rhPH-20. The disaccharide (n_1) continuously accumulated. However, standardized peak areas were much lower than for n_3, which should have been formed in equal amounts from hydrolysis ($n_4 \rightarrow n_1 + n_3$). Therefore, it is conceivable that, by rhHyal-1, n_1 was also transferred to an acceptor molecule by transglycosylation as suggested for BTH.[27]

However, bearing in mind the sensitivity of the analytical method optimized for n_2–n_4 (*cf*. Chapter 3), it should be noted that the amount of n_1 might be partially underestimated comparing the peak areas. The lack of n_5 and the accumulation of n_1, albeit on a relatively low level, are hints that hydrolysis prevailed. In their study on this topic, Hofinger et al. also reported that the catalytic action of their rhHyal-1 preparation was restricted to hydrolysis at 100 µM of n_4, whereas at high concentrations (1 mM) the formation of transglyosylation products was proven.[3] Hence, at 500 µM transglycosylation might occur, although to a much lower extent than hydrolysis. In the respective article, the concentration of n_1 was reported to be close to the limit of detection of the CZE–UV method, even at low substrate concentrations.[3] Nevertheless, n_3 was the major product resulting from digestion of n_4 by rhHyal-1.[3] Provided that this discrepancy was not due to methodological reasons, this finding (ratio of n_3 and n_1), which is basically in agreement with the CZE–ESI-TOF-MS results, is incompatible with a simple hydrolytic mechanism. Thus, further research will be necessary to elucidate the exact catalytic mechanism of rhHyal-1.

As already described in literature,[3] n_3 (Figure 7.14) and n_2 (Figure 7.15) were not accepted as substrates by rhHyal-1.

A

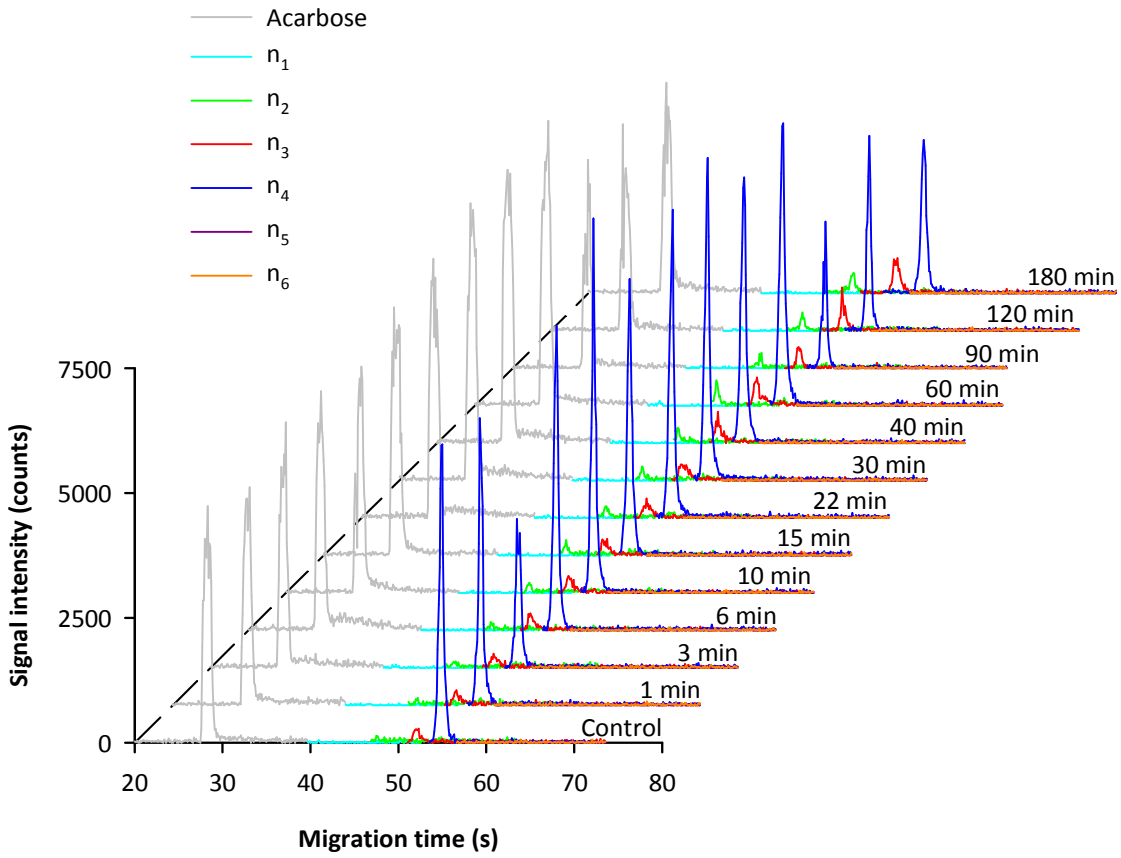

B

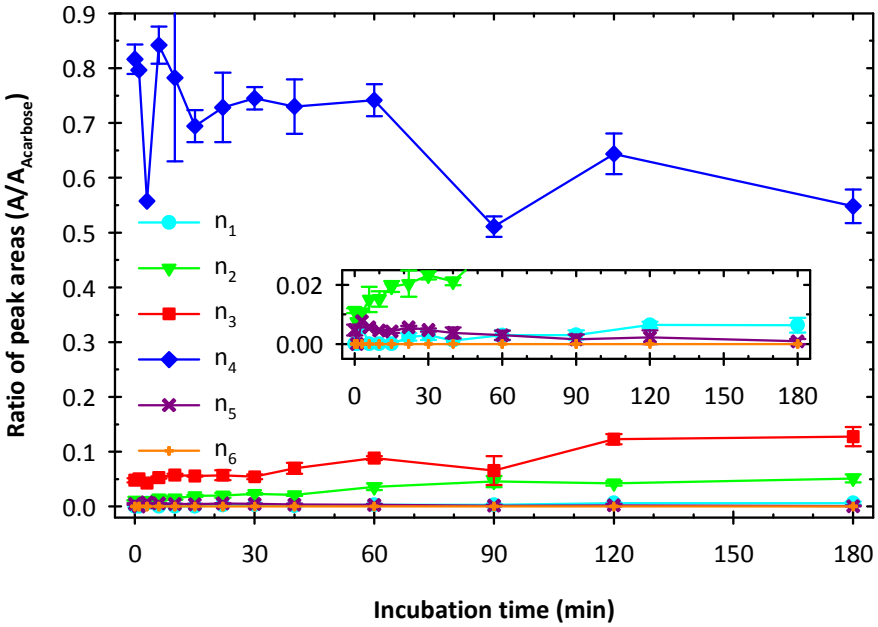

Figure 7.12: Incubation of the octasaccharide (n_4, 500 µM) with rhHyal-1 (55.56 IU/mL) at pH = 3.5. Electropherograms (A) and standardized peak areas (B). Mean ± SEM for multiple injections. CZE: 1:10 sample dilution, 30 s injection, 25 µm × 28 cm capillary, ammonium acetate (25 mM, pH = 8.5), 35 kV.

A

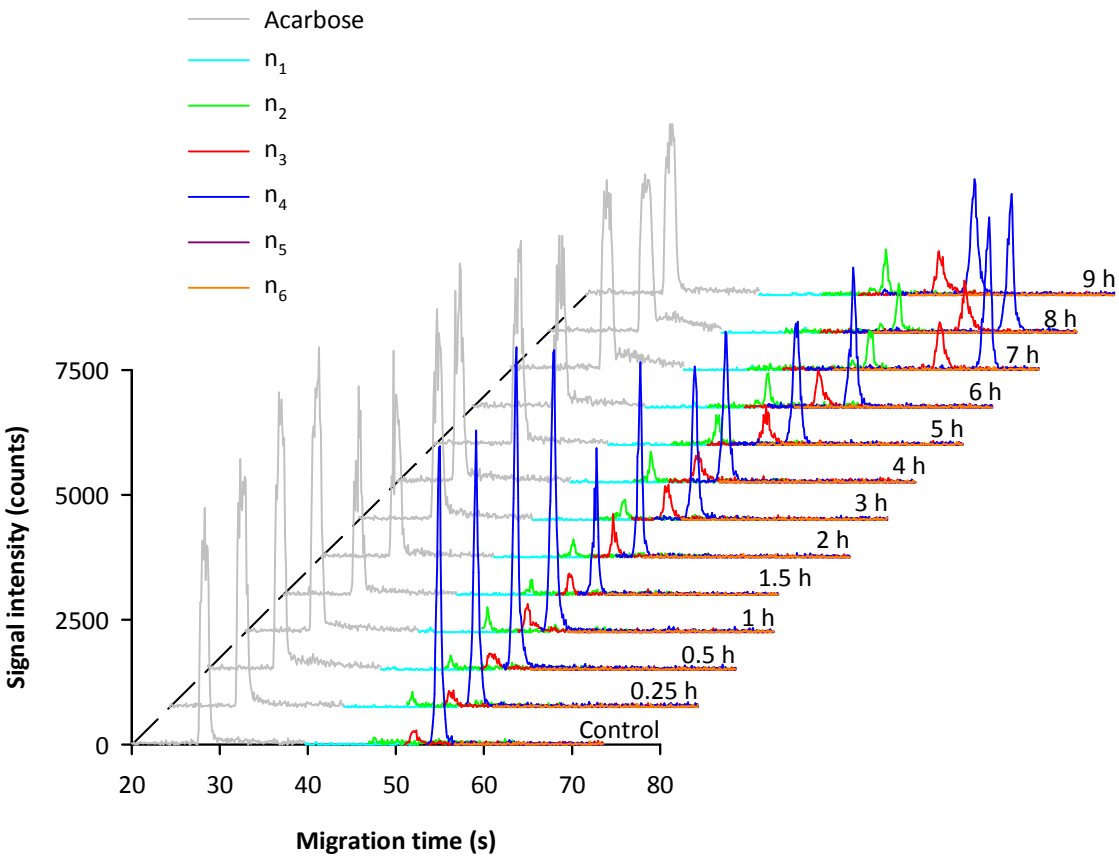

B

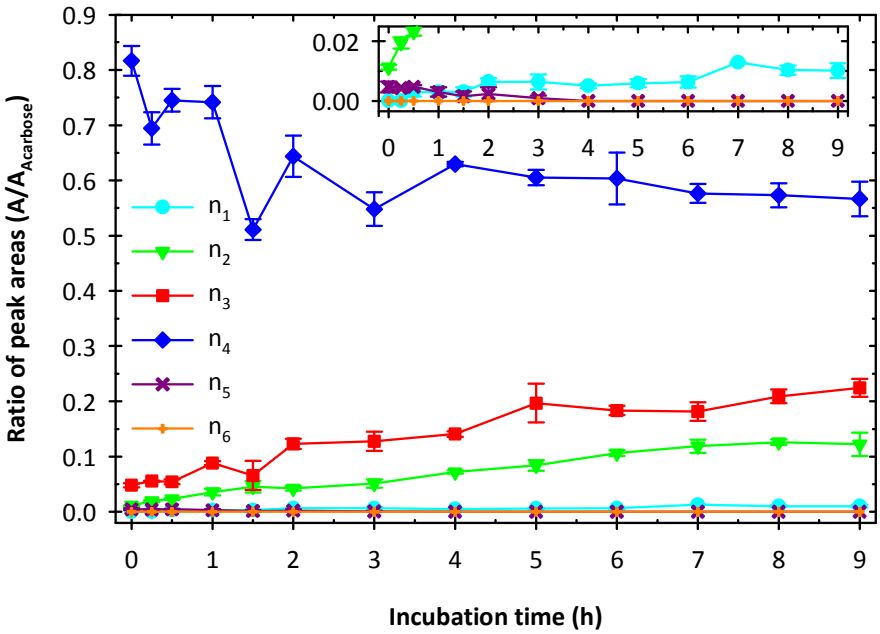

Figure 7.13: Prolonged incubation of the octasaccharide (n_4, 500 µM) with rhHyal-1 (55.56 IU/mL) at pH = 3.5. Electropherograms (A) and standardized peak areas (B). Mean ± SEM for multiple injections. CZE: 1:10 sample dilution, 30 s injection, 25 µm × 28 cm capillary, ammonium acetate (25 mM, pH = 8.5), 35 kV.

A

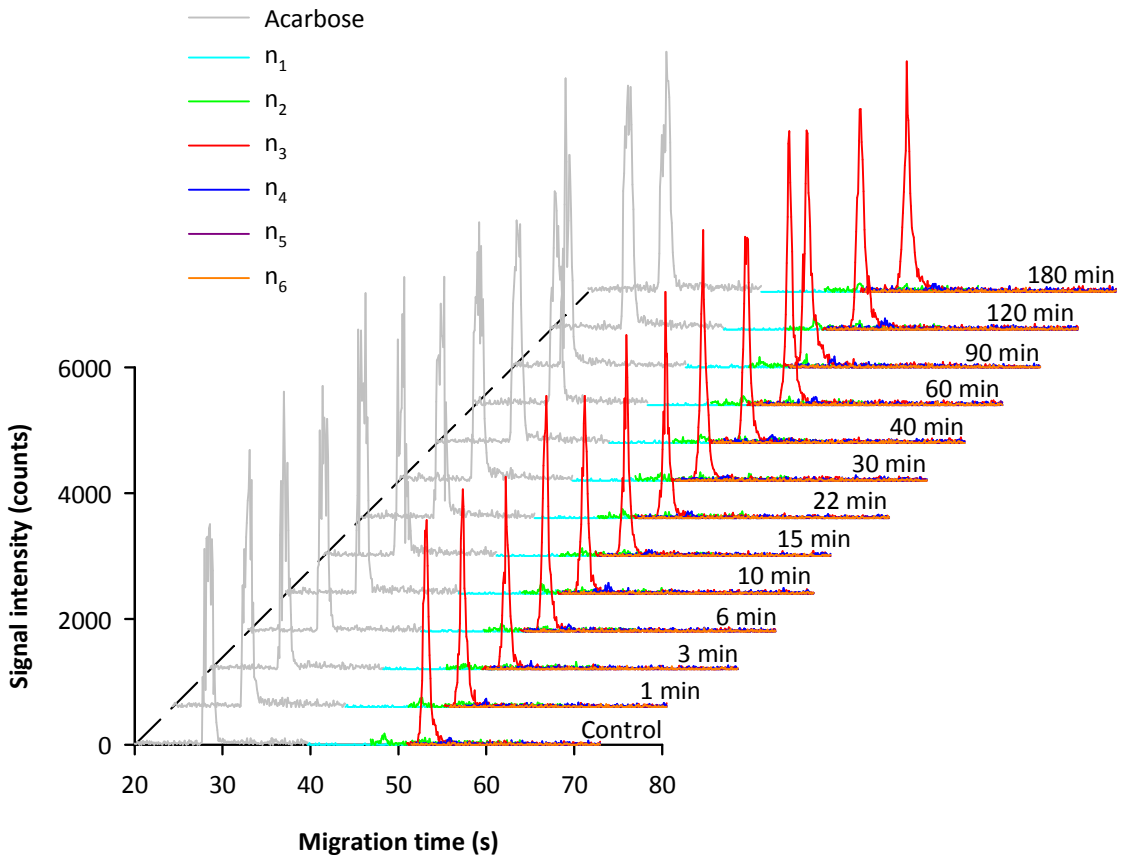

B

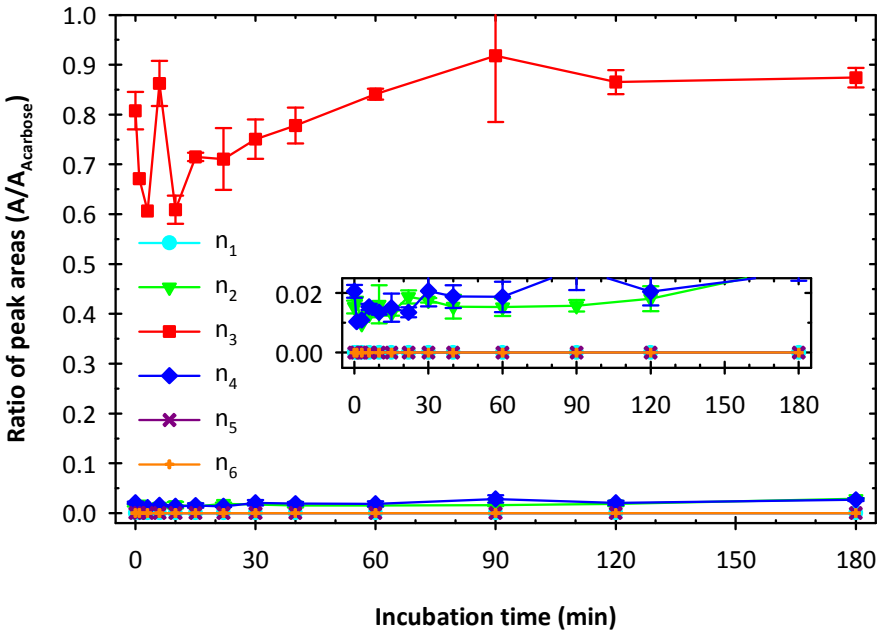

Figure 7.14: Incubation of the hexasaccharide (n_3, 500 µM) with rhHyal-1 (55.56 IU/mL) at pH = 3.5. Electropherograms (A) and standardized peak areas (B). Mean ± SEM for multiple injections. CZE: 1:10 sample dilution, 30 s injection, 25 µm × 28 cm capillary, ammonium acetate (25 mM, pH = 8.5), 35 kV.

A

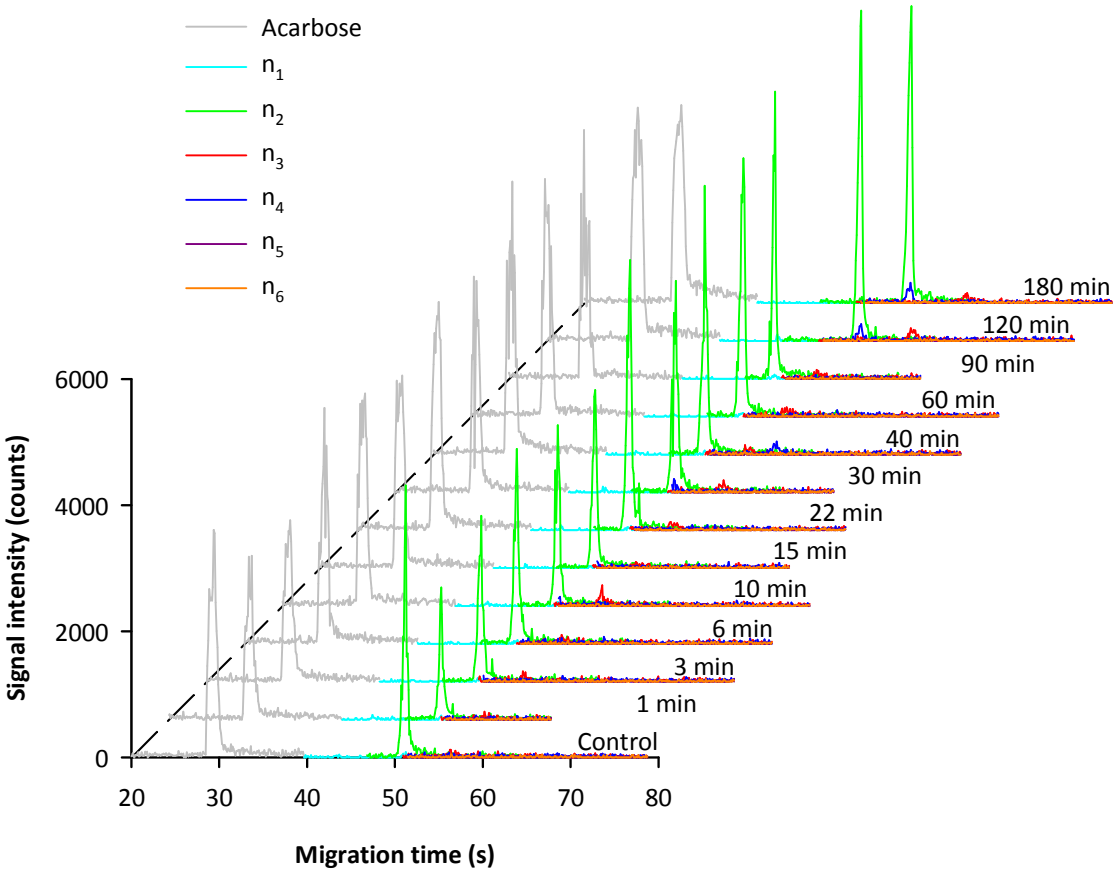

B

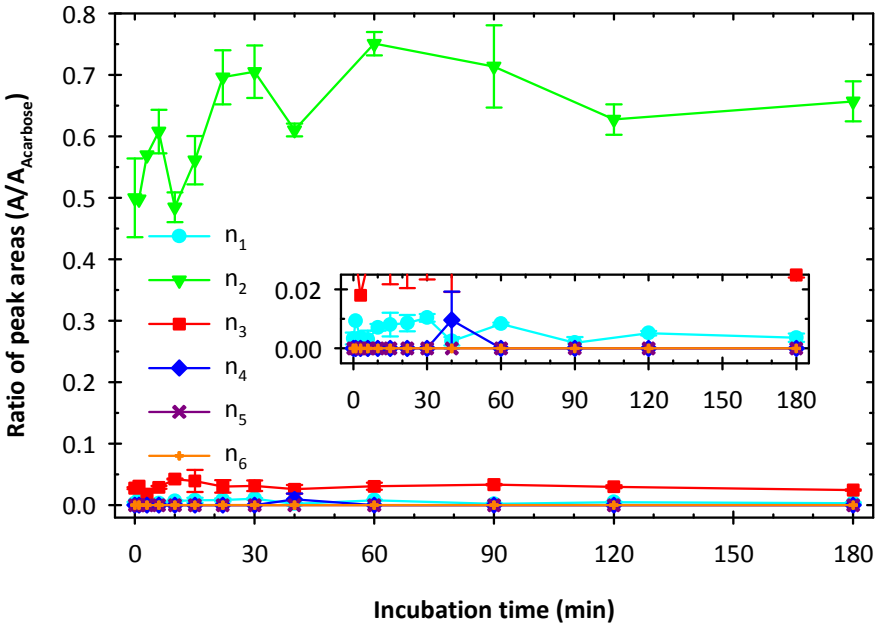

Figure 7.15: Incubation of the tetrasaccharide (n_2, 500 µM) with rhHyal-1 (55.56 IU/mL) at pH = 3.5. Electropherograms (A) and standardized peak areas (B). Mean ± SEM for multiple injections. CZE: 1:10 sample dilution, 30 s injection, 25 µm × 28 cm capillary, ammonium acetate (25 mM, pH = 8.5), 35 kV.

7.3.7 The quest for inhibitors

For the study of the physiological and pathophysiological role of human hyaluronidases, potent and selective inhibitors of these enzymes are strongly needed as pharmacological tools. Therefore, the search for such substances has been the matter of several PhD projects in our group. Commonly used reference compounds with inhibitory activity on hyaluronidases are diclofenac, indomethacin, and L-ascorbic acid-6-*O*-hexadecanoate (vitamin C palmitate).[30] Especially vitamin C palmitate was proven to be a potent inhibitor of bovine testicular hyaluronidase as well as the bacterial hyaluronidases from *Streptococcus agalactiae* and *Streptococcus pneumoniae*.[31]

To assess the potency of the reference inhibitors with regard to these particular enzyme preparations, the inhibitory effects on rhPH-20 at pH = 5.0 (Figure 7.16) and rhHyal-1 at pH = 3.5 (Figure 7.17) were determined within a concentration range of 50–1000 µM. Different enzyme activities and incubation periods were compared. With increasing enzyme activity, the maximum inhibition decreased significantly. Only at low enzyme concentrations and prolonged incubation, evaluable curves were obtained. It must be noted that enzyme activities are expressed as activities of the enzyme solution added to the incubation mixture. For the final concentration in the assay, the dilution of 1:7.3 has to be considered.

Diclofenac and indomethacin showed inhibition of rhPH-20 only at very high concentrations, whereas IC_{50} values of 156 ± 14 µM (10 IU/mL enzyme solution, 4.5 h) and 168 ± 48 µM (10 IU/mL enzyme solution, 2 h) could be calculated from the concentration-response curves of vitamin C palmitate. Values are expressed as mean ± SEM from three independent experiments.

By contrast, both vitamin C palmitate and diclofenac had no inhibitory effect on rhHyal-1 at pH = 3.5. Only indomethacin was able to inhibit enzyme activity at very high concentrations. From these results, it becomes obvious that human hyaluronidases still pose a particular challenge with regard to identification of inhibitors. Hence, the quest for inhibitors of these isoenzymes is still in the early stages.

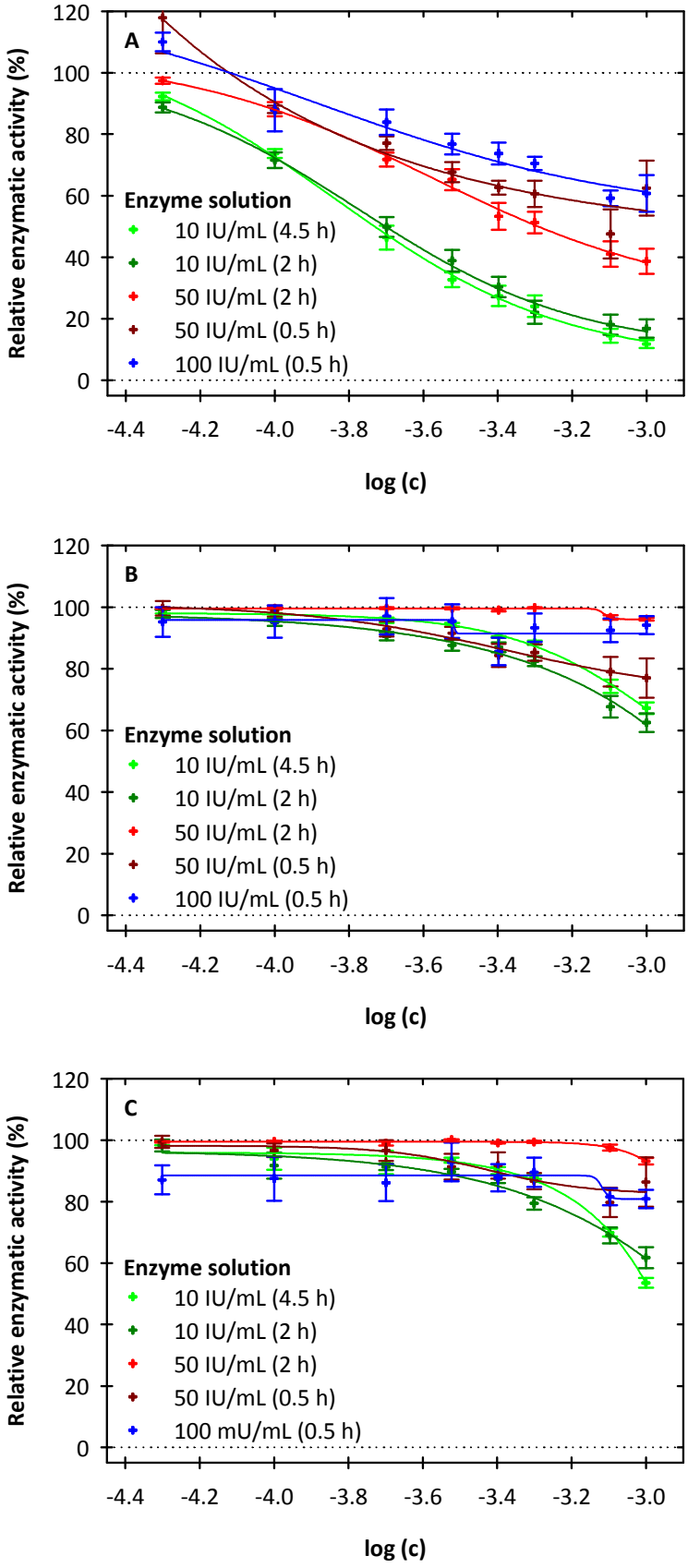

Figure 7.16: Inhibition of rhPH-20 (at pH = 5.0) by vitamin C palmitate (A), diclofenac (B), and indomethacin (C). Determination by the turbidimetric assay using 96-well plates. Concentrations of the enzyme solutions are given as values of the prepared solution (prior to addition to the incubation mixture, dilution in assay: 1:7.3). Incubation time is stated in parentheses. Data presented as mean ± standard error of three independent experiments (each performed in triplicate), curves were fitted with SigmaPlot.

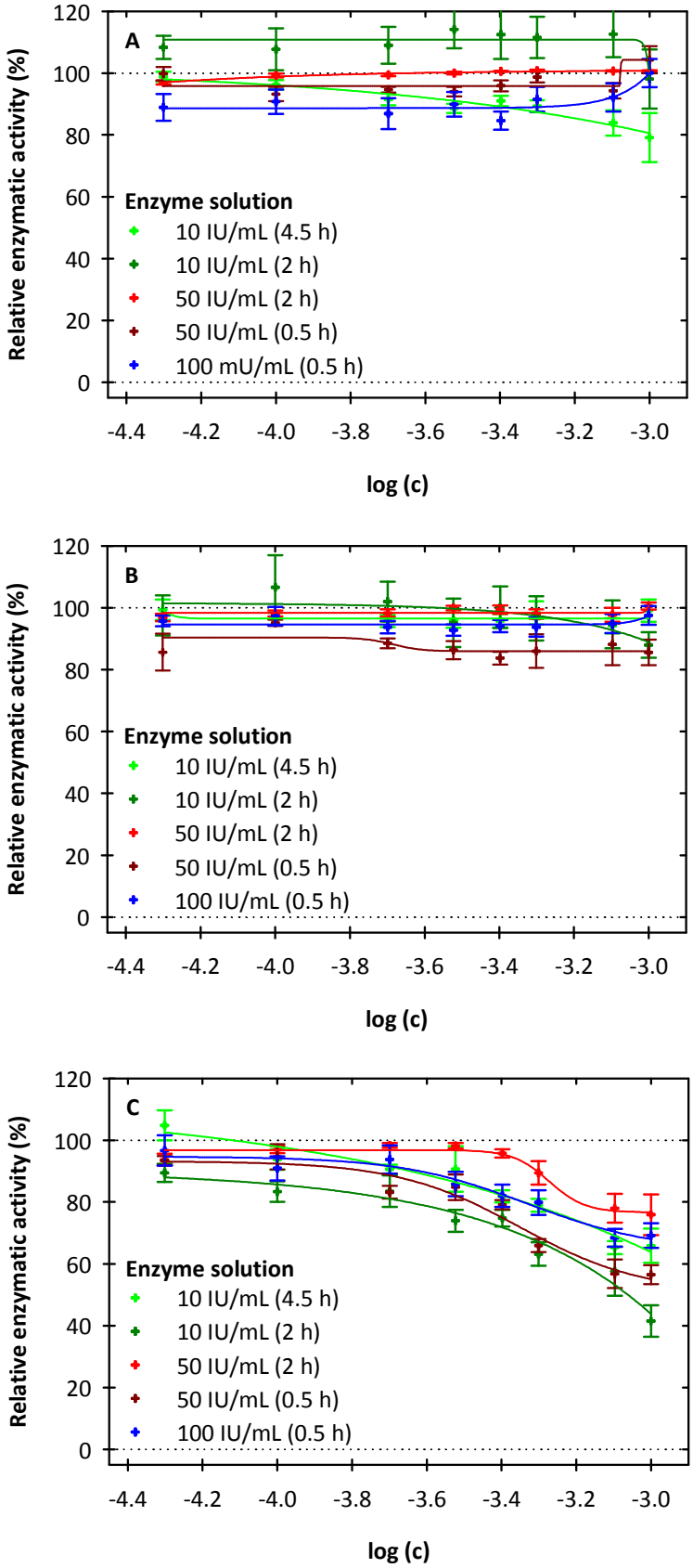

Figure 7.17: Inhibition of rhHyal-1 (at pH = 3.5) by vitamin C palmitate (A), diclofenac (B), and indomethacin (C). Determination by the turbidimetric assay using 96-well plates. Concentrations of the enzyme solutions are given as values of the prepared solution (prior to addition to the incubation mixture, dilution in assay: 1:7.3). Incubation time is stated in parentheses. Data presented as mean ± standard error of three independent experiments (each performed in triplicate), curves were fitted with SigmaPlot.

7.4 Summary and conclusion

Recombinant human PH-20 (rhPH-20), PEGylated rhPH-20 (PEG-rhPH-20) and recombinant human Hyal-1 (rhHyal-1) were characterized *in vitro*. All of them showed maximum activity at acidic pH values of 4 (rhPH-20 and PEG-rhPH-20) or 3.5 (rhHyal-1). In contrast to bovine testicular hyaluronidase (BTH) and a different preparation of rhPH-20,[2] neither rhPH-20 nor PEG-rhPH-20 exhibited assay-dependent differences regarding pH profiles.

The degradation of hyaluronan oligosaccharides by the different isoenzymes was monitored by HPAEC–PAD and fast at-line CZE–ESI-TOF-MS. Thereby, differences between BTH and rhPH-20 became obvious, whereas PEG-rhPH-20 and its non-PEGylated form, rhPH-20 showed essentially the same behavior. In general, the characteristics reported for recombinant human hyaluronidases[2, 3] were confirmed. Nevertheless, the conversion of hyaluronan and hyaluronan oligosaccharides by these enzymes obviously follows a complex mechanism including hydrolysis as well as transglycosylation steps.

Vitamin C palmitate, indomethacin, and diclofenac showed very low inhibitory effects on the examined preparations of rhPH-20 and rhHyal-1. Varying the period of incubation with rhPH-20, IC_{50} values of 156 ± 14 µM and 168 ± 48 µM (mean ± SEM), respectively, were determined for vitamin C palmitate. No inhibitory effect on rhHyal-1 was observed. On both enzymes, indomethacin and diclofenac had no or only weak inhibitory effects at very high concentrations of around 1 mM. Moreover, maximum inhibitory effect was considerably reduced with increasing enzyme concentrations, although the time of incubation was adjusted to the respective degradation velocity. Hence, evaluable curves were only obtained at low enzyme activities, requiring long incubation periods up to 4.5 h.

7.5 References

1. Jedrzejas, M. J.; Stern, R. Structures of vertebrate hyaluronidases and their unique enzymatic mechanism of hydrolysis. *Proteins* **2005,** 61, 227-238.

2. Hofinger, E. S. A.; Hoechstetter, J.; Oettl, M.; Bernhardt, G.; Buschauer, A. Isoenzyme-specific differences in the degradation of hyaluronic acid by mammalian-type hyaluronidases. *Glycoconj. J.* **2008,** 25, 101-109.

3. Hofinger, E. S. A.; Bernhardt, G.; Buschauer, A. Kinetics of Hyal-1 and PH-20 hyaluronidases: comparison of minimal substrates and analysis of the transglycosylation reaction. *Glycobiology* **2007,** 17, 963-971.

4. Gmachl, M.; Sagan, S.; Ketter, S.; Kreil, G. The human sperm protein PH-20 has hyaluronidase activity. *FEBS Lett.* **1993,** 336, 545-548.

5. Cherr, G. N.; Yudin, A. I.; Overstreet, J. W. The dual functions of GPI-anchored PH-20: hyaluronidase and intracellular signaling. *Matrix Biol.* **2001,** 20, 515-525.

6. Evison, M.; Pretty, C.; Taylor, E.; Franklin, C. Human recombinant hyaluronidase (Cumulase) improves intracytoplasmic sperm injection survival and fertilization rates. *Reprod. Biomed. Online* **2009,** 18, 811-814.

7. Taylor, T. H.; Elliott, T.; Colturato, L. F.; Straub, R. J.; Mitchell-Leef, D.; Nagy, Z. P. Comparison of bovine- and recombinant human-derived hyaluronidase with regard to fertilization rates and embryo morphology in a sibling oocyte model: a prospective, blinded, randomized study. *Fertil. Steril.* **2006,** 85, 1544-1546.

8. Bookbinder, L. H.; Hofer, A.; Haller, M. F.; Zepeda, M. L.; Keller, G. A.; Lim, J. E.; Edgington, T. S.; Shepard, H. M.; Patton, J. S.; Frost, G. I. A recombinant human enzyme for enhanced interstitial transport of therapeutics. *J. Control. Release* **2006,** 114, 230-241.

9. Frost, G. I. Recombinant human hyaluronidase (rHuPH20): an enabling platform for subcutaneous drug and fluid administration. *Expert Opin. Drug Deliv.* **2007,** 4, 427-440.

10. Frost, G. I.; Csóka, A. B.; Wong, T.; Stern, R. Purification, cloning, and expression of human plasma hyaluronidase. *Biochem. Biophys. Res. Commun.* **1997,** 236, 10-15.

11. Hofinger, E. S. A.; Spickenreither, M.; Oschmann, J.; Bernhardt, G.; Rudolph, R.; Buschauer, A. Recombinant human hyaluronidase Hyal-1: insect cells versus *Escherichia coli* as expression system and identification of low molecular weight inhibitors. *Glycobiology* **2007,** 17, 444-453.

12. Afify, A. M.; Stern, M.; Guntenhöner, M.; Stern, R. Purification and characterization of human serum hyaluronidase. *Arch. Biochem. Biophys.* **1993,** 305, 434-441.

13. Gold, E. W. Purification and properties of hyaluronidase from human liver. Differences from and similarities to the testicular enzyme. *Biochem. J.* **1982,** 205, 69-74.

14. Csóka, A. B.; Frost, G. I.; Wong, T.; Stern, R. Purification and microsequencing of hyaluronidase isozymes from human urine. *FEBS Lett.* **1997,** 417, 307-310.

15. Hofinger, E. S. A. Recombinant expression, purification and characterization of human hyaluronidases. PhD thesis, University of Regensburg, Regensburg, **2007**.

16. Asari, A. Novel functions of hyaluronan oligosaccharides. *Glycoforum* **2005**. (http://www.glycoforum.gr.jp/science/hyaluronan/HA12a/HA12aE.html)

17. Oettl, M. Biochemische Charakterisierung boviner testikulärer Hyaluronidase und Untersuchungen zum Einfluß von Hyaluronidase und Hyaluronsäure auf das Wachstum von Tumoren. PhD thesis, University of Regensburg, Regensburg, **2000**.

18. Bradford, M. M. A rapid and sensitive method for the quantitation of microgram quantities of protein utilizing the principle of protein-dye binding. *Anal. Biochem.* **1976,** 72, 248-254.

19. Muckenschnabel, I.; Bernhardt, G.; Spruß, T.; Dietl, B.; Buschauer, A. Quantitation of hyaluronidases by the Morgan-Elson reaction: comparison of the enzyme activities in the plasma of tumor patients and healthy volunteers. *Cancer Lett.* **1998,** 131, 13-20.

20. Gacesa, P.; Savitsky, M. J.; Dodgson, K. S.; Olavesen, A. H. A recommended procedure for the estimation of bovine testicular hyaluronidase in the presence of human serum. *Anal. Biochem.* **1981,** 118, 76-84.

21. Reissig, J. L.; Storminger, J. L.; Leloir, L. F. A modified colorimetric method for the estimation of *N*-acetylamino sugars. *J. Biol. Chem.* **1955,** 217, 959-966.

22. Morgan, W. T.; Elson, L. A. A colorimetric method for the determination of *N*-acetylglucosamine and *N*-acetylchrondrosamine. *Biochem. J.* **1934,** 28, 988-995.

23. Di Ferrante, N. Turbidimetric measurement of acid mucopolysaccharides and hyaluronidase activity. *J. Biol. Chem.* **1956,** 220, 303-306.

24. Oettl, M.; Hoechstetter, J.; Asen, I.; Bernhardt, G.; Buschauer, A. Comparative characterization of bovine testicular hyaluronidase and a hyaluronate lyase from *Streptococcus agalactiae* in pharmaceutical preparations. *Eur. J. Pharm. Sci.* **2003,** 18, 267-277.

25. Gorham, S. D.; Olavesen, A. H.; Dodgson, K. S. Effect of ionic strength and pH on the properties of purified bovine testicular hyaluronidase. *Connect. Tissue Res.* **1975,** 3, 17-25.

26. Saitoh, H.; Takagaki, K.; Majima, M.; Nakamura, T.; Matsuki, A.; Kasai, M.; Narita, H.; Endo, M. Enzymic reconstruction of glycosaminoglycan oligosaccharide chains using the transglycosylation reaction of bovine testicular hyaluronidase. *J. Biol. Chem.* **1995,** 270, 3741-3747.

27. Kakizaki, I.; Ibori, N.; Kojima, K.; Yamaguchi, M.; Endo, M. Mechanism for the hydrolysis of hyaluronan oligosaccharides by bovine testicular hyaluronidase. *FEBS J.* **2010,** 277, 1776-1786.

28. Meyer, K. Hyaluronidases. In: *The Enzymes*, Boyer, P. D. (Ed.). Academic Press: New York, **1971**, Vol. 3, pp 307-320.

29. Vercruysse, K. P.; Lauwers, A. R.; Demeester, J. M. Kinetic investigation of the degradation of hyaluronan by hyaluronidase using gel permeation chromatography. *J. Chromatogr. B, Biomed. Appl.* **1994,** 656, 179-190.

30. Spickenreither, M. Inhibitors of bacterial and mammalian hyaluronidases: design, synthesis and structure-activity relationships with focus on human enzymes. PhD thesis, University of Regensburg, Regensburg, **2008**.

31. Botzki, A.; Rigden, D. J.; Braun, S.; Nukui, M.; Salmen, S.; Hoechstetter, J.; Bernhardt, G.; Dove, S.; Jedrzejas, M. J.; Buschauer, A. L-Ascorbic acid 6-hexadecanoate, a potent hyaluronidase inhibitor. X-ray structure and molecular modeling of enzyme-inhibitor complexes. *J. Biol. Chem.* **2004,** 279, 45990-45997.

8 Analysis of synovial fluid samples

8.1 Introduction

In 1939, Meyer et al. reported the isolation of a polysaccharide, consisting of *N*-acetyl-D-glucosamine and glucuronic acid, from synovial fluid.[1] The authors identified this polysaccharide as hyaluronan, which was isolated from many different sources in the 1930s and 1940s.[2] In 1950, Sundblad published a chemical characterization of synovial fluid and described the crucial role of hyaluronan in determining the viscosity of the synovial fluid.[3] He also found high amounts, but a decreased degree of polymerization of hyaluronan in case of degenerative and inflammatory joint diseases.[3] One year before, Ragan and Meyer had published similar results for rheumatoid arthritis and had suggested a defect in synthesis as the reason for the occurrence of incompletely polymerized hyaluronan.[4] Regardless of the increased total amount of hyaluronan, other authors reported a reduced concentration in synovial fluids from patients due to dramatically increased volume and concomitant dilution effects.[5, 6]

Recently, the pathological degradation of hyaluronan from synovial fluid to smaller fragment has been doubted, at least in osteoarthritis.[7] Hence, even more than seven decades after the isolation by Meyer et al.,[1] the exact role of hyaluronan in synovial fluid and in the pathology of arthritis is far from being completely understood. Therefore, synovial fluid remains an interesting matrix for hyaluronan analysis. Although the hyaluronan content of 3–4 mg/mL is rather high,[8] this material is challenging for an application of a new method of hyaluronan and hyaluronan oligosaccharide analysis due to the complexity of biological matrices. Consequently, CZE–ESI-TOF-MS and HPAEC–PAD were used in combination with colorimetry, rheology, gel electrophoresis, and zymography to characterize 12 synovial fluid samples, which were available at our lab.

8.2 Materials and methods

8.2.1 Origin of samples

Synovial fluid samples, kindly provided by the Department of Orthopedics (University of Regensburg/Asklepios Klinikum, Bad Abbach, Germany), had been obtained from 12 patients during knee surgery in 2007 and stored at −80 °C until analysis. Patient data (as provided by the Department of Orthopedics) are listed in Table 8.1.

Table 8.1: Patient data. Sex abbreviated as f (female) or m (male).

Patient (Sample)	Age	Sex	Diagnosis
1	78	f	Osteoarthritis (left knee)
2	69	f	Change of implant
3	71	f	Osteoarthritis (right knee)
4	59	f	Osteoarthritis (left knee)
5	67	f	Osteoarthritis (left knee), chondromalacia, meniscopathy
6	61	m	Osteoarthritis (left knee)
7	58	f	Osteoarthritis (right knee)
8	69	f	Osteoarthritis (left knee)
9	67	f	Osteoarthritis (left knee), rheumatoid arthritis
10	76	f	Osteoarthritis (right knee)
11	66	m	Osteoarthritis (left knee)
12	55	f	Osteoarthritis (left knee)

It should be noted that, in addition to osteoarthritis, patient 9 was also suffering from chronic rheumatoid arthritis.

8.2.2 Macroscopic characterization and microscopy of smears

The samples were characterized macroscopically with regard to color. For reproducible description, a RAL K7 CLASSIC® card (RAL German Institute of Quality Assurance and Certification, Sankt Augustin, Germany) was used. In addition, smears of the synovial fluids were examined microscopically after Pappenheim's staining.

8.2.3 Rheology

Rheological characterization of the viscoelastic properties was carried out on a TA Instruments AR 2000 rheometer (TA Instruments, Eschborn, Germany) with parallel plate geometry (diameter of upper steel plate: 20 mm) at 22 °C. 310 µL of the respective sample were transferred to the bottom plate of the instrument with a syringe. Then, the upper plate was lowered to reach a gap width of 1000 µm. Two consecutive experiments were performed. In a non-destructive frequency sweep experiment, oscillatory frequency was varied from 0.01 Hz to 10 Hz with torque control set at 10 µNm (oscillatory stress: 6.366 Pa).

Afterwards, a destructive stress sweep was carried out at constant frequency of 1 Hz, increasing oscillatory stress from 1 Pa to 1000 Pa.

8.2.4 Determination of protein content

Protein content of the samples was determined by the Bradford method[9] using human serum albumin (Behringwerke, Marburg, Germany) as calibration standard. Samples were diluted 1:100 with phosphate buffer (pH = 7.2, 10 mM). 50 µL of this dilution were mixed with 2.5 mL of an aqueous dilution (1:5) of the Bio-Rad protein assay dye reagent concentrate (Bio-Rad, Munich, Germany). Absorbance at 595 nm was measured with a CARY 100 photometer (Agilent Technologies, Darmstadt, Germany). A single experiment was performed in duplicate.

8.2.5 Preparation of samples for hyaluronan analysis

With regard to hyaluronan analysis, the synovial fluid samples were deproteinized by boiling. Boiling of the undiluted samples, however, led to a clot of denaturated protein from which no liquid supernatant was obtained. Consequently, the synovial fluid was diluted 1:5 with purified water prior to boiling. The volume of the synovial fluid was measured with a plastic syringe. The use of a normal microliter pipette was not feasible due to the high viscosity of the samples. After boiling, the precipitated protein was removed by centrifugation at 13000 × *g* and the supernatant was used for further analysis.

8.2.6 Enzymatic digestion of hyaluronan

To determine the total hyaluronan content of the samples, the polysaccharide was digested by addition of bovine testicular hyaluronidase (BTH, Neopermease®, kindly provided by Sanabo, Vienna, Austria) as described in Chapter 6 (Section 6.2.2) but using the supernatant, prepared accoding to Section 8.2.5 instead of hyaluronan solution as substrate. To ensure exhaustive digestion, an enzyme solution of 20000 IU/mL (based on the declaration by the supplier) was prepared. 50 µL of the enzyme solution were added to 400 µL of the incubation mixture. The digestion mixture was then placed in a water bath and incubated at 37 °C for 72 h.

8.2.7 Colorimetric quantification

The exhaustively digested samples from Section 8.2.6 as well as analogously diluted aliquots of the undigested counterparts from Section 8.2.5 were subjected to the Morgan-Elson reaction[10-13] and the absorbance was measured at 586 nm as explained in detail in Chapter 5

(Section 5.2.3). By this procedure, the total content of hyaluronan was determined from the digested samples by the amount of *N*-acetyl-D-glucosamine ends liberated during enzymatic cleavage. In contrast, from the undigested synovial fluid the reducing (*N*-acetyl-D-glucosamine) ends, initially present in the sample, were measured, allowing for a rough comparison of the average chain length. *N*-Acetyl-D-glucosamine (Fluka, Buchs, Switzerland) served as calibration standard. Therefore, the measured values were expressed as *N*-acetyl-D-glucosamine equivalents.

8.2.8 Determination of hyaluronan content by CZE–ESI-TOF-MS

In addition to the colorimetric quantification, the digested synovial fluids (*cf*. Section 8.2.6) were analyzed by CZE–ESI-TOF-MS (*cf*. Chapter 3). Samples were filtrated through a Phenex-NY 4 mm syringe filter 0.2 µm (Phenomenex, Aschaffenburg, Germany) and injected (pressure-free injection, 30 s) into the capillary (25 µm × 28 cm). The tetrasaccharide (n_2) liberated by enzymatic cleavage was quantified using the respective oligosaccharide standard (oligoHA from Hyalose, Oklahoma City, OK, USA) for calibration. The standard was purchased from AMSBIO (Abingdon, UK). Hyaluronan content was calculated from the peak heights of three consecutive injections of the same sample.

8.2.9 HPAEC–PAD of digested and undigested samples

After filtration through a Phenex-NY 4 mm syringe filter 0.2 µm (Phenomenex, Aschaffenburg, Germany), aliquots of the digested samples were also analyzed using the HPAEC–PAD method from Chapter 4. In this case, the amount of tetrasaccharide (n_2) was determined from the peak area by calibration with the standard substance oligoHA (Hyalose, Oklahoma City, OK, USA). Furthermore, HPAEC–PAD was applied to determine small oligosaccharides in the undigested synovial fluids (diluted 1:5, *cf*. Section 8.2.5). For this purpose, protein and high molecular weight hyaluronan were removed by ultrafiltration at 13900 × *g* using Nanosep® Centrifugal Devices 10 K (Pall Life Sciences, Ann Arbor, MI, USA).

8.2.10 Hyaluronan analysis by gel electrophoresis

Polyacrylamide gel electrophoresis of hyaluronan was carried out according to previously reported protocols[14-16] using 10% polyacrylamide separation gels and 5% stacking gels. A tris/borate/EDTA (TBE) buffer (pH = 8.3) was used as gel buffer as well as running buffer. In detail, the buffer contained 89 mM tris(hydroxymethyl)aminomethane (tris, USB, Cleveland, OH, USA), 82 mM boric acid (Merck, Darmstadt, Germany), and 2 mM EDTA (Merck, Darmstadt, Germany). For one separation gel, 5 mL of TBE buffer were mixed with 2.5 mL of acrylamide/bisacrylamide solution 30% (Sigma-Aldrich, Munich, Germany). 3.75 µL of

N,*N*,*N'*,*N'*-tetramethylethylenediamine (TEMED, Serva, Heidelberg, Germany) and 37.5 µL of a 10% (w/v) solution of ammonium peroxodisulfate (APS, Serva, Heidelberg, Germany) started the reaction. By contrast, the stacking gel was prepared from 4.1 mL of TBE buffer, 0.85 mL of acrylamide/bisacrylamide solution 30%, 3.75 µL of TEMED, and 50 µL of APS solution (10% in water). Gel chambers were 10 cm × 10 cm × 0.8 cm in size.

Due to incomplete precipitation of protein by boiling, residual protein was found to interfere with hyaluronan detection. Therefore, samples were additionally incubated with proteinase K from *Tritirachium album* (Merck, Darmstadt, Germany). The activity of the enzyme was specified by the supplier as 0.027 Anson units per mg. A solution of 20 mg/mL in phosphate buffered saline (PBS) with 10 mM calcium chloride was prepared. 3 µL of this solution were added to 27 µL of sample. The mixture was incubated at 50 °C for 17 h. 5 parts of the sample were mixed with 1 part of 2 M sucrose (Merck, Darmstadt, Germany) in TBE buffer. 10 µL per lane were applied to the gel. The tracking dye bromophenol blue (Aldrich, Beerse, Belgium) and aqueous solutions of sulfonated polystyrenes (Fluka, Buchs, Switzerland) as size markers (990 kDa, 32 kDa, and 17 kDa) were treated equally.

Electrophoresis was performed with a PerfectBlue gel electrophoresis system (Twin S, Peqlab, Erlangen, Germany) at 250 V for 20 min, at 500 V for additional 10 min, and finally at 400 V for approximately 15 min. Under the given conditions (TBE running buffer, pH = 8.3), proteinase K did not migrate into the gel and, hence, did not interfere with the subsequent visualization of the saccharides.

The combined alcian blue and silver staining was based on a method by Ikegami-Kawai and Takahashi[14] and performed following the protocol described by Hamberger.[16] At first, the gel was stained in the dark with a 0.5% (w/v) solution of alcian blue 8GX (Sigma, St. Louis, MO, USA) in 2% (v/v) acetic acid (prepared from concentrated acetic acid, Merck, Darmstadt, Germany). After 30 min the gel was transferred to 2% (v/v) acetic acid and destained for additional 30 min. After alcian blue staining, a silver staining procedure according to Merril et al.,[17] basically performed in four steps (plus several washing steps), was carried out. All reagents used for silver staining were from Merck (Darmstadt, Germany). In the first step, the gel was treated with an oxidation solution of potassium dichromate (3.4 mM) and nitric acid (3.2 mM) for 5 min. After three short washing intervals (5 min each) with water, the gel was soaked in a silver nitrate solution (12 mM) for 20 min. Prior to the developing step, the gel was again washed in water for 3 × 5 min, and then transferred to a solution of 5 g of sodium carbonate and 100 µL of formaldehyde in 200 mL of water. When bands had become visible, the reaction was stopped by transferring the gel to 5% (v/v) acetic acid. After 15 min, the gel was put into water and stored for further analysis.

8.2.11 Zymography

Zymography with hyaluronan substrate gels, previously described by Cherr et al.,[18] was essentially carried out according to Hamberger.[16] Polyacrylamide gels were prepared in chambers of 10 cm × 10 cm × 0.8 cm. Reagents were obtained from the same suppliers as stated in Section 8.2.10. Sodium dodecyl sulfate (SDS) was from Sigma-Aldrich (Munich, Germany). For the separation gel (12% polyacrylamide), 2.4 mL of acrylamide/bisacrylamide solution 30%, 1.56 mL of buffer A (1.5 M tris, 0.4% SDS, pH = 8.8), and 2.0 mL of water were mixed. 81.5 µL of a 5 mg/mL solution of hyaluronan from *Streptococcus zooepidemicus* (Aqua Biochem, Dessau, Germany) were added to yield a substrate gel containing 67 µg/mL hyaluronan. Polymerization was started by addition of 3 µL of TEMED and 40 µL of a 10% (m/v) solution of APS in water. The stacking gel (5% polyacrylamide) was produced analogously from 0.5 mL of acrylamide/bisacrylamide solution 30%, 1.25 mL of buffer B (0.5 M tris, 0.4% SDS, pH = 6.8), 3.25 mL of water, 3 µL of TEMED, and 50 µL of APS solution (10% in water). Running buffer (pH = 8.3) contained 25 mM tris, 200 mM glycine (Merck, Darmstadt, Germany), and 0.1% (w/v) SDS.

Sample buffer (kindly provided by Dr. Janina Hamberger) consisted of 200 mM tris-HCl buffer (pH = 6.8), 20% (v/v) glycerol (Merck, Darmstadt, Germany), 10% (w/v) SDS (Sigma-Aldrich, Munich, Germany), and 0.05% (w/v) bromophenol blue (Aldrich, Beerse, Belgium). Tris was from USB (Cleveland, OH, USA). Untreated (not boiled) synovial fluid samples were diluted 1:10 by addition of phosphate buffer (pH = 7.2, 10 mM). Human citrate-phosphate-dextrose (CPD) plasma, diluted in the same manner, served as control. 10 µL of the sample dilution were mixed with 10 µL of sample buffer. From this mixture, 10 µL per lane were applied to the gel. Electrophoresis was performed at 150 kV with the PerfectBlue gel electrophoresis system (Twin S, Peqlab, Erlangen, Germany) for approximately 90 min.

After electrophoresis, SDS was replaced by triton X-100 (Carl Roth, Karlsruhe, Germany). For this purpose, the gel was treated with a 2.5% (v/v) solution of triton X-100 for 30 min. Afterwards the gel was washed with water for 5 min and with incubation buffer for additional 30 min. The gel was transferred to a glass trough with incubation buffer. The buffer had been prepared as described in Chapter 6 (Section 6.2.2) but adjusted to a pH value of 4.0 instead of 5.0. After incubation at 37 °C overnight (24 h), the gel was stained with a 0.5% (w/v) solution of alcian blue 8GX (Sigma, St. Louis, MO, USA) in acetic acid. In contrast to Section 8.2.10, the staining reagent contained 7% (v/v) of acetic acid instead of 2% (v/v). The gel was destained with 7% (v/v) acetic acid until light bands became visible on the blue background.

Proteins were counterstained with a 0.1% (w/v) solution of Coomassie Brillant Blue G-250 (Serva, Heidelberg, Germany) in 50% (v/v) methanol and 10% (v/v) acetic acid. After a final destaining step in an aqueous solution of 7% (v/v) acetic acid and 10% (v/v) methanol, the

gel was scanned with a Bio-Rad GS-710 gel scanner using Bio-Rad Quantity One software (Bio-Rad, Munich, Germany). The scanner settings were chosen by analogy with the settings for Coomassie-stained gels. Glacial acetic acid and methanol were from Merck (Darmstadt, Germany).

8.3 Results and discussion

8.3.1 Macroscopic characterization and microscopic findings

Aliquots of the synovial fluid samples were transferred to a white glass plate to characterize the macroscopic appearance (Figure 8.1). In addition, the color was also assessed directly in a 1.5 mL plastic vial. Due to the increased thickness of the light absorbing layer, appearance was slightly darker. The detailed color descriptions according to RAL K7 CLASSIC® are listed in Table 8.2 for all samples.

Table 8.2: Color description of the synovial fluid samples by comparison with RAL K7 CLASSIC® standard. Colors of a drop on a white glass plate and of a relatively thick sample layer in a 1.5 mL plastic vial are listed.

Sample	**Drop color on white glass plate**		**Color as seen in 1.5 mL plastic vial**	
	RAL number	**RAL color name**	**RAL number**	**RAL color name**
1	2000	Yellow orange	2001	Red orange
2	1014	Ivory	1017	Saffron yellow
3	—	*(colorless)*	1014	Ivory
4	1015	Light ivory	1017	Saffron yellow
5	—	*(colorless)*	1015	Light ivory
6	1014	Ivory	1000	Green beige
7	1013	Oyster white	1015	Light ivory
8	—	*(colorless)*	1014	Ivory
9	1015	Light ivory	1017	Saffron yellow
10	1015	Light ivory	1034	Pastel yellow
11	2000	Yellow orange	2001	Red orange
12	2002	Vermilion	3003	Ruby red

Figure 8.1: Aliquots of the synovial fluid samples on a white glass plate. Colors of the drops are compared to a RAL K7 CLASSIC® card. Numbers on the glass plate indicate sample numbers.

Samples 1 and 11 were of reddish color, sample 12 was intensely red. In addition, the latter also contained noticeable blood clots. Small traces of blood were also observed in sample 9. It should be noted that especially the blood content does not necessarily reflect the original situation in the joint. Contamination could also have occurred during surgery. In contrast,

samples 3, 5, and 8 were clear and colorless. The other samples were also clear, being slightly white to beige or yellowish in color.

Microscopically, significant numbers of neutrophils were found in one sample (Figure 8.2 A), whereas all other smears contained only low amounts of leucocytes, mainly lymphocytes (Figure 8.2 B, C).

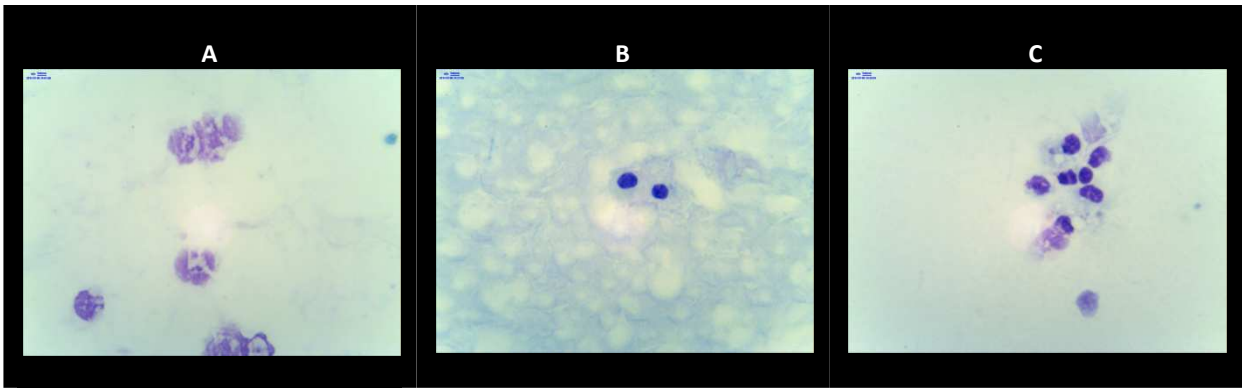

Figure 8.2: Microscopic images of synovial fluid smears after Pappenheim's staining. Neutrophils were observed in sample 7 (A). All other samples contained only small amounts of leucocytes (mainly lymphocytes), examples from the samples 1 (B) and 11 (C).

High numbers of neutrophils are typically observed in synovial fluid of patients suffering from inflammatory joint diseases like rheumatoid arthritis[19, 20] or gout.[21] Surprisingly, this was not the case for sample 9, the only one associated with rheumatoid arthritis. In contrast, neutrophils were observed in the synovial fluid number 7. However, neutrophils have also been reported in synovial fluids from patients with non-rheumatoid arthritis.[19]

8.3.2 Viscoelastic properties

Normal synovial fluid is a non-Newtonian fluid. Its rheological properties were reported to depend on the content and molecular mass of hyaluronan.[3, 22] More detailed rheological studies clearly suggested that the viscoelastic properties of pathological synovial fluids differ for inflammatory and non-inflammatory arthritis.[23, 24] For this reason, rheological characterization of the synovial fluid samples was carried out by oscillatory experiments with parallel plate geometry. Thereby, the viscoelastic properties can be described by a complex number, the complex shear rigidity modulus (G*, absolute value: |G*|). This complex shear rigidity modulus can be expressed by its real part (G', storage modulus) and its imaginary part (G'', loss modulus). Briefly, the storage modulus represents the elastic component of the shear rigidity. The loss modulus reflects the viscous properties. The whole system can also be characterized by the phase angle (δ) of the sinusoidal curves of shear rate and shear stress versus time, ranging from 0° (elastic behavior) to 90° (viscous behavior).

In a frequency sweep experiment (Figure 8.3), oscillatory frequency was continuously increased, torque was kept low. Consequently, this kind of experiment does not destruct the sample.

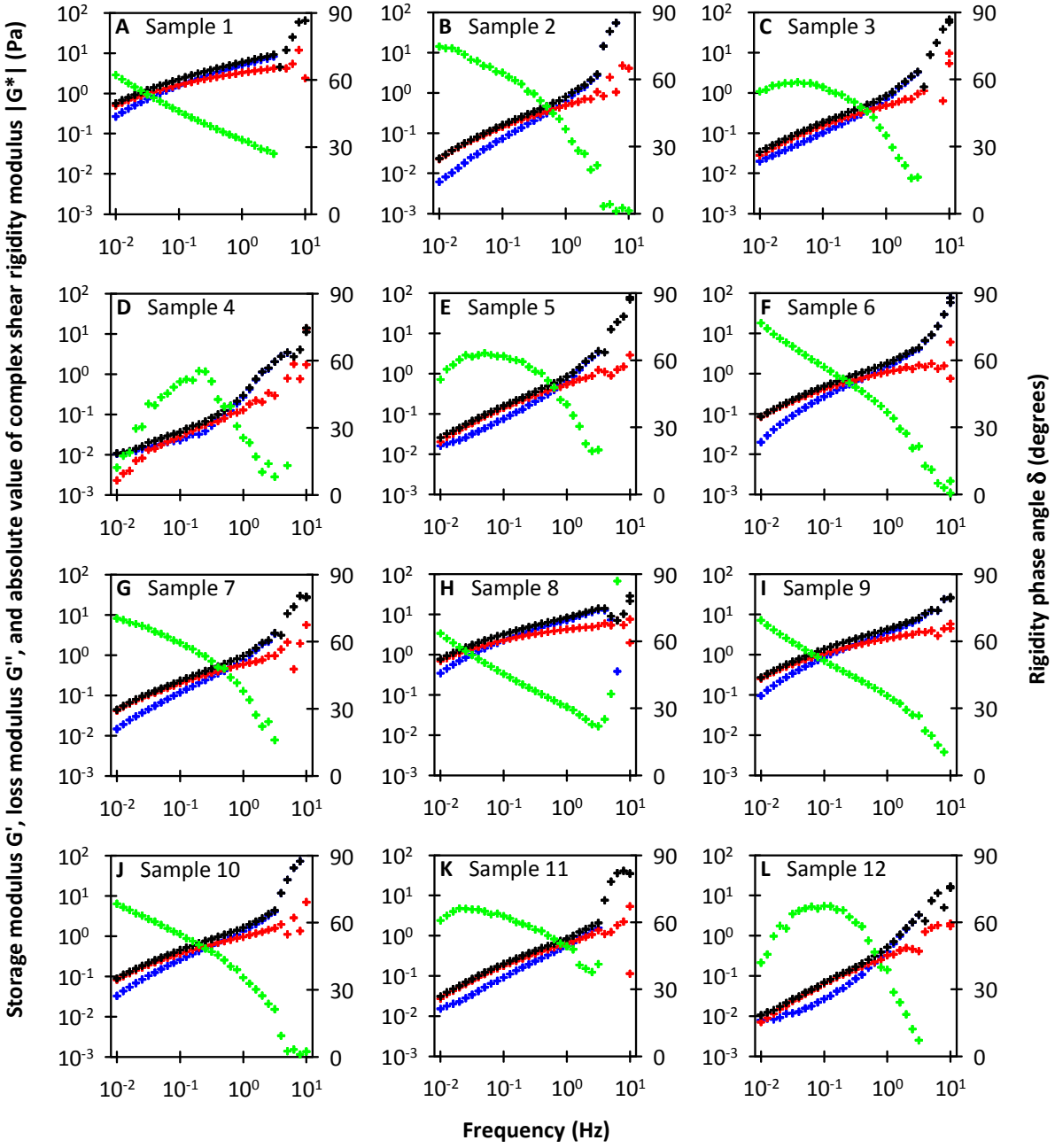

Figure 8.3: Frequency sweep experiment. At controlled torque, frequency of the oscillation was varied in a range of 0.01–10 Hz. Storage modulus (G', blue), loss modulus (G'', red), absolute value of the complex shear rigidity modulus (|G*|, black), and rigidity phase angle (δ, green) are plotted versus frequency.

Taking a closer look at the obtained curves, several differences can be identified. Firstly, the values of the moduli (|G*|, G', and G'') observed at low frequency (at the beginning of the frequency sweep) vary in a range of approximately two orders of magnitude. Although the experiments described in literature cannot be compared directly to the experiment presented here, generally higher values for the measured viscosity parameters were

observed for the physiological state and non-inflammatory arthritis than for inflammatory joint diseases.[23, 24] With increasing frequency, comparable values are reached for all samples, but the curves differ in their slope. Finally, the relative positions of the curves for G' and G'' are of interest. In general, the viscous (G'') component of complex shear rigidity is dominant for low frequencies, the elastic component (G') is more pronounced at high frequencies. However, the curves intersect at different frequency values.

It was previously described that high molecular weight hyaluronan is responsible for the elastic properties of synovial fluid and that enzymatic cleavage results in a loss of viscoelastic properties.[24] The same study reported that the gap between the curves expressing the elastic and viscous component is more pronounced for inflammatory arthritis than for non-inflammatory joint diseases.[24] Therefore, it may be speculated that a relatively high storage modulus (G') compared to the loss modulus (G'') reflects an intact structure and high average molecular weight of hyaluronan in the synovial fluid. Assuming this correlation, low relative values for G' and crossovers at higher frequency values would be hints for pronounced fragmentation, probably due to enzymatic cleavage, defects in synthesis, and inflammatory processes. Three samples (numbers 4, 5, and 12), however, clearly showed two crossovers of the curves (Figure 8.3 D, E, L). The observation is even more obvious for the phase angle curves. Regarding the occurrence of a maximum for δ, two additional graphs (Figure 8.3 C, K), belonging to the samples 3 and 11, probably show additional crossovers for G' and G'' at lower frequency (outside the measured range). Similar observations, probably due to two elastic species, were also reported in the article by Thurston and Greiling.[24]

In a second experiment, the oscillatory stress was steadily increased at a constant frequency of 1 Hz (Figure 8.4). These conditions led to destruction of the samples. The drop in the storage modulus accompanied by a simultaneous increase in the rigidity phase angle indicates the breakup of the sample structure.

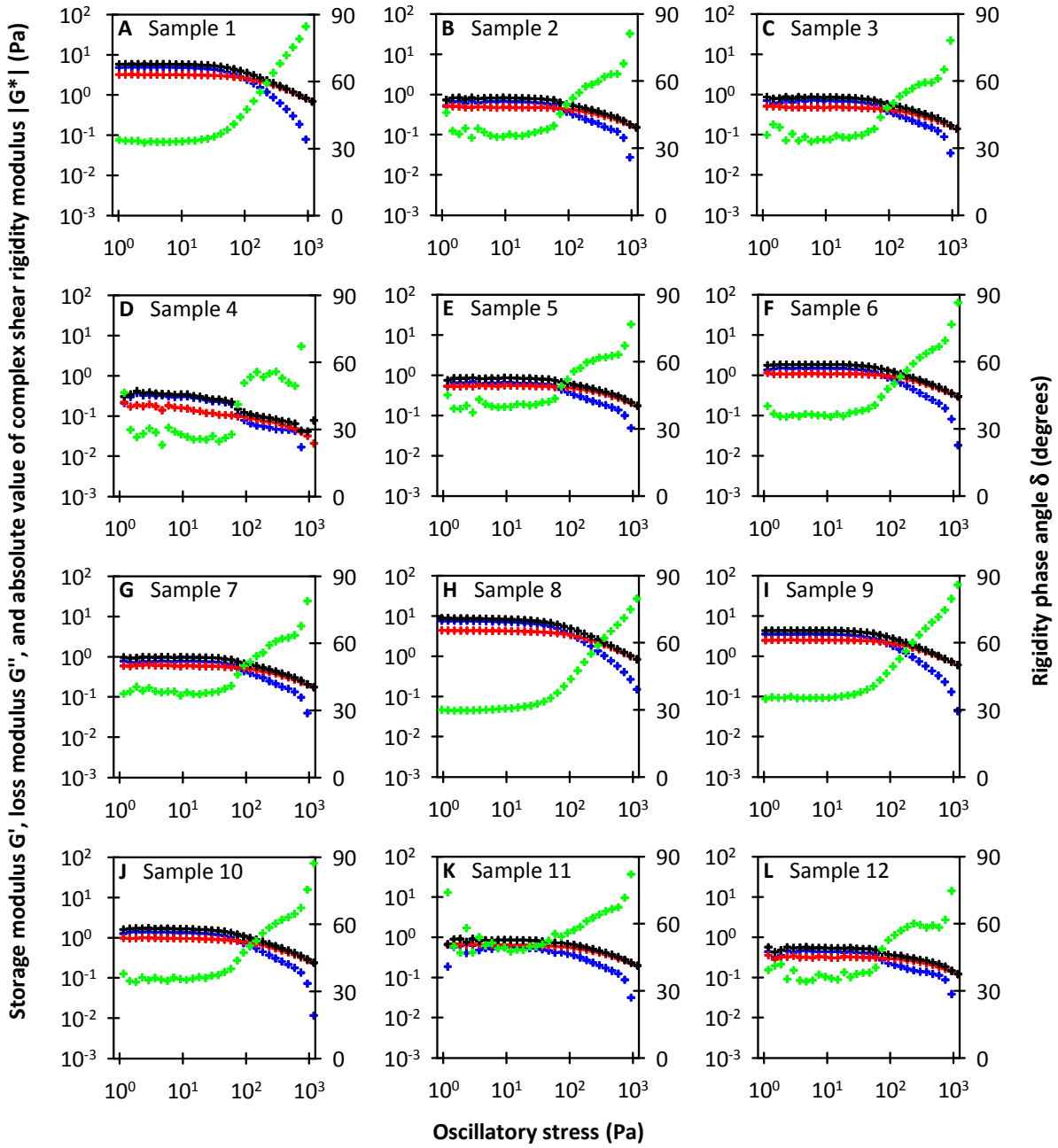

Figure 8.4: Stress sweep experiment. Increasing oscillatory stress of 1–1000 Pa was applied at a constant frequency of 1 Hz. Storage modulus (G', blue), loss modulus (G'', red), absolute value of the complex shear rigidity modulus (|G*|, black), and rigidity phase angle (δ, green) are plotted versus oscillatory stress.

Except for sample 11 (Figure 8.4 K), G'' was initially higher than G'. The faster decrease in the storage modulus, confirmed that mainly the elastic component got lost when the structure of the hyaluronan containing matrix was broken. In all cases, the destruction began at an oscillatory stress of 10–100 Pa. As a matter of course, the differences of about two orders of magnitude for |G*|, G', and G'', observed in the frequency sweep experiment (*cf*. Figure 8.3.), were confirmed.

8.3.3 Protein content

Protein content of the synovial fluid samples was determined by a single experiment in duplicate. The results are depicted in Figure 8.5. All samples contained relatively high amounts of protein, ranging from 26.9 mg/mL (number 4) to 59.8 mg/mL (number 12).

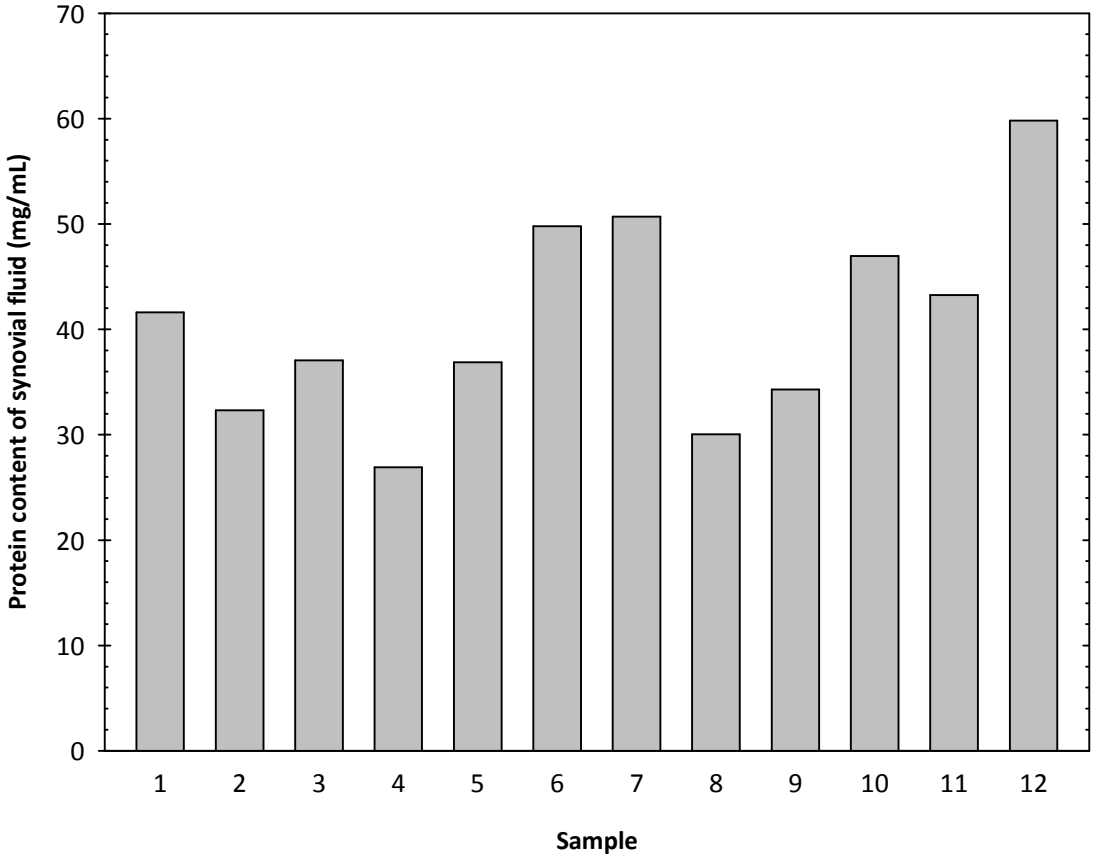

Figure 8.5: Protein content of the synovial fluid samples as determined by the Bradford method. Data are presented as mean values of one experiment performed in duplicate.

8.3.4 Total hyaluronan content

Hyaluronan of all samples was enzymatically degraded to give the tetrasaccharide (n_2). The initial content of hyaluronan was determined by quantification of n_2. Analysis according to the Morgan-Elson assay was performed in three independent experiments. A single injection was performed for analysis by HPAEC–PAD, and three consecutive injections of the same sample were carried out for CZE–ESI-TOF-MS. Figure 8.6 compares the results from the different quantification methods. It should again be noted that for the colorimetric quantification *N*-acetyl-D-glucosamine served as calibration standard, whereas commercially available tetrasaccharide was used as reference compound for chromatography and electrophoresis.

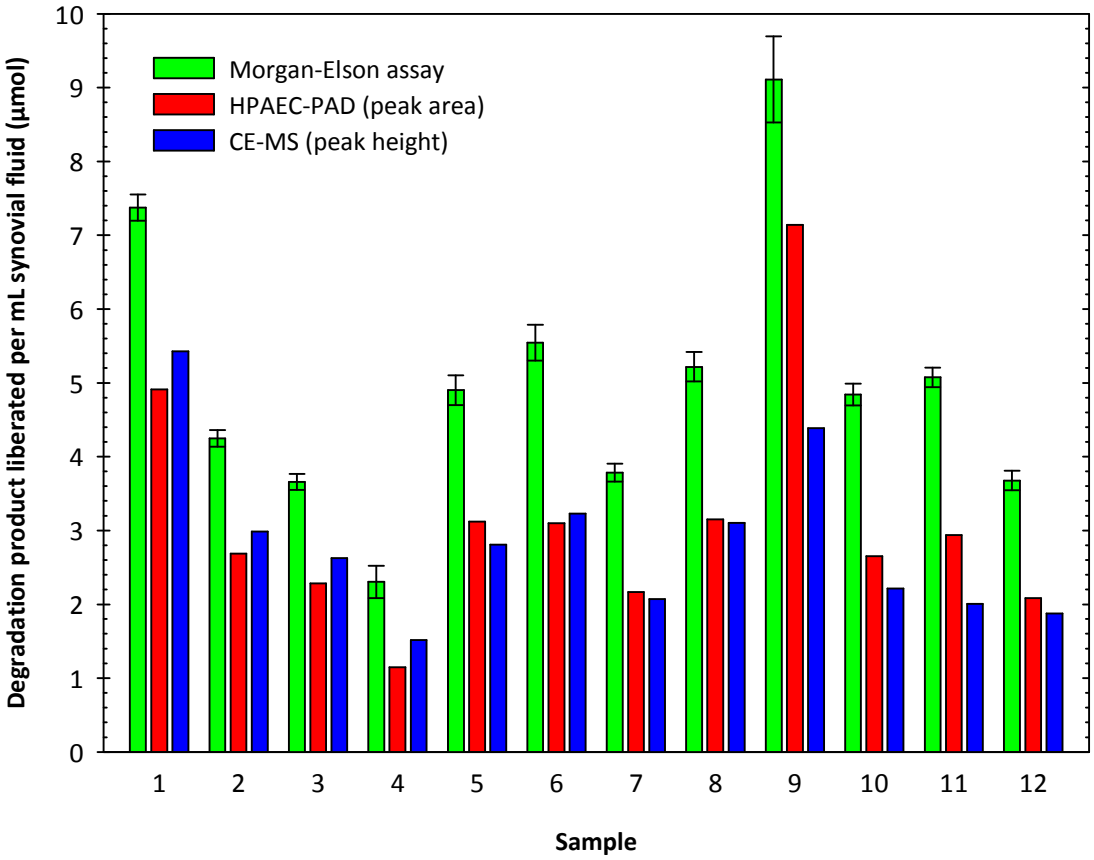

Figure 8.6: Total hyaluronan content of the synovial fluids determined via quantification of the product of enzymatic cleavage. Morgan-Elson reaction (green): quantification of free ends, calibration with *N*-acetyl-D-glucosamine, mean ± SEM of three independent experiments ($N = 3$). HPAEC–PAD (red): tetrasaccharide (n_2) as calibration standard, evaluation of peak areas of the n_2 peak, single injection. CZE–ESI-TOF-MS (blue): tetrasaccharide (n_2) as calibration standard, evaluation of peak heights of the n_2 peak, three consecutive injections of the same sample, mean.

Due to methodological reasons and especially because of the differences regarding the calibration standard, the absolute values, determined by colorimetry compared to the chromatographic and electrophoretic quantification, varied. Nevertheless, the relative comparison of the samples and the general results are in good accordance. The highest hyaluronan contents were determined in samples 1 and 9, the lowest in sample 4. All other values were in a medium range.

8.3.5 Size distribution of hyaluronan

The amount of reducing ends of hyaluronan polysaccharide chains, originally present in the synovial fluid, can act as a first rough indicator for the average molecular weight of hyaluronan. Therefore, the undigested samples were analyzed using the colorimetric method with *N*-acetyl-D-glucosamine as calibration standard. Three independent experiments were performed. The results are summarized in Figure 8.7.

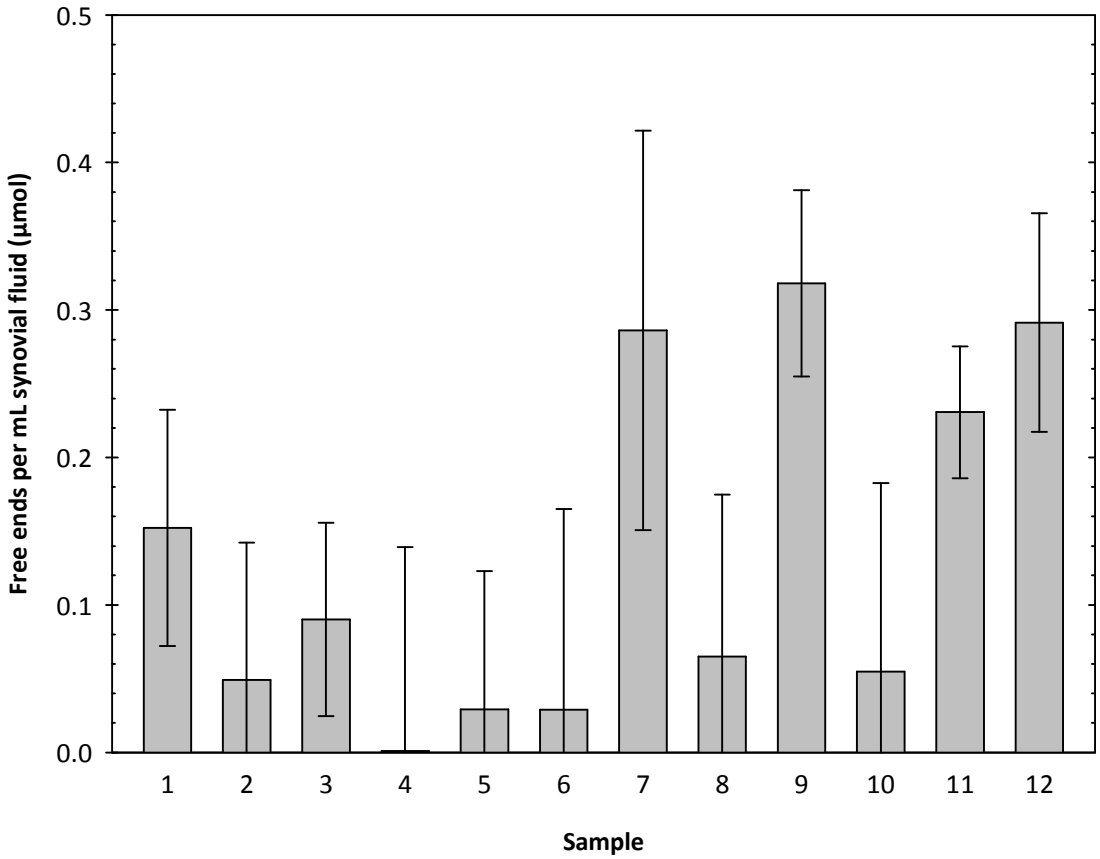

Figure 8.7: Free hyaluronan ends in the undigested synovial fluids given as *N*-acetyl-D-glucosamine equivalents from the colorimetric assay. All dilution steps were considered. Data are presented as mean ± SEM of three independent experiments (*N* = 3).

The highest "concentrations of reducing ends" were measured for samples 7, 9, 11, and 12. Whereas the high total hyaluronan content has to be considered for number 9, the other samples had only a medium content of hyaluronan (*cf*. Figure 8.6). Therefore, it may be assumed that in the samples 7, 11, and 12 hyaluronan is degraded or incompletely polymerized to a relatively high extent. When the hyaluronan content was extremely low (especially for sample 4), the amount of free ends in the undigested synovial fluids, of course, was extremely low, too. In these cases, it cannot be ruled out that the tiny amounts of hyaluronan might have been degraded, and the concentrations of the resulting fragments (free ends) were below the limit of quantification.

To further scrutinize the size distribution of the hyaluronan from the synovial fluid samples, a gel electrophoretic separation was performed (Figure 8.8). According to gel electrophoresis, samples 3, 5, and 8 showed the lowest degradation of hyaluronic acid. Interestingly, this finding is in good accordance to the macroscopically clear and colorless (physiological) appearance observed in Section 8.3.1. Samples 1, 4, 9, 10, and 12 contained the highest band intensity in the low molecular weight sector. For number 9 and number 12 this is consistent with the estimation from Figure 8.7. However, there was no general correlation. The high amount of low molecular weight hyaluronan together with high

hyaluronan content in sample 9, associated with the diagnosis of rheumatoid arthritis (*cf*. Table 8.1), confirm the findings of Ragan and Meyer.[4] They suggested an elevated synthesis of hyaluronan with a low degree of polymerization rather than increased hyaluronidase action in rheumatoid arthritis.[4] Finally, sample 4 is worth a closer look. This particular synovial fluid showed the lowest protein content, the lowest viscoelastic moduli, the lowest total hyaluronan content, and high degree of degradation in gel electrophoresis. Obviously, a low content of protein and hyaluronan, in addition to low average molecular weight of the hyaluronan, result in the weak viscoelastic properties observed.

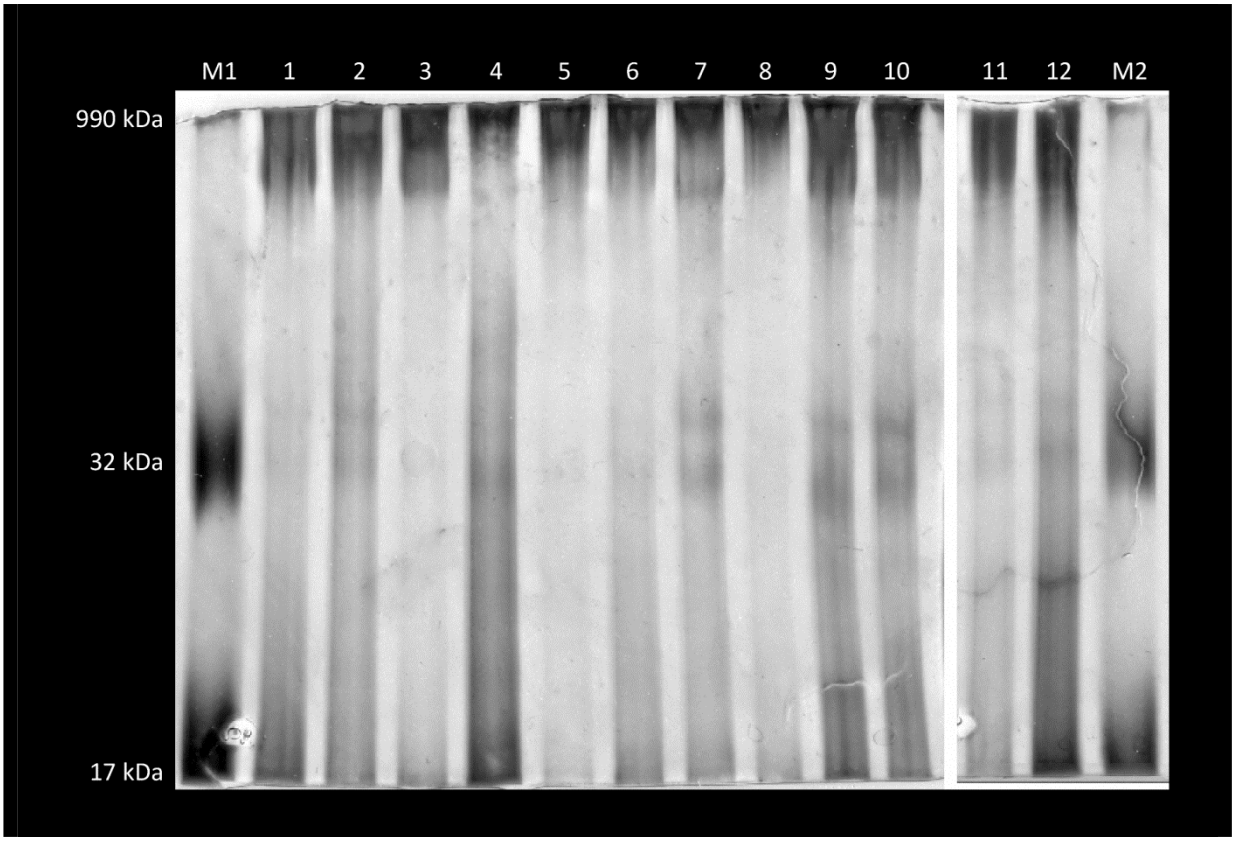

Figure 8.8: Determination of hyaluronan by polyacrylamide gel (10%) electrophoresis, combined alcian blue and silver staining. Synovial fluid samples (after boiling and treatment with proteinase K) labeled according to the sample number (1–12). M1 (10 µL) and M2 (5 µL): sulfonated polystyrenes as size markers.

By polyacrylamide gel electrophoresis, oligosaccharides could be detected down to a molecular weight of approximately 17 kDa. In search for very small oligosaccharides derived from enzymatic hyaluronan degradation, ultrafiltrated aliquots of the diluted but undigested synovial fluids were additionally analyzed by HPAEC–PAD (Figure 8.9).

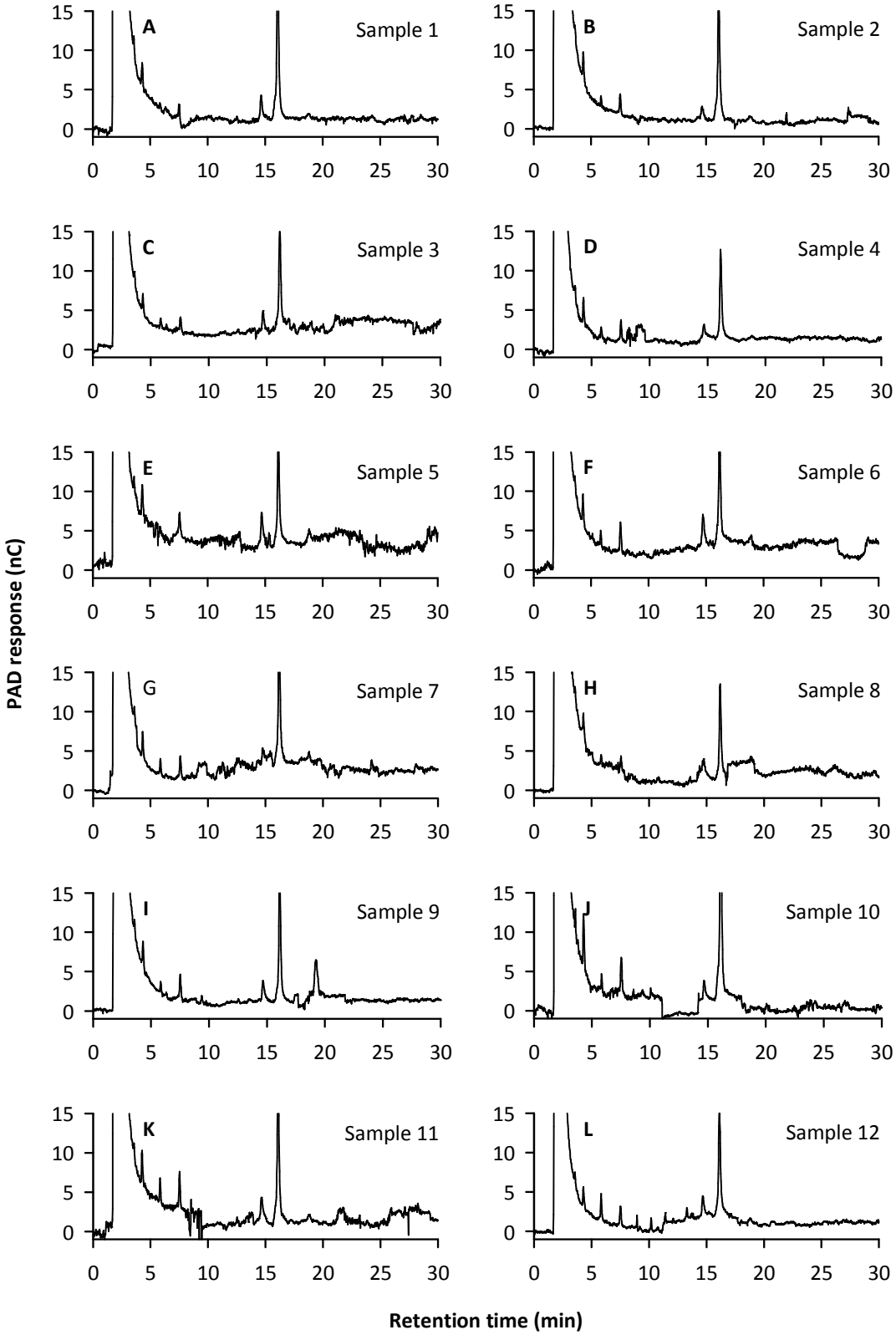

Figure 8.9: HPAEC–PAD of the ultrafiltrated synovial fluids. Chromatography conditions: CarboPac™ PA200, 100 mM sodium hydroxide, gradient of 200–900 mM sodium acetate, 40 °C, 0.5 mL/min.

Although the peaks detected in the samples 1–12 are supposed to correspond, at least in part, to the expected analytes, chromatography was insufficient to unambiguously assign the signals to hyaluronan oligosaccharides or other matrix components. Unfortunately, due to the very low analyte concentrations, CZE–ESI-TOF-MS was not sensitive enough. Consequently, a different approach was chosen. Sample 12 (Figure 8.9 L), which was the only one to show a clear series of small peaks in the respective region of the chromatogram, was spiked with the standard oligosaccharides (n_2, n_3, n_4). In this way, three peaks could be assigned to these oligosaccharides by their retention time (Figure 8.10). Nevertheless, the n_2 peak seems to overlap with a second peak from an unidentified matrix component.

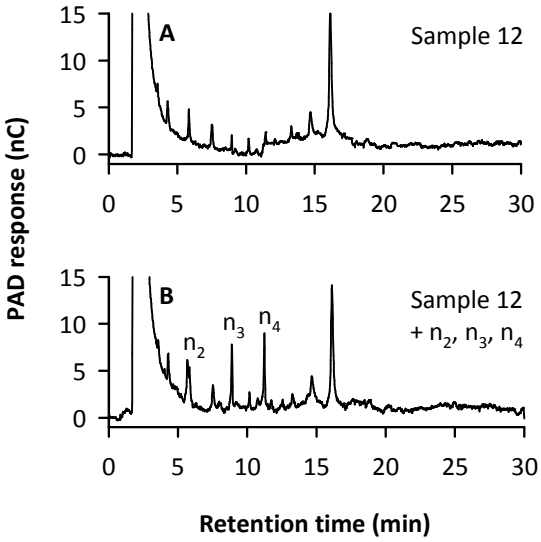

Figure 8.10: Spiking of the ultrafiltrate from sample 12 with standard oligosaccharides (n_2, n_3, n_4). HPAEC–PAD: CarboPac™ PA200, 100 mM sodium hydroxide, gradient of 200–900 mM sodium acetate, 40 °C, 0.5 mL/min.

Except for sample 12, the n_3 and n_4 peaks were not observed. The peak at the retention time observed for n_2, owing to the mentioned overlap, cannot be unambiguously assigned to the hyaluronan tetrasaccharide. Thus, the presence of small hyaluronan oligosaccharides was only proven for sample 12.

8.3.6 Hyaluronidase activity

To evaluate if different amounts of hyaluronidase as a potential constituent of synovial fluid caused the observed differences in viscoelastic properties as well as hyaluronan size distribution, zymography with hyaluronan substrate gels was performed. After incubation at pH = 4 and staining of the gels, light bands on dark background indicated enzymatic activity (Figure 8.11).

Hyaluronidase activity was found in almost all synovial fluid samples to variable extent. Only sample 8 showed no significant activity. Furthermore, in sample 6 and in sample 7 the

activity was rather weak. Relatively high activity was determined for sample 4, which had also shown low viscoelastic moduli, low hyaluronan content, and high degradation in the gel electrophoresis experiment.

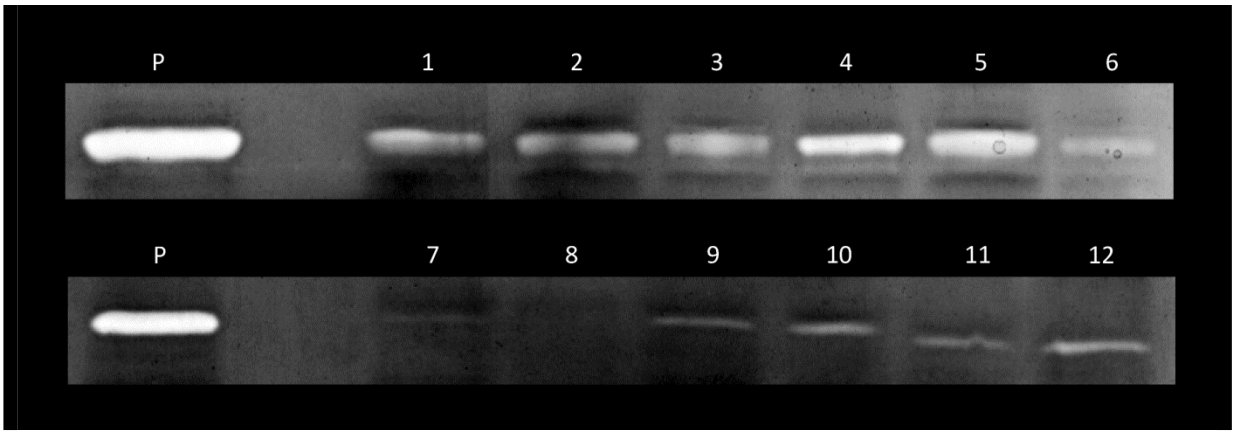

Figure 8.11: Determination of hyaluronidase activity by zymography (incubation at pH = 4.0) followed by alcian blue staining and Coomassie counterstaining. Light bands on dark background indicate enzymatic activity. Synovial fluid samples labeled according to the sample number (1–12). Human CPD plasma (P) served as control. Samples and control were diluted in the same manner.

By comparison to a plasma control, the active protein in synovial fluid samples was proven to be identical to plasma hyaluronidase. However, enzymatic activity was much higher in plasma than in the synovial fluids. Moreover, it cannot be ruled out that hyaluronidase activity in the synovial fluid might, at least in part, result from blood contamination.

8.4 Summary and conclusion

CZE–ESI-TOF-MS and HPAEC–PAD were successfully applied to the quantification of hyaluronan in synovial fluids after digestion of the polysaccharide. HPAEC–PAD also proved to be a valuable tool for the search of traces of small hyaluronan oligosaccharides in biological matrices. In combination with several complementary methods, a detailed characterization of 12 synovial fluid samples was achieved. Especially rheology yielded obvious differences in the viscoelastic properties. Polyacrylamide gel electrophoresis proved that the hyaluronan from the synovial fluids was fragmented into low molecular weight saccharides to a variable extent. For extremely low hyaluronan contents and high fragmentation (sample 4), the relation to very weak viscoelastic properties was self-evident. Hyaluronidase activity was found in most samples. Nevertheless, this could also originate from blood contamination. Although diagnoses were similar, differences in synovial fluid analysis were obvious. However, no general correlation between diagnoses and the analytical results was observed.

Dunn et al. reported on high variability in the properties of synovial fluids under controlled conditions and therefore found no statistically significant differences between osteoarthritis patients and healthy volunteers.[7] Consequently, although it cannot be ruled out that in our experiments artifacts (long-term freezing of the samples) contributed to variability, the results probably reflect the interindividual natural situation.

8.5 References

1. Meyer, K.; Smyth, E. M.; Dawson, M. H. The isolation of a mucopolysaccaride from synovial fluid. *J. Biol. Chem.* **1939,** 128, 319-327.

2. Meyer, K. The biological significance of hyaluronic acid and hyaluronidase. *Physiol. Rev.* **1947,** 27, 335-359.

3. Sundblad, L. The chemistry of synovial fluid with special regard to hyaluronic acid. *Acta Orthop. Scand.* **1950,** 20, 105-113.

4. Ragan, C.; Meyer, K. The hyaluronic acid of synovial fluid in rheumatoid arthritis. *J. Clin. Invest.* **1949,** 28, 56-59.

5. Dahl, L. B.; Dahl, I. M.; Engstrom-Laurent, A.; Granath, K. Concentration and molecular weight of sodium hyaluronate in synovial fluid from patients with rheumatoid arthritis and other arthropathies. *Ann. Rheum. Dis.* **1985,** 44, 817-822.

6. Stafford, C. T.; Niedermeier, W.; Holley, H. L.; Pigman, W. Studies on the concentration and intrinsic viscosity of hyaluronic acid in synovial fluids of patients with rheumatic diseases. *Ann. Rheum. Dis.* **1964,** 23, 152-157.

7. Dunn, S.; Kolomytkin, O. V.; Marino, A. A. Pathophysiology of osteoarthritis: evidence against the viscoelastic theory. *Pathobiology* **2009,** 76, 322-328.

8. Hascall, V. C.; Laurent, T. C. Hyaluronan: structure and physical properties. *Glycoforum* **1997**. (http://glycoforum.gr.jp/science/hyaluronan/HA01/HA01E.html)

9. Bradford, M. M. A rapid and sensitive method for the quantitation of microgram quantities of protein utilizing the principle of protein-dye binding. *Anal. Biochem.* **1976,** 72, 248-254.

10. Muckenschnabel, I.; Bernhardt, G.; Spruß, T.; Dietl, B.; Buschauer, A. Quantitation of hyaluronidases by the Morgan-Elson reaction: comparison of the enzyme activities in the plasma of tumor patients and healthy volunteers. *Cancer Lett.* **1998,** 131, 13-20.

11. Gacesa, P.; Savitsky, M. J.; Dodgson, K. S.; Olavesen, A. H. A recommended procedure for the estimation of bovine testicular hyaluronidase in the presence of human serum. *Anal. Biochem.* **1981,** 118, 76-84.

12. Reissig, J. L.; Storminger, J. L.; Leloir, L. F. A modified colorimetric method for the estimation of *N*-acetylamino sugars. *J. Biol. Chem.* **1955,** 217, 959-966.

13. Morgan, W. T.; Elson, L. A. A colorimetric method for the determination of *N*-acetylglucosamine and *N*-acetylchrondrosamine. *Biochem. J.* **1934,** 28, 988-995.

14. Ikegami-Kawai, M.; Takahashi, T. Microanalysis of hyaluronan oligosaccharides by polyacrylamide gel electrophoresis and its application to assay of hyaluronidase activity. *Anal. Biochem.* **2002,** 311, 157-165.

15. Min, H.; Cowman, M. K. Combined alcian blue and silver staining of glycosaminoglycans in polyacrylamide gels: application to electrophoretic analysis of molecular weight distribution. *Anal. Biochem.* **1986,** 155, 275-285.

16. Hamberger, J. Characterization of mammalian hyaluronidase-2 activity and identification of inhibitors of *Streptococcal* hyaluronan lyase. PhD thesis, University of Regensburg, Regensburg, **2012**.

17. Merril, C. R.; Goldman, D.; Sedman, S. A.; Ebert, M. H. Ultrasensitive stain for proteins in polyacrylamide gels shows regional variation in cerebrospinal fluid proteins. *Science* **1981,** 211, 1437-1438.

18. Cherr, G. N.; Meyers, S. A.; Yudin, A. I.; VandeVoort, C. A.; Myles, D. G.; Primakoff, P.; Overstreet, J. W. The PH-20 protein in cynomolgus macaque spermatozoa: identification of two different forms exhibiting hyaluronidase activity. *Dev. Biol.* **1996,** 175, 142-153.

19. Bayliss, C. E.; Dawkins, R. L.; Cullity, G.; Davis, R. E.; Houliston, J. B. Laboratory diagnosis of rheumatoid arthritis. Prospective study of 85 patients. *Ann. Rheum. Dis.* **1975,** 34, 395-402.

20. Harris, E. D., Jr. Rheumatoid arthritis. Pathophysiology and implications for therapy. *N. Engl. J. Med.* **1990,** 322, 1277-1289.

21. Cronstein, B. N.; Terkeltaub, R. The inflammatory process of gout and its treatment. *Arthritis Res. Ther.* **2006,** 8 Suppl 1, S3.

22. Sundblad, L. Determination of anomalous viscosity in pathological joint fluids. *Scand. J. Clin. Lab. Invest.* **1954,** 6, 288-294.

23. Schurz, J.; Ribitsch, V.; Rainer, F. Rheologische Untersuchungen an Synovia und Synoviamodellen. *Rheol. Acta* **1979,** 18, 139-150.

24. Thurston, G. B.; Greiling, H. Viscoelastic properties of pathological synovial fluids for a wide range of oscillatory shear rates and frequencies. *Rheol. Acta* **1978,** 17, 433-445.

9 *In vitro* studies on the interaction of hyaluronan and hyaluronan oligosaccharides with human cells

9.1 Introduction

Hyaluronan and hyaluronan oligosaccharides are supposed to play an important role in tissue regeneration and wound repair.[1, 2] West and Kumar reported stimulating effects of hyaluronan oligosaccharides comprising 3–16 disaccharide units (n_3–n_{16}) on proliferation of bovine aortic endothelial cells, whereas high molecular weight hyaluronan (at concentrations above 100 µg/mL) inhibited cell proliferation and disrupted newly formed monolayers.[3] Animal studies also provided hints to angiogenic effects of small oligosaccharides leading to accelerated wound healing.[4] The hyaluronan receptors CD44 and RHAMM are supposed to influence the complex processes of wound healing and vascularization.[5-7] Previous studies by Hamberger aimed at elucidating the effect of products from enzymatic digests of hyaluronan on the proliferation of human microvascular endothelial cells (HMEC-1).[8] Inspired by these experiments, we decided to follow up this matter combining the conventional crystal violet assay with the sensitive approach of electric cell–substrate impedance sensing (ECIS).

Electric cell–substrate impedance sensing is based on the observation that changes in morphology and density of cells growing on a gold film electrode can be measured via the impedance of the system when alternating electric fields are applied.[9] While attaching and spreading on the gold film electrode, cells cause a measurable change in impedance, allowing for quantitative and continuous real-time analysis.[10] Hence, ECIS has already been successfully applied to determine attachment and spreading of cells on artificial surfaces,[11] cell motility,[12] and invasive behavior of metastatic cells *in vitro*.[13] Noiri et al. used a direct current pulse to wound a layer of endothelial cells and measured the recovery of the cell layer by ECIS.[14] Later, this approach was further optimized and characterized in detail.[15] Thereby, an alternating current pulse was used, causing a defined lesion only on the surface of the electrode.[15] In view of the high sensitivity of ECIS concerning a broad range of changes in cell shape, cell movement, and proliferation, this method was considered for studying the cellular effects of hyaluronan and hyaluronan oligosaccharides.

Apart from wound healing and angiogenesis, the polysaccharide itself, hyaluronidase activity, and the enzymatic degradation products of hyaluronan are supposed to be involved in cancer and metastasis.[16, 17] Overexpression of hyaluronidase by human colorectal adenocarcinoma cells (HT-29) increased the number of metastases especially in the liver and lung of nude mice bearing orthotopic xenografts.[18] Hyaluronidase activity was proven in

tumor cell lysates as well as, after sample concentration, in conditioned cell culture media at the pH optimum of the enzymes.[18] However, metabolic products of hyaluronan or hyaluronan oligosaccharides were not detected in the surrounding cell culture medium due to the lack of suitable analytical methods. Thus, we envisaged the analysis of hyaluronan oligosaccharides in cell culture media with regard to cellular uptake or alteration in size distribution by hyaluronidase activity.

9.2 Materials and methods

9.2.1 Cell lines and cell culture conditions

Immortalized human microvascular endothelial cells (HMEC-1)[19] were kindly provided by Prof. Dr. Joachim Wegener (Institute of Analytical Chemistry, Chemo- and Biosensors, University of Regensburg). Human colorectal adenocarcinoma cells (HT-29), the human breast adenocarcinoma cell line MDA-MB-231, and the human melanoma cell line SK-MEL-3 were obtained from the American Type Culture Collection (ATCC, Rockville, MD, USA) and stored according to the seed stock concept.[20] SK-MEL-3 cells overexpressing human PH-20 (clone SK-MEL-3 PH # 14) were established and characterized by Oettl.[21] HT-29 cells were modified by Jarzyna with regard to overexpression of human hyaluronidase-1 (clone V_{alt}).[18]

All cells were grown in suitable cell culture media (Table 9.1) at 37 °C in water-saturated atmosphere of 95% air and 5% carbon dioxide (CO_2). Cell culture flasks were from Sarstedt (Nümbrecht, Germany). Fetal calf serum (FCS) was from Biochrom (Berlin, Germany). Sodium hydrogen carbonate ($NaHCO_3$) was from Merck (Darmstadt, Germany). For passaging, cells were trypsinized with 0.05% trypsin and 0.02% EDTA in PBS, prepared from a trypsin/EDTA concentrate (PAA Laboratories, Pasching, Austria).

Table 9.1: Cell culture media. HT-29 cells with Hyal-1 overexpression and control cells were cultured with 10% FCS instead of 5% (standard conditions).

Cell line	Cell culture medium	FCS	Other supplements
HMEC-1	Endothelial Cell Growth Medium	10%	Supplement mix
MDA-MB-231	McCoy's 5 A Medium with L-glutamine	5%	$NaHCO_3$ (2.2 g/L)
HT-29	McCoy's 5 A Medium with L-glutamine	5% or 10%	$NaHCO_3$ (2.2 g/L)
SK-MEL-3	McCoy's 5 A Medium with L-glutamine	10%	$NaHCO_3$ (2.2 g/L)

Endothelial Cell Growth Medium and corresponding supplement mix were from PromoCell (Heidelberg, Germany). The complete medium (after addition of supplement mix) contained FCS (2%, v/v, in addition to FCS supplementation listed in Table 9.1), endothelial cell growth

supplement (0.4%, v/v), recombinant human epidermal growth factor (0.1 ng/mL), recombinant human basic fibroblast growth factor (1 ng/mL), heparin (90 µg/mL), and hydrocortisone (1 µg/mL). McCoy's 5 A Medium with L-glutamine was prepared from powder (Sigma-Aldrich, Munich, Germany).

According to previously described conditions, parallel cultures of clones with hyaluronidase overexpression were cultured in selective media to ensure maintenance of phenotype. Medium for SK-MEL-3 with PH-20 overexpression contained geniticin (G-418) sulfate (500 µg/mL, Biochrom, Berlin, Germany).[21] Hygromycin B (800 µg/mL, A. G. Scientific, San Diego, CA, USA) was used for HT-29 with Hyal-1 overexpression.[18]

In contrast to the conditions in our lab, FCS for culture of HMEC-1 in Prof. Wegener`s (Institute of Analytical Chemistry, Chemo- and Biosensors, University of Regensburg) lab was from PAA (Pasching, Austria). Penicillin G (100 U/mL) and streptomycin (100 µg/mL) were added, using a penicillin/streptomycin concentrate (100 x, PAA, Pasching, Austria). Additionaly, medium was supplemented with 2.5 µg/mL amphotericin B (AppliChem, Darmstadt, Germany). Apart from these exceptions, composition of the medium (*cf*. Table 9.1) and cell culture conditions were as described above.

9.2.2 Test substances

Hyaluronan from *Streptococcus zooepidemicus* (Aqua Biochem, Dessau, Germany), Hyalo-Oligo with an average molecular weight below 10 kDa (Kewpie, also named Q. P. Corp., Tokyo, Japan), and the purified hexasaccharide (n_3, prepared and quantified by colorimetry as described in Chapter 5) were investigated in cellular assays. As the hexasaccharide (n_3) is the prevailing reaction product when hyaluronan is degraded by rhHyal-1 (*cf*. Chapter 7), this oligosaccharide was chosen. Bovine testicular hyaluronidase (BTH, Neopermease®) was a kind gift from Sanabo (Vienna, Austria). *N*-Acetyl-D-glucosamine (NAG) was from Fluka (Buchs, Switzerland), D-glucuronic acid (GA) and cisplatin were from Sigma-Aldrich (Munich, Germany).

9.2.3 Flow cytometry

The flow cytometric determination of hyaluronan receptors was based on the protocol by Hamberger.[8] After trypsinization, cells were suspended in phosphate-buffered saline (PBS) containing 10% (v/v) of fetal calf serum (FCS). The suspension was centrifuged at 400 × *g* for 5 min, washed once with PBS (without FCS), and centrifuged again. A suspension of $1 \cdot 10^6$ to $2 \cdot 10^6$ cells/mL was prepared with PBS/FCS. To aliquots of 500 µL, the respective primary antibody was added to yield an appropriate dilution (anti-RHAMM: 1:500, anti-CD44: 1:100). The monoclonal rabbit antibody against human CD168/RHAMM (catalog #: 3139-1, clone ID: EPR4055, lot: YH031609C, Epitomics, Burlingame, CA, USA) was identical to that used by

Hamberger.[8] In contrast to Hamberger's conditions, a polyclonal anti-CD44 antibody produced in rabbit (human protein atlas #: HPA005785, lot: B41535, Prestige Antibodies/Sigma-Aldrich, Steinheim, Germany) was used. Cells were incubated with the primary antibody for 1 h. After three washing steps with PBS, cells were suspended in PBS supplemented with 3% (w/v) of bovine serum albumin containing the secondary antibody (goat anti-rabbit IgG, phycoerythrin-conjugated, code # 611-108-122, Rockland Immunochemicals, Gilbertsville, PA, USA) at a dilution of 1:250. Cells were incubated in the dark for 1 h, washed twice with PBS, and suspended in PBS/BSA. Flow cytometric analysis was conducted with a FACSCalibur™ (Becton Dickinson, Heidelberg, Germany) using the following instrument settings: FSC: E−1, SSC: 310, FL-2, flow: high. WinMDI 2.9 software was used for data evaluation.

9.2.4 Electric cell–substrate impedance sensing (ECIS) of endothelial cells

Electric cell–substrate impedance sensing (ECIS) was performed in Prof. Wegener`s (Institute of Analytical Chemistry, Chemo- and Biosensors, University of Regensburg) lab. Measurements were carried out with an ECIS 1600R system (Applied BioPhysics, Troy, NY, USA), equipped with an Elevated Field Module (EFM). Prior to usage, electrode arrays were coated with collagen (Biochrom, Berlin, Germany). High molecular weight hyaluronan, a low molecular weight hyaluronan oligosaccharide mixture, and purified hexasaccharide (n_3, 100 mg/mL stock solution) were dissolved in FCS-free cell culture medium (without supplement mix, without antibiotics). The solutions were sterilized by filtration through a 0.22 µm filter. After addition of 2.5% FCS, the medium contained 1 mg/mL of the test compounds. It should be noted again that n_3 was not weighted but quantified by colorimetry. Standard cell culture medium (with supplement, 10% FCS) and blank assay medium (without supplement, 2.5% FCS) served as control.

For an electric wound healing assay,[15] HMEC-1 cells were seeded to form a confluent monolayer in 8W1E (8 wells, 1 electrode/well, Figure 9.1 A) disposable electrode arrays (Applied BioPhysics, Troy, NY, USA). After incubation overnight (37 °C, 5% CO_2), medium was replaced by fresh medium containing the test substances. The measurement was started. After approximately 2 h of equilibration, an electric wounding pulse (sine pulse, frequency: 40 kHz, amplitude: 5 V, duration: 30 s) was applied to kill the cells on the electrode surface. After recovery of the cell layer the experiment was repeated, applying a second (identical) wounding pulse.

For monitoring cell proliferation, 8W10E+ (8 wells, 40 electrodes/well, Figure 9.1 B) arrays (Applied BioPhysics, Troy, NY, USA) were used. Cells were seeded at 2% confluency and increasing coverage of the electrodes as a function of time was measured for 142 h. All other conditions were identical to the wound healing assay. After 142 h, an additional electric wounding pulse was elicited as described above.

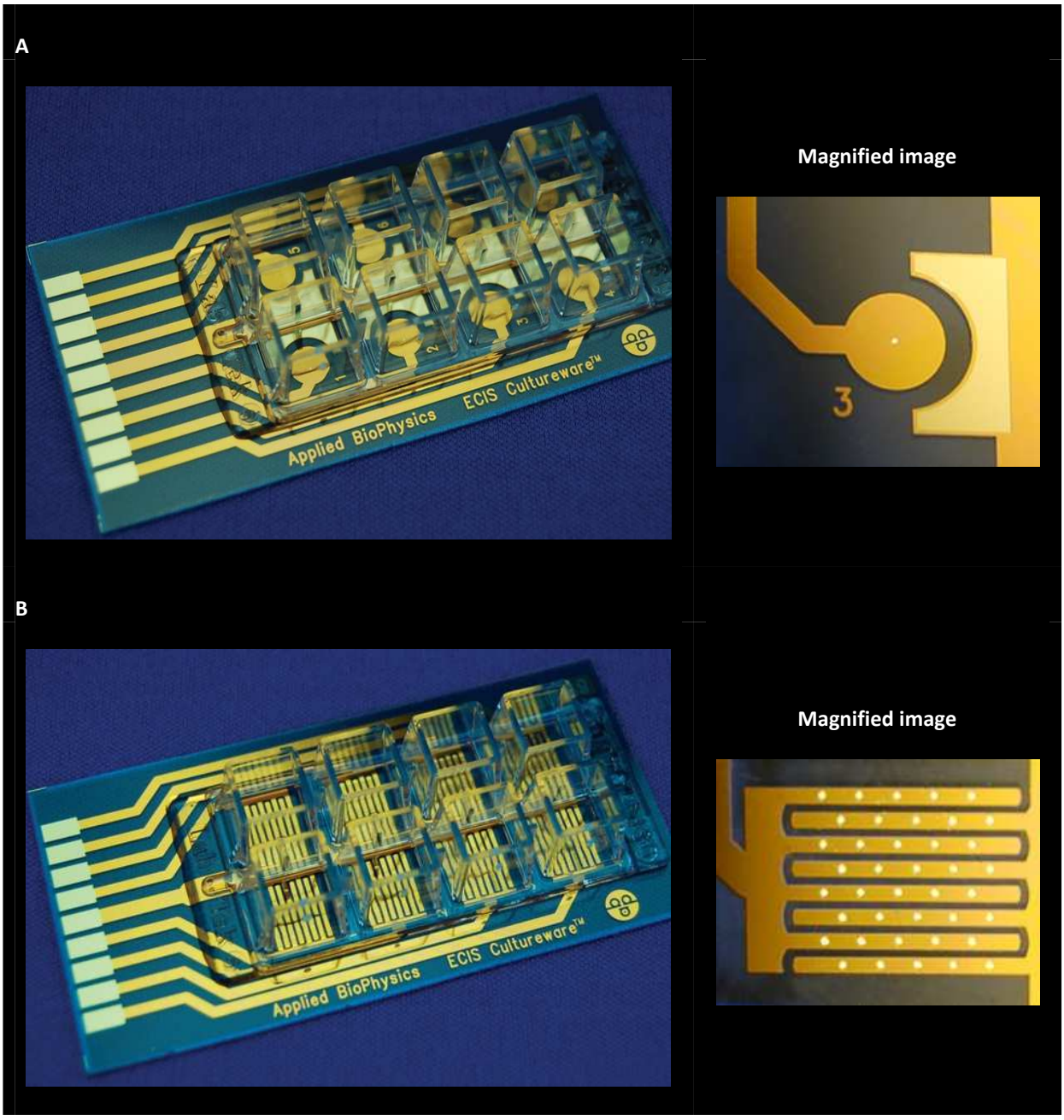

Figure 9.1: Arrays 8W1E (A) and 8W10E+ (B) for ECIS. Images of the whole arrays taken from the product information sheet (http://www.biophysics.com/Product%20Sheets/ABP_ArraySheet.pdf), magnified images (high resolution) kindly provided by Applied BioPhysics. Use of all images with kind permission from Applied BioPhysics (Troy, NY, USA).

9.2.5 Crystal violet cell proliferation assay

A previously desribed crystal violet assay[22, 23] was applied to measure proliferation of the HMEC-1 cells. By analogy with ECIS arrays (*cf*. Section 9.2.3) flat-bottomed 96-well plates (Greiner, Frickenhausen, Germany) were coated with collagen. 100 µL of cell suspension per well were seeded in the plate to reach 2% confluency. After 24 h of incubation under standard conditions (37 °C, 5% CO_2) the medium was replaced by 200 µL of fresh medium containing the test compounds. As described in Section 9.2.3, the substances were dissolved

in FCS-free cell culture medium (without supplement mix) and filtrated through Millex-GP 0.22 µm syringe filter units (Merck-Millipore, Darmstadt, Germany). By addition of 2.5% of sterile FCS, the desired concentration of the test compounds was yielded. Cisplatin was applied as concentrated (100 µM) stock solution in dimethylformamide. For each substance or concentration, 16 wells were used.

After different periods of incubation (37 °C, 5% CO_2), cell culture medium was discarded. Cells were fixed with 1% (v/v) glutardialdehyde (Merck, Darmstadt, Germany) in PBS. Afterwards, cells were covered with PBS and the plates were stored at 4 °C until the end of the experiment. PBS was discarded and cells in all 96-well plates were stained simultaneously with an aqueous solution (0.02%, w/v) of crystal violet (Merck, Darmstadt, Germany). Unbound dye was washed off with water. Finally, cell-bound crystal violet was dissolved by addition of 180 µL of 70% ethanol per well.

Absorbance was measured at 580 nm with a Tecan GENios Pro plate reader (Tecan, Crailsheim, Germany). Data were recorded with the corresponding XFluor GENios Pro software V.4.55. Cell proliferation curves were obtained by plotting absorbance versus incubation time with SigmaPlot for Windows 11.2.0.5 (Systat Software Inc., San Jose, CA, USA).

To exclude pH effects at high concentrations of acidic saccharides, an additional experiment with HEPES-buffered medium was performed. A 1 M aqueous solution of HEPES (Serva, Heidelberg, Germany) was prepared and adjusted to pH = 8.2. Due to the concentration dependency of the pKa value, a pH of 7.4 was reached after addition to the medium yielding a final HEPES concentration of 30 mM. After dissolution of the hyaluronan oligosaccharides and prior to filtration, pH was additionally titrated to physiological values by addition of sodium hydroxide solution if necessary (at high concentrations of HA oligosaccharides).

9.2.6 Collection and analysis of wound material

Wound material from volunteers was provided by Prof. Dr. Sigrid Karrer (Department of Dermatology, University of Regensburg). Three silicone-coated foam dressings (Mepilex®, Mölnlycke Health Care, Erkrath, Germany), soaked with exudate, were collected. However, sufficient amounts of material were only obtained from one foam dressing by squeezing and subsequent centrifugation. An additional sample of debris, scraped off from the wound, was also provided. After ultrafiltration using Nanosep® Centrifugal Devices 10 K (Pall Life Sciences, Ann Arbor, MI, USA), samples were analyzed by HPAEC–PAD as described in Chapter 4. In addition, 1:10 dilutions were analyzed and compared to human CPD plasma by zymography according to the protocol from Chapter 8 (Section 8.2.11). Until analysis, all samples were stored at −80 °C.

9.2.7 Analysis of conditioned cell culture media

Hyaluronidase overexpressing SK-MEL-3 and HT-29 clones and the respective wild type controls were seeded in a 24-well plate (2 mL of $1.5 \cdot 10^5$ cells/mL suspension per well). After 24 h (37 °C, 5% CO_2), culture medium was replaced by FCS-free (to prevent hyaluronidase contamination from serum) medium containing 1 mg/mL of a hyaluronan oligosaccharide mixture (MW < 10 kDa). The oligosaccharides were dissolved in the medium and filtrated through Millex-GP 0.22 µm syringe filter units (Merck-Millipore, Darmstadt, Germany). Cell-free controls with oligosaccharide mixture alone (negative control) or oligosaccharide mixture with 1000 IU/mL of BTH (positive control) were incubated under the same conditions. After 7 days, cell culture media were deproteinized by boiling for 10 min, centrifugation at 13000 × *g* for 10 min, and filtration through a Phenex-NY 4 mm syringe filter 0.2 µm (Phenomenex, Aschaffenburg, Germany). Samples were diluted 1:2 with purified water and analyzed by HPAEC–PAD (*cf*. Chapter 4).

9.3 Results and discussion

9.3.1 Flow cytometry

The hyaluronan receptor CD44 was previously detected on the surface of the human microvascular endothelial cell line HMEC-1.[24] Having observed an inhibitory effect of an anti-CD44 antibody on migration and proliferation of HMEC-1 cells, Trochon et al. proposed CD44 to be involved in these processes.[25] Moreover, wound healing in mice was reported to be promoted by hyaluronan oligosaccharides,[4] whereas delayed wound healing was observed in CD44-deficient mice.[26] Savani et al. suggested that both CD44 and RHAMM are involved in proliferation and migration of endothelial cells.[6] Thereby, proliferation of the human endothelial cell line HUVEC could only be inhibited by an anti-CD44 (not by anti-RHAMM) antibody, whereas migration was inhibited by anti-RHAMM (not by anti-CD44).[6] Based on studies with porcine iliac vascular endothelial cells (PIEC), Gao et al. suggested that RHAMM, rather than CD44, was responsible for the proposed stimulation of angiogenesis and wound healing processes by hyaluronan oligosaccharides.[27] Hence, the expression of CD44 and RHAMM was investigated by flow cytometry. After binding of the primary antibody, directed against the respective receptor protein, bound antibody was detected with a phycoerythrin-conjugated secondary antibody (Figure 9.2).

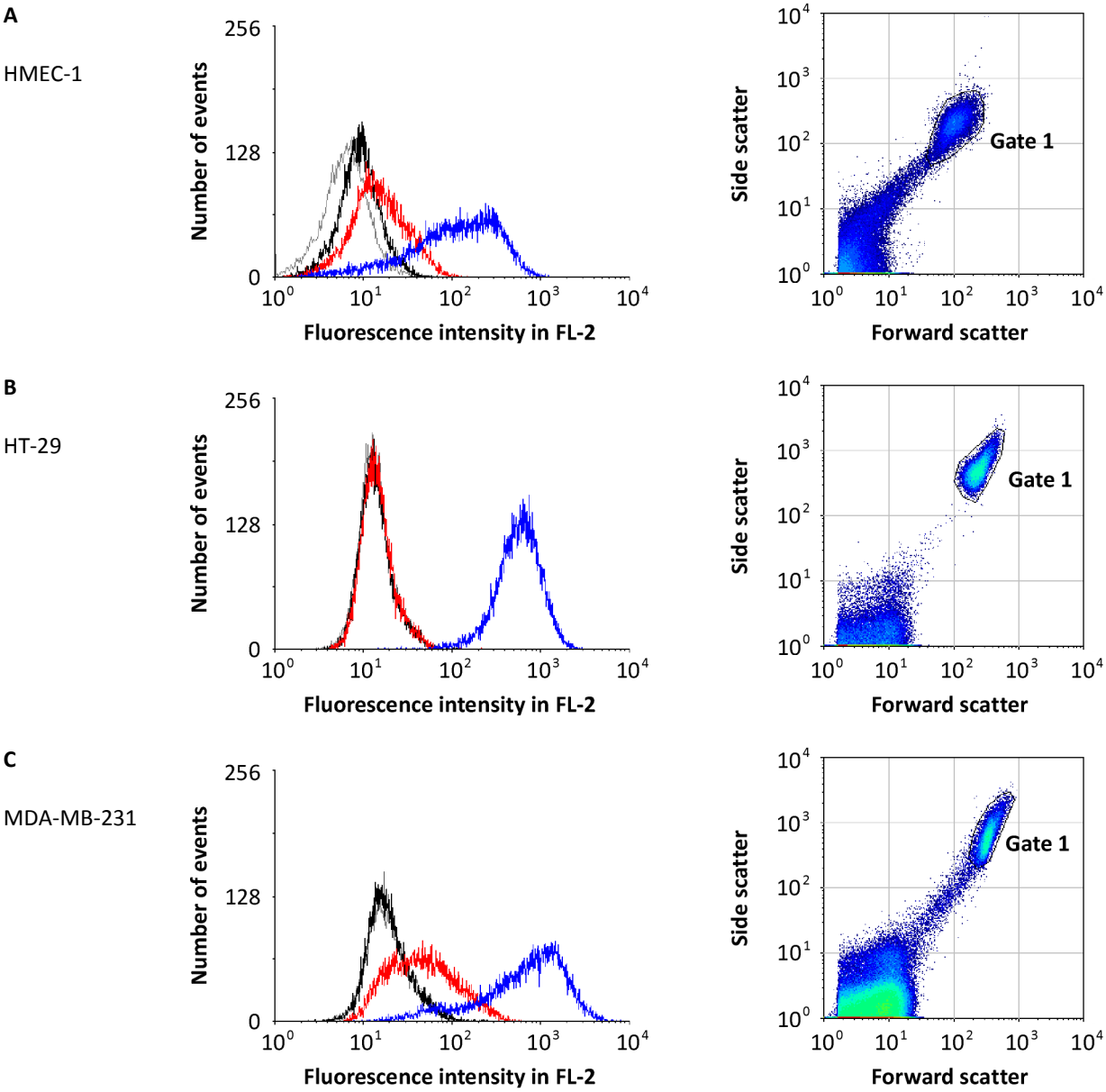

Figure 9.2: Flow cytometric determination of hyaluronan receptors RHAMM and CD44 on HMEC-1 (A), HT-29 (B), and MDA-MB-231 (C) cells. Curves show autofluorescence of the cells (grey), phycoerythrin-conjugated secondary antibody alone (black), monoclonal anti-RHAMM (red), and polyclonal anti-CD44 (blue). Cell populations in gate 1 were considered in the histograms.

In a previous study, RHAMM but not CD44 was detected on HMEC-1 cells by flow cytometry with monoclonal primary antibodies against the respective proteins.[8] Nevertheless, using a polyclonal anti-CD44 antibody instead, we succeeded in proving the protein on these cells. As already speculated by Hamberger, the monoclonal primary antibody probably was not suitable for the recognition of the CD44 isoform present on HMEC-1 cells.[8] With regard to RHAMM, previous results[8, 24] were confirmed (Figure 9.2 A). Moreover, comparable expression of CD44 and RHAMM was measured by Savani et al. on different human endothelial cells (HUVEC).[6] This is in accordance with the results of Xu et al., who compared HMEC-1 and HUVEC with respect to CD44.[24]

The human colorectal adenocarcinoma cell line HT-29 is known to express the CD44 protein.[28] MDA-MB-231 cells were previously reported to express elevated levels of both RHAMM and CD44.[29] Hence, these cell lines were chosen as references. Both controls showed the expected high expression of CD44. RHAMM was additionally detected on MDA-MB-231, but not on HT-29 cells (Figure 9.2 B, C).

9.3.2 Electric wound healing model

In an electric wound healing model, based on the assay by Keese et. al.,[15] the influence of hyaluronan and hyaluronan oligosaccharides on the recovery HMEC-1 cell layers was studied. Two arrays were measured in parallel. It was previously reported that capacitance measurements at high frequencies are ideal for determination of electrode coverage, showing a linear correlation.[11] Hence, capacitance measured at 32 kHz was plotted versus incubation time for both arrays (Figure 9.3). Owing to the insulating properties of cells, a high degree of electrode coverage results in low capacitance and vice versa. Hence, an immediate increase in capacitance was observed as soon as the wounding pulse was applied. Along with recovery of the cell layer the capacitance continuously decreased until it reached the initial values for the cell-covered electrode.

As becomes obvious from Figure 9.3, high molecular weight hyaluronan and the oligosaccharide mixture (both at 1 mg/mL) did not influence this process. Interestingly, there was also no difference between the control medium (2.5% FCS, no supplement mix) and the supplemented medium with high FCS content. Probably, the supplement mix and higher amount of FCS are only necessary for longer periods of incubation. By contrast, the hexasaccharide (n_3) led to a measurable delay in recovery after the high electric field pulse. The effect was even more pronounced after the second wounding pulse. In this case, the initial capacitance values (indicating a completely covered electrode) were not reached.

Hyaluronan oligosaccharides were often related to increased endothelial cell proliferation and wound healing.[3, 4] By contrast, our observations suggest an inhibitory, rather than a stimulating, effect of the hexasaccharide (n_3) at a concentration of 1 mg/mL. Hence, our results are in line with the observation by Banarjee and Toole that 500 µg/mL of the hexasaccharide (but not the tetrasaccharide, D-glucuronic acid, and *N*-acetyl-D-glucosamine) completely inhibited endothelial cell migration and tube formation.[30]

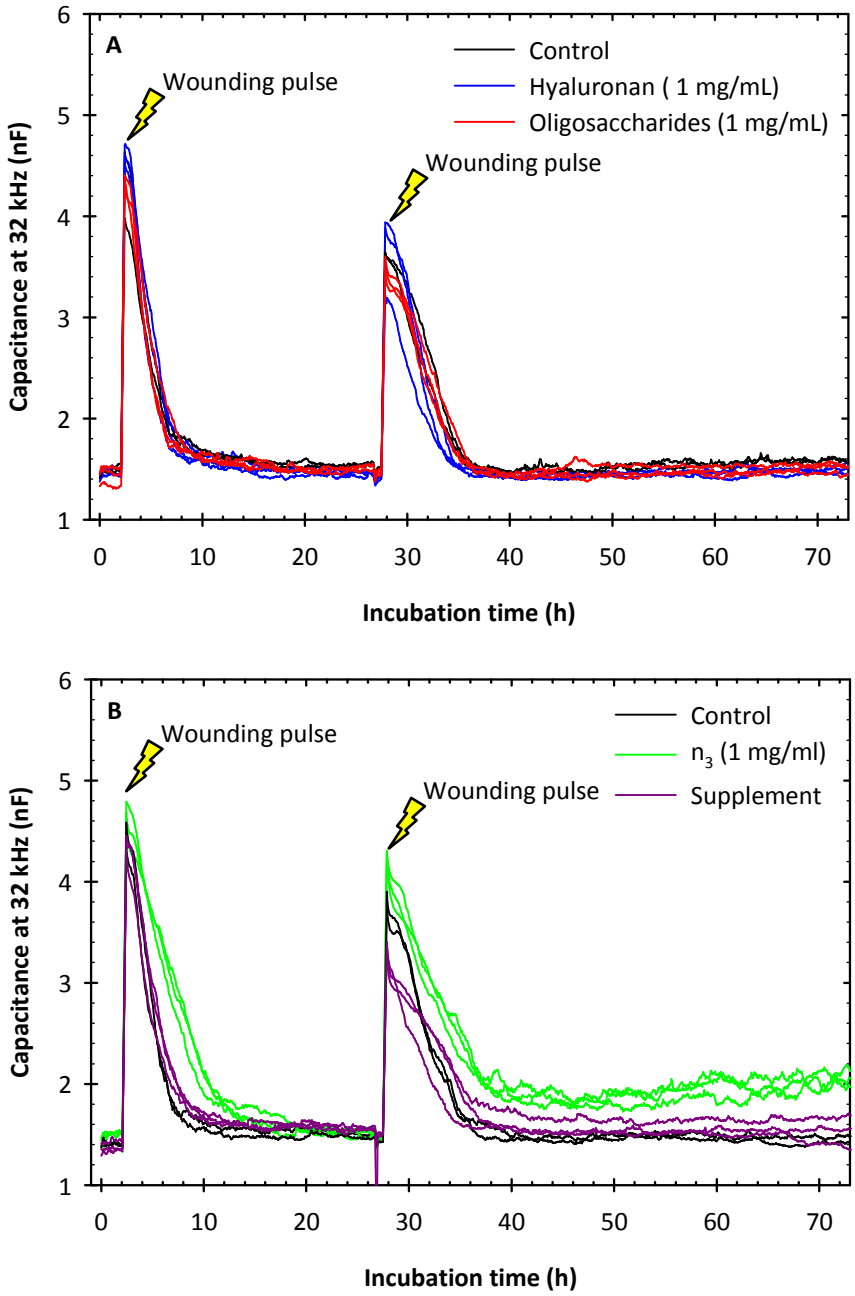

Figure 9.3: Electric wound healing assay using HMEC-1 cells. Array 1 (A): high molecular weight hyaluronan (1 mg/mL) and hyaluronan oligosaccharide mixture (1 mg/mL) compared to control (medium + 2.5% FCS). Array 2 (B): purified hexasaccharide (n_3, 1 mg/mL) and supplemented medium (supplement mix, 10% FCS) compared to control. Capacitance measured at 32 kHz. Wounding pulses: 5 V (amplitude), 40 kHz, 30 s.

9.3.3 Proliferation of HMEC-1 cells

Proliferation assays were performed to investigate if the inhibition of cell layer recovery in the wounding experiment by n_3 originated from reduced cell proliferation or other parameters, for instance, cell migration or differences in attachment to the electrode surface. Thereby, ECIS was combined with the conventional crystal violet assay.

Real-time measurement by ECIS (Figure 9.4) revealed considerable acceleration of cell proliferation by addition of the supplement mix and high FCS content. The hyaluronan hexasaccharide (n_3) obviously inhibited cell proliferation.

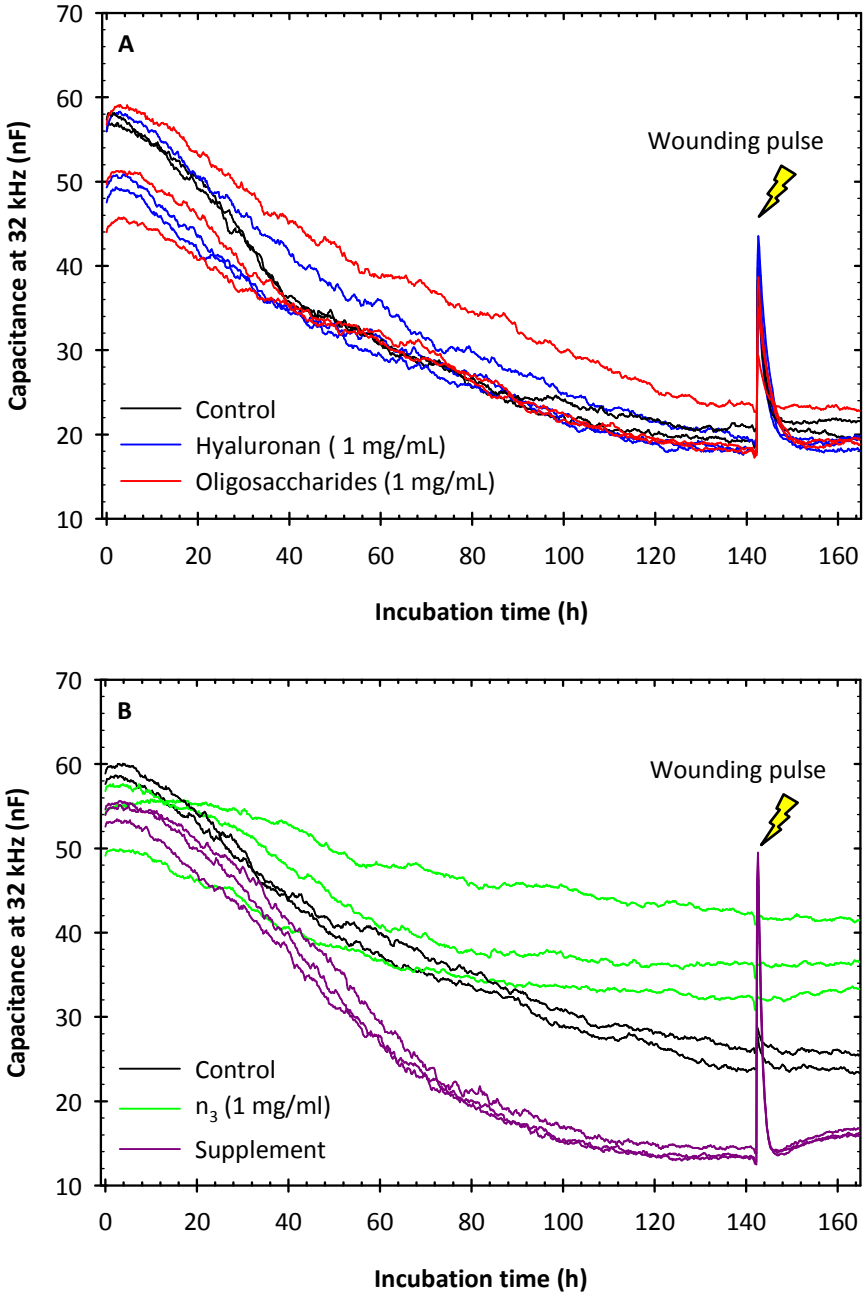

Figure 9.4: Electric cell proliferation assay using HMEC-1 cells. Array 1 (A): high molecular weight hyaluronan (1 mg/mL) and hyaluronan oligosaccharide mixture (1 mg/mL) compared to control (medium + 2.5% FCS). Array 2 (B): purified hexasaccharide (n_3, 1 mg/mL) and supplemented medium (supplement mix, 10% FCS) compared to control. Capacitance measured at 32 kHz. Additional wounding pulse: 5 V (amplitude), 40 kHz, 30 s.

The curves for high molecular weight hyaluronan and the oligosaccharide mixture were comparable to the control, but showed a relatively high variability considering absolute values. With regard to the absolute values of capacitance, it should be noted that the differences between Figure 9.3 and Figure 9.4 are caused by the number of electrodes per

well (1 versus 40) for the respective arrays. For the same reason, identical wounding did not lead to effective killing of the cells in the experiment depicted in Figure 9.4. Applying the same voltage pulse, the average current at each electrode of the 8W10E+ array (parallel circuit) was only 1/40 of the current using the 8W1E array, according to Kirchhoff's nodal rule.

In view of better interpretability, the curves from Figure 9.4 were normalized by dividing the measured capacitance (C) by the respective capacitance at t = 0 (C_0). The normalized curves for the initial 140 h of the experiment (proliferation without the wounding pulse) are depicted in Figure 9.5.

By normalization, small differences between the ECIS curves for hyaluronan, the oligosaccharide mixture, and control became visible. Under the influence of high molecular weight hyaluronan the decrease in capacitance, which is proportional to the increase in electrode coverage,[11] was slightly slower compared to control but reached similar values after 140 h. Furthermore, the hyaluronan oligosaccharide mixture tended to further decelerate the occupation of the electrode surface by the cells, not reaching exactly the same values as control after 140 h. These findings are reflected by the results from a crystal violet cell proliferation assay, performed simultaneously under identical conditions (Figure 9.6 A). In a second assay, different concentrations of the hyaluronan oligosaccharide mixture were tested. Previous studies had revealed no effect of this mixture on proliferation of HMEC-1 cells at concentrations of 5–100 µg/mL.[8] Hence, we focused on the range of 0.5–10 mg/mL (Figure 9.6 B). In contrast to the first experiment, proliferation was not inhibited at 1 mg/mL. At higher concentrations, proliferation was decelerated and completely inhibited at 10 mg/mL. However, at these high concentrations the addition of hyaluronan oligosaccharides significantly acidified the cell culture medium. This issue will be discussed later in this section.

To exclude that the suppression of cell proliferation by n_3 was caused by unspecific effects, mixtures of *N*-acetyl-D-glucosamine and D-glucuronic acid (each 10–1000 µM) and each of the sugars alone (1000 µM) were investigated (Figure 9.6 C). No effect was detected, suggesting that a specific interaction is responsible for the lack of cell proliferation in the presence of n_3 at a concentration of 1 mg/mL (≈ 865 µM). Co-incubation of the cells with hyaluronan and bovine testicular hyaluronidase (BTH) revealed no difference compared to hyaluronan alone (Figure 9.6 C). However, the slight reduction of proliferation rate by hyaluronan (*cf*. Figure 9.6 A) was confirmed, whereas BTH alone had no effect.

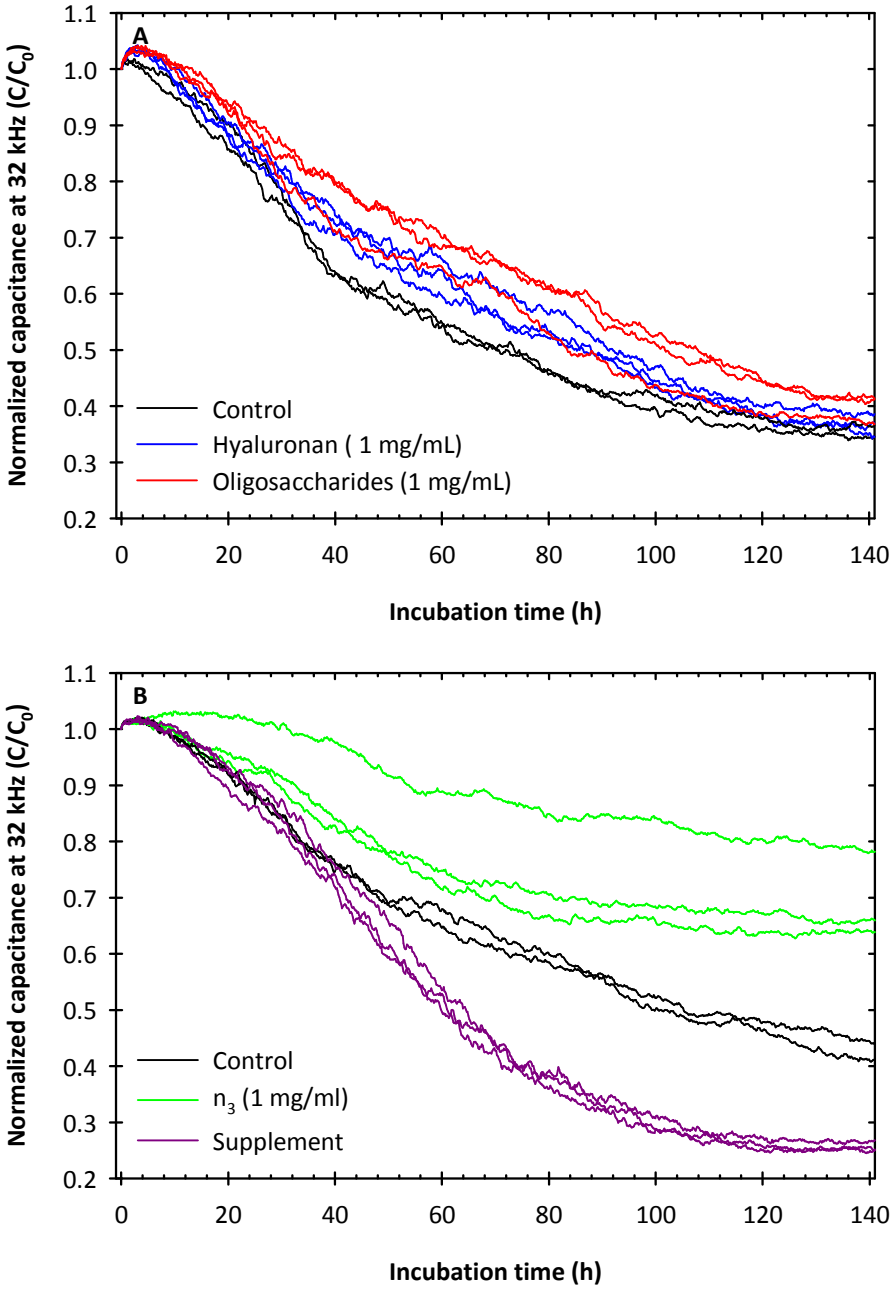

Figure 9.5: Normalization of the HMEC-1 proliferation curves from Figure 9.4. Capacitance divided by the respective value at t = 0 (C_0). Only the first 140 h of the experiment are depicted. Array 1 (A): high molecular weight hyaluronan (1 mg/mL) and hyaluronan oligosaccharide mixture (1 mg/mL) compared to control (medium + 2.5% FCS). Array 2 (B): purified hexasaccharide (n_3, 1 mg/mL) and supplemented medium (supplement mix, 10% FCS) compared to control. Capacitance measured at 32 kHz.

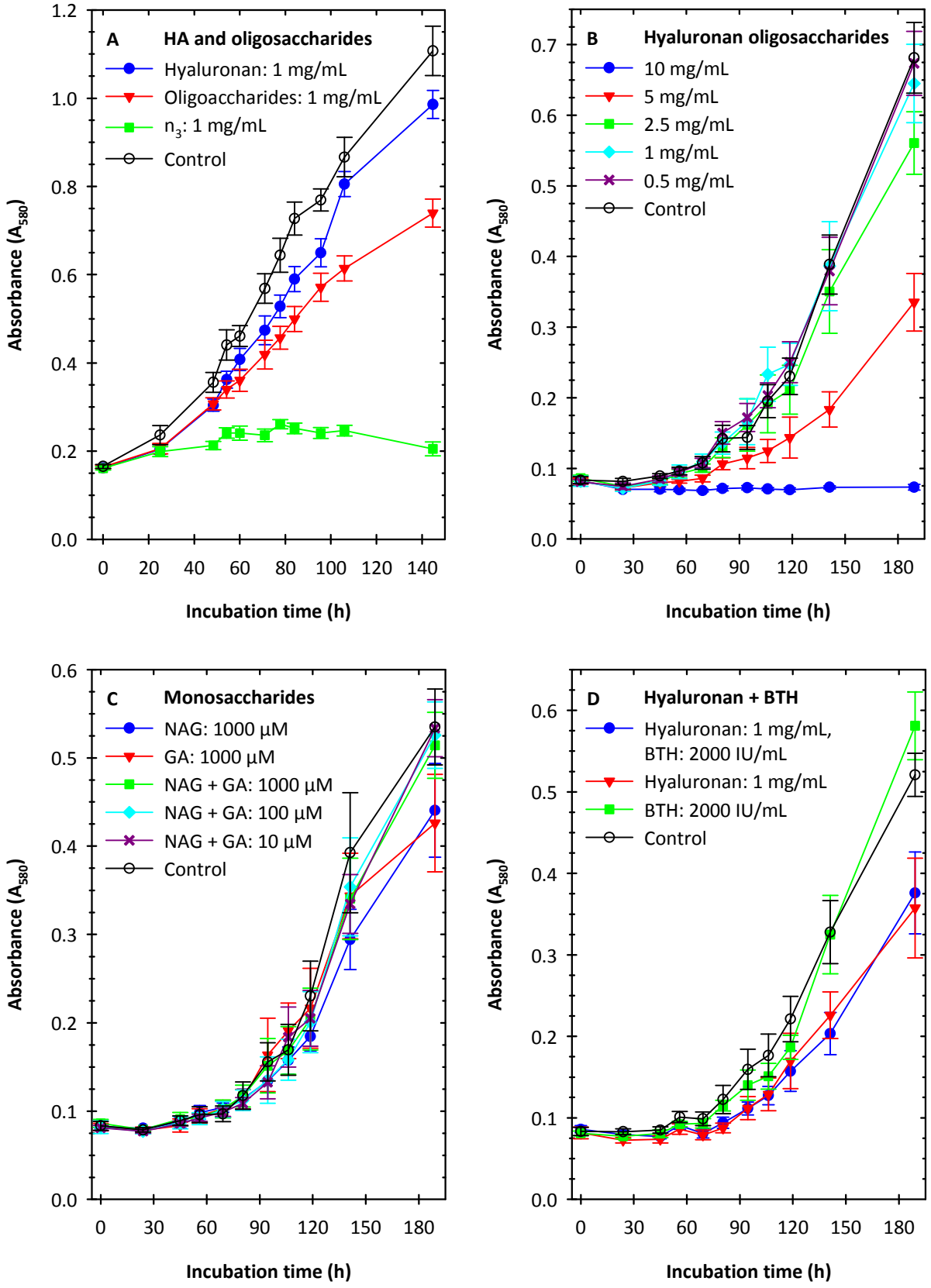

Figure 9.6: Influence of hyaluronan and hyaluronan oligosaccharides on the proliferation of HMEC-1 cells. Growth curves determined by the crystal violet assay. Comparison of hyaluronan and hyaluronan oligosaccharides (A), concentration-dependent effect of a hyaluronan oligosaccharide mixture (B), D-glucuronic acid (GA) and *N*-acetyl-D-glucosamine (NAG) alone and in combination (C), co-incubation with hyaluronan and BTH (D). Data presented as means ± SD of 16 wells on the same plate.

The stimulating effect of medium containing the supplement mix and additional FCS on HMEC-1 proliferation, observed in the ECIS experiment (*cf*. Figure 9.4 and Figure 9.5), was confirmed by simultaneously performed crystal violet assays (Figure 9.7 A). The reference compound cisplatin (100 nM) considerably inhibited cell proliferation (Figure 9.7 A), albeit the effect was much less prominent than observed for 1 mg/mL (≈ 865 µM) of the hyaluronan hexasaccharide (*cf*. Figure 9.6 A). Moreover, we were interested in the effect of the supplement mix alone. Hence, the FCS content was reduced to 2.5%, the same content used for negative control. As the supplement mix already contains FCS (yielding 2.0% FCS in the readily prepared medium), this portion was considered in an additional test medium to investigate the contribution of the other ingredients of the supplement mix (Figure 9.7 B). Both supplemented media clearly stimulated cell proliferation. Thereby, no differences between 2.5% and 4.5% FCS content were found, indicating other components of the supplement mix to be responsible for the stimulation of cell growth.

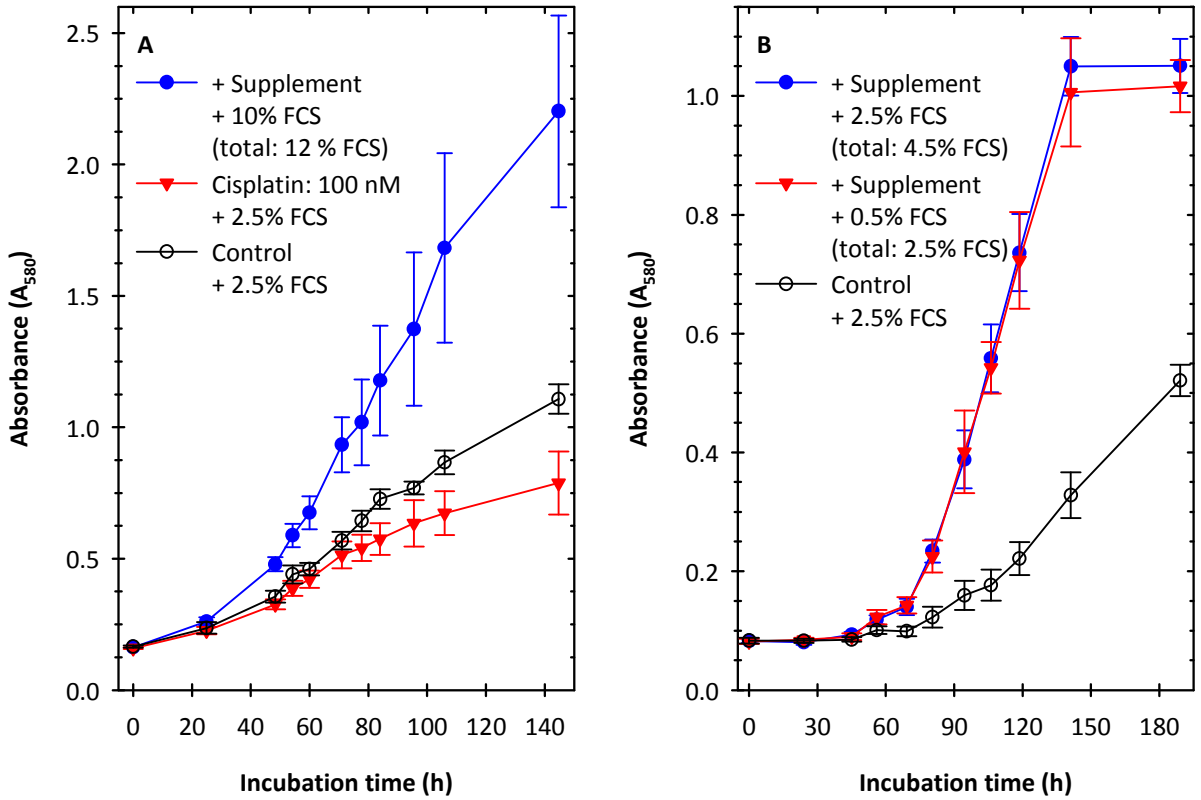

Figure 9.7: Influence of supplement, FCS content, and the reference substance cisplatin on proliferation of HMEC-1 cells. Growth curves determined by the crystal violet assay. Stimulating effect of supplemented medium (supplement mix + 10% FCS) and inhibition of cell proliferation by cisplatin (A), influence of the supplement mix (containing FCS) and its non-FCS components alone (B). Data presented as means ± SD of 16 wells on the same plate.

The mixture of hyaluronan oligosaccharides affected endothelial cell proliferation only at concentrations, at which acidification of the culture medium must be kept in mind (*cf*. Figure 9.6 B). To exclude this parameter, buffering capacity of the cell culture medium was

increased by addition of HEPES at a concentration of 30 mM (Figure 9.8). In HEPES-buffered medium, the oligosaccharide mixture did not influence proliferation of HMEC-1 cells. However, the inhibitory effect of the hyaluronan hexasaccharide (n_3) was confirmed.

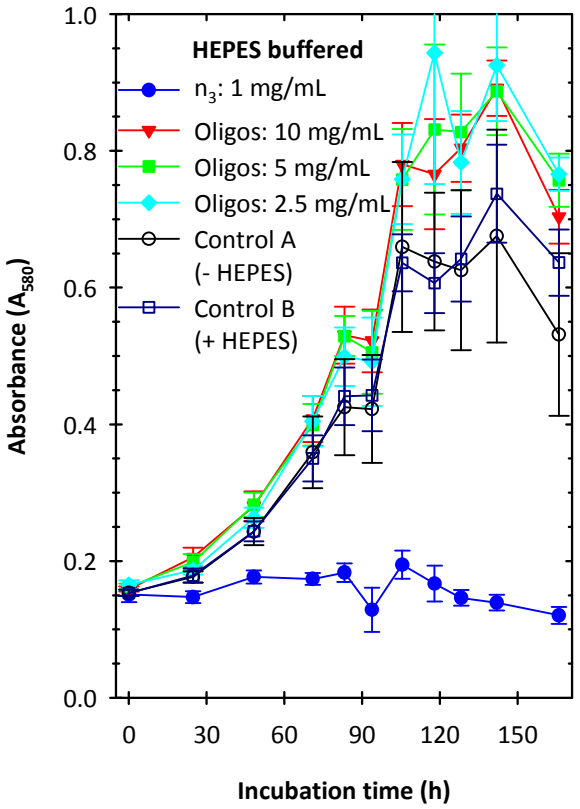

Figure 9.8: Influence of the hyaluronan hexasaccharide (n_3, 1 mg/mL) and high concentrations of hyaluronan oligosaccharides (2.5–10 mg/mL) on proliferation of HMEC-1 cells in additionally HEPES-buffered (30 mM) medium. Growth curves determined by the crystal violet assay. Data presented as means ± SD of 16 wells on the same plate.

In summary, high molecular weight hyaluronan and a low molecular weight hyaluronan oligosaccharide mixture had no clear-cut effect on endothelial cell proliferation. At 1 mg/mL no response or only a slight inhibitory effect was observed. Stronger inhibition by higher concentrations of the oligosaccharide mixture was probably caused by acidification of the culture medium. In accordance with previous studies,[30] a high concentration (1 mg/mL) (≈ 865 µM) of the hyaluronan hexasaccharide (n_3) completely inhibited endothelial cell proliferation in both ECIS and crystal violet assay.

It is known from binding experiments using a different cell line that n_3 binds to hyaluronan receptors on the cell surface, albeit with lower affinity than the polymer.[31] A common model suggests that polyvalent (high affinity) binding of high molecular weight hyaluronan to CD44 and other hyaluronan receptors induces the respective signaling cascades, whereas competitive monovalent (low affinity) binding of small oligosaccharides (n_3–n_9) inhibits constitutive kinase activation.[32, 33] In this context, hyaluronan oligosaccharides are discussed

as possible sensitizers in view of overcoming drug resistance in cancer cells.[34, 35] As discussed (*cf*. Section 9.3.1), hyaluronan receptors are presumably involved in the proliferation of endothelial cells.[6, 25-27] In contrast to our findings, Gao et. al described stimulation of (porcine) endothelial cell proliferation by hyaluronan oligosaccharides (mixture of n_2–n_{10}) via RHAMM-mediated signaling.[27] With bovine endothelial cells, small oligosaccharides (n_3–n_{16}) were also reported to induce proliferation and to show an inhibitory effect only at high concentrations of 2–4 mg/mL.[3] Thus, specific effects of hyaluronan oligosaccharides are discussed controversially. Moreover, the biological responses seem to depend not only on size but also on the concentration of the respective saccharides.

9.3.4 Analysis of wound material

Applicability of HPAEC–PAD to ultrafiltrates of exudate and debris from wounds was proven. Although exudate and debris gave different chromatograms, numerous peaks were visible in both of them (Figure 9.9). However, none of these peaks could be assigned to one of the hyaluronan oligosaccharides.

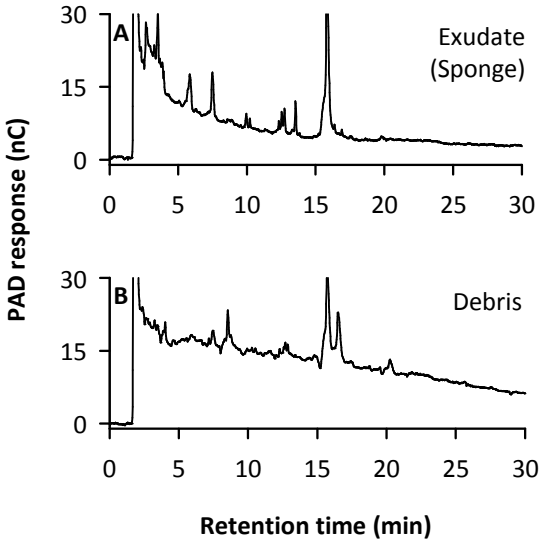

Figure 9.9: Ultrafiltrates of wound material analyzed by HPAEC–PAD: exudate isolated from a sponge/foam dressing (A) and debris (B). Chromatography conditions: CarboPac™ PA200, 10 µL of sample injected, 100 mM sodium hydroxide, gradient of 200–900 mM sodium acetate, 40 °C, 0.5 mL/min.

Zymography revealed no measurable hyaluronidase activity in the samples at pH = 4.0 (not shown). As hyaluronidase activity had been detected in human plasma and in synovial fluids (*cf*. Chapter 8), comparable results were expected for wound material. However, the exudation process possibly leads to strong dilution, resulting in much lower enzymatic activity compared to plasma. Nevertheless, it cannot be ruled out that difficulties in sample collection and preparation, especially obtaining the material from the foam dressing, are responsible for the negative zymographic results. Hence, optimization of sample collection should precede further analytical studies.

9.3.5 HPAEC–PAD of hyaluronan oligosaccharide-supplemented conditioned cell culture media

Like wound material (*cf*. Section 9.3.4) and synovial fluids (*cf*. Chapter 8), conditioned cell media were successfully analyzed by HPAEC–PAD. However, conditioned media, from wild type and from hyaluronidase overexpressing clones of HT-29 (Figure 9.10) and SK-MEL-3 (Figure 9.11) cells, showed no signs of hyaluronidase activity or oligosaccharide internalization.

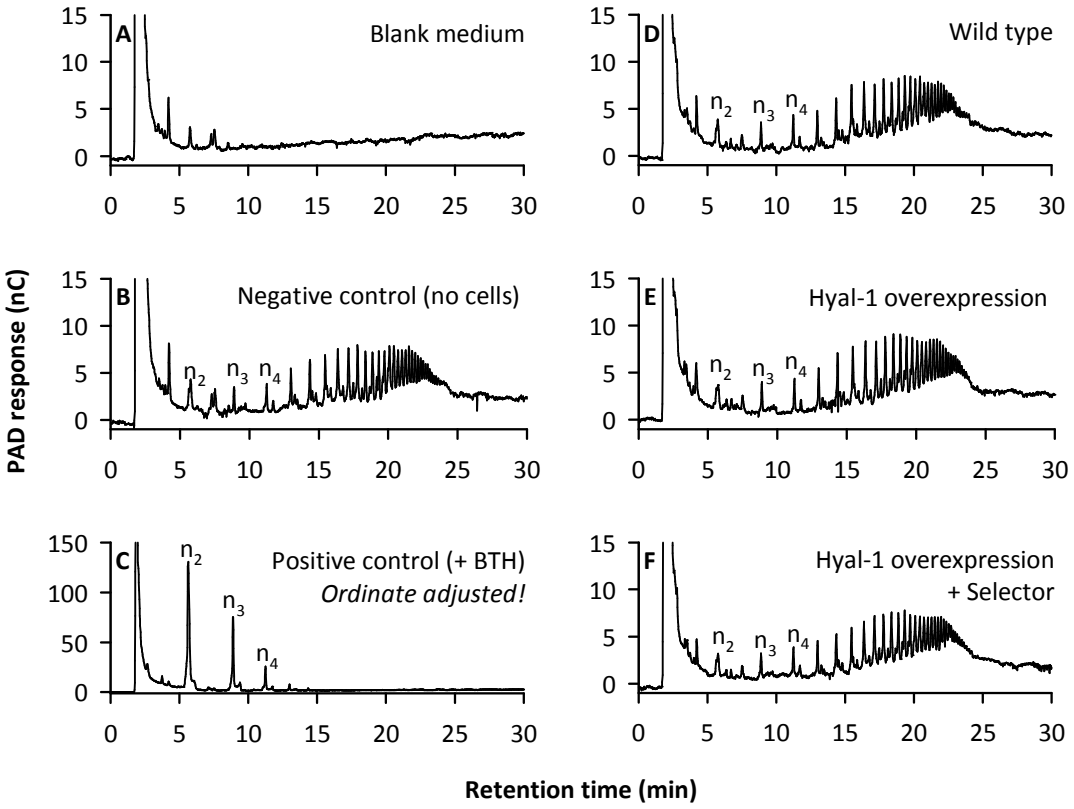

Figure 9.10: HPAEC–PAD of cell culture media from HT-29 cells, supplemented with hyaluronan oligosaccharide mixture (1 mg/mL). Controls: blank medium (A), negative control without cells (B), positive control containing 1000 IU/mL of BTH (C). Conditioned media: wild type cells (D), Hyal-1 overexpressing clone without (E) and with addition of hygromycin B (F). Oligosaccharides (n_x) labeled according to the number of disaccharide units (*x*). Chromatography conditions: CarboPac™ PA200, 10 µL of sample (1:2 dilution) injected, 100 mM sodium hydroxide, gradient of 200–900 mM sodium acetate, 40 °C, 0.5 mL/min.

The composition of the added oligosaccharide mixture was not altered compared to a cell-free control. Nevertheless, previous work by Jarzina showed that activity in conditioned media was very low and could be determined by colorimetry only after sample concentration and at optimum pH.[18] Hence, it may be doubted that formation of relevant amounts of small oligosaccharides occurs under physiological conditions. Nevertheless, it should be mentioned that cells were kept in FCS-free medium to exclude serum as a source of hyaluronidase activity. As a consequence, cells showed almost no proliferation. However, cells with high proliferation rate might behave differently with regard to degradation of

components of the extracellular matrix, particularly hyaluronan. The positive control (with BTH) contained n_2–n_4 and minor amounts of n_5. As discussed in Chapter 6, the tetrasaccharide (n_2) could be found as the main product of BTH. Hence, the distribution observed in the cell culture medium is congruent with the observations from Chapter 6. In conditioned media from SK-MEL-3 cells (Figure 9.11 D–F), an additional peak, eluting shortly before the n_3 peak, occurred. As this peak was not present in control and HT-29 media, it probably has to be assigned to a specific product of SK-MEL-3 cell metabolism.

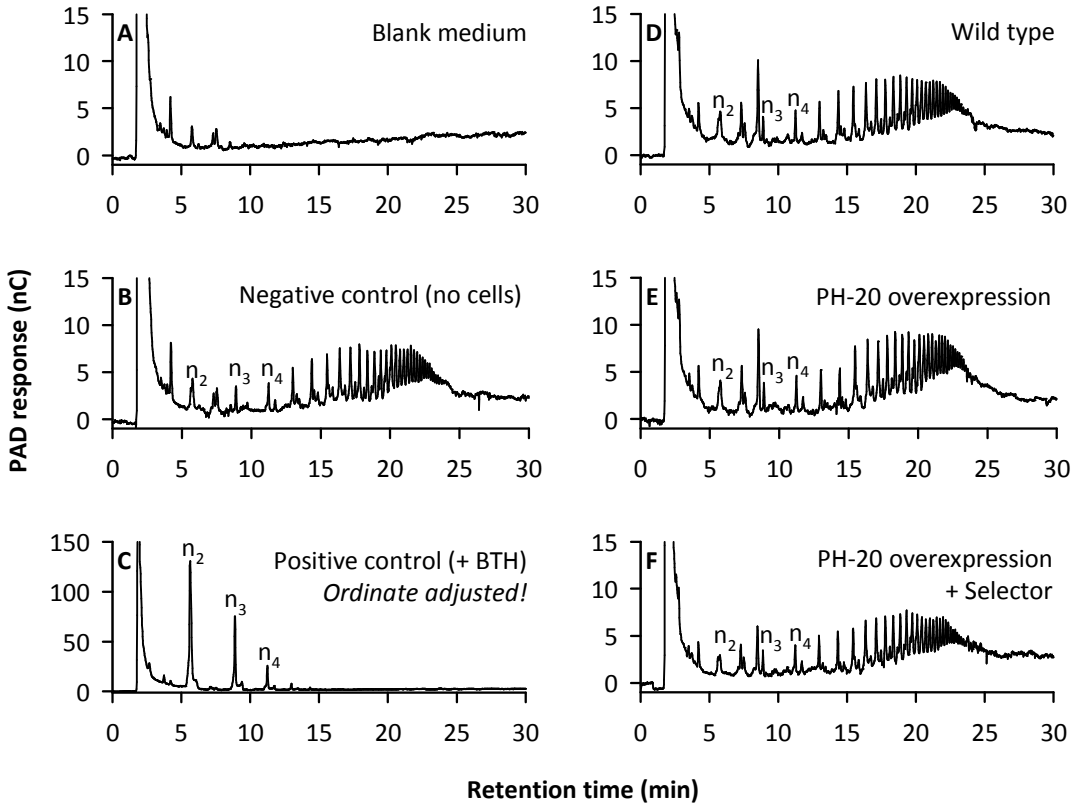

Figure 9.11: HPAEC–PAD of cell culture media from SK-MEL-3 cells, supplemented with 1 mg/mL of hyaluronan oligosaccharide mixture. Controls: blank medium (A), negative control without cells (B), positive control containing 1000 IU/mL of BTH (C). Conditioned media: wild type cells (D), PH-20 overexpressing clone without (E) and with addition of geniticin sulfate (F). Oligosaccharides (n_x) labeled according to the number of disaccharide units (*x*). Chromatography conditions: CarboPac™ PA200, 10 µL of sample (1:2 dilution) injected, 100 mM sodium hydroxide, gradient of 200–900 mM sodium acetate, 40 °C, 0.5 mL/min.

9.4 Summary and conclusion

The hyaluronan receptors CD44 and RHAMM were proven on the surface of a human microvasular endothelial cell line (HMEC-1) by flow cytometry. Further studies focused on the effect of hyaluronan and its degradation products on migration and proliferation of these cells. Thereby, an electric wound healing model was used. Cells on an electrode surface were killed by an alternating current pulse. Recovery of the cell layer by migration and proliferation was measured by electric cell–substrate impedance sensing (ECIS). ECIS

was also successfully applied in combination with the conventional crystal violet assay to determine cell proliferation.

Hyaluronan and a low molecular weight hyaluronan oligosaccharide mixture exhibited no or only slight inhibitory effects. At higher concentrations of the oligosaccharide mixture, acidic pH was identified as the reason for reduced cell proliferation. In good accordance with previous studies by Banerjee and Toole,[30] strong inhibition by 1 mg/mL (≈ 865 µM) of the hyaluronan hexasaccharide (n_3) was observed in both, the wound healing and the proliferation experiment. Considering a common hypothesis, it may be assumed that monovalent binding of n_3 (present at high concentrations) thereby prevents polyvalent binding of hyaluronan to its receptors on the cell surface.[33] By contrast, hyaluronan oligosaccharides are often reported to stimulate endothelial cell proliferation and angiogenesis.[3, 4, 27]

From analysis of wound material and conditioned cell culture media it may be doubted that distinct oligosaccharides are produced in relevant concentrations *in vivo*. In a dynamic process of anabolic and catabolic hyaluronan metabolism, the portion of the smallest oligosaccharides must be assumed to be far below the tested concentration of 1 mg/mL. Supplementation of cell culture media with an oligosaccharide mixture did not reveal any changes in size distribution of the saccharides even when hyaluronidase overexpressing cells were cultured in these media, indicating no or only extremely low hyaluronidase activity in the environment of the cells at physiological pH. However, applicability of HPAEC–PAD on samples of wound material and cell culture media was proven.

Nevertheless, biological processes like angiogenesis and wound healing are much more complex than reflected by *in vitro* assays. Moreover, the effects of hyaluronan oligosaccharides may vary not only in a size-dependent manner but also with regard to their concentration and the biological model. Hence, further studies in view of angiogenesis were performed, using the more complex test system of the chorioallantoic membrane (CAM) assay (*cf*. Chapter 10).

9.5 References

1. Chen, W. Y.; Abatangelo, G. Functions of hyaluronan in wound repair. *Wound Repair Regen.* **1999,** 7, 79-89.

2. Noble, P. W. Hyaluronan and its catabolic products in tissue injury and repair. *Matrix Biol.* **2002,** 21, 25-29.

3. West, D. C.; Kumar, S. The effect of hyaluronate and its oligosaccharides on endothelial cell proliferation and monolayer integrity. *Exp. Cell Res.* **1989,** 183, 179-196.

4. Gao, F.; Liu, Y.; He, Y.; Yang, C.; Wang, Y.; Shi, X.; Wei, G. Hyaluronan oligosaccharides promote excisional wound healing through enhanced angiogenesis. *Matrix Biol.* **2010,** 29, 107-116.

5. Matou-Nasri, S.; Gaffney, J.; Kumar, S.; Slevin, M. Oligosaccharides of hyaluronan induce angiogenesis through distinct CD44 and RHAMM-mediated signalling pathways involving Cdc2 and γ-adducin. *Int. J. Oncol.* **2009,** 35, 761-773.

6. Savani, R. C.; Cao, G.; Pooler, P. M.; Zaman, A.; Zhou, Z.; DeLisser, H. M. Differential involvement of the hyaluronan (HA) receptors CD44 and receptor for HA-mediated motility in endothelial cell function and angiogenesis. *J. Biol. Chem.* **2001,** 276, 36770-36778.

7. Slevin, M.; Krupinski, J.; Gaffney, J.; Matou, S.; West, D.; Delisser, H.; Savani, R. C.; Kumar, S. Hyaluronan-mediated angiogenesis in vascular disease: uncovering RHAMM and CD44 receptor signaling pathways. *Matrix Biol.* **2007,** 26, 58-68.

8. Hamberger, J. Characterization of mammalian hyaluronidase-2 activity and identification of inhibitors of *Streptococcal* hyaluronan lyase. PhD thesis, University of Regensburg, Regensburg, **2012**.

9. Giaever, I.; Keese, C. R. Monitoring fibroblast behavior in tissue culture with an applied electric field. *Proc. Natl. Acad. Sci. U. S. A.* **1984,** 81, 3761-3764.

10. Giaever, I.; Keese, C. R. A morphological biosensor for mammalian cells. *Nature* **1993,** 366, 591-592.

11. Wegener, J.; Keese, C. R.; Giaever, I. Electric cell–substrate impedance sensing (ECIS) as a noninvasive means to monitor the kinetics of cell spreading to artificial surfaces. *Exp. Cell Res.* **2000,** 259, 158-166.

12. Giaever, I.; Keese, C. R. Micromotion of mammalian cells measured electrically. *Proc. Natl. Acad. Sci. U. S. A.* **1991,** 88, 7896-7900.

13. Keese, C. R.; Bhawe, K.; Wegener, J.; Giaever, I. Real-time impedance assay to follow the invasive activities of metastatic cells in culture. *Biotechniques* **2002,** 33, 842-844, 846, 848-850.

14. Noiri, E.; Hu, Y.; Bahou, W. F.; Keese, C. R.; Giaever, I.; Goligorsky, M. S. Permissive role of nitric oxide in endothelin-induced migration of endothelial cells. *J. Biol. Chem.* **1997,** 272, 1747-1752.

15. Keese, C. R.; Wegener, J.; Walker, S. R.; Giaever, I. Electrical wound-healing assay for cells *in vitro*. *Proc. Natl. Acad. Sci. U. S. A.* **2004,** 101, 1554-1559.

16. Boregowda, R. K.; Appaiah, H. N.; Siddaiah, M.; Kumarswamy, S. B.; Sunila, S.; Thimmaiah, K. N.; Mortha, K.; Toole, B.; Banerjee, S. Expression of hyaluronan in human tumor progression. *J. Carcinog.* **2006,** 5, 2.

17. Stern, R. Hyaluronidases in cancer biology. *Semin. Cancer Biol.* **2008,** 18, 275-280.

18. Jarzyna, P. Preclinical investigations on the effect of the human hyaluronidase Hyal-1 on growth and metastasis of human colon carcinoma. PhD thesis, University of Regensburg, Regensburg, **2007**.

19. Ades, E. W.; Candal, F. J.; Swerlick, R. A.; George, V. G.; Summers, S.; Bosse, D. C.; Lawley, T. J. HMEC-1: establishment of an immortalized human microvascular endothelial cell line. *J. Invest. Dermatol.* **1992,** 99, 683-690.

20. Hay, R. J. The seed stock concept and quality control for cell lines. *Anal. Biochem.* **1988,** 171, 225-237.

21. Oettl, M. Biochemische Charakterisierung boviner testikulärer Hyaluronidase und Untersuchungen zum Einfluß von Hyaluronidase und Hyaluronsäure auf das Wachstum von Tumoren. PhD thesis, University of Regensburg, Regensburg, **2000**.

22. Bernhardt, G.; Reile, H.; Birnböck, H.; Spruß, T.; Schönenberger, H. Standardized kinetic microassay to quantify differential chemosensitivity on the basis of proliferative activity. *J. Cancer Res. Clin. Oncol.* **1992,** 118, 35-43.

23. Reile, H.; Birnböck, H.; Bernhardt, G.; Spruß, T.; Schönenberger, H. Computerized determination of growth kinetic curves and doubling times from cells in microculture. *Anal. Biochem.* **1990,** 187, 262-267.

24. Xu, Y.; Swerlick, R. A.; Sepp, N.; Bosse, D.; Ades, E. W.; Lawley, T. J. Characterization of expression and modulation of cell adhesion molecules on an immortalized human dermal microvascular endothelial cell line (HMEC-1). *J. Invest. Dermatol.* **1994,** 102, 833-837.

25. Trochon, V.; Mabilat, C.; Bertrand, P.; Legrand, Y.; Smadja-Joffe, F.; Soria, C.; Delpech, B.; Lu, H. Evidence of involvement of CD44 in endothelial cell proliferation, migration and angiogenesis *in vitro*. *Int. J. Cancer* **1996,** 66, 664-668.

26. Cao, G.; Savani, R. C.; Fehrenbach, M.; Lyons, C.; Zhang, L.; Coukos, G.; Delisser, H. M. Involvement of endothelial CD44 during *in vivo* angiogenesis. *Am. J. Pathol.* **2006,** 169, 325-336.

27. Gao, F.; Yang, C. X.; Mo, W.; Liu, Y. W.; He, Y. Q. Hyaluronan oligosaccharides are potential stimulators to angiogenesis via RHAMM mediated signal pathway in wound healing. *Clin. Invest. Med.* **2008,** 31, E106-116.

28. Richter, U.; Wicklein, D.; Geleff, S.; Schumacher, U. The interaction between CD44 on tumour cells and hyaluronan under physiologic flow conditions: implications for metastasis formation. *Histochem. Cell Biol.* **2012,** 137, 687-695.

29. Hamilton, S. R.; Fard, S. F.; Paiwand, F. F.; Tolg, C.; Veiseh, M.; Wang, C.; McCarthy, J. B.; Bissell, M. J.; Koropatnick, J.; Turley, E. A. The hyaluronan receptors CD44 and Rhamm (CD168) form complexes with ERK1,2 that sustain high basal motility in breast cancer cells. *J. Biol. Chem.* **2007,** 282, 16667-16680.

30. Banerjee, S. D.; Toole, B. P. Hyaluronan-binding protein in endothelial cell morphogenesis. *J. Cell Biol.* **1992,** 119, 643-652.

31. Underhill, C. B.; Toole, B. P. Binding of hyaluronate to the surface of cultured cells. *J. Cell Biol.* **1979,** 82, 475-484.

32. Ghatak, S.; Misra, S.; Toole, B. P. Hyaluronan oligosaccharides inhibit anchorage-independent growth of tumor cells by suppressing the phosphoinositide 3-kinase/Akt cell survival pathway. *J. Biol. Chem.* **2002,** 277, 38013-38020.

33. Toole, B. P.; Ghatak, S.; Misra, S. Hyaluronan oligosaccharides as a potential anticancer therapeutic. *Curr. Pharm. Biotechnol.* **2008,** 9, 249-252.

34. Cordo Russo, R. I.; Garcia, M. G.; Alaniz, L.; Blanco, G.; Alvarez, E.; Hajos, S. E. Hyaluronan oligosaccharides sensitize lymphoma resistant cell lines to vincristine by modulating P-glycoprotein activity and PI3K/Akt pathway. *Int. J. Cancer* **2008,** 122, 1012-1018.

35. Misra, S.; Ghatak, S.; Zoltan-Jones, A.; Toole, B. P. Regulation of multidrug resistance in cancer cells by hyaluronan. *J. Biol. Chem.* **2003,** 278, 25285-25288.

10 Studies on potential effects of hyaluronan and its oligosaccharides on angiogenesis in the CAM assay

10.1 Introduction

Hyaluronan is supposed to be responsible for the formation and maintenance of avascular regions in certain tissues.[1] In contrast, oligosaccharides from hyaluronan degradation were reported to induce angiogenesis in the chorioallantoic membrane (CAM) assay.[2, 3] Furthermore, a size-dependent effect of hyaluronan on endothelial cell proliferation was described.[4] In 2001, an article by Savani et al. proposed an involvement of the hyaluronan receptors CD44 and RHAMM in endothelial cell function and angiogenesis.[5] Moreover, Gao et al. reported on potential proangiogenic effects in wound healing models *in vitro*.[6] In a consecutive study, the same group confirmed these results by *in vivo* experiments on dermal wound healing in mice.[7] Also in rat skin, an increase in the number of blood vessels was observed after application of hyaluronan oligosaccharides.[8]

Due to their putative relevance in angiogenic processes, hyaluronan and its degradation products were also suggested to play an important role in tumor vascularization.[9, 10] In line with this assumption, hyaluronidase expression by tumor cells was reported to induce angiogenesis.[11] Thus, hyaluronidase isoenzymes might be involved in the regulation of normal and pathological angiogenic processes by formation of characteristic degradation products. Therefore, potential effects of hyaluronan and hyaluronan oligosaccharides were investigated in the chorioallantoic membrane (CAM) assay. This assay was chosen due to its feasibility and because there are reports in literature on similar studies.[2, 3] Moreover, the outcome of experiments with this system (in between *in vitro* and *in vivo* conditions) was expected to facilitate the decision if further *in vivo* studies were reasonable.

The CAM assay can be performed in various modifications and is applicable to studies of both induction and inhibition of angiogenesis.[12] After the CAM has formed from the allantois and the chorion epithelium on the fourth day of embryonic development, a phase of proliferation and differentiation of primitive blood vessels into a complex vascular system follows until day eight.[12] The rate of capillary formation remains extremely high until day eleven.[12] Within this period of CAM development, usually the assay is performed with six to ten days old embryos. In the following experiments, substances were applied to the CAM on the sixth day. Vascularization was evaluated on day seven or nine, respectively. Thereby, previously reported protocols for the CAM assay[13-16] were adopted with slight modifications.

10.2 Materials and methods

10.2.1 Test substances

Hyaluronan from *Streptococcus zooepidemicus* (Aqua Biochem, Dessau, Germany), Hyalo-Oligo with an average molecular weight below 10 kDa (Kewpie, also named Q. P. Corp., Tokyo, Japan), and the purified hexasaccharide (n_3, prepared as described in Chapter 5) were tested. Thalidomide (Calbiochem-Novabiochem, La Jolla, CA, USA), sodium dodecyl sulfate (Sigma-Aldrich, Munich, Germany), and basic fibroblast growth factor (bFGF, PeproTech, Rocky Hill, NJ, USA) served as reference substances. The growth factor was kindly provided by Dr. Jörg Teßmar (Department of Pharmaceutical Technology, University of Regensburg). 5(6)-Carboxyfluorescein, used as fluorescent marker, was purchased from Fluka (Buchs, Switzerland). Substances were dissolved in water purified with a Milli-Q system (Millipore, Eschborn, Germany) or phosphate buffered saline (PBS), respectively.

10.2.2 Eggs and incubation conditions

Fertilized chicken eggs were purchased from Brüterei Süd (Regenstauf, Germany). Eggshells were wiped with 70% ethanol to avoid contamination. Afterwards, the eggs were kept in an incubator (Hemel, Verl, Germany) at 80% relative humidity and 37 °C for three days. Lying in a horizontal position, the eggs were rotated several times.

10.2.3 Opening of the chicken eggs

On the third day, eggs were positioned vertically with the blunt side to the top. Eggs were left in this position for 30 min before they were opened as depicted in Figure 10.1. After the eggshell had been removed at the blunt side and the opened egg had been covered with a piece of plastic wrap, the eggs were further incubated at 37 °C until day six.

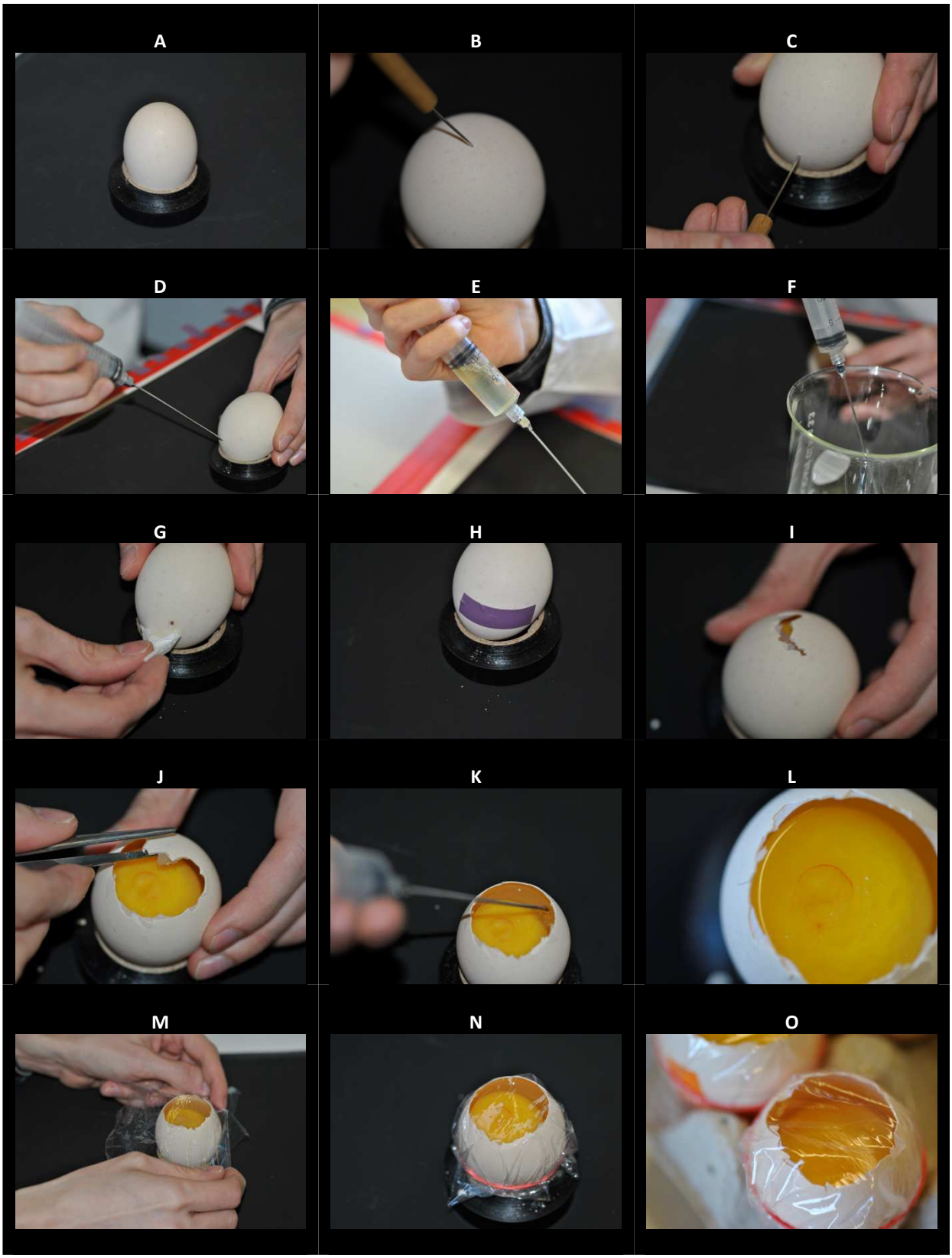

Figure 10.1: Opening of the eggs. The egg was positioned with the blunt side to the top (A). Afterwards, the eggshell was pierced at the blunt side (B) and in the lower third of the egg (C). Through the lower hole, 10–15 mL of albumen were aspired with a syringe (D–F). Residual albumen around the hole was wiped off (G) and the hole closed with a piece of adhesive tape (H). With a pair of tweezers the eggshell at the blunt side was removed carefully, starting from the hole at the top (I, J). If necessary, additional albumen was removed with the syringe (K). The opened egg (L) was covered with a piece of plastic wrap (M) which was additionally fixed with a rubber band (N, O).

10.2.4 Application of the test compounds

A 2.5% solution of pegGOLD Universal Agarose (Peqlab, Erlangen, Germany) was used to prepare pellets (Figure 10.2 B, C) or rings (Figure 10.2 G, H) as supports for the test compounds. On day six of the incubation period, 50 µg of the test substances (0.5 µg for bFGF) were administered to the agarose supports, which were positioned on the CAM. The exact procedure is illustrated by the photographs in Figure 10.2.

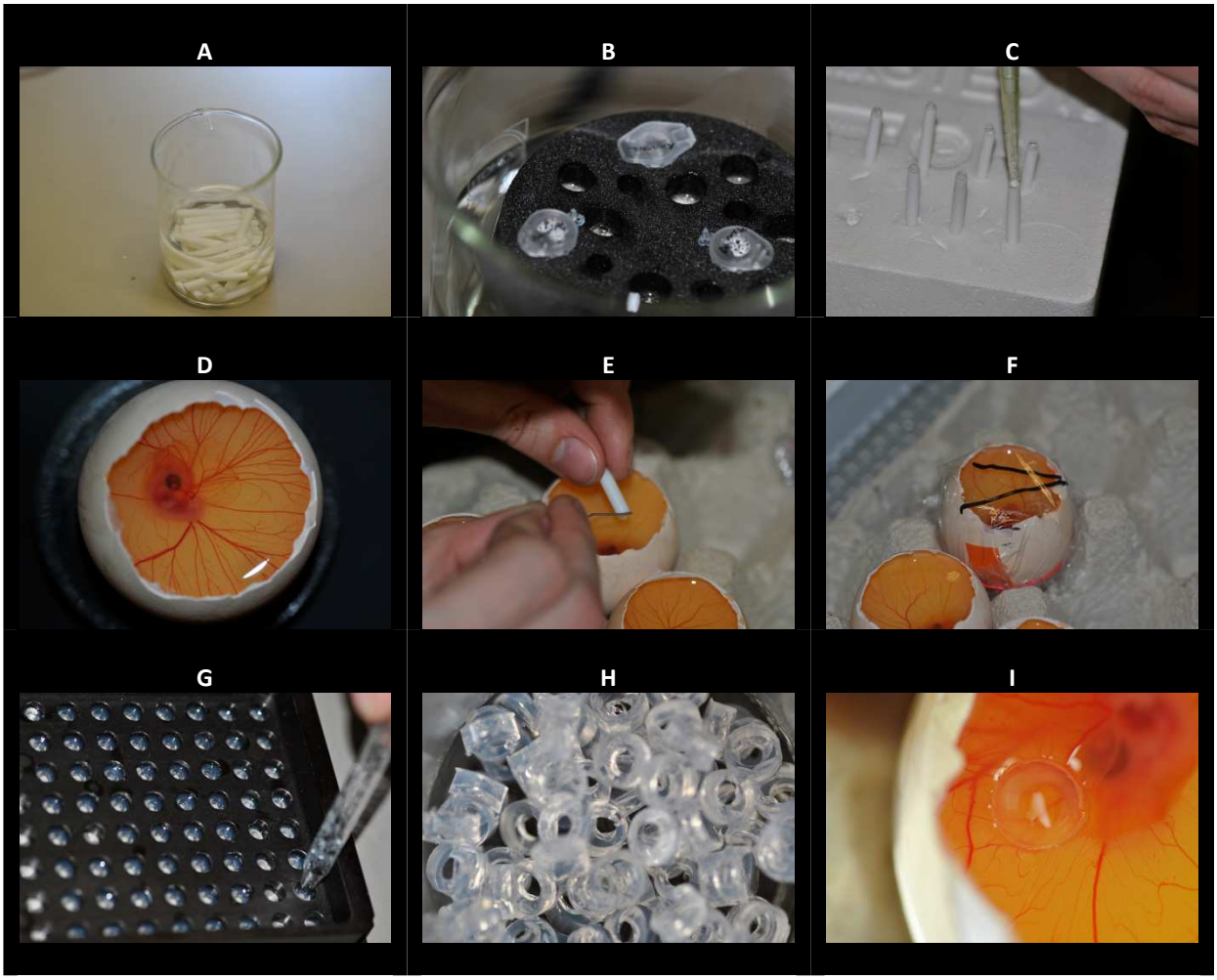

Figure 10.2: Application of test compounds. For the preparation of pellets, polytetrafluoroethylene sticks were sanitized with 70% ethanol (A). Agarose was dissolved at 60 °C together with heat-stable test compounds (B). Heat-sensitive substances were added after complete dissolution of agarose. 10 µL of the agarose solution were pipetted on top of the fixed sticks (C). On day six, the CAM was clearly visible (D). The agarose pellet was carefully placed on the membrane (E). Eggs were covered with a labeled piece of plastic wrap (F). Alternatively, agarose rings were prepared in a metal plate by filling the holes with agarose and subsequent punching (G). The rings (H) could equally be placed on the CAM and filled with a test solution (I).

When using agarose pellets, heating of the test substances cannot be avoided. Heat-sensitive substances were added after dissolving the agarose at 60 °C. When applying the biopolymer hyaluronan in a pellet, the polysaccharide is most probably enclosed in the gel structure and will show only minimal diffusion. Consequently, the biological effect might be

biased. For this reason, agarose rings were preferred for the investigation of hyaluronan and the corresponding oligosaccharides. For the preparation of these rings (*cf*. Figure 10.2 G, H), 30–50 µL of agarose solution were pipetted into the holes of a metal plate which had been closed with adhesive foil from one side. The plate was comparable to common 96-well plates in size and shape. After punching and after removing the foil, the obtained rings could be easily pressed out of the plate. Rings prepared from 50 µL of agarose solution were preferred due to higher stability. By the use of agarose rings, 10 µL of test solution or suspension (in the case of thalidomide) could be placed on the CAM without any heating of the test compound. After substance application, eggs were again incubated until day seven or day nine, respectively.

10.2.5 Stereo microscopy and evaluation score

On day seven or day nine of incubation, the vascularization of the CAM was assessed by stereo microscopy with an Olympus SZ-III zoom stereo microscope (Olympus, Tokyo, Japan). To optimize the distance for convenient handling and to improve the illumination, the stereo microscope was equipped with an accessory lens (factor: 0.5) and an LED ring light with four lighting zones (Müller Optronics, Erfurt, Germany). Prior to stereo microscopy, long-life cream from a local LIDL store (Regensburg, Germany) was injected underneath the CAM to increase contrast (Figure 10.3). The vascularization of the membrane was evaluated according to a score discussed below (*cf*. Section 10.3.4).

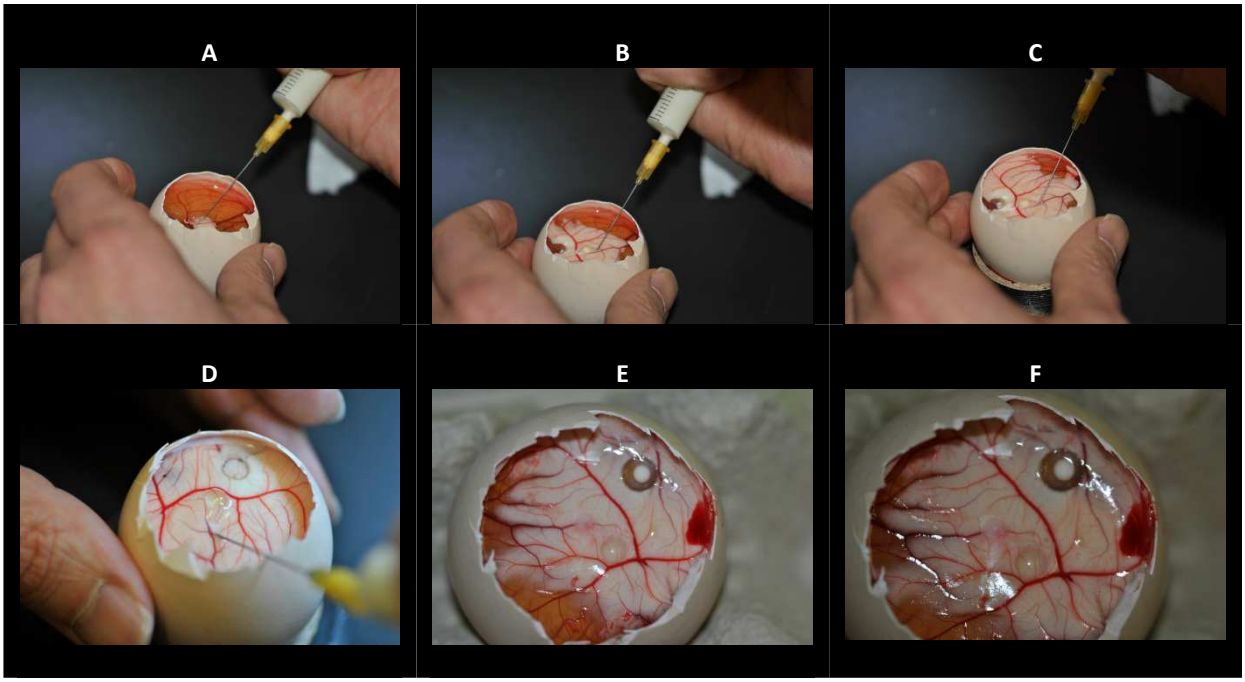

Figure 10.3: Preparation of eggs for stereo microscopy. Long-life cream was injected underneath the CAM to increase contrast. Blood vessels became clearly visible on the white background.

10.2.6 Preparation, staining, and microscopy of chorioallantoic membranes

Representative membranes from all groups were dissected and placed in Bouin's solution for fixation. The CAM was embedded in paraffin, cut with a microtome, and stained with hematoxilin and eosin (H&E stain). The preparations were then microscopically examined with regard to histological peculiarities, especially concerning blood vessels.

10.3 Results and discussion

10.3.1 Suitability of agarose rings

A solution of the fluorescent dye 5(6)-carboxyfluorescein was placed in the middle of an agarose ring to study its ability to hold applied test substances *in situ*. Only little spreading into the agarose gel and along larger blood vessels was observed, proving the suitability of agarose rings for this test system (Figure 10.4).

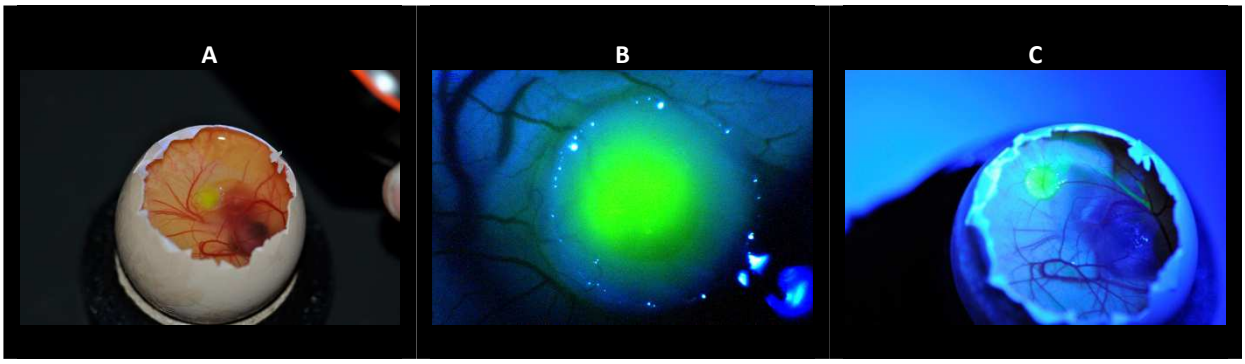

Figure 10.4: Evaluation of agarose rings for substance application. 5(6)-Carboxyfluorescein was placed in the agarose ring (A). A microscopic image (illuminated with blue light) clearly shows the flurorescence inside the ring (B). Later, the fluorescent dye was also detected in the middle of the ring, in the agarose gel, and associated with larger blood vessels (C).

10.3.2 Normal chorioallantoic membranes

On day seven (Figure 10.5 A) as well as on day nine (Figure 10.5 B, C), the normal CAM was characterized by uniform vascularization. Homogeneously branched blood vessels were found outside and inside the PBS-filled agarose ring (Figure 10.5 C). Figure 10.5 B and Figure 10.5 C show the same egg before and after injection of long-life cream, respectively. By comparison of the two images, two beneficial effects of this procedure become obvious. Apart from increasing the contrast, the injection of the contrast agent underneath the CAM facilitates the discrimination between blood vessels of the yolk and the CAM.

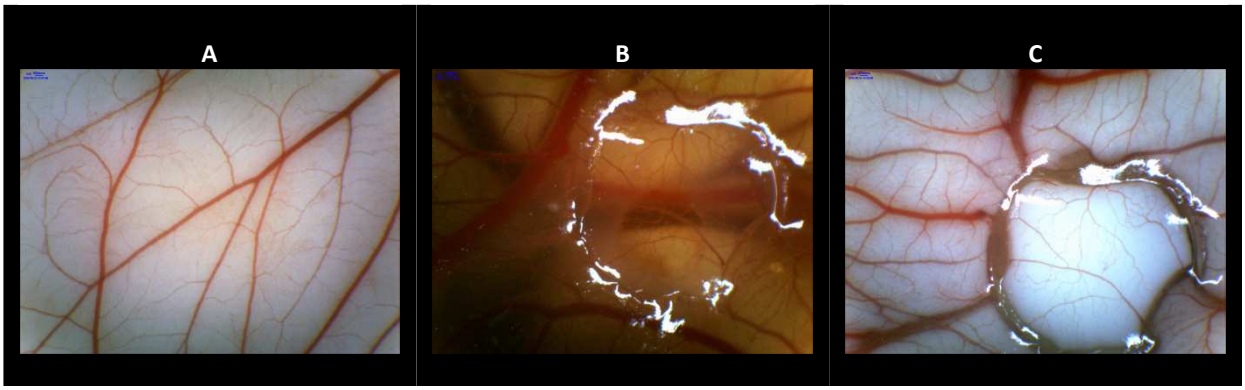

Figure 10.5: The normal CAM on day seven (A) and on day nine with PBS-filled agarose ring (B). Comparison of the same egg before (B) and after injection of long-life cream (C) demonstrates the beneficial effect of the increased contrast and better discrimination between blood vessels of yolk and CAM.

10.3.3 Irritation of the chorioallantoic membrane

Sodium dodecyl sulfate (SDS) served as model substance to cause irritation of the CAM. 50 µg of SDS were applied using agarose pellets. On day seven, wheel-shaped irritations with central necroses, accompanied by hemorrhages, were observed (Figure 10.6 A). Zooming in on the necrotic structure, a ring of blood vessels around the necrotic center was clearly visible (Figure 10.6 B). In some cases, necrosis without a pronounced ring structure occurred (Figure 10.6 C).

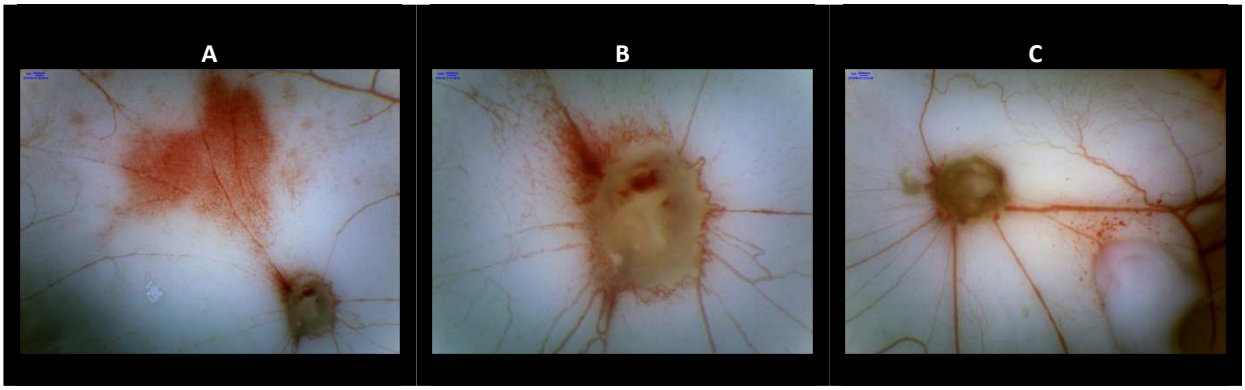

Figure 10.6: CAM irritation caused by SDS. Overview (A) and detailed image (B) of a wheel-shaped irritation with central necrosis, example of a necrotic area without pronounced blood vessel ring (C).

10.3.4 Scoring of effects

The reference substance thalidomide led to a reduction of blood vessel density. The assignment of inhibition score values, as described in literature,[13-16] was performed with the help of expert knowledge, contributed by PD Dr. Dietrich Paper (personal communication). In contrast to literature,[13] score values of 0.5 were not set 0, when calculating the overall scores. Typical examples for the assignment of the individual score values are depicted in (Figure 10.7). The score value 0 was assigned to a normal CAM with homogeneous

vascularization (example from day seven, A). Figure 10.7 B and Figure 10.7 C show inhibition of angiogenesis on day seven (after application of pellets) with score values of 1 and 2, respectively. Examples from day nine (rings) had score values of 0.5 due to slightly reduced vascularization inside the ring (Figure 10.7 D), 1 (Figure 10.7 E), and 2 (Figure 10.7 F). The highest score value (2) was used when large areas inside and around the ring were avascular. A value of 0.5 was used in case of abnormal shapes of blood vessels or slightly reduced densities, lacking avascular regions.

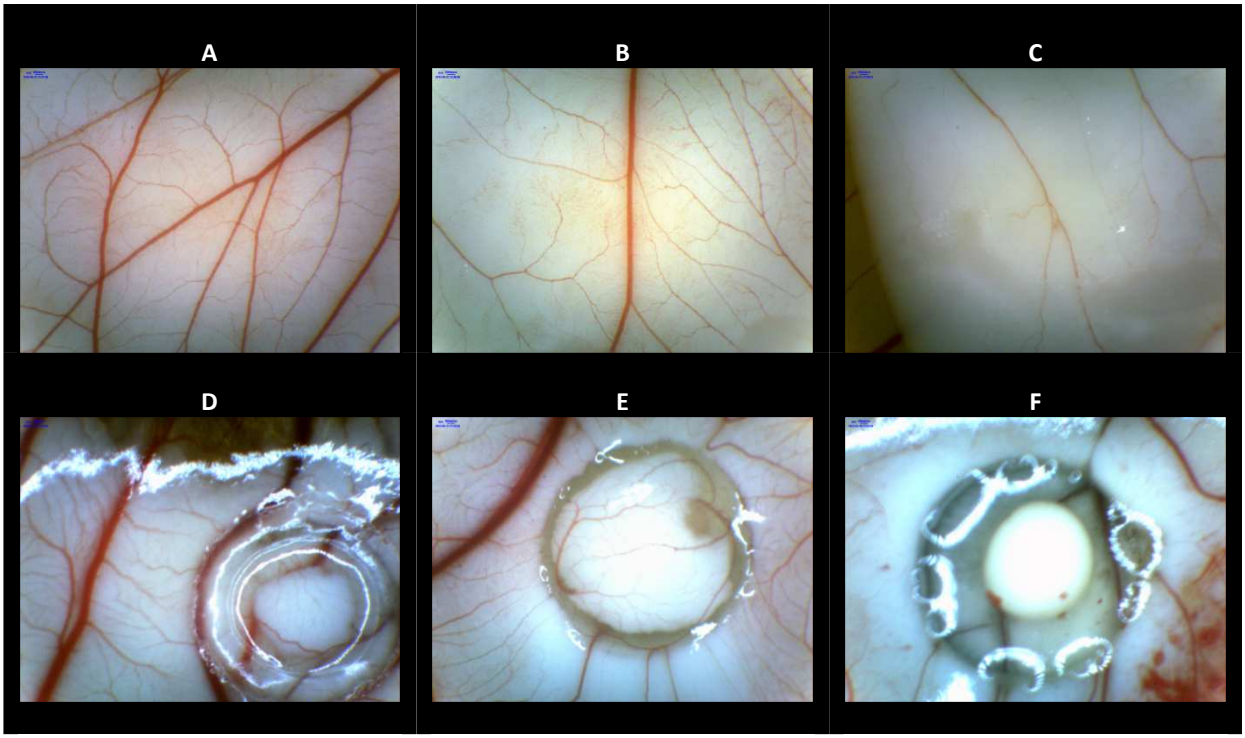

Figure 10.7: Assignment of score values. Examples from day seven: score 0 (A), score 1 (B), and score 2 (C). Examples from day nine: score 0.5 (D), score 1 (E), and score 2 (F).

10.3.5 Impact of hyaluronan and hyaluronan oligosaccharides on angiogenesis

The influence of hyaluronan and hyaluronan oligosaccharides on angiogenesis was investigated in two ways. In the first study, purified water was used as solvent for the test substances. In a second approach, PBS was used instead to exclude irritation caused by pH or hypoosmolarity. The results were heterogeneous. Overall, there was no evidence for induction of angiogenesis, not even in the bFGF group. Particularly, wheel-shaped structures, as described by West et al.,[2] were not observed at all. Hence, further evaluation was focused on the reduction of vascularization and defects in blood vessel formation. For this purpose, the score described in Section 10.3.4 was applied. The results are presented in Figure 10.8. The score values for all substances are summarized in Figure 10.8 A–F. For each series of eggs, total scores were calculated. Each score value was multiplied by the respective number

of eggs. The sum of these products was divided by the total number of living eggs in the series (Figure 10.8 G).

In comparison to PBS, score values were higher for water. Although the eggs in the two experiments might also have differed in blood vessel formation, this indicates some additional effect of the solvent water. Interestingly, the total score was identical for both experiments in the group with high molecular weight hyaluronan. Possibly, the water-binding properties of hyaluronan reduced an irritation of the CAM. However, more reliable results were probably obtained with PBS as solvent. Focusing on these values, the total score was considerably increased for both, thalidomide and high molecular weight hyaluronan, compared to all other groups. Low molecular weight hyaluronan oligosaccharide mixture, purified hexasaccharides (n_3), and bFGF yielded values comparable to blank. Although there was no clear evidence on the impact of hyaluronan on angiogenesis in this experiment, high molecular weight hyaluronan seemed antiangiogenic to some extent. The formation of avascular zones in the presence of high molecular weight hyaluronan is in good accordance with observations by Feinberg and Beebe.[1] In contrast, induction of CAM vascularization, previously reported for hyaluronan oligosaccharides,[2, 3] was not confirmed by our experiments. Moreover, histological examination of CAM preparations did not reveal any peculiarities (not shown).

Finally, the failure of bFGF as a proangiogenic control deserves a closer look. It might be speculated that the used human growth factor is not suitable for the hen's egg system. However, the rate of vascularization was extremely high in the respective period of CAM development. Therefore, the sensitivity of a biological system, optimized by nature, to identify potential proangiogenic stimuli (both, growth factors and oligosaccharides) can be expected to be low. In addition, although generally accepted, visual assessment might be too imprecise for evaluation.

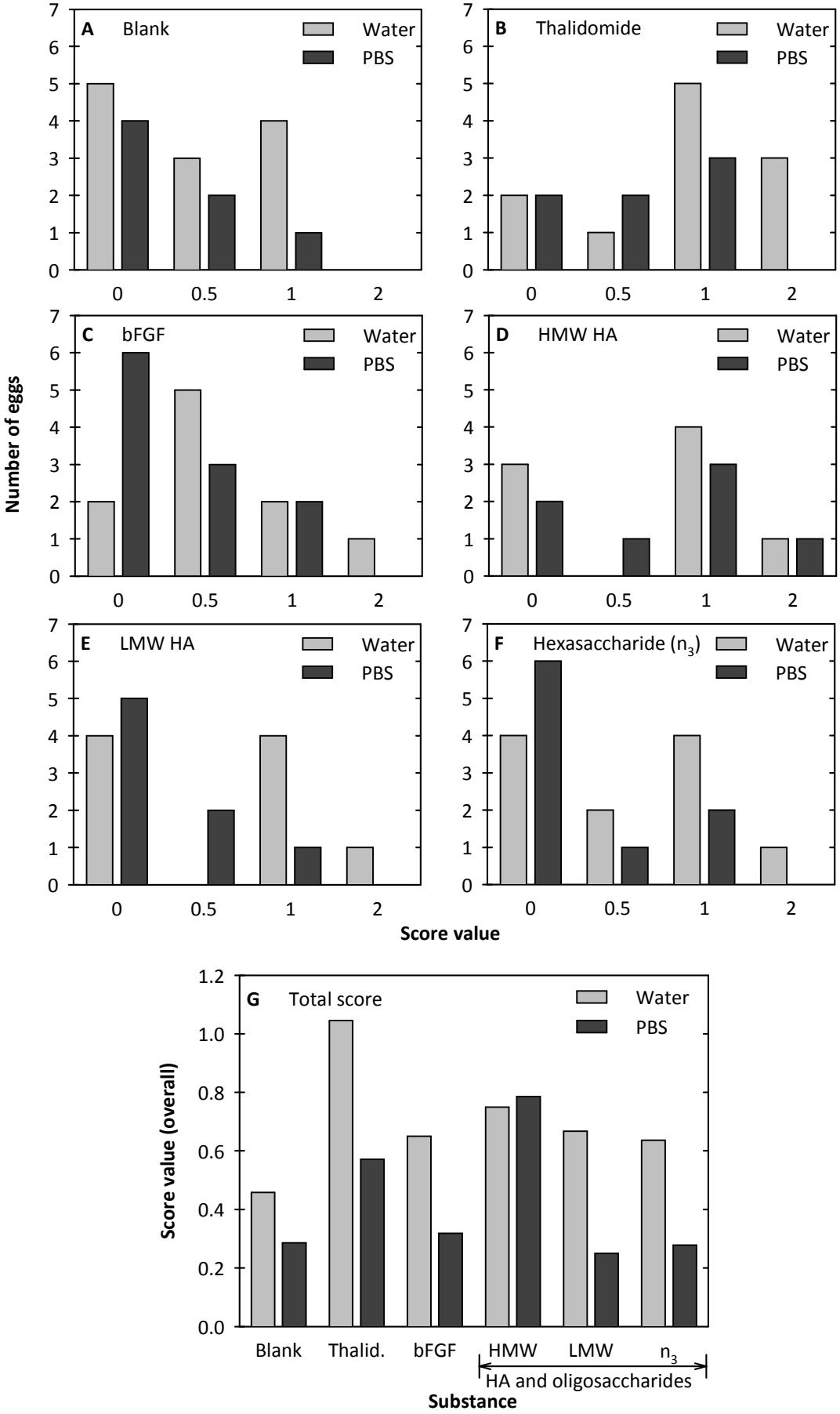

Figure 10.8: Score values for solvent (water/PBS) alone (A), thalidomide (B), bFGF (C), high molecular weight hyaluronan (HMW HA, D), oligosaccharide mixture (LMW HA, E), and hexasaccharide (n_3, F). Total score (G).

10.4 Summary and conclusion

The chorioalantoic membrane (CAM) assay was used for studies on the potential size-dependent impact of hyaluronan and its oligosaccharides on angiogenesis. Instead of pellets, agarose rings were used to administer the test compounds. The application of a fluorescent dye thereby proved the ability of the rings to hold the test solution *in situ*.

Our experiments raised doubts regarding the reported proangiogenic effect of hyaluronan oligosaccharides.[2, 3] Wheel-shaped structures, very roughly comparable to the description by West et al.,[2] were only observed for unspecific irritation of the CAM by sodium dodecyl sulfate. In contrast, high molecular weight hyaluronan tended to induce avascular regions in a higher number of eggs compared to the controls. Of course, this observation is no proof of antiangiogenic effects by the polysaccharide. Nevertheless, this conclusion would be in accordance with literature.[1] However, the poor outcome of this study does not justify subsequent animal experiments.

10.5 References

1. Feinberg, R. N.; Beebe, D. C. Hyaluronate in vasculogenesis. *Science* **1983,** 220, 1177-1179.

2. West, D. C.; Hampson, I. N.; Arnold, F.; Kumar, S. Angiogenesis induced by degradation products of hyaluronic acid. *Science* **1985,** 228, 1324-1326.

3. Cui, X.; Xu, H.; Zhou, S.; Zhao, T.; Liu, A.; Guo, X.; Tang, W.; Wang, F. Evaluation of angiogenic activities of hyaluronan oligosaccharides of defined minimum size. *Life Sci.* **2009,** 85, 573-577.

4. West, D. C.; Kumar, S. The effect of hyaluronate and its oligosaccharides on endothelial cell proliferation and monolayer integrity. *Exp. Cell Res.* **1989,** 183, 179-196.

5. Savani, R. C.; Cao, G.; Pooler, P. M.; Zaman, A.; Zhou, Z.; DeLisser, H. M. Differential involvement of the hyaluronan (HA) receptors CD44 and receptor for HA-mediated motility in endothelial cell function and angiogenesis. *J. Biol. Chem.* **2001,** 276, 36770-36778.

6. Gao, F.; Yang, C. X.; Mo, W.; Liu, Y. W.; He, Y. Q. Hyaluronan oligosaccharides are potential stimulators to angiogenesis via RHAMM mediated signal pathway in wound healing. *Clin. Invest. Med.* **2008,** 31, E106-116.

7. Gao, F.; Liu, Y.; He, Y.; Yang, C.; Wang, Y.; Shi, X.; Wei, G. Hyaluronan oligosaccharides promote excisional wound healing through enhanced angiogenesis. *Matrix Biol.* **2010,** 29, 107-116.

8. Sattar, A.; Rooney, P.; Kumar, S.; Pye, D.; West, D. C.; Scott, I.; Ledger, P. Application of angiogenic oligosaccharides of hyaluronan increases blood vessel numbers in rat skin. *J. Invest. Dermatol.* **1994,** 103, 576-579.

9. West, D. C.; Kumar, S. Tumour-associated hyaluronan: a potential regulator of tumour angiogenesis. *Int. J. Radiat. Biol.* **1991,** 60, 55-60.

10. Rooney, P.; Kumar, S.; Ponting, J.; Wang, M. The role of hyaluronan in tumour neovascularization (review). *Int. J. Cancer* **1995,** 60, 632-636.

11. Liu, D.; Pearlman, E.; Diaconu, E.; Guo, K.; Mori, H.; Haqqi, T.; Markowitz, S.; Willson, J.; Sy, M. S. Expression of hyaluronidase by tumor cells induces angiogenesis *in vivo*. *Proc. Natl. Acad. Sci. U. S. A.* **1996,** 93, 7832-7837.

12. Ribatti, D.; Vacca, A.; Roncali, L.; Dammacco, F. The chick embryo chorioallantoic membrane as a model for *in vivo* research on angiogenesis. *Int. J. Dev. Biol.* **1996,** 40, 1189-1197.

13. Bürgermeister, J. Wirkmechanistische Untersuchungen antiangiogener Galactansulfate. PhD thesis, University of Regensburg, Regensburg, **2002**.

14. Bürgermeister, J.; Paper, D. H.; Vogl, H.; Linhardt, R. J.; Franz, G. LaPSvS1, a (1→3)-β-galactan sulfate and its effect on angiogenesis *in vivo* and *in vitro*. *Carbohydr. Res.* **2002,** 337, 1459-1466.

15. Käsbauer, C. W.; Paper, D. H.; Franz, G. Sulfated β-(1→4)-galacto-oligosaccharides and their effect on angiogenesis. *Carbohydr. Res.* **2001,** 330, 427-430.

16. Paper, D. H.; Vogl, H.; Franz, G.; Hoffman, R. Defined carrageenan derivatives as angiogenesis inhibitors. *Macromol. Symp.* **1995,** 99, 219-225.

11 Summary and outlook

11.1 Method development

Hyaluronan and hyaluronan oligosaccharides, which are produced when the polysaccharide is enzymatically degraded by the action of hyaluronidases, are supposed to have various size-dependent biological effects. To study the (patho)physiological role of these oligosaccharides, appropriate analytical and bioanalytical methods are a prerequisite. Hence, hyphenated chromatographic and electrophoretic techniques were developed and optimized. Focusing on small oligosaccharides, these hyphenated methods complement the conventional approaches (Figure 11.1).

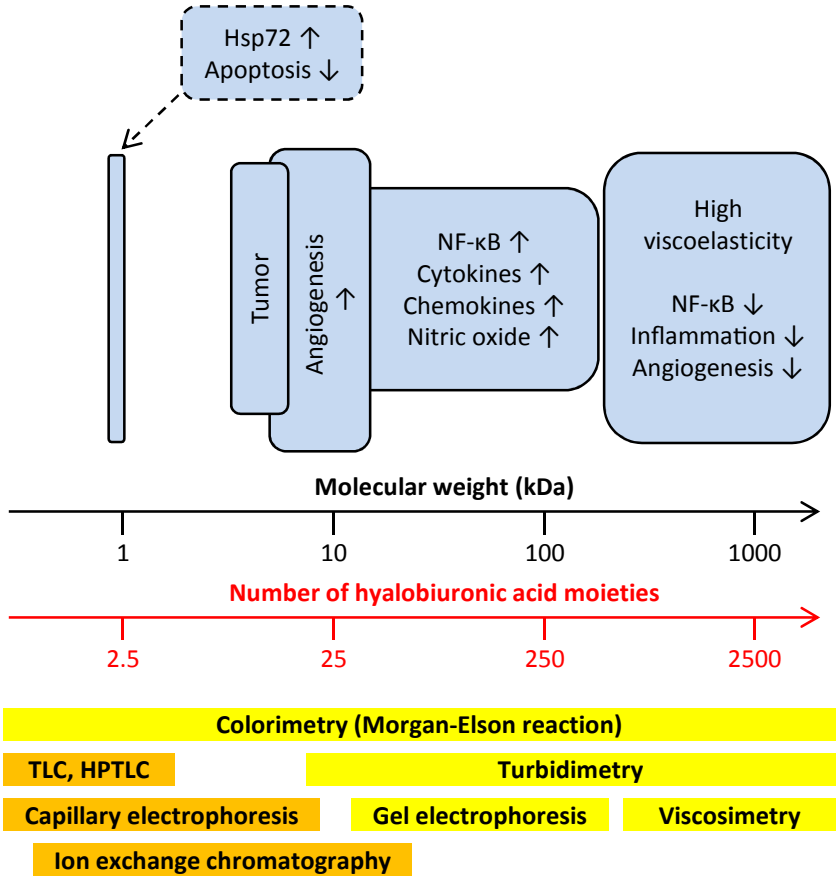

Figure 11.1: Hyaluronan and hyaluronan oligosaccharides: their proposed size-dependent biological effects and the respective analytical approaches. Methods developed and optimized in this work are highlighted in orange. Modified from: Asari, A. Novel functions of hyaluronan oligosaccharides. *Glycoforum* **2005.** (http://www.glycoforum.gr.jp/science/hyaluronan/HA12a/HA12aE.html).

Each method has its particularities, predestining a technique for a certain size range of the oligosaccharides as well as for specific analytical problems (Table 11.1).

Table 11.1: Suggested analytical methods depending on the number of hyalobiuronic acid moieties.

Hyalobiurionic acid moieties	Method	Detection	Particularities
All	Morgan-Elson	Colorimetry	No information on size distribution
> 1500	Viscosimetry	Outflow time	Sensitive for changes in average size, no information on size distribution
25–80	Gel electrophoresis	Alcian blue/silver staining	Suitable for polysaccharide to medium-sized oligosaccharides
> 20	Turbidimetry	Light scattering	No information on size distribution
2–25	Anion exchange chromatography	Pulsed amperometry	High sensitivity, wide range of oligosaccharides
1–20	Capillary zone electrophoresis	Far-UV, ESI-TOF-MS	Fast at-line analysis and mass information using MS, low sample volume
1–4	HPTLC, TLC	Reflectometry, MS coupling	Simple procedure, parallel analysis of multiple samples

Capillary zone electrophoresis coupled to time-of-flight mass spectrometry (CZE–ESI-TOF-MS) is suited for oligosaccharides comprising up to 20 disaccharide moieties (n_1–n_{20}). The method was optimized with regard to fast separations. Together with minimal sample pretreatment, this allows for assessment of hyaluronidase activity quasi in real-time. MS also enables the unambiguous identification of substrates and products. Moreover, CZE–ESI-TOF-MS with short capillaries requires only very small sample volumes (about 990 pL). Hence, this method should be chosen if only small amounts of sample solution are available (*cf*. Chapter 3).

High performance anion exchange chromatography with pulsed amperometric detection (HPAEC–PAD) was optimized for the sensitive determination of oligosaccharides comprising 2–25 hyalobiuronic acid moieties (n_2–n_{25}). Oligosaccharides with higher degree of polymerization can also be detected at a lower resolution. Hence, HPAEC and gel electrophoresis perfectly complement each other for studying hyaluronan degradation covering a broad range of differently sized products. High sensitivity with an LOD of 0.2–0.3 pmol (depending on the analyte) for oligosaccharides consisting of 2–4 disaccharide units (n_2–n_4) recommends the method for determination of low concentrations (*cf*. Chapter 4).

High performance thin layer chromatography (HPTLC) is most convenient for rapid quality control of purified oligosaccharides (n_2–n_4). Using a reagent-free derivatization of amino-modified silica, HPTLC enabled the rapid densitometric quantification. Coupling of thin layer chromatography (TLC) on normal phase with mass spectrometry was successfully applied to the qualitative analysis of these samples (*cf*. Chapter 5)

Hence, together with conventional techniques, the developed approaches solve a broad variety of analytical problems associated with the biological role of hyaluronan and hyaluronidases. To develop these methods further, future work may focus on automation especially of the CZE–ESI-TOF-MS protocol. Moreover, application of the presented techniques to other analytes of interest (e. g. chondroitin sulfates) should be possible.

11.2 *In vitro* studies on hyaluronidases

Enzymological *in vitro* characterization of hyaluronidases is a prerequisite for understanding the particularities of different isoenzymes. However, conclusions with regard to the biological role of these enzymes *in vivo* remain speculative without knowledge of the specific substrates, the degradation mechanisms, and the products. Thus, the newly developed analytical methods were applied to the study of hyaluronidases of different origins. HPAEC–PAD proved to be ideal for monitoring the time-dependent degradation of a low molecular weight hyaluronan oligosaccharide mixture. By contrast, fast CZE–ESI-TOF-MS was preferably used for at-line analysis of the degradation of purified oligosaccharides.

Product spectra of bovine testicular hyaluronidase (BTH) and bacterial hyaluronidase from *Streptococcus agalactiae*, strain 4755, were compared (*cf*. Chapter 6). BTH exhibited a complex degradation profile of hydrolysis and transglycosylation reactions, leading to a mixture of different oligosaccharides as end products. With the bacterial enzyme, the unsaturated disaccharide (n_1*) accumulated, other oligosaccharides were liberated intermediately during the reaction. Thereby, the unsaturated tetrasaccharide (n_2*) seemed to be preferred. By analogy with n_2*, the saturated tetrasaccharide (n_2) was also accepted as substrate. Hence, this minimal substrate was used for determination of kinetic parameters according to the Michaelis-Menten theory for *Streptococcus agalactiae* hyaluronidase. The minimal substrate was digested at pH = 5.0, using 5 IU/mL (according to the declaration of the supplier) of the enzyme. Samples were analyzed by HPAEC–PAD. K_m = 923 ± 106 µM and v_{max} = 3.68 ± 0.20 nmol/min were determined.

Recombinant human Hyal-1 (rhHyal-1), PH-20 (rhPH-20), and PEGylated PH-20 (PEG-rhPH-20) were characterized with regard to pH profiles and degradation of hyaluronan oligosaccharides (*cf*. Chapter 7). All three enzymes had optima at acidic pH values of 4.0 (rhPH-20 and PEG-rhPH-20) and 3.5 (rh-Hyal-1), respectively. No assay-dependent differences were observed. Degradation of hyaluronan oligosaccharides was similar to BTH. Nevertheless, differences with regard to the product spectra, depending on pH, were identified.

Testing of L-ascorbic acid-6-*O*-hexadecanoate (vitamin C palmitate), indomethacin, and diclofenac (within a concentration range of 50–1000 µM) with regard to inhibitory effects on rhHyal-1 and rhPH-20 (*cf*. Chapter 7) revealed only very weak inhibition. Only vitamin C palmitate showed IC_{50} values of 156 ± 14 µM and 168 ± 48 µM, depending on the assay conditions. As increasing concentration of the enzyme led to dramatic loss in maximum inhibition, evaluable curves were only obtained at low enzyme activity. Necessarily, long incubation periods were required for the assay.

As the applicability of HPAEC–PAD and CZE–ESI-TOF-MS for *in vitro* studies on hyaluronidase isoenzymes has been proven, these methods can easily be used for the characterization of hyaluronidases from other sources like venoms from snakes and hymenoptera, additional bacterial species (especially pathogens), or isolates from human tissues. Moreover, determination of the Michaelis-Menten kinetics of the different isoenzymes is necessary for characterization of both the enzymes and the inhibitors. However, potent and selective inhibitors for human hyaluronidases, needed as pharmacological tools as well as potential drugs, are still lacking. Hence, the search for these substances is still a challenging task.

11.3 Bioanalytical and biological investigations

In view of the biological role of hyaluronan, hyaluronan oligosaccharides, and hyaluronidases, synovial fluid samples were analyzed (*cf*. Chapter 8). Although the samples differed with regard to hyaluronan content, size distribution of hyaluronan, hyaluronidase activity, and viscoelastic properties, no correlation of the different parameters could be identified. Nevertheless, HPAEC–PAD and CZE–ESI-TOF-MS were proven to be suitable for the determination of hyaluronan and hyaluronan oligosaccharides from a biological matrix. In combination with colorimetry, gel electrophoresis, rheology, and zymography a broad characterization of the samples was possible.

Finally, hyaluronan, a hyaluronan oligosaccharide mixture, and purified oligosaccharides were used for biological investigations in different assays. By electrical cell–substrate impedance sensing (ECIS), an inhibitory effect of the hexasaccharide (n_3) on recovery of electrode coverage with endothelial cells (HMEC-1) after an electrical wounding pulse was observed. Similar effects were found in an ECIS cell proliferation experiment and in the crystal violet assay (*cf*. Chapter 9). However, the hexasaccharide (n_3) was applied at 1 mg/mL (≈ 865 µM). It may be doubted that such high concentrations occur under physiological conditions. Native hyaluronan and a more complex mixture of oligosaccharides (both 1 mg/mL) had no effects on endothelial cells. At very high concentrations, the oligosaccharide mixture led to an acidification of the culture media.

As cell migration and proliferation are important in wound healing processes, single samples of wound exudate and debris were analyzed by HPAEC–PAD and zymography. Neither small oligosaccharides nor hyaluronidase activity were proven. In view of their putative role in hyaluronan oligosaccharide signaling, expression of hyaluronan receptors RHAMM and CD44 by different cell lines was analyzed using flow cytometry (*cf*. Chapter 9).

Oligosaccharides added to cell culture media were not degraded, even during culture of hyaluronidase overexpressing cells (*cf*. Chapter 9). Hence, it may be concluded that no considerable amounts of hyaluronidases were secreted into the media or that activity at physiological pH was too low to affect the size distribution of a supplemented oligosaccharide mixture.

A chorioallantoic membrane (CAM) assay was performed (*cf*. Chapter 10) to study putative effects of hyaluronan oligosaccharides on angiogenesis. Oligosaccharides had no effect, whereas there was a weak tendency to antiangiogenesis in the presence of high molecular weight hyaluronan. Nevertheless, further studies would be necessary to verify this observation.

Hyaluronan and its degradation products are supposed to be involved in manifold (patho)physiological processes. Hence, cellular assays and other biological tests will always be necessary to elucidate their biological role (e. g. in cancer or inflammation). The analytical approaches presented in this work are valuable tools for quality control of purified oligosaccharides for biological assays as well as for the determination of hyaluronan and hyaluronan oligosaccharides (resulting from hyaluronidase activity) in biological matrices.

Eidesstattliche Erklärung

Ich erkläre hiermit an Eides statt, dass ich die vorliegende Arbeit ohne unzulässige Hilfe Dritter und ohne Benutzung anderer als der angegebenen Hilfsmittel angefertigt habe; die aus anderen Quellen direkt übernommenen Daten und Konzepte sind unter Angabe des Literaturzitats gekennzeichnet.

Einige der experimentellen Arbeiten wurden in Zusammenarbeit mit anderen Institutionen und Personen durchgeführt. Entsprechende Vermerke finden sich in den betreffenden Kapiteln. Eine detaillierte Auflistung aller Kooperationen enthält zudem der Abschnitt „Acknowledgements and declaration of collaborations“.

Weitere Personen waren an der inhaltlich-materiellen Herstellung der vorliegenden Arbeit nicht beteiligt. Insbesondere habe ich hierfür nicht die entgeltliche Hilfe eines Promotionsberaters oder anderer Personen in Anspruch genommen. Niemand hat von mir, weder unmittelbar noch mittelbar, geldwerte Leistungen für Arbeiten erhalten, die im Zusammenhang mit dem Inhalt der vorgelegten Dissertation stehen.

Die Arbeit wurde bisher weder im In- noch im Ausland in gleicher oder ähnlicher Form einer anderen Prüfungsbehörde vorgelegt.

Regensburg, _____ _____

Martin Rothenhöfer